HIGHWAY RESEARCH RECORD

Number 71

Flexible Pavement Design
1963 and 1964
10 Reports

Presented at the
43rd ANNUAL MEETING
January 13-17, 1964

and

44th ANNUAL MEETING
January 11-15, 1965

HIGHWAY RESEARCH BOARD
of the
Division of Engineering and Industrial Research
National Academy of Sciences—
National Research Council
Washington, D. C.
1965

Department of Design

T. E. Shelburne, Chairman
Director of Research, Virginia Department of Highways
Charlottesville

COMMITTEE ON FLEXIBLE PAVEMENT DESIGN

(As of December 31, 1963)

R. E. Livingston, Chairman
Planning and Research Engineer
Colorado State Highway Department, Denver

Stuart Williams, Secretary
Supervisory Highway Research Engineer
U. S. Bureau of Public Roads, Washington, D. C.

A. C. Benkelman, Altamonte Springs, Florida
John A. Bishop, Director, Soils and Pavement Division, U. S. Naval Civil Engineering Laboratory, Port Hueneme, California
Thomas L. Bransford, Engineer of Research and In-Service Training, Florida State Road Department, Gainesville
W. H. Campen, Manager, Omaha Testing Laboratories, Omaha, Nebraska
George H. Dent, Benjamin E. Beavin Company, Baltimore, Maryland
James M. Desmond, Assistant State Materials Engineer, Wyoming State Highway Department, Cheyenne
T. V. Fahnestock, Bituminous Engineer, North Carolina State Highway Commission, Raleigh
Charles R. Foster, Coordinator of Research, National Bituminous Concrete Association, Texas A & M College, College Station
F. H. Gardner, Transportation Engineer Office, Transportation Research Command, Fort Eustis, Virginia
J. E. Gray, Engineering Director, National Crushed Stone Association, Washington, D. C.
John M. Griffith, Director of Research and Development, The Asphalt Institute, University of Maryland, College Park
R. A. Helmer, Research Engineer, Oklahoma Department of Highways, Oklahoma City
Frank B. Hennion, Assistant Chief, Civil Engineering Branch, Engineering Division, Military Construction, Office, Chief of Engineers, Department of the Army Washington, D. C.
Raymond C. Herner, Consulting Engineer, Indianapolis, Indiana
W. S. Housel, University of Michigan, Ann Arbor
F. N. Hveem, Materials and Research Engineer, California Division of Highways, Sacramento
Charles W. Johnson, Engineer of Construction, New Mexico State Highway Department, Santa Fe
Henry J. Lichtefeld, Federal Aviation Agency, Airports Division, Washington, D. C.
Wallace J. Liddle, Chief Materials Engineer, Materials Testing Laboratory, Utah State Department of Highways, Salt Lake City
Chester McDowell, Supervising Soils Engineer, Texas Highway Department, Austin
Alfred W. Maner, Staff Engineer, The Asphalt Institute, University of Maryland, College Park
C. E. Minor, Materials and Research Engineer, Washington Department of Highways, Olympia
Carl L. Monismith, University of California, Berkeley
A. O. Neiser, Assistant State Highway Engineer, Kentucky Department of Highways, Frankfort
Frank P. Nichols, Jr., Highway Research Engineer, Virginia Department of Highways, Charlottesville

R. L. Peyton, Assistant State Highway Engineer, State Highway Commission of Kansas, Topeka
E. G. Robbins, Portland Cement Association, Chicago, Illinois
Rollin J. Smith, Engineer-Manager, Asphalt Department, Skelly Oil Company, Kansas City, Missouri
Fred Sternberg, Senior Highway Engineer—Research, Connecticut State Highway Department, Hartford
John H. Swanberg, Chief Engineer, Minnesota Department of Highways, St. Paul
B. A. Vallerga, Vice President, Golden Bear Oil Company, Bakersfield, California

PAVEMENT DIVISION

Milton E. Harr, Chairman
Professor of Soil Mechanics, School of Civil Engineering
Purdue University, Lafayette, Indiana

COMMITTEE ON FLEXIBLE PAVEMENT DESIGN

(As of December 31, 1964)

R. E. Livingston, Chairman
Deputy Manager, Department of Public Works, City and County of Denver
Denver, Colorado

Stuart Williams, Secretary
Supervisory Highway Research Engineer
U. S. Bureau of Public Roads, Washington, D. C.

A. C. Benkelman, Altamonte Springs, Florida
John A. Bishop, Director, Soils and Pavement Division, U. S. Naval Civil Engineering Laboratory, Port Hueneme, California
Thomas L. Bransford, Engineer of Research and In-Service Training, Florida State Road Department, Gainesville
W. H. Campen, Manager, Omaha Testing Laboratories, Omaha, Nebraska
Bonner S. Coffman, Associate Professor of Civil Engineering, Ohio State University, Columbus
Robert A. Crawford, Assistant Research Engineer, South Dakota Department of Highways, Pierre
George H. Dent, Benjamin E. Beavin Company, Baltimore, Maryland
James M. Desmond, State Materials Engineer, Wyoming State Highway Department, Cheyenne
T. V. Fahnestock, Bituminous Engineer, North Carolina State Highway Commission, Raleigh
Charles R. Foster, Coordinator of Research, National Bituminous Concrete Association, Texas A & M University, College Station
J. E. Gray, Engineering Director, National Crushed Stone Association, Washington, D. C.
John M. Griffith, Director of Research and Development, The Asphalt Institute, University of Maryland, College Park
R. A. Helmer, Research Engineer, Oklahoma Department of Highways, Oklahoma City
Frank B. Hennion, Assistant Chief, Civil Engineering Branch, Engineering Division, Military Construction, Office, Chief of Engineers, Department of the Army, Washington, D. C.
Raymond C. Herner, Consulting Engineer, Indianapolis, Indiana
W. S. Housel, University of Michigan, Ann Arbor

Charles W. Johnson, Engineering Director, New Mexico State Highway Department, Santa Fe
Henry J. Lichtefeld, Federal Aviation Agency, Airports Service (AS-58), Washington, D. C.
Wallace J. Liddle, Engineer of Materials and Research, Utah State Department of Highways, Salt Lake City
Alfred W. Maner, Staff Engineer, The Asphalt Institute, University of Maryland, College Park
Chester McDowell, Supervising Soils Engineer, Texas Highway Department, Austin
C. E. Minor, Materials and Research Engineer, Washington Department of Highways, Olympia
Carl L. Monismith, University of California, Berkeley
A. O. Neiser, Assistant State Highway Engineer, Kentucky Department of Highways, Frankfort
Frank P. Nichols, Jr., Highway Research Engineer, Virginia Department of Highways, Charlottesville
R. L. Peyton, Assistant State Highway Engineer, State Highway Commission of Kansas, Topeka
E. G. Robbins, Portland Cement Association, Chicago, Illinois
George B. Sherman, Assistant Materials and Research Engineer, California Division of Highways, Sacramento
Rollin J. Smith, Engineer—Manager, Asphalt Department, Skelly Oil Company, Kansas City, Missouri
John H. Swanberg, Chief Engineer, Minnesota Department of Highways, St. Paul
B. A. Vallerga, Director of Engineering, Materials Research and Development, Oakland, California

Foreword

THE ten papers in this Record cover various aspects of the general subject of flexible pavement design. Six of the papers were presented at the 43rd Annual Meeting of the Highway Research Board and four at the 44th Annual Meeting. They are combined into a single record for reader convenience and to facilitate the early release of the latter group.

The paper by Bengt B. Broms describes an analytical method of evaluating the effect of the degree of saturation of the subgrade on the bearing capacity of a flexible pavement. This paper should be interesting to all who are called upon to design flexible pavements under a variety of conditions.

One other paper is of a specialized nature. Zube and Forsyth report on a series of tests to determine the effect of flotation type tires on flexible pavements.

Of the remaining eight papers three are concerned with road test data and five with analytical methods of flexible pavement design. All these papers will be of interest to those responsible for flexible pavement design.

In his analysis of the AASHO Road Test data, L. J. Painter develops equations relating performance to traffic volume, axle load and pavement structure thickness. In doing this he eliminates local environmental factors of the test site. R. A. Helmer relates the history and reports the findings of a long-term flexible pavement research project in Oklahoma. George F. Sowers has studied selected flexible pavements in Georgia employing the serviceability-performance concept developed at the AASHO Road Test. Ties established between the AASHO Road Test design charts and Georgia materials and environment make it possible to utilize the AASHO interim design method for the design of pavements in Georgia.

Under the general subject of analytical pavement design studies, S. Thenn de Barros reviews the state of knowledge on the problem of rational thickness design. Dorman and Metcalf have developed a practical method of applying the three-layer elastic theory to flexible pavement design. Tons, Chambers and Kamin have developed a flexible pavement design method for the Massachusetts Department of Public Works. The methods used on the AASHO Road Test were used as a guide but the method accounts for local operations and conditions. Hagstrom, Chambers and Tons have developed a computer solution for bending and shear stresses and vertical deflections in the asphalt-bound layers of a flexible pavement by application of the Westergaard theory. In a continuation of "Some Notes on Pavement Structural Design" begun in Highway Research Record 13, Norman W. McLeod investigates the application of Burmister's analysis of layered systems to the design of flexible pavements. For subgrades with CBR ratings from 4 to 20, the Burmister equation and the design methods of the Canadian Department of Transport and the Corps of Engineers, U. S. Army, produce very similar results.

Contents

Effect of Degree of Saturation on Bearing Capacity of Flexible Pavements

BENGT B. BROMS
Associate Professor of Civil Engineering, Cornell University, Ithaca, N. Y.

The bearing capacity of flexible pavements is frequently governed by the bearing capacity of the subgrade soil. The bearing capacity of the subgrade is reduced considerably during the spring breakup period due to reduction in the relative density and increase in the degree of saturation. A method for the evaluation of the bearing capacity of partially saturated soils has been developed. The effects of the apparent shear strength parameters c' and ϕ', the pore pressure coefficients $\bar{A}$ and B, the coefficient X, the coefficient of lateral earth pressure at rest K_o, and the location of the initial groundwater table have been investigated. The method is based on the assumption that the rate of loading of the subgrade soil caused by moving traffic loads is rapid enough that no or very small changes in moisture content of the subgrade soil take place during loading.

• THE BEARING capacity of flexible pavements is reduced considerably during the spring breakup period. This reduction is partly a result of a decrease of the relative density of the base course and subgrade materials as caused by heave, partly a result of an increase of the degree of saturation of the soil, and partly a result of excess pore pressures in the soil caused by rapid melting of the ice lenses present in the soil. A method for the evaluation of the bearing capacity of flexible pavements subject to frost action has been presented previously (5). A comparison of this method with a method proposed by Linell (12) showed good agreement.

The method proposed by the author (5) can be used as a basis for design of flexible pavements. This method is based on the assumption that failure takes place in the subgrade and that the subgrade soil is fully saturated. However, subgrades constructed according to modern methods reach saturation only within limited areas and over a brief period during the spring months. It may, therefore, be uneconomical to use this method for the design of highway pavements under all conditions. An optimum design may be reached if the design is based on more favorable conditions, for example, 90 percent saturation of the soil; but it should be expected that a few failures will take place if such a method is used. The degree of saturation to be used in design depends on such factors as type of traffic, local soil conditions, purpose of road, initial cost, and cost of repair in the case of failure.

The purpose of this investigation is the evaluation of the effect on the bearing capacity of flexible pavements of the degree of saturation of the subgrade soil.

NOMENCLATURE

$\bar{A}$ = pore pressure coefficient,
B = pore pressure coefficient,
c = cohesion (lb/sq ft),
c_u = cohesion as measured by undrained triaxial or direct shear tests (Q-tests) (lb/sq ft),
c' = cohesion with respect to effective stresses as measured by consolidated-undrained triaxial tests with pore pressure measurements (R-tests) (lb/sq ft),

Paper sponsored by Committee on Flexible Pavement Design and presented at the 43rd Annual Meeting.

d = width of loaded area (ft),
$(dp_1 - dp_3)$ = increase in stress difference or deviator stress, (lb/sq ft),
dp_3 = increase of ambient or hydrostatic stress (lb/sq ft),
dp_v = stress increase at level of subgrade (lb/sq ft),
du_a = pore pressure increase caused by increase of stress difference by $(dp_1 - dp_3)$ under undrained conditions (lb/sq ft),
du_b = pore pressure increase caused by increase of ambient stress by dp_3 under undrained conditions (lb/sq ft),
g = pressure in gas phase of soil (lb/sq ft),
g_f = pressure in gas phase at failure (lb/sq ft),
K_o = coefficient of lateral earth pressure at rest,
K_c, K, K_q = shape factors,
ℓ = length of loaded area (ft),
N_c, N_γ, N_q = bearing capacity factors,
p_o = total overburden pressure at level of subgrade (lb/sq ft),
$(p_1)_o$ = initial major total principal stress (lb/sq ft),
$(p_3)_o$ = initial minor total principal stress (lb/sq ft),
$(\overline{p}_1)_o$ = initial major effective principal stress (lb/sq ft),
$(\overline{p}_3)_o$ = initial minor effective principal stress (lb/sq ft),
$(p_1)_f$ = major total principal stress at failure (lb/sq ft),
$(p_3)_f$ = minor total principal stress at failure (lb/sq ft),
$(\overline{p}_1)_f$ = major effective principal stress at failure (lb/sq ft),
$(\overline{p}_3)_f$ = minor effective principal stress at failure (lb/sq ft),
t = thickness of wearing and base courses (ft),
S_r = degree of saturation (%),
u = pore pressure (lb/sq ft),
u_f = pore pressure at failure (lb/sq ft),
u_o = initial pore pressure (lb/sq ft),
W = applied load (lb),
X = parameter (Eq. 8),
ϕ_u = angle of internal friction as measured by undrained direct shear or triaxial tests (Q-tests) (deg), and
ϕ' = angle of internal friction with respect to effective stresses as measured by consolidated-undrained triaxial tests with pore pressure measurements (R-tests) (deg).

BEARING CAPACITY OF FLEXIBLE PAVEMENTS

Failure of a flexible pavement caused by failure of the subgrade soil is illustrated in Figure 1. Failure takes place along an approximately cylindrical failure surface within the subgrade when the load intensity at the bottom of the base course, at the level of the subgrade, reaches the bearing capacity of the subgrade. The ultimate bearing capacity of a flexible pavement, as governed by the bearing capacity of the subgrade, depends on the load-carrying capacity of the base course, as well as on the shear strength parameters, c and ϕ, of the subgrade soils along the failure surface.

The load-distributing ability of the base and wearing courses can be calculated, at low load levels, by a method based on the theory of elasticity, assuming that the materials in the base and wearing courses behave as ideal elastic materials (6). When the applied load approaches the bearing capacity of the soil, elastic methods are no longer

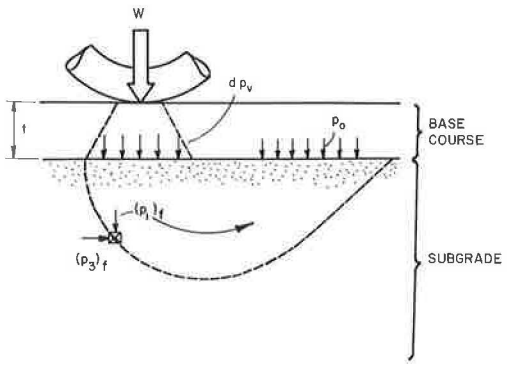

Figure 1. Failure of flexible pavement.

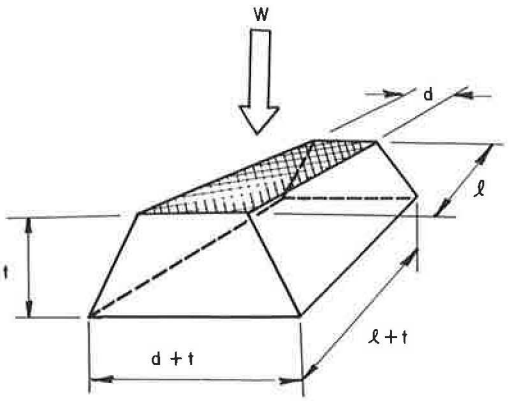

Figure 2. Assumed load distribution at failure.

applicable. In the following analysis, it has been assumed that the applied load is distributed over an area which increases linearly with the distance from the point of loading, the so-called 2:1 method (11, 13). Thus, it has been assumed in the following calculations (Fig. 2) that the soil pressure increase, dp_v, at the depth, t, below the point of loading as caused by the moving load, W, can be calculated from the equation:

$$dp_v = W/(d + t)\ (\ell + t) \tag{1}$$

in which ℓ d is the loaded area at the ground surface (Fig. 2). Failure will take place when the pressure increase dp_v reaches the ultimate bearing capacity of the subgrade soil.

The ultimate bearing capacity of the subgrade soil depends on the bearing capacity factors N_c, N_γ and N_q as expressed by the equation (7, 14, 17):

$$q_{ult} = K_c\, c\, N_c + K_\gamma\, d\, N_\gamma + K_q\, p_o\, N_q \tag{2}$$

in which

c = apparent cohesion,
K_c, K_γ, and K_q = factors depending on the shape of the loaded area, and
p_o = overburden pressure at the level of the subgrade (Fig. 1).

The apparent angle of internal friction of the soil, ϕ, and the cohesion, c, are functions of the rate of loading and the compressibility, void ratio and permeability of the subgrade soil. The most important of these factors are the rate of loading and the permeability of the subgrade soil. In the following analysis, it has been assumed that the rate of loading is high and that the change in moisture content of the soil is small as the soil is loaded to failure. The permeability of soils decreases rapidly with increasing percentage of silt and clay size particles. The change in moisture content of the soil as the soil is loaded to failure by a moving traffic load is small when the permeability of the soil is less than approximately 10^{-3} cm/sec. Under these conditions, the shearing strength of a soil and the bearing capacity factors, Nc, N_γ and Nq, are governed by the apparent angle of internal friction, ϕ_u, and the apparent cohesion, c_u, of the soil, the shear strength parameters of the soil as determined by undrained triaxial or direct shear tests (Q-tests). N_c, N_γ and N_q are functions of the apparent shear strength parameters, c_u and ϕ_u. The bearing capacity factor, N_q, can be determined from the equation:

$$N_q = e^{\pi \tan \phi_u} (1 + \sin \phi_u)/(1 - \sin \phi_u) \tag{3}$$

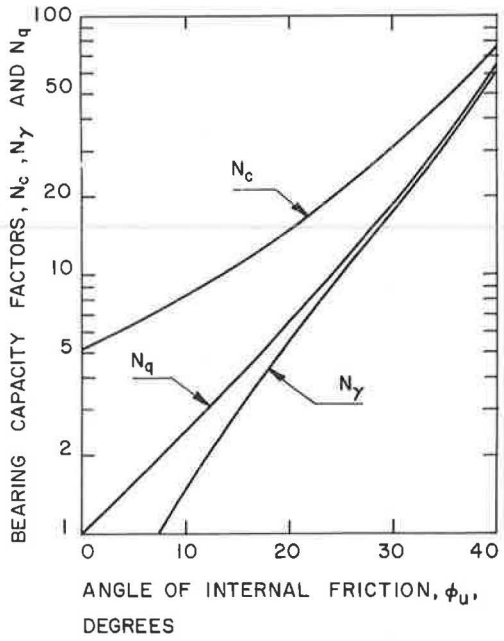

Figure 3. Bearing capacity factors, N_c, N_γ and N_q.

N_q is equal to 1.0 and 64.0 at apparent angles of internal friction of 0° and 40°, respectively.

The bearing capacity factor, N_c, can be computed from the equation:

$$N_c = (N_q - 1) \cot \phi_u \qquad (4)$$

N_c is equal to 5.14 and 75.0 at apparent angles of internal friction of 0° and 40°, respectively.

The bearing capacity factor, N_γ, cannot be calculated exactly by presently (1963) available methods. However, a number of approximate solutions are available. Its value can be determined conservatively from the expression:

$$N_\gamma = N_q - 1 \qquad (5)$$

N_γ as calculated from Eq. 5 attains the values 0.0 and 63.0 at apparent angles of internal friction, ϕ_u, of 0° and 40°, respectively. The relationships between the bearing capacity factors, N_c, N_γ and N_q, and the shear strength parameter, ϕ_u, have been computed and plotted in Figure 3.

The shape factors, K_c, K_γ and K_q, depend on the shape of the loaded area. The factors, K_c, K_γ and K_q, are equal to 1.0, 0.5 and 1.0, respectively, for large values of the length-to-width ratio ℓ/d of the loaded area and equal to approximately 1.25, 0.4 and 1.0, respectively, for a square or circular shape of the loaded area (1, 8, 9, 10, 14).

SHEAR STRENGTH AND PORE PRESSURE PARAMETERS

Definitions

The apparent cohesion, c_u, and apparent angle of internal friction, ϕ_u, can be expressed in terms of the shear strength parameters c' and ϕ', the pore pressure coefficients $\bar{A}$ and B, the parameter X, the coefficient of lateral earth pressure at rest K_o, the initial pore pressure u_o, and the initial effective overburden pressure $(\bar{p}_1)_o$. This relationship has been derived in the Appendix.

The shear strength parameter, ϕ', the apparent angle of internal friction with respect to effective pressures in the soil, does not vary appreciably with the degree of saturation of the soil, whereas the apparent cohesion, c', decreases rapidly with increasing degree of saturation; c' approaches zero as the degree of saturation of the soil approaches 100 percent. The apparent cohesion at the optimum water content may attain a value ranging from 0 to 2,500 lb/sq ft. This variation of c' affects the apparent shear strength parameters, c_u and ϕ_u.

The pore pressure coefficients, $\bar{A}$ and B, are defined by the equations:

$$\bar{A} = du_a/(dp_1 - dp_3) \qquad (6)$$

and

$$B = du_b/dp_3 \qquad (7)$$

in which du_a is the pore pressure increase caused by an increase of the deviator stress or stress difference within the soil by $(dp_1 - dp_3)$, and du_b is the pore pressure increase caused by an increase of the total ambient or total hydrostatic pressure by dp_3 under

undrained conditions. The pore pressure coefficient, B, is equal to 1.0 for saturated soils but decreases rapidly with decreasing degree of saturation. The pore pressure coefficient, B, is approximately equal to zero when the degree of saturation is in the range of 30 to 70 percent.

The pore pressure coefficient, $\bar{A}$, is also a function of the degree of saturation of the soil. $\bar{A}$ at a constant relative density is approximately proportional to the pore pressure coefficient, B. The relationship, $\bar{A} = 0.5\,B$, corresponds to a soil with a low relative density, and the relationship, $\bar{A} = -0.2\,B$, corresponds to a soil with a relatively high relative density.

The parameter X affects the effective stress distribution in a soil and, thus, the apparent shear strength parameters, c_u and ϕ_u. X (3, 4) is defined by the equation:

$$\bar{p} = p - u\,X - g\,(1.0 - X) \qquad (8)$$

in which $\bar{p}$ is the effective normal stress corresponding to the total normal stress p, u is the pore pressure and g is the gas pressure in the soil. X can, as a first approximation, be taken equal to the degree of saturation of the soil. It is equal to 1.0 for a fully saturated soil and to zero when the degree of saturation approaches zero.

The initial effective and total pressures in the subgrade are affected by the coefficient of lateral earth pressure at rest, K_o. The total vertical pressure, $(p_1)_o$, as shown in Figure 1, before the application of any external loads, is equal to the total overburden pressure; the corresponding effective vertical pressure, $(\bar{p}_1)_o$, can be calculated from Eq. 8 if the initial pore and gas pressures, u_o and g_o, respectively, are known. The corresponding initial lateral confining pressure, $(\bar{p}_3)_o$, can be expressed in terms of the initial effective overburden pressure by the equation:

$$(\bar{p}_3)_o = K_o\,(\bar{p}_1)_o \qquad (9)$$

in which K_o is the coefficient of lateral earth pressure at rest. K_o may attain a value as low as 0.4 for a normally consolidated clay (2), and as high as 2.5 for a heavily overconsolidated clay (16). The coefficient of lateral earth pressure for a compacted, partially saturated soil depends mainly on the compaction procedure. A value of K_o of 1.0 has been used in the following analysis.

Interrelationships Between Shear Strength and Pore Pressure Parameters

Pore Pressure Coefficients $\bar{A}$ and B. —The relationship between the apparent friction angle, ϕ_u, and the pore pressure coefficients, $\bar{A}$ and B, is illustrated in Figure 4. This relationship has been calculated from Eq. 22 (Appendix) at a value of X and K_o equal to 1.0. The apparent friction angle, ϕ', has been assumed equal to 30°. At a value of the pore pressure coefficient, $\bar{A}$, of 0.0, the apparent angle of internal friction, ϕ_u, varies between 0° for the case when the soil is saturated (B = 1.0) and 30° when the degree of saturation of the soil is equal to 30 to 70 percent (B = 0.0). The relationship between the apparent friction angle, ϕ_u, and the pore pressure coefficient, B, has been calculated for values of $\bar{A}$ equal to 0.5, 0.2, 0.0 and -0.2, corresponding to relative densities of the soil ranging from low to high.

The pore pressure coefficient, $\bar{A}$, is, at constant relative density of the soil, approximately proportional to the pore pressure coefficient, B. The relationships, $\bar{A} = 0.5\,B$ and $\bar{A} = -0.2B$, correspond to a low and high relative density of the soil, respectively. The effect of these relationships on the apparent angle of internal friction, ϕ_u, is shown in Figure 4. It can be seen that the effect of the relative density of the soil is the largest at an intermediate value of the pore pressure coefficient, B, when the degree of saturation of the soil is approximately 80 to 90 percent.

The effect of the pore pressure coefficient, B, on the apparent cohesion, c_u, can be evaluated by Eq. 23. This relationship has been calculated and plotted in Figure 5 (lower part). The apparent cohesion, c_u, has been calculated at a depth of 2.0 ft below the ground surface. The initial pore pressure, u_o, and the apparent cohesion, c', have been assumed equal to zero. The coefficient, X, and the coefficient of lateral

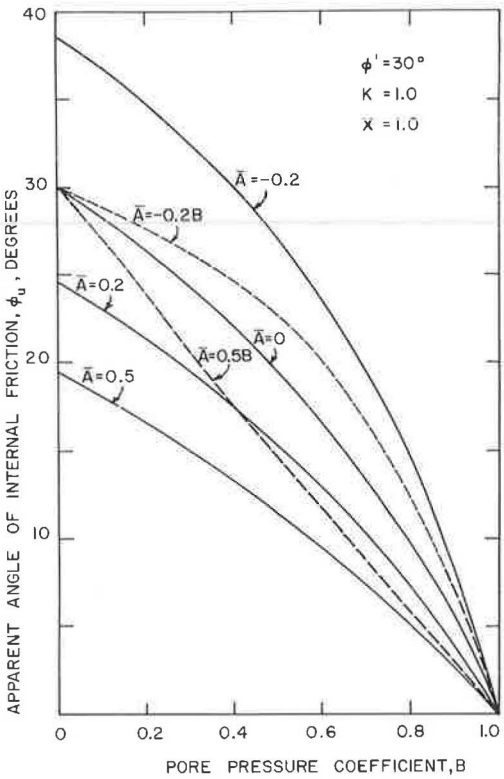

Figure 4. ϕ_u vs pore pressure coefficients, $\bar{A}$ and B.

earth pressure, K_o, have been taken as 1.0. The apparent angle of internal friction, ϕ', has been assumed equal to 30°. Figure 5 indicates that c_u increases rapidly with increasing values of B (thus, with increasing degree of saturation) and with decreasing values of $\bar{A}$ (thus, with increasing relative density of the soil). The apparent cohesion, c_u, ranges from 130 to 430 lb/sq ft as $\bar{A}$ ranges from 0.5 to -0.2. It may be concluded that, at small values of c', c_u is greatly affected by the degree of saturation of the soil.

The effects of the pore pressure coefficients, $\bar{A}$ and B, on the shear strength parameter, c_u, have also been calculated for a value of the apparent cohesion, c', equal to 400 lb/sq ft (Fig. 5, upper part). It can be seen that the effect of c' on c_u is large. Thus, in the calculation of c_u, all terms on the right-hand side of Eq. 23, except the first term ($2c' \cos \phi'$), can be neglected when the apparent cohesive strength of the soil exceeds approximately 400 lb/sq ft.

Coefficient X. —The coefficient X affects the apparent angle of internal friction, ϕ_u, of the soil. Its effect can be evaluated from Eq. 22 as a function of the pore pressure coefficient, B, and is presented in Figure 6. X can, as a first approximation, be taken as the degree of saturation of the soil. The effect of X has been calculated at a value of the coefficient of lateral earth pressure at rest, K_o, equal to 1.0, at a value of the apparent friction angle, ϕ', of 30° and at a value of the pore pressure coefficient, $\bar{A}$, of 0.0. The pore pressure coefficient, B, is always less than the degree of saturation, S_r, and thus, less than X. The relationship, X = B, therefore, represents a lower limit of the pore pressure coefficient, X. It can be seen from Figure 6. that the effect of X on the apparent friction angle, ϕ_u, is relatively small and can be neglected. X also has an effect on the apparent cohesion, c_u. Its effect is small as compared to the effect of the apparent cohesion, c', when the value of c' exceeds approximately 400 lb/sq ft (Fig. 5).

Initial Pore Pressure u_o. —The effect of the initial pore pressure, u_o, on the shear strength parameters, ϕ_u and c_u, can also be evaluated by Eqs. 22 and 23. The apparent friction angle, ϕ_u, is unaffected by the initial pore pressure, u_o. Its effect on the apparent cohesion, c_u, has been evaluated and presented in Figure 7. A variation of the initial location of the groundwater table by 2.0 ft affects c_u by 70 lb/sq ft at low values of the pore pressure coefficient, B, and by 120 lb/sq ft for a value of B equal to 1.0. This effect is small and can be neglected in comparison with the effect of the apparent cohesion, c', when c' exceeds approximately 400 lb/sq ft.

NUMERICAL EXAMPLES

The ultimate bearing capacity of a flexible pavement as governed by the ultimate strength of the subgrade can be calculated from Eqs. 1 and 2. It has been assumed that the load applied to the surface of the pavement is distributed to the subgrade over an area which increases in proportion to the thickness of the base and wearing courses (the 2:1 method). It has been further assumed that failure of the subgrade takes place

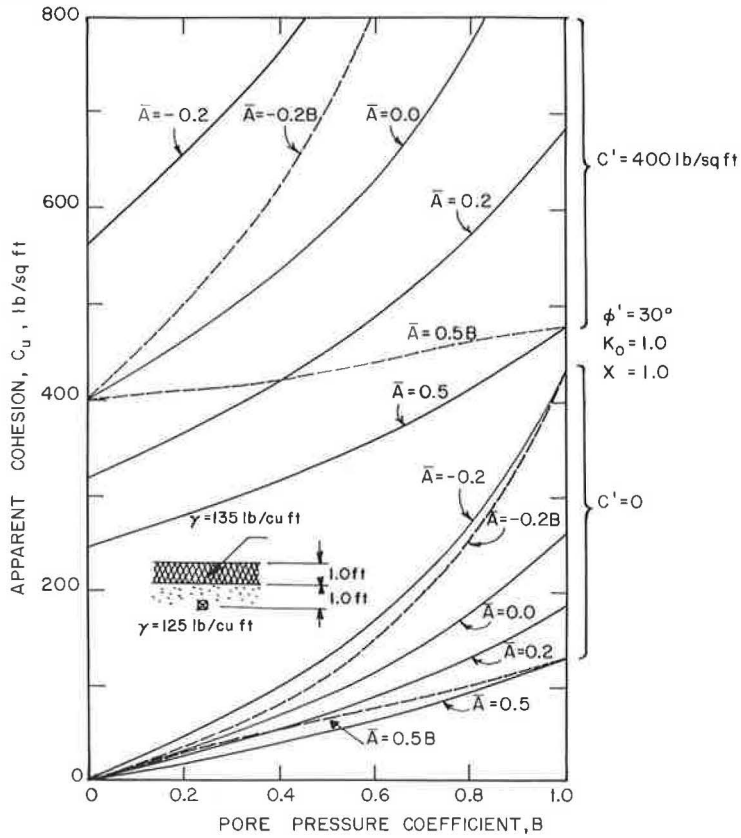

Figure 5. c_u vs pore pressure coefficients, $\bar{A}$ and B.

when the pressure increase, dp_v, at the level of the subgrade is equal to the ultimate bearing capacity, q_{ult}, as determined by Eq. 2. The ultimate bearing capacity can be expressed in terms of the bearing capacity factors, N_c, N_γ and N_q. These bearing capacity factors are functions of the apparent angle of internal friction of the soil, ϕ_u, in the case when the rate of loading is sufficiently high that no or very small changes of the water content of the soil take place when the soil is loaded to failure. The relationship between the apparent friction angle, ϕ_u, and the pore pressure coefficients, $\bar{A}$ and B, have been presented in Figure 4.

The ultimate bearing capacity depends also on the apparent cohesion, c_u, which can be evaluated directly from Figure 5 as a function of the pore pressure coefficients, $\bar{A}$ and B.

The ultimate bearing capacity of a flexible pavement has been calculated for

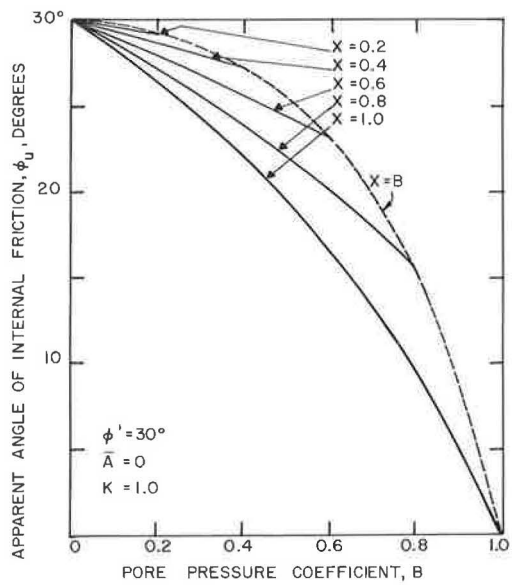

Figure 6. Effect of parameter X on friction angle, ϕ_u.

two soils denoted Soil I and Soil II, with assumed shear strength and pore pressure relationships as shown in Table 1. Soil I (with an apparent angle of internal friction, ϕ', and apparent cohesion, c', of 30° and zero, respectively) will, in general, be classified as an inorganic silt with low compressibility and Soil II (with ϕ' of 25° and c' varying from 0 to 800 lb/sq ft, depending on the degree of saturation) as an inorganic clay of medium plasticity.

The ultimate bearing capacity has been calculated assuming that the coefficient of lateral earth pressure, K_o, for the subgrade is equal to 1.0 and that the initial groundwater table is located 1.0 ft below the surface of the subgrade (at a depth of t + 1.0 ft below the ground surface). It has been assumed further that no excess pore pressures exist in the subgrade before application of load and that no change in moisture content of the subgrade soil takes place during loading.

The calculated ultimate bearing capacity is shown in Figures 8 through 13 for Soils I and II as a function of the contact pressure (tire pressure), the thickness of the wearing and base courses, and the degree of saturation of the two soils.

It can be seen from Figures 8 through 12 that the degree of saturation of the soil greatly affects the ultimate bearing capacity. A decrease of the degree of saturation from 1.0 to 0.9 increases the bearing capacity of Soil I and Soil II by approximately two and eight times, respectively. It can also be seen that the ultimate total bearing capacity increases with decreasing contact pressure (tire pressure).

The ultimate bearing capacity has been plotted in Figure 13 as a function of the thickness of the wearing and base courses at the contact pressures (tire pressures) of 250 and 100 lb/sq in., respectively. Relationships similar to those shown in Figure 13 can be constructed for other soil types with different shear strength and pore pressure relationships. These relationships can then be used as a basis for design of flexible highway or airport pavements. It should, however, be noted that the relationships shown in Figure 13 refer to the ultimate bearing capacity and that a safety factor (approximately 2.0 to 3.0) should be used, sufficient to prevent excessive deformations at working loads.

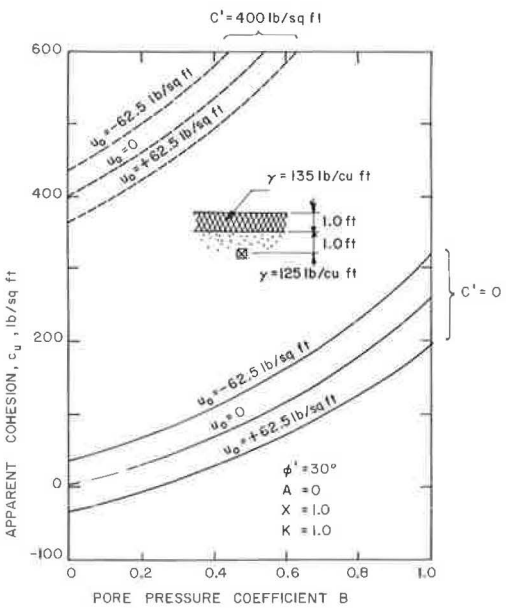

Figure 7. Effect of location of groundwater table on cohesion, c_u.

TABLE 1

ASSUMED SHEAR STRENGTH AND PORE PRESSURE RELATIONSHIPS

S_r (%)	X	c' (lb/sq ft)
	(a) Soil I[a]	
1.0	1.0	0
0.9	0.9	0
0.8	0.8	0
	(b) Soil II[b]	
1.0	1.0	0
0.9	0.9	400
0.8	0.8	800

[a] ϕ', 30°; unit weight, 125 lb/cu ft.
[b] ϕ', 25°; unit weight, 115 lb/cu ft.

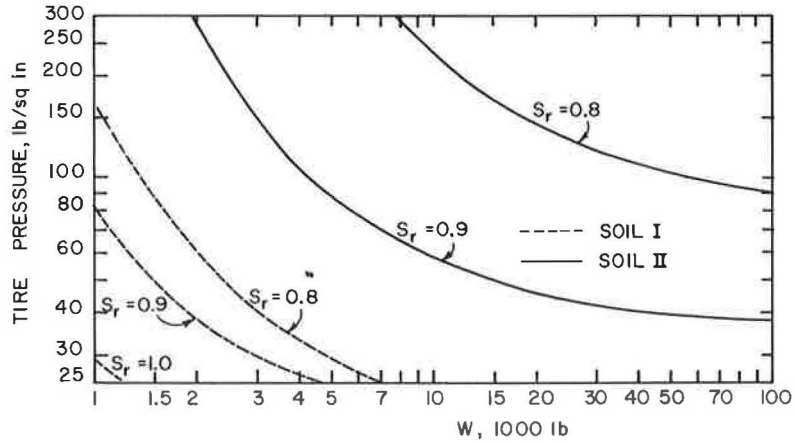

Figure 8. Ultimate bearing capacity, W, of flexible pavement, 6.0 in. total thickness.

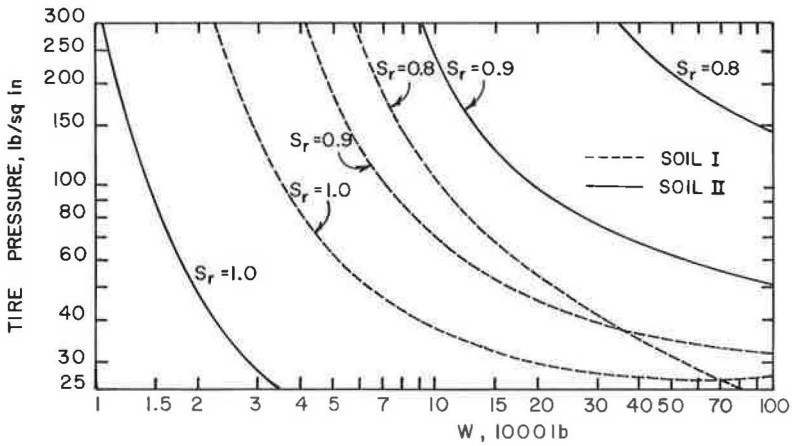

Figure 9. Ultimate bearing capacity, W, of flexible pavement, 12 in. total thickness.

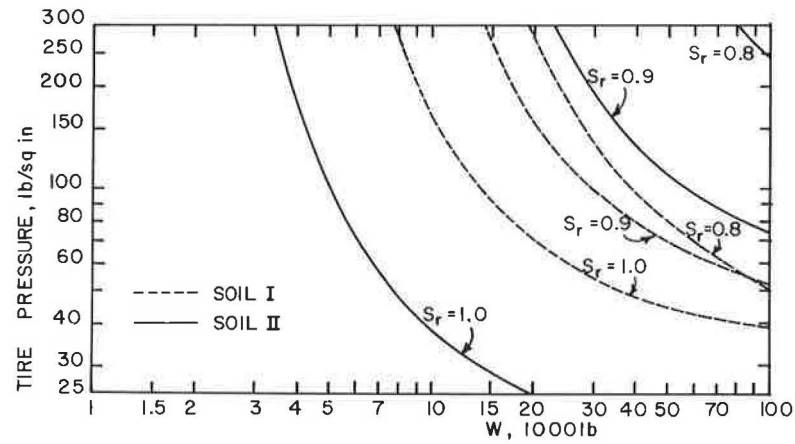

Figure 10. Ultimate bearing capacity, W, of flexible pavement, 18 in. total thickness.

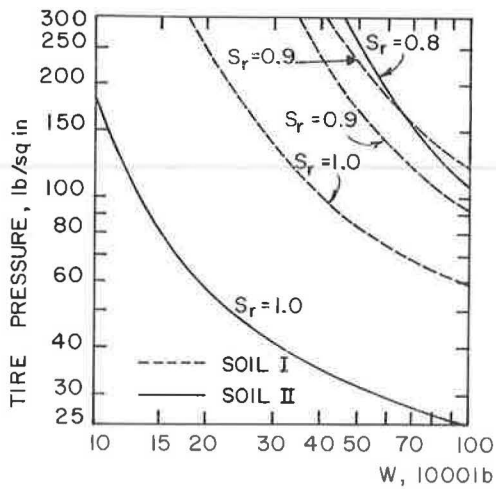

Figure 11. Ultimate bearing capacity, W, of flexible pavement, 24 in. total thickness.

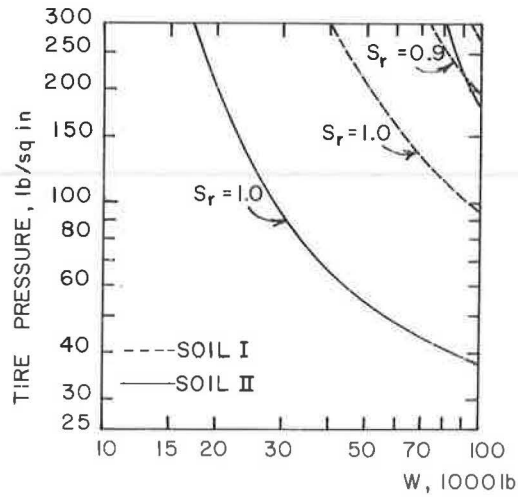

Figure 12. Ultimate bearing capacity, W, of flexible pavement, 30 in. total thickness.

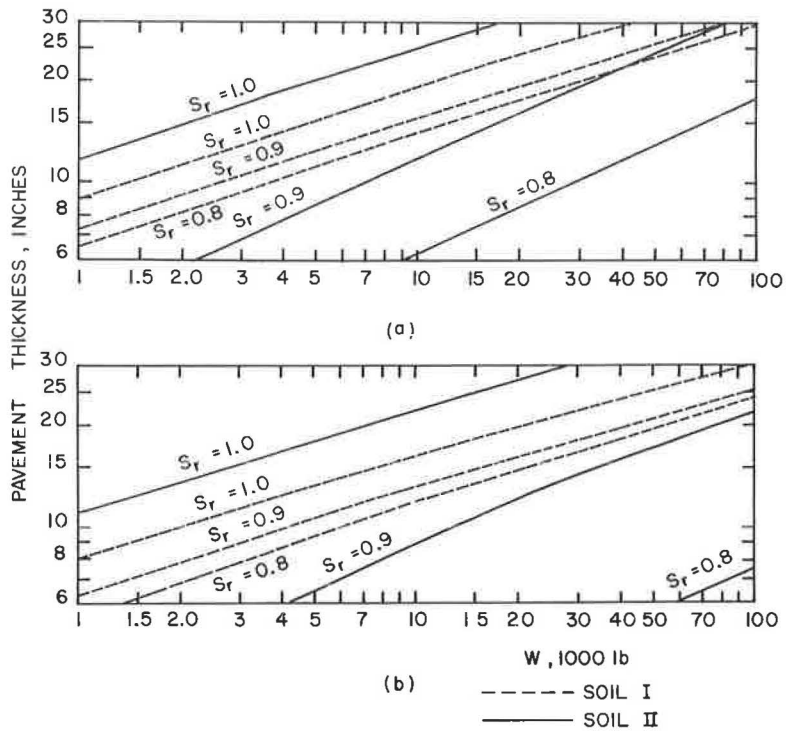

Figure 13. Ultimate bearing capacity, W, of flexible pavement: (a) tire pressure, 250 lb/sq in., and (b) tire pressure, 100 lb/sq in.

SUMMARY

Failure of flexible pavements may occur by failure of the subgrade soil when the load at the level of the subgrade reaches the bearing capacity of the subgrade. The ultimate bearing capacity of the subgrade can be evaluated by the bearing capacity factors, N_c, N_γ and N_q. The bearing capacity factors and the ultimate bearing capacity of the subgrade are functions of the apparent angle of internal friction, ϕ_u, and the apparent cohesion, c_u, as evaluated by undrained triaxial or direct shear tests (Q-tests). These shear strength parameters can be expressed in terms of the apparent shear strength parameters ϕ' and c', the pore pressure coefficients $\bar{A}$ and B, the empirical factor X, and the coefficient of lateral earth pressure at rest K_o.

The apparent friction angle, ϕ_u, was found to decrease rapidly with increasing value of the pore pressure coefficient, B, and thus, with the degree of saturation of the soil. On the other hand, the apparent cohesion, c_u, increased rapidly with increasing degree of saturation of the soil and with increasing value of the pore pressure coefficient, B. The effects of overburden pressure, the coefficient of lateral earth pressure at rest K_o, the empirical coefficient K, and the location of the groundwater table were found to be small when the apparent cohesion of the soil, c', exceeded approximately 400 lb/sq ft.

The ultimate bearing capacity of flexible pavements has been calculated for two subgrade soils (a silt of low compressibility and a clay of medium plasticity) as a function of the thickness of the wearing and base courses, the contact pressure (tire pressure) and of the degree of saturation of the subgrade soils. It was found that the degree of saturation affected greatly the bearing capacity of flexible pavements.

Appendix

The apparent angle of internal friction, ϕ_u, and apparent cohesion, c_u, depend on the degree of saturation of the soil, the pore pressure coefficients $\bar{A}$ and B, the coefficient X, the coefficient of lateral earth pressure at rest K_o, the effective shear strength parameters c' and ϕ' and the initial pore pressure u_o. The relationship between the apparent cohesion, c_u, the apparent angle of internal friction, ϕ_u, and these coefficients are derived in the following.

Failure of the soil takes place when the Mohr's stress circle with respect to effective stresses is tangent to the envelope curve corresponding to the shear strength parameters, ϕ' and c', as shown in Figure 13. From geometry the following relationship can be derived:

$$\sin \phi' \left[2c'/\tan \phi' + (\bar{p}_1 + \bar{p}_3)_f \right] = (\bar{p}_1 - \bar{p}_3)_f \qquad (10)$$

This equation can be rewritten in terms of total stresses, $(p_1)_f$ and $(p_3)_f$, if it is observed that:

$$(\bar{p}_1)_f = (p_1)_f - u_f X - g_f (1 - X) \qquad (11)$$

and

$$(\bar{p}_3)_f = (p_3)_f - u_f X - g_f (1 - X) \qquad (12)$$

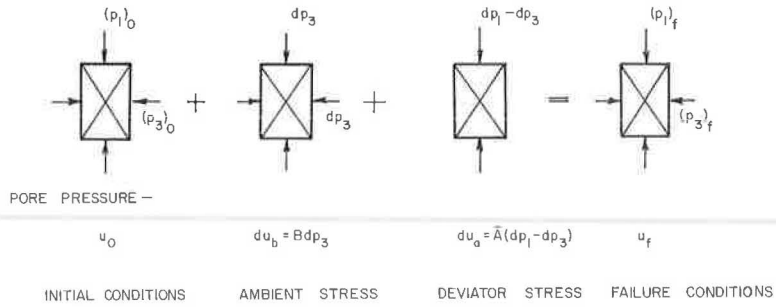

Figure 14. Pore pressures in partly saturated soil.

The gas pressure, g_f, at failure is, in general, low. If the gas phase is continuous, then g_f is equal to the atmospheric pressure and can be neglected. In the following analysis, g_f has been assumed equal to zero.

The pore pressure, u_f, at failure (Eqs. 11, 12) can be determined from the equation:

$$u_f = u_o + du_b + du_a \tag{13}$$

in which u_o is the initial pore pressure in the soil, du_b is the pore pressure increase caused by an increase of the ambient or hydrostatic pressure by dp_3, and du_a is the pore pressure increase caused by an increase of the deviator stress or stress difference by $(dp_1 - dp_3)$. The pore pressure increases, du_b and du_a, can be determined from the relationships (Fig. 14):

$$du_b = B\ dp_3 \tag{14}$$

$$du_a = \bar{A}\ (dp_1 - dp_3) \tag{15}$$

in which $\bar{A}$ and B are pore pressure coefficients. B depends on the degree of saturation of the soil and is equal to 1.0 when the degree of saturation of the soil approaches 100 percent and equal to zero when the degree of saturation of the soil is 30 to 70 percent. The pore pressure coefficient $\bar{A}$ depends on the degree of saturation, as well as on the relative density of the soil.

The ambient and deviator stress increases, dp_3 and $(dp_1 - dp_3)$, respectively, depend on the initial principal total stresses in the soil, $(p_1)_o$ and $(p_3)_o$, as well as on the stress conditions at failure, $(p_1)_f$ and $(p_3)_f$. The initial total stresses depend on the coefficient of lateral earth pressure at rest, K_o, and can be determined from the equations:

$$(p_1)_o = (\bar{p}_1)_o + X\ u_o \tag{16}$$

and

$$(p_3)_o = K\ (\bar{p}_1)_o + X\ u_o \tag{17}$$

The ambient pressure increase dp_3 can then be calculated from Eq. 17 as:

$$dp_3 = (p_3)_f - \left[K_o\ (\bar{p}_1)_o + X\ u_o \right] \tag{18}$$

and the deviator stress $(dp_1 - dp_3)$ from Eq. 16 as:

$$(dp_1 - dp_3) = (p_1)_f - (p_3)_f + (\bar{p}_1)_o \left[K_o - 1.0 \right] \tag{19}$$

By substituting Eqs. 18 and 19 into Eqs. 14 and 15, the pore pressure at failure can be determined from Eq. 13. The relationship between total pressures at failure $(p_1)_f$ and $(p_3)_f$ can be determined by substituting Eqs. 11, 12, and 13 into Eq. 10:

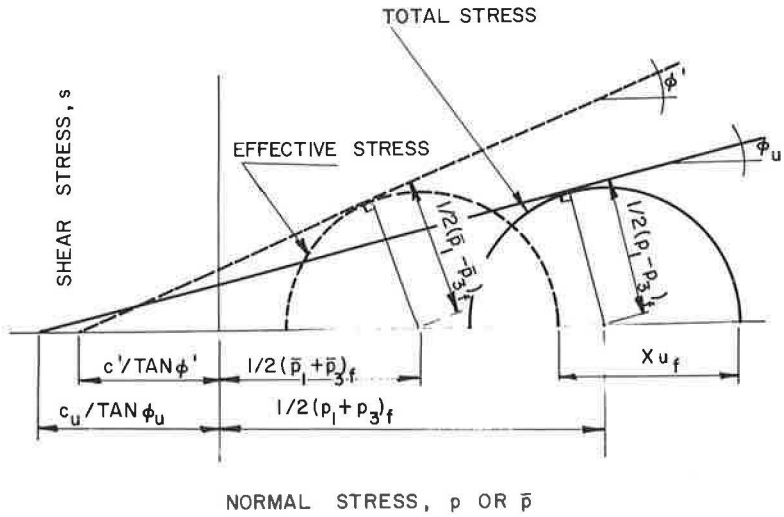

Figure 15. Pore pressures in partly saturated soil.

$$(p_1)_f \left[1.0 + 2X\bar{A} \sin\phi' - \sin\phi' \right] = (p_3)_f \left\{ 1.0 + 2X\bar{A} \sin\phi' - 2XB \sin\phi' + \sin\phi' + 2c' \cos\phi' 2Xu_o \sin\phi' + 2XBK (\bar{p}_1) \sin\phi' + 2BX^2 u_o \sin\phi' - 2X\bar{A}(\bar{p}_1)_o \left[K_o - 1.0 \right] \sin\phi' \right\} \quad (20)$$

The relationship between the principal total stresses at failure can also be expressed in terms of the shear strength parameters, c_u and ϕ_u. From geometry the following relationship (Fig. 15) can be derived:

$$(p_1)_f (1.0 - \sin\phi_u) = (p_3)_f (1.0 + \sin\phi_u) + 2c_u \cos\phi_u \quad (21)$$

A comparison between Eqs. 20 and 21 yields the relationships:

$$\frac{1.0 + \sin\phi_u}{1.0 - \sin\phi_u} + \frac{1.0 + 2X\bar{A} \sin\phi' - 2XB \sin\phi' + \sin\phi'}{1.0 + 2X\bar{A} \sin\phi' - \sin\phi'} \quad (22)$$

and

$$\frac{2c_u \cos\phi_u}{1.0 - \sin\phi_u} =$$

$$\frac{2c' \cos\phi' - 2Xu_o \sin\phi' + 2XBK_o(\bar{p}_1)_o \sin\phi' + 2BX^2 u_o \sin\phi' - 2X(\bar{p}_1)_o(K_o - 1.0) \sin\phi'}{1.0 + 2X\bar{A} \sin\phi' - \sin\phi'} \quad (23)$$

By means of Eqs. 22 and 23, the shear strength parameters, ϕ_u and c_u, can be expressed in terms of the pore pressure coefficients $\bar{A}$ and B, the coefficient X, the coefficient of lateral earth pressure at rest K_o and the shear strength parameters c' and ϕ'.

REFERENCES

1. deBeer, E. E., and Ladanyi, B. Etude Experimentale de la Capacite Portante du Sable Sous des Foundations Circulaires Stablies en Surface. Proc. 5th Int. Conf. on Soil Mech. and Found. Eng., Vol. 1, pp. 577-585, 1961.
2. Bishop, A. W. Test Requirements for Measuring the Coefficient of Earth Pressure at Rest. Brussels Conf. 58 on Earth Press. Prob., Vol. 1, pp. 2-14, 1958.
3. Bishop, A. W., Alpan, I., Blight, G. E., and Donald, I. B. Factors Controlling the Strength of Partly Saturated Cohesive Soils. Proc. ASCE Conf. on Shear Strength of Cohesive Soils, Boulder, pp. 503-532, 1960.
4. Bishop, A. W. Discussion. Proc. Conf. on Pore Pressure and Suction in Soils, pp. 38-46, 1961.
5. Broms, B. B. Bearing Capacity of Flexible Pavements Subject to Frost Action. Highway Research Record No. 39, pp. 66-180, 1963.
6. Burmister, D. M. The Theory of Stresses and Displacements in Layered Systems and Applications to Design of Airport Runways. Highway Research Board Proc., pp. 126-148, 1943.
7. Caquot, A., and Kerisel, J. Tables for the Calculation of Passive Earth Pressure, Active Earth Pressure and Bearing Capacity of Foundations. Paris, Gauthier-Villars, 1948.
8. Feda, J. Research on the Bearing Capacity of Loose Soil. Proc. 5th Int. Conf. on Soil Mech. and Found. Eng., Vol. 1, pp. 635-642, 1961.
9. Hansen, B. The Bearing Capacity of Sand Tested by Loading Circular Plates. Proc. 5th Int. Conf. on Soil Mech. and Found. Eng., Vol. 1, pp. 659-664, 1961.
10. l'Herminier, R., Habib, P., Tcheng, Y., and Bernede, J. Foundations Superficielles. Proc. 5th Int. Conf. on Soil Mech. and Found. Eng., Vol. 1, pp. 713-717, 1961.
11. Hough, B. K. Basic Soils Engineering. New York, Ronald Press Co., 1957.
12. Linell, K. A. Frost Design Criteria for Pavement. Highway Research Board Bull. 71, pp. 18-32, 1953.
13. Lundgren, H., and Brinch-Hansen, J. Geoteknik. Copenhagen, Teknisk Forlag, 1958.
14. Meyerhof, G. G. The Ultimate Bearing Capacity of Foundations. Geotechnique, Vol. 2, pp. 301-332, 1951.
15. Skempton, A. W. The Pore-Pressure Coefficients A and B. Geotechnique, Vol. 4, pp. 143-147, 1954.
16. Skempton, A. W. Horizontal Stresses in an Over-Consolidated Eocene Clay. Proc. 5th Int. Conf. on Soil Mech. and Found. Eng., Vol. 1, pp. 351-357, 1961.
17. Terzaghi, K. Theoretical Soil Mechanics. New York, John Wiley and Sons, 1943.

Analysis of AASHO Road Test Asphalt Pavement Data by The Asphalt Institute

L. J. PAINTER
Research Statistician, California Research Corporation, Richmond, California

• THIS REPORT is the result of the need, as foreseen by The Asphalt Institute, for independent analyses of the results of the AASHO Road Test. The Asphalt Institute took cognizance of this need in 1960 in setting up its Road Test Board of Study. The Institute reasoned that in an area so new, because of its vastly increased scope, examination of the research results from many different points of view could only help to shed still more light on the problem of adequate highway structural design.

In addition to the independent analysis of the AASHO Road Test presented here, the Road Test Board of Study was charged with developing thickness design relationships to be used in a revised edition of The Asphalt Institute's Thickness Design manual. The resulting thickness design method, distinct from but not unrelated to the work presented in this paper, is based on many sources of data besides the AASHO Road Test and has been reported elsewhere (9).

SUMMARY

This report presents a system of equations which describe all the measures of asphalt pavement performance made at the AASHO Road Test.

These measures include the Present Serviceability Index (PSI), the slope variance, the transverse profile (rutting), major cracking (Class 2 and Class 3), and roughness as indicated by the AASHO BPR-type roughometer. Each item was investigated in both the inner and outer wheelpath of each test section of the main asphalt experiment. In addition, the average serviceability index for each test section was studied. The serviceability indexes (Appendix B) used were calculated from the equations developed by The Asphalt Institute (1).

The results of our analysis as presented in this report are based on the complete data from the AASHO Road Test as released by the Highway Research Board at the time of its May 1962 special meeting in St. Louis, Mo. (2). These final results agree very well with our previous analysis of the average serviceability through the first 40 percent of the test traffic. The results of the preliminary analysis were presented at the International Conference on the Structural Design of Asphalt Pavements in August 1962 (3).

The results of our analysis are in the form of a group of equations relating performance to traffic volume, axle load, and pavement structure thicknesses. As such, they are easily used for the solution of thickness design problems or for estimating the remaining useful life of in-service highways. The effects of applied axle loads have been accounted for in a manner permitting the evaluation of mixed-traffic effects.

The effect of the Illinois environment has been evaluated by a climatic factor. This has been done to make the major part of the analysis free from any influence of the spring thaw effects of the Illinois environment. The development of the climatic factor points a way to possible evaluation of such factors for other climatic areas.

In the development of the models presented here, very deliberate efforts were made to identify and eliminate from the analysis any possible biases arising from specific conditions such as time, traffic rate, and initial pavement condition prevailing at the Road Test during testing. These factors are extraneous influences compared to the more basic engineering boundary conditions such as soil strength, materials, and methods of construction. In the course of the analyses, it became apparent that these extraneous boundary conditions would, in fact, bias the results if not accounted for.

Paper sponsored by Committee on Flexible Pavement Design and presented at the 43rd Annual Meeting.

The methods used to test for and eliminate these sources of bias are described in the appropriate sections of this report.

The form of the equations relating thickness to applications (traffic), axle load, and the several measures of pavement performance is such as to permit solution for the minimum cost design (surface, base and subbase thicknesses) for any specific situation. This could be done by the technique of linear programing, a method of obtaining the optimum solution for large systems of linear equations. A simplified example of its use with the results of our analysis is given in the section of this report on "Minimum Cost Design."

Our models should be applicable to the analysis of satellite testing programs conducted in the various states. Of particular interest is the possibility of using our equations to describe the performance of in-service highways. This is possible because the basic parameters in the equations are independent of the age of the pavement. Thus, it would not be necessary to make any assumptions of traffic rate or condition prior to the time of starting a measurement program.

It is most important to keep in mind that the equations presented here give only a description (although a mathematical one) of what happened at the AASHO Road Test. However, a strong point in favor of the validity of our results is the fact that the deterioration rates determined by our analyses correlate very well with critical stresses and strains calculated for the pavement structures by theoretical stress-strain relationships for layered systems (4, 5).

As was pointed out earlier, there are certain real limitations on these analyses. There is no way to tell from the Road Test data how, for example, soils of different strengths will perform. To determine this will require similar data on different soils with proper measurements of the strength properties of the soils. Such extensions of the AASHO Road Test findings are urgently needed.

BASIC PERFORMANCE RELATIONSHIPS

This section describes the form of the equations used to represent the Road Test results. The development of the equations is given in Appendix A.

Present Serviceability Index

The basic equation form for the present serviceability index, P_t, average of both wheelpaths, is

$$P_t = P_o e^{-b\ W_t} \qquad (1)$$

or the logarithmic transformation

$$\ln (P_o/P_t) = b\ W_t \qquad (2)$$

in which

- P_t = present serviceability index at time, t_j;
- P_o = the same index at start of traffic ($t = 0$);
- b = deterioration rate parameter; and
- W_t = millions of accumulated load applications to time, t.

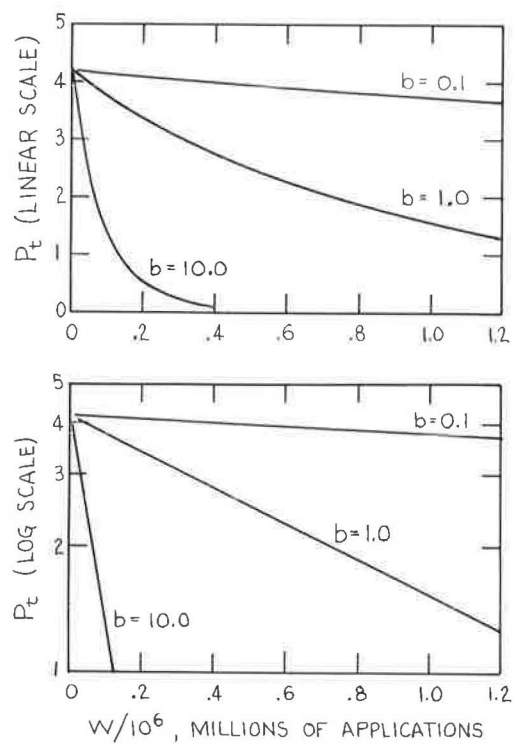

Figure 1. Basic performance relationships.

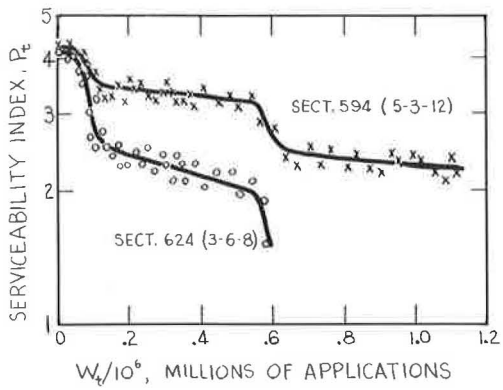

Figure 2. Typical performance data.

The shapes of these equation forms are shown in Figure 1.

In the equation, b is the deterioration rate of the pavement, dependent on thickness and strength of surface, base and subbase, subgrade soil strength, and the load applied to the pavement. Analysis of the Road Test data shows that, for a given pavement, b is constant throughout the year, except for the spring thaw periods. During these times, the deterioration rate increases to some higher value and then returns gradually to its original, nonspring thaw, value. This increase of the deterioration rate is the result of a loss of strength in the pavement structure, most likely in the subgrade soil and the granular layers. Figure 2 shows some typical Road Test data, illustrating very well this seasonal variation in the deterioration rate.

The variation of b follows a very definite and consistent pattern. The value of b can be described, at any time, i, by the equation:

$$b_i = b_o [\, 1 + k(x_i - 2x_i^2 + x_i^3) \,] \tag{3}$$

in which b_o is the value of b prevailing during most of the year, x_i is the real time fraction (modulo one) of the spring thaw already passed, and k is a parameter, determined from the data, measuring the relative loss of strength in the pavement structure during a spring thaw period. An important point is that the variation of b is independent of design thickness and applied load.

If b_i is the rate of deterioration when a single load application is made, the performance equation can be written as:

$$\Delta \ln (P_o/P_t) = b_o \, v_i/10^6 \tag{4}$$

in which

$$v_i = 1 + k(x_i - 2x_i^2 + x_i^3) \tag{5}$$

If we had knowledge of the exact time, i, when each load application was made, we could sum Eq. 4:

$$\ln (P_o/P_t) = \sum_{i=1}^{t} b_o \, v_i/10^6 \tag{6}$$

As the Road Test data give load applications only in two-week counts, if the applications (again in millions) occurring in each biweekly period are denoted by n_i, Eq. 6 can be approximated by:

$$\ln (P_o/P_t) = \sum_{i=1}^{t} b_o \, \bar{v}_i \, n_i \tag{7}$$

in which $\bar{v}_i$ is the integral average of v_i for each two-week period ending on Index Day, i. This average assumes that the traffic rate is constant during the index period.

As b_o is constant for a given design and load, Eq. 7 may be written as:

$$\ln (P_o/P_t) = b_o \sum_{i=1}^{t} \bar{v}_i \, n_i \tag{8}$$

Here, the acceleration function, $\bar{v}_i$, operates as a weighting function on n_i, the applications during period i. This is convenient for defining

$$\text{Weighted applications} = \sum_{i=1}^{t} \bar{v}_i \, n_i = W_t^* \tag{9}$$

so that we can write

$$\ln (P_o/P_t) = b_o \, W_t^* \tag{10}$$

It must be kept in mind that this concept of weighted applications is only a convenience. What has really occurred is an increase of the basic deterioration rate, b_o, during the spring thaw period.

By considering the increase of b_o in this way in our analysis, we avoid any bias in the data caused by having had the traffic start in late October 1958. Most of the test sections which failed during the first spring thaw would have accumulated many more load applications before failure if traffic startup had been late June.

The weighted applications, W_t^*, as defined in Eq. 9, can be interpreted as the real load applications one would require to change the serviceability from P_o to P_t for a pavement of strength b_o in an area with no spring thaw or similar acting period of accelerated deterioration. As a result, the analysis yields performance relationships for two climatic conditions: (a) the Ottawa, Ill., environment; and (b) an ideal environment (no spring thaw, etc.). Environments in most areas of this country undoubtedly fall between these two points.

If, as for design purposes, we assume a constant rate of load application, we can define an annual adversity (climatic or regional) factor, F, using N periods covering exactly one year, as:

$$F = \sum_{i=1}^{N} \bar{v}_i / N \tag{11}$$

That is, F equals the average value of $\bar{v}_i$ over the entire year.

For practical design work, some estimate of an average F value must be used, because conditions such as spring thaws vary from year to year in their effect on pavements. An average value of F based on Y years observed is most easily calculated as:

$$\bar{F} = 1 + \left(\sum_{j=1}^{Y} k_j \, m_j \right) / (12YN) \tag{12}$$

in which

k_j = the value of the thaw parameter, k, for year j;
m_j = the number of observation periods in which the adverse spring thaw conditions exist in year j;
$1/12$ = the integral of $x - 2x^2 + x^3$ between x = 0 and x = 1;
Y = number of years observed; and
N = number of observation periods per year.

There are likely also large effects of subgrade soil, drainage, etc., on this adversity factor. The Road Test gives only two estimates of F, one for each complete year of testing. Satellite test programs in the various states would provide the information required to determine reasonably accurate values of F for the different areas of the country.

It follows from the definition of F that for each year

$$W_t^* = F \, W_t \tag{13}$$

or for F derived from several years' data

$$W_t* = \bar{F}\, W_t \tag{14}$$

Therefore, by substitution of Eq. 14, Eq. 10 can be written in terms of real applications:

$$\ln (P_o/P_t) = b_o\, \bar{F}\, W_t \tag{15}$$

We can now consider the adversity factor operating as a weight on b_o. The F factor is the average acceleration of b_o, as defined in Eq. 11. Hence, $\bar{F}\, b_o$ is the annual average rate of pavement deterioration. In this form, the equation is most convenient for design use because F may be incorporated directly into the relationship of b_o with factors such as thickness.

Relation of Performance to Design and Load.—The basic deterioration rate, b_o, in Eq. 15 is related to design and load as follows:

$$\ln b_o = a_o + a_1 D_1 + a_2 D_2 + a_3 D_3 + a_4 L \tag{16}$$

in which

D_1 = asphalt concrete surface thickness (in.),
D_2 = crushed stone base (in.),
D_3 = sand gravel subbase (in.),
$L = L_1/L_2 + a_5 (L_2 - 1)$,
L_1 = gross axle load (kips), and
L_2 = 1 for single axles and 2 for tandem axles.

The deterioration rate, b_o, is completely independent of the age of the pavement, being a function only of the thickness and load variables.

Rewriting Eq. 16 as

$$\ln b_o = a_o + a_1 \left[D_1 + \frac{a_2}{a_1} D_2 + \frac{a_3}{a_1} D_3 \right] + a_4 L \tag{17}$$

we see that the term in brackets defines an equivalent thickness of surface, D_a, wherein the ratios a_2/a_1 and a_3/a_1 are the surface equivalencies of base and subbase, respectively. The coefficient, a_o, is almost certainly dependent on subgrade soil strength. Possibly a_1, a_2, and a_3 are also dependent on soil strength. Certainly a_1, a_2, and a_3 should be dependent on the respective strength properties of the surface, base and subbase.

Substituting D_a, equivalent surface thickness, for the bracketed term gives:

$$\ln b_o = a_o + a_1 D_a + a_4 L . \tag{18}$$

Combining Eq. 18 with the logarithmic transform of Eq. 15 and solving for D_a gives the design formula:

$$D_a = \frac{-[a_o + \ln F - \ln \ln (P_o/P_t) + \ln (W_t) + a_4 L]}{a_1} \tag{19}$$

The load term can be combined with the W_t term:

$$\ln W_t + a_4 L = \ln [W_t\, e^{a_4 L}] \tag{20}$$

The bracketed portion of Eq. 20 defines axle-load effects in a way that permits development of axle-load equivalencies. This is possible because the value of $W_t\, e^{a_4 L}$, regardless of the particular values of W_t and L, will require some fixed value of D_a once

P_o, P_t, and F are specified. This permits a rather straightforward evaluation of mixed traffic. A term $e^{a_4(L - L')}$ defines a load factor relating W applications of load L to W′ applications of some other load L′:

$$W' = W\, e^{a_4(L - L')} \tag{21}$$

The theory underlying this definition of axle-load equivalencies is discussed in Appendix A.

In this report, we have chosen to use the 18-kip, single-axle load as a base or reference load, defining equivalent 18-kip, single-axle loads, W_{18}, as:

$$W_{18} = W_L\, e^{a_4(L-18)} \tag{22}$$

By combining this with Eq. 19, we can write a final design equation:

$$D_a = \frac{-[a_o + \ln F - \ln \ln (P_o/P_t) + \ln (W_{18})]}{a_1} \tag{23}$$

Other Measures of Performance

Criticisms have been made of the use of the serviceability index in defining pavement failure These criticisms are based on the contention that the index is too big a melting pot, in which the various physical forms of distress lose their identity and meaning.

In a certain sense, this criticism is a valid one; knowing only that a pavement has too quickly reached an unacceptably low serviceability certainly gives no clue to the possible cause of the rapid decline. However, the serviceability index does give a good overall picture of the riding quality which the customer-taxpayer is paying for. In a sense, the serviceability index was meant to be a melting pot to provide a single measurement of the riding quality of a pavement. It is difficult, if not impossible, to analyze the index, a subjective thing, in the engineering terms of stress, strain, and strength. For this we must look at each form of pavement distress separately.

In this section of this report is given the form of the equations used to analyze, by wheelpath, the following forms of distress measured at the AASHO Road Test: (a) serviceability index, (b) slope variance, (c) rutting, (d) roughness index, and (e) cracking. In all cases, I and ϕ will be used to identify the inner and outer wheelpaths, respectively.

Basic Equation Forms.

Wheelpath Serviceability Index, P_t. —The basic equation form for the individual wheelpaths is identical to that for the average serviceability index. For the inner wheelpath:

$$P_{t,\,I} = P_o\, e^{-b_I W_t} \tag{24}$$

and for the outer wheelpath:

$$P_{t,\,\phi} = P_o\, e^{-b_\phi W_t} \tag{25}$$

The logarithmic forms of these equations used in analyzing for b_I and b_ϕ are:

$$\ln (P_o/P_{t,\,I}) = b_I W_t \tag{26}$$

$$\ln (P_o/P_{t,\,\phi}) = b_\phi W_t \tag{27}$$

P_0 is the same initial serviceability used for the average P_t analysis. The b's, of course, are the deterioration rates for the individual wheelpaths and are analogous to the b_0 defined for the average P_t performance.

Wheelpath Slope Variance, SV. —The slope variance is a statistical measure of the variability of the slope of the pavement. As such, it is a direct measure of the longitudinal roughness of a pavement. At the AASHO Road Test, a new instrument (the AASHO Profilometer) was developed to measure and record a continuous analog trace of the pavement slope. This analog trace was then sampled at 1-ft intervals to obtain point measurements of the slope, s_i. The slope variance, σ_s^2, was then calculated as:

$$\sigma_s^2 = \sum_{i=1}^{n} (s_i - \bar{s})^2/(n - 1) \tag{28}$$

For convenience, these values were scaled by a factor of 10^6 to obtain more manageable numbers. These scaled values, called SV, are the ones used in all phases of the Road Test work (including our analyses) to denote slope variance. SV = 10^6 x slope variance, according to Eq. 28.

The slope variance is by far the most important single variable influencing the serviceability index. Consequently, it was no surprise to find that the best mathematical form for analyzing slope variance was derivable from the serviceability index performance model and the serviceability index equations developed by The Asphalt Institute (1). The equations used are as follows:

for the inner wheelpath

$$\sqrt{\overline{SV}_I} = \sqrt{\overline{SV}_0} + b_I W_t \tag{29}$$

and for the outer wheelpath

$$\sqrt{\overline{SV}_\phi} = \sqrt{\overline{SV}_0} + b_\phi W_t \tag{30}$$

SV_0 is the average initial slope variance for the test section. The b's are the rates at which slope variance increased with traffic.

Wheelpath Rutting, RD. —The rut depth measures the amount of permanent deformation in the transverse profile of the pavement. At the Road Test, the rut depth was measured below the center of a 4-ft span placed across the wheelpath. The values reported are actually the average of a number of rut depth measurements made throughout the length of the test section.

Rutting plays only a secondary role in determining the serviceability index. In fact, it was not included in the index equations originally developed by the Road Test staff because the amount of rutting found on the in-service highways panel rated for serviceability was insignificant and minor in extent. As serious rutting appeared on the Road Test, some of the test sections were panel rated and rutting was found to have a significant, although secondary, effect on serviceability.

The serious rutting observed at the Road Test seems to have been a peculiar effect caused by the unnatural (though necessary) isolation of the specific axle loads. When the results of our analysis are applied to specific real traffic situations on practical sections, the level of rutting estimated at the end of, say, 20 years of traffic is very minor.

The equations found best suited for analyzing rutting are as follows:

for the inner wheelpath

$$RD_I^2 = b_I W_t \tag{31}$$

and for the outer wheelpath

$$RD_\phi^2 = b_\phi W_t \tag{32}$$

The b's are the rates of rutting in each wheelpath for the particular load and test section being studied. The initial value of RD was zero, which accounts for the lack of an RD_o term. It should be noted that the growth of rutting is a decelerating function of load applications, that is, the change in rutting (RD) per application becomes smaller with increasing load applications.

Wheelpath Roughness, RI. —Part of the AASHO Road Test measurement program involved periodic measurements of the roughness index by the AASHO roughometer, modeled after the familiar BPR roughometer. This type of instrument measures the total positive vertical displacements of the pavement surface, longitudinally, in the wheelpaths.

Theoretically, this measurement can be related to the slope variance of a pavement. However, analysis of data obtained on asphalt pavements by both methods shows only moderate correlation between the two types of measurement. This is due, it appears, to two mechanical features of the BPR-type roughometer:

1. Even on relatively smooth pavements, there seems to be extraneous vibration of the measuring wheel relative to its reference frame. As a result, there seems to be a minimum of 40 to 50 in. per mile roughness measurable on even a perfectly smooth pavement.
2. The reaction-time (inertial) characteristics of the BPR-type roughometer are such that the device is sensitive to (i.e., measures) only the higher frequency distortions in a pavement surface, filtering out, for the most part, the lower frequencies. The profilometer, on the other hand, will measure virtually all distortion frequencies.

As a result, although both types of equipment attempt to measure the same thing, they will, in fact, measure somewhat different properties of the pavement profile because of their mechanical differences. This is not to say that one measurement is any better than the other, only that they are different. Each has its advantages and disadvantages.

The profilometer has an advantage in that it measures slope variance which, as noted, was used as the major variable in defining serviceability. Also, there is a stronger correlation of riding quality with the slope variance than with roughness index. However, the profilometer is designed to operate at a speed of about 3 mph, compared to as high as 20 mph for a roughometer. Besides the obvious economic advantages of the faster instrument, some state highway departments are greatly concerned with the safety hazards involved in operating such equipment at extremely low speeds on major highways.

The decision of which type of instrument to use on in-service pavement research or in routine maintenance/condition surveys must be made by any user agency by balancing the relative merits and demerits of the two types of instruments.

The form of the roughness-applications equation was governed by consideration of the AASHO Road Test data. This form agrees with the results obtained by Housel (6) and the theoretical relation between slope variance and roughness index developed by Painter (1):

for the inner wheelpath:

$$RI_I = RI_o + b \ W_t \tag{33}$$

and the outer wheelpath:

$$RI_\phi = RI_o + b_\phi \ W_t \tag{34}$$

in which RI_o is the average initial roughness of the test section, and the b's are the rates of increase of roughness with traffic.

Cracking and Patching, CP. —The appearance of cracking in an asphalt surface is used by many highway engineers as a direct indication of a structural inadequacy somewhere in the pavement system. Pavement cracking was used as the principal criterion of pavement failure at the WASHO Road Test. Major cracking (Class 2 and Class 3)

and patching (to cover up previously cracked areas) was found to have only a minor role in determining the serviceability (riding quality) of a pavement. This does not mean that cracking is of minor structural importance. Indications are that by the time cracking has progressed far enough to impair greatly the riding quality of a pavement, that pavement has become very rough in terms of slope variance; hence, the slope variance term accounts for most of the detrimental effects of cracking.

Cracking can be the result of two types of failure in the pavement structure:

1. Shear failure in one or more of the pavement layers caused by complete overstressing by a single load application; or
2. Fatigue failure of the asphalt surface caused by the repeated applications of loads, no one of which is necessarily even close to causing shear failure.

Neither type of failure is unique to highway pavements. Steel and concrete beams exhibit the same behavior.

In general, any pavement likely to crack because of shear failure is already woefully underdesigned; hence, the study of cracking can be limited to cases of fatigue failure. On no asphalt section at the AASHO Road Test was cracking observed until after almost a thousand load applications. Many sections exhibited no cracking at the end of the testing period after having received over 1.1 million load applications.

Because there was very little cracking observed in the inner wheelpath, it was necessary to restrict the analysis to the outer wheelpath only. The equation form is

$$\sqrt{(C + P)}_{\phi} = b_{\phi} W_t \tag{35}$$

In terms of C + P (cracking + patching), this is an accelerating function, i.e.,

$$(C + P)_{\phi} = b_{\phi}^2 W_t^2 \tag{36}$$

Relation of Other Performance Measures to Design and Load. —The rates of deterioration for the several other performance measures studied were related to design and load by equations of the same form as the average serviceability, with the addition of a term to account for wheelpath differences.

$$\ln b = a_0 + a_1 D_1 + a_2 D_2 + a_3 D_3 + a_4 L + a_6 WP \tag{37}$$

in which WP = wheelpath indicating variable, with a value of 1 for the inner wheelpath and 0 for the outer wheelpath and all other terms are as defined previously for Eq. 16.

For each different performance equation, it is then possible to define an equivalent surface thickness as a function of the performance measure and equivalent 18-kip, single-axle applications, giving equations of the form:

$$D_a = \frac{-[a_0 + \ln F - f(\text{Performance}) + \ln(W_{18})]}{a_1} \tag{38}$$

The functions of performance, f(Performance), for each of the performance measures, are as follows:

Performance Measure	f(Performance)
PSI	$\ln \ln(P_0/P)$
Slope variance	$\ln (\sqrt{SV} - \sqrt{SV_0})$
Rut depth	$2 \ln RD$
Roughness index	$\ln (RI\text{-}RI_0)$
Cracking	$\frac{1}{2} \ln (C + P)$

The subscript o, as in P_o, denotes the initial value (prior to traffic startup) of that variable.

NUMERICAL RESULTS

The results presented here are all based on the complete data from the AASHO Road Test, representing a total of 1,114,000 load applications on the test pavements. The data were released to The Asphalt Institute after the Highway Research Board's St. Louis Conference on the AASHO Road Test in May 1962. Complete details of the fitting techniques used in our analyses have been described by Painter (11).

Climatic Factor

The first step in the analysis was to obtain values for the climatic factor, F, for each of the two years of testing. This was done to define the "weighted applications" scale. The average serviceability histories of all possible test sections were used for obtaining the F values. Obviously, each measure of performance could be used to define a climatic factor; however, we restricted our attention to the average serviceability so as to have only one such factor.

The average serviceability index history for each test section was fit by an equation of the form:

$$\ln P_t = a_o - a_1 - a_2 - b_o W_t \tag{39}$$

in which

a_o = fitted initial P,
a_1 = first spring drop in P in excess of traffic effect,
a_2 = second spring drop in P in excess of traffic effect, and
b_o = deterioration rate due to traffic outside spring thaw.

For each section surviving the first full year of testing (i.e., still in service on Index Day 26), an individual F value was obtained from the ratio of annual average deterioration rate over b_o, the basic deterioration rate:

$$F_1 = \frac{-a_1 - b_o W_{26}}{-b_o W_{26}} = 1 + \frac{a_1}{b_o W_{26}} \tag{40}$$

For each section still in service after two full years (on Day 52), an F value was obtained from

$$F_2 = \frac{-a_2 - b_o (W_{52} - W_{26})}{-b_o (W_{52} - W_{26})} = 1 + \frac{a_2}{b_o (W_{52} - W_{26})} \tag{41}$$

No significant effect of either structural design or load could be found to explain the variations in the F_1 or F_2 values. Accordingly, they were averaged over all sections to give $\bar{F}_1 = 3.760$ (based on 100 sections) and $\bar{F}_2 = 2.655$ (based on 44 sections). These gave values for the two spring thaw parameters (k_1 and k_2) of 174 and 119, respectively.

The overall average value of F for design purposes, computed according to Eq. 12, is $F_D = 4.0$. For each year, the design F (Eq. 12) is $F_{D,1} = 5.5$ and $F_{D,2} = 2.5$.

Table 1 lists the actual applications (W), the weighting function ($\bar{v}_t$), and the weighted applications ($W_{t*} = \sum_1^t v_t n_t$) obtained in this analysis. The relation of weighted to actual applications is shown graphically in Figure 3.

TABLE 1

WEIGHTED MEAN LOAD APPLICATIONS

Index Day	W (millions)	v_t	W_t* (millions)
1	0.0007	1.00	0.0007
2	0.0052	1.00	0.0052
3	0.0114	1.00	0.0114
4	0.0217	1.00	0.0217
5	0.0287	1.00	0.0287
6	0.0356	1.00	0.0356
7	0.0457	1.00	0.0457
8	0.0584	1.00	0.0584
9	0.0696	10.16	0.1722
10	0.0762	22.26	0.3191
11	0.0797	26.47	0.4118
12	0.0860	24.56	0.5665
13	0.0978	20.22	0.8051
14	0.1072	12.56	0.9231
15	0.1205	6.01	1.0031
16	0.1341	1.84	1.0281
17	0.1512	1.00	1.0451
18	0.1686	1.00	1.0626
19	0.1820	1.00	1.0760
20	0.1992	1.00	1.0932
21	0.2169	1.00	1.1109
22	0.2331	1.00	1.1271
23	0.2499	1.00	1.1439
24	0.2710	1.00	1.1650
25	0.2891	1.00	1.1831
26	0.3053	1.00	1.1993
27	0.3239	1.00	1.2179
28	0.3383	1.00	1.2323
29	0.3527	1.00	1.2467
30	0.3729	1.00	1.2669
31	0.3853	1.00	1.2793
32	0.4078	1.00	1.3018
33	0.4446	1.00	1.3386
34	0.4800	1.00	1.3740
35	0.5055	1.00	1.3995
36	0.5397	1.00	1.4337
37	0.5699	11.37	1.7771
38	0.6014	17.72	2.3352
39	0.6340	11.50	2.7102
40	0.6692	3.00	2.8158
41	0.7047	1.00	2.8512
42	0.7336	1.00	2.8802
43	0.7713	1.00	2.9178
44	0.8068	1.00	2.9534
45	0.8329	1.00	2.9794
46	0.8677	1.00	3.0142
47	0.9014	1.00	3.0480
48	0.9291	1.00	3.0756
49	0.9512	1.00	3.0978
50	0.9838	1.00	3.1303
51	1.0156	1.00	3.1622
52	1.0496	1.00	3.1962
53	1.0805	1.00	3.2270
54	1.0996	1.00	3.2462
55	1.1138	1.00	3.2604

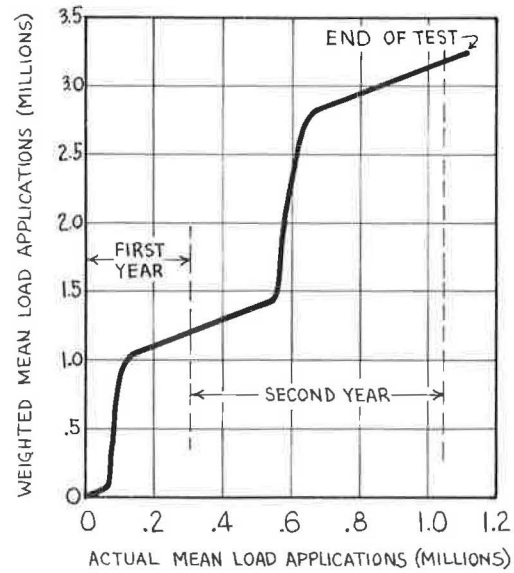

Figure 3. Weighted vs actual load applications.

Design and Load Effects

The data for each performance measure, in each wheelpath of each section, were correlated against weighted applications using the equation forms discussed previously. These equations are all of the general form:

$$g(\text{Performance})_t = b\ W_t^* \qquad (42)$$

The mathematical function, g(Performance), is the antilogarithm of f(Performance).

The b's thus obtained for all measures of performance (except cracking because of incompleteness) were then analyzed (as ln b) by routine factorial analysis methods, loop by loop, for the design, lane, and (except for average serviceability) wheelpath effects. With the possible exception of the Loop 2 analyses, no definite trends in the values of the effects could be noted. The coefficients for thickness and wheelpath effects were then averaged across all five loops.

Using the average thickness effects for each performance measure, the mean ln b values for each loop were adjusted to a common thickness (zero for all layers, for convenience) to study the load effects. This adjustment was necessary because the average thickness of each layer was different, generally, in each loop. The

TABLE 2

LAYER SUBSTITUTION RATIOS

Performance Measure	D_1	D_2	D_3	
PSIA	1	0.282	0.210	$= D_a$
PSI	1	0.291	0.171	$= D_a$
SV	1	0.313	0.200	$= D_a$
RD	1	0.145	0.046	$= D_a$
RI	1	0.245	0.167	$= D_a$
C + P	1	0.284	0.228	$= D_a$

TABLE 3

LOAD FACTORS

Axles	L_1 (kips)	L, Equivalent SA Load	Load Factor	Avg. Axle Factor
Single	2	2	0.0545	0.0545
	6	6	0.1128	0.1673
	12	12	0.336	0.375
	18	18	1.000	1.0564
	22.4	22.4	2.23	2.29
	30	30	8.88	8.90
Tandem	24	14.36	0.515	0.571
	32	18.36	1.068	1.165
	40	22.36	2.21	2.31
	48	26.36	4.57	4.74
Steering	2	2	0.0545	-
	4	4	0.0783	-
	6	6	0.1128	-
	9	9	0.1944	-
	12	12	0.336	-

lane effects were then added to account for the load differences between lanes.

The load effect for each performance measure was obtained by regression of these adjusted lane means ($a_{O,\ L}$) against the load terms shown in Eq. 16. Steering axle effects were accounted for, as shown in Eqs. 2 and 10, in accordance with the load equivalency concept developed in this analysis. The load effect was found to be virtually the same for all performance measures. Accordingly, the data were pooled and reanalyzed to obtain a single value for the effect of load.

The thickness effects are given in Table 2 as "layer substitution" ratios, relative to asphalt concrete surface.

The load effect which we obtained, expressed in terms of equivalent 18-kip, single-axle applications, is

$$W_{18} = W_L \cdot 10^{0.0790(L - 18)} \qquad (43)$$

with $L = L_1$ for single-axle loads or $L_1/2 + 2.36$ for tandem-axle loads.

Load factors $\left(10^{0.0790(L - 18)}\right)$ for the various loads used at the Road Test are shown in Table 4. This table also contains values of average axle load factors which include the effect of the steering-axle load for each of the vehicles as used at the Road Test.

The single tandem-axle load relationship $L = L_1/2 + 2.36$ can be used to estimate the relative effect of tandem-axle loads. Consider a load, L, applied to a single axle with 2L applied to a tandem axle. Using the form of Eq. 21, we obtain

$$W_S = W_T \cdot 10^{0.079(L_T - L_S)} = W_T \cdot 10^{0.079(2.36)} = W_T \cdot 1.54 \qquad (44)$$

Thus, one application of a load 2L on a tandem axle is equivalent to only 1.54 applications of load L on a single axle. For example, consider a 36-kip total load. If this is split over two single axles (18 kips each), we have, of course, two 18-kip, single-axle loads. If we put the 36 kips all on a tandem-axle combination, we have only 1.54 equivalent 18-kip, single-axle loads. In terms of asphalt pavement deterioration, therefore, it is advantageous to put loads on tandem axles rather than half loads on single axles. This type of effect does not apply to portland cement concrete pavements. In fact, from the Road Test equations developed by the Highway Research Board, 36 kips on a tandem axle is roughly equivalent to 2.5 18-kip, single-axle loads (7). (The corresponding Road Test equations for asphalt pavements give a value of about 1.4 for the 18-kip equivalency of a 36-kip, tandem-axle load.)

A possible explanation of this observed tandem-axle effect on the asphalt pavements may be that the relatively wide spacing of the single axles permits two full deflections of the pavement, with virtually complete recovery between the axles, whereas there is not complete deflection recovery between the tandem axles.

TABLE 4

DESIGN EQUATIONS[a]

Performance Measure		Constant	log W_{18}	IWP	f(Performance)
PSIA	D_a =	3.764	2.910	-	-2.910 log log (P_o/P)
PSI	D_a =	3.623	3.565	-0.938	-3.565 log log (P_o/P)
SV	D_a =	7.412	3.477	-0.737	-3.477 log $(\sqrt{SV} - \sqrt{SV_o})$
RD	D_a =	1.617	4.208	-1.796	-8.416 log RD
RI	D_a =	9.782	2.416	-0.454	-2.416 log $(RI - RI_o)$
C+P	D =	9.403	2.931	-	-1.466 log (C + P)

[a]See Eq. 43.

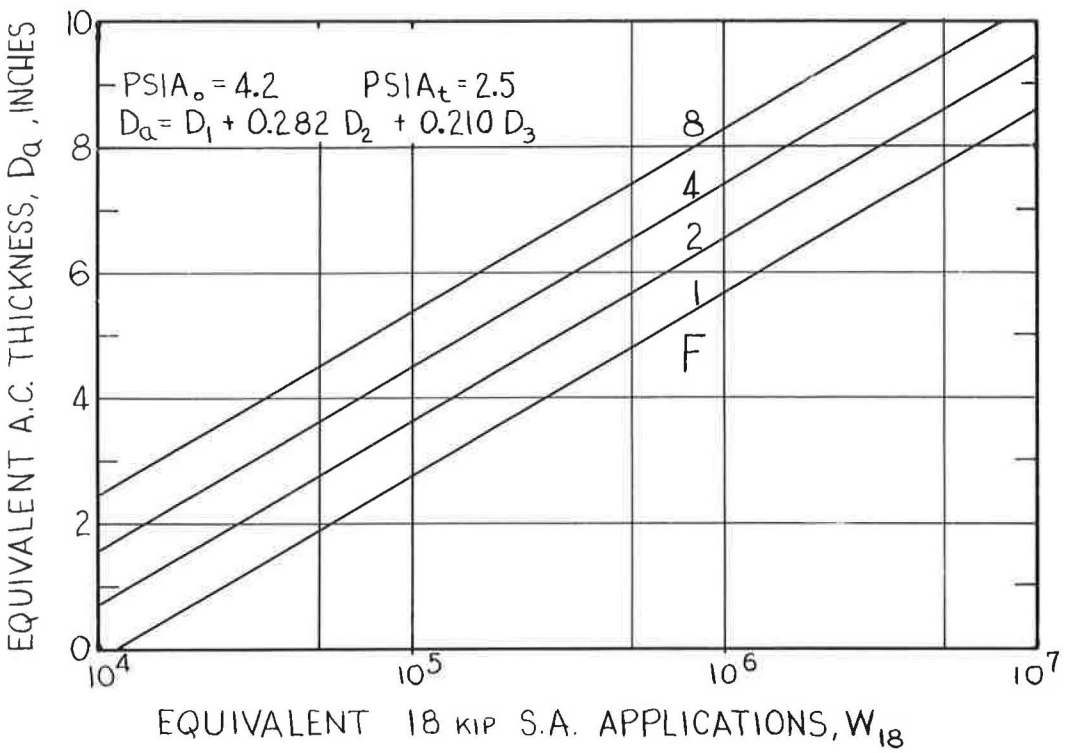

Figure 4. Design chart for average serviceability.

The final design equations for each measure of performance (according to the forms of Eqs. 23 and 28) are given in Table 4. These equations are plotted in Figures 4 through 9 for specified levels of performance. These charts are, in effect, design charts for soils of a strength of that of the AASHO embankment, with the actual level of the design thickness determined by the value of the climatic factor, F, and the total expected traffic, W_{18}.

Figures 4 and 5, for serviceability index, are based on an assumed terminal serviceability level of 2.5 and an initial value of 4.2 (Road Test asphalt pavement average). The choice of 2.5 for the terminal P_t value was somewhat arbitrary. It conforms, however, to the terminal value used by the Road Test staff in their reports.

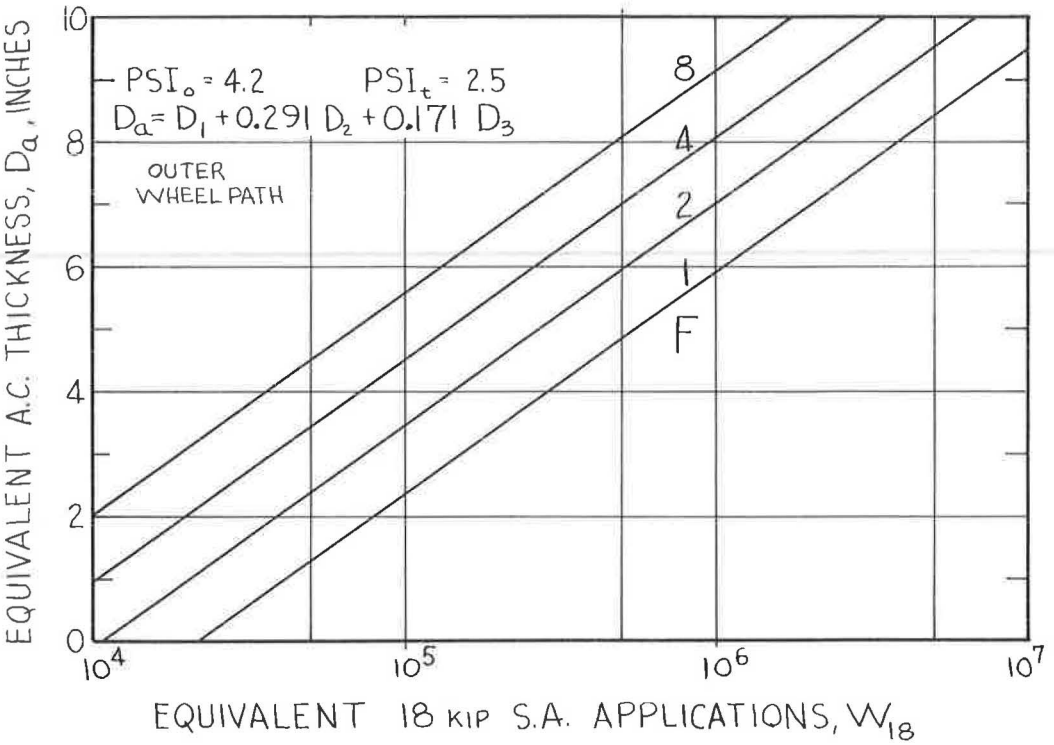

Figure 5. Design chart for outer wheelpath serviceability.

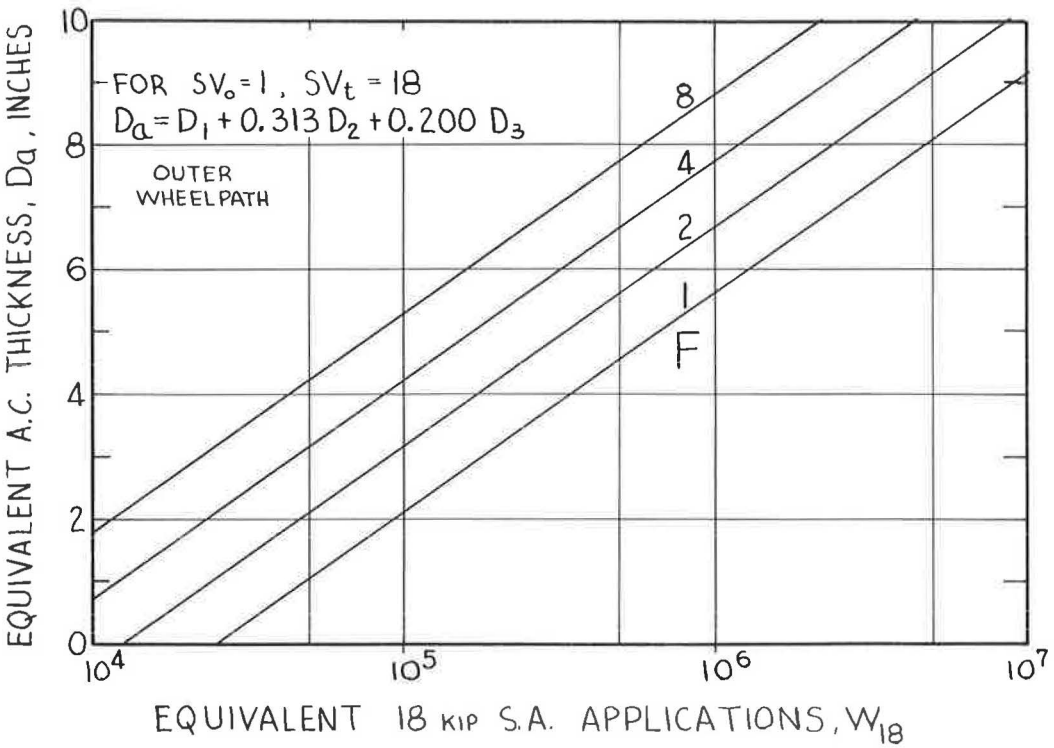

Figure 6. Design chart for slope variance.

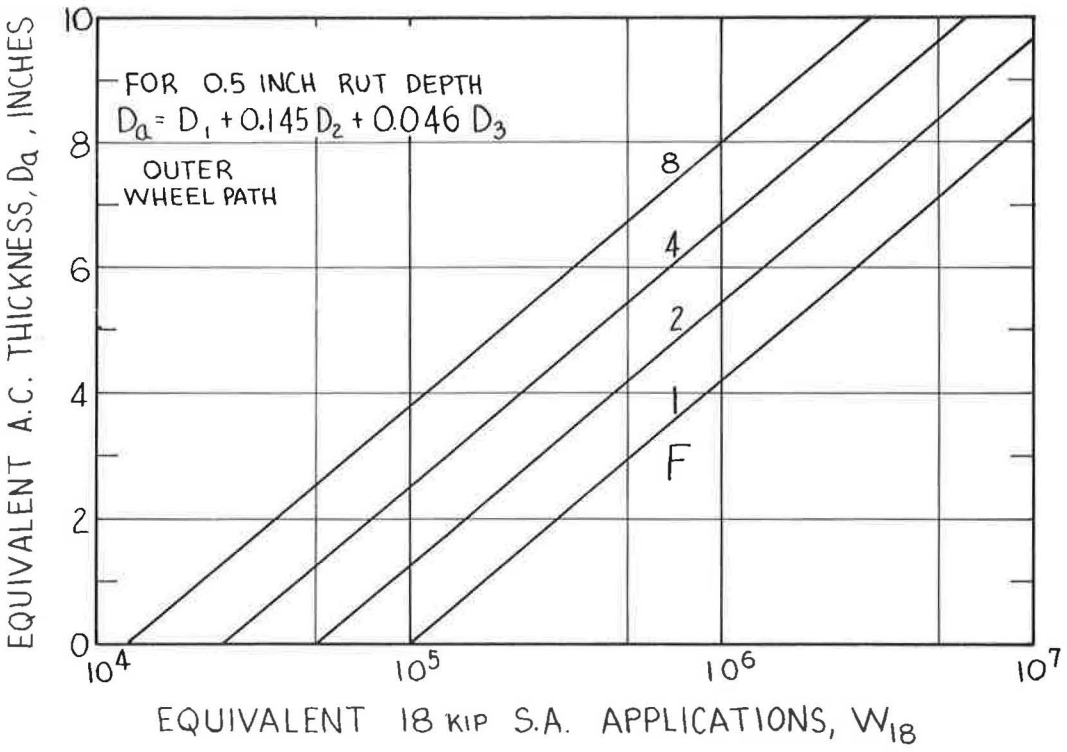

Figure 7. Design chart for rut depth.

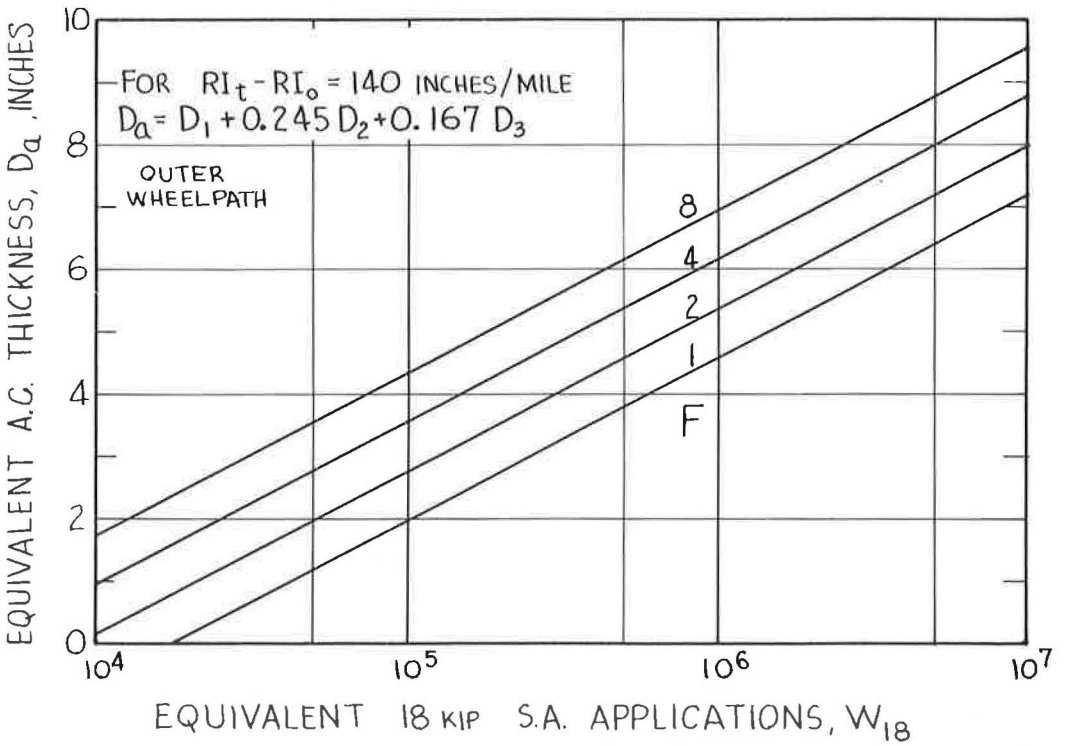

Figure 8. Design chart for roughness index.

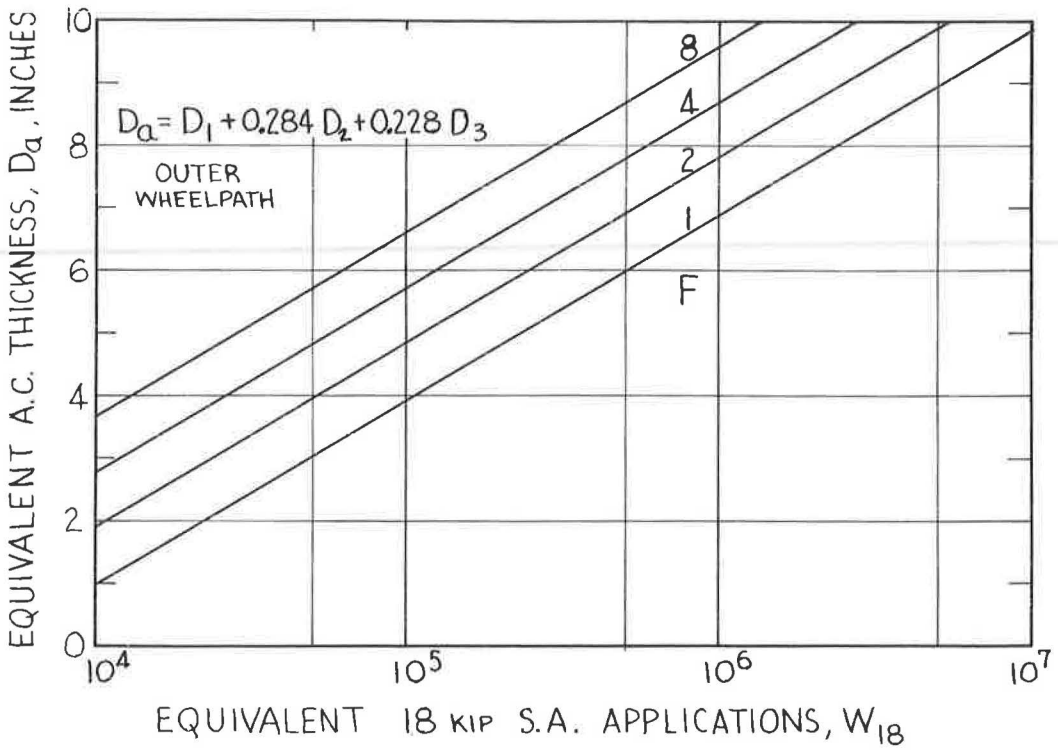

Figure 9. Design chart for 5 percent Class 2 + 3 cracking.

In the development of the serviceability index concept (8), it was found that, on the average, the rating panel members considered serviceabilities less than about 2.5 to be unacceptable for heavy-duty highways. Implicit in this finding is the possibility that lower terminal values may be acceptable on secondary roads. More research is needed along these lines to establish the relation between minimum acceptable serviceability and road type (usage patterns, etc.). Chastain and Burke (9) have shown that 2.5 is a fair average terminal value for main-line highways being "retired" by overlaying or reconstruction in Illinois.

For all other performance measures (Figs. 6 through 9) values were also chosen arbitrarily so as to give approximately 2.5 serviceability if all terminal values are reached. There is no support, similar to that referenced for serviceability index, for any of the individual values used.

It must be kept in mind that the D_a's obtained from the design equations (Table 4 or Figs. 4 through 9) are only equivalent to each other in terms of an all-asphalt pavement structure. For example, 10-in. D_a from the PSIA equation does not represent the same real structural section (with base and subbase courses) as does 10 in. of D_a from the rut depth equation. This is because the layer substitution ratios are, in general, different for all the different measures of performance. It is recommended that when the full set of equations is to be used, the total D_a be allocated among surface, base, and subbase by a linear programing study.

COMPARISON OF RESULTS WITH DATA

Predicted values of log W were compared with the observed values at a particular "terminal" level of performance for each performance measure. The standard errors in log W and the corresponding error in D_a are shown in Table 5, together with the terminal (and initial) values used for each performance measure. For all test sections,

TABLE 5

ERROR SUMMARY

Performance Measure	Initial	Terminal	Standard Errors	
			log W	D_a
PSIA	4.2	2.5	0.247	0.72
PSI	4.2	2.5	0.297	1.06
SV	1.0	18.0	0.335	1.17
RD	0	0.5	0.389	1.64
RI	70	210	0.364	0.88
C + P (owp), %	0	5	0.359	1.05

the observed log W was adjusted to account for the section's initial performance measure not having been exactly the value used in this comparison. (The initial values used here are approximately the average initial values for each measure at the Road Test.) The amount of adjustment in log W is determined by the models used to analyze the data, but is independent of the fitted parameters.

The errors given in Table 5 include only the data on sections which reached the "terminal" level of performance during the two years of traffic testing. The serviceability errors are less than the corresponding errors reported by the Road Test staff (7) or in the analysis by Shook and Finn (10). The Road Test report (7) shows a mean absolute error of 0.23 (standard error approximately 0.30) in log W, considering all levels of terminal serviceability. Shook and Finn (10) report a standard error of 0.35 in log W and 2.2 in their thickness factor, corresponding to about 0.9 in the D_a

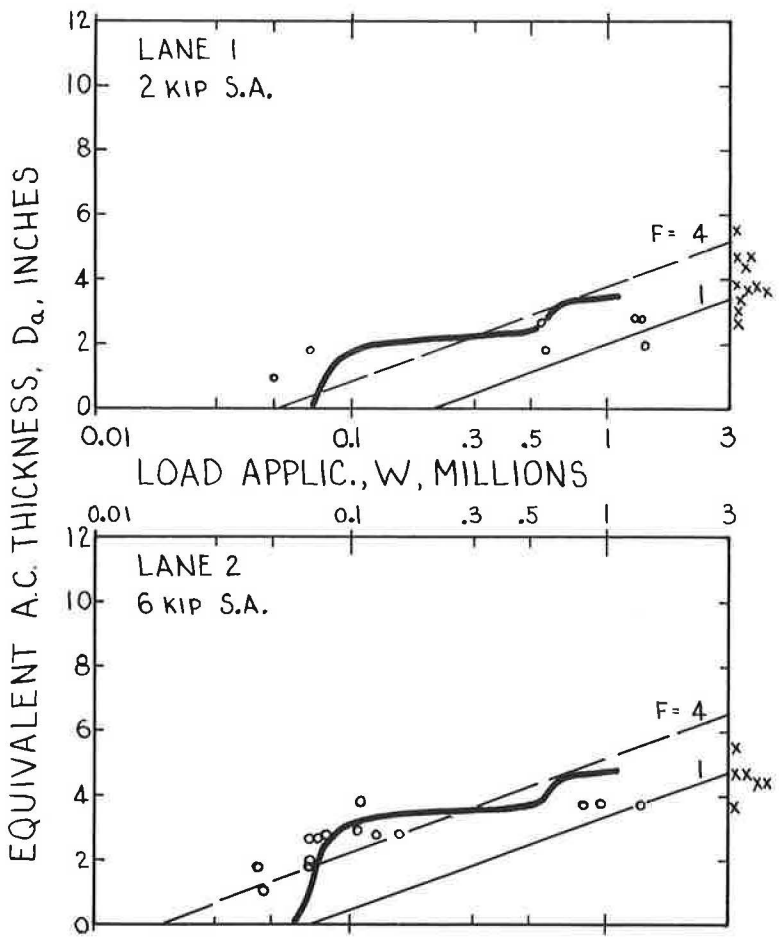

Figure 10. D_a vs actual application for PSIA = 2.5, Loop 2.

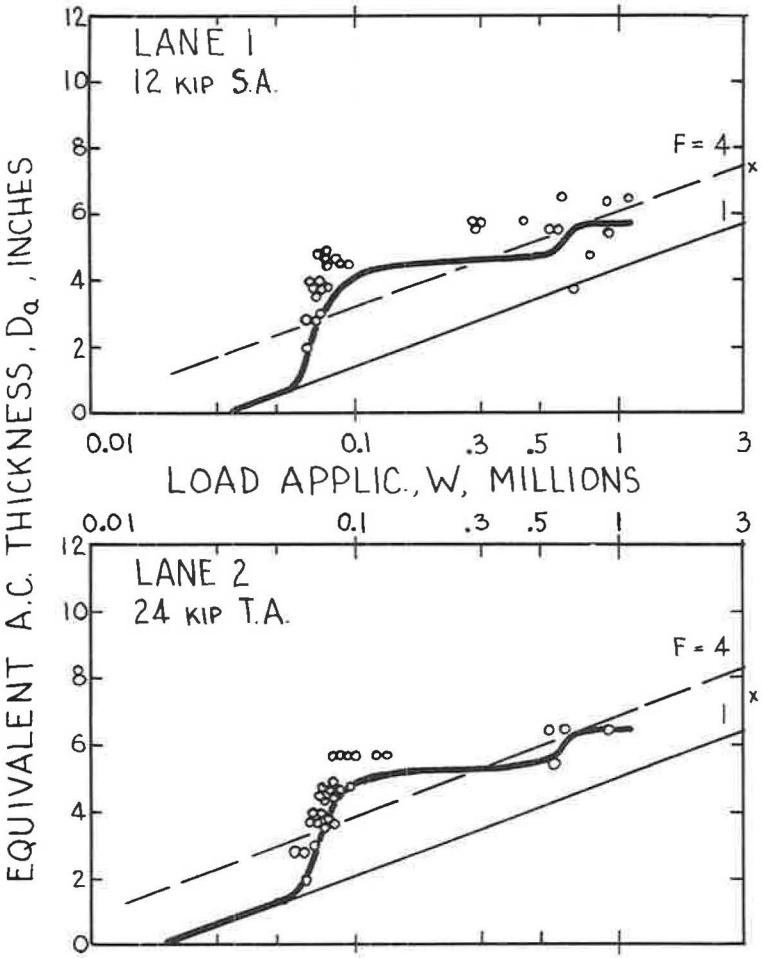

Figure 11. D_a vs actual application for PSIA = 2.5, Loop 3.

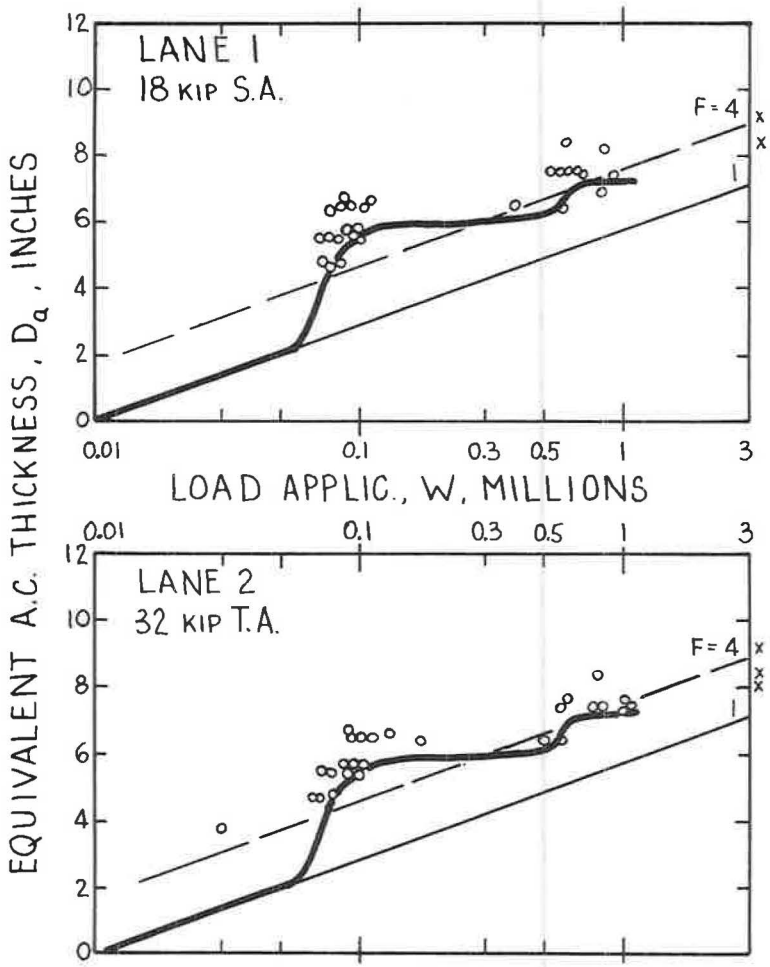

Figure 12. D_a vs actual application for PSIA = 2.5, Loop 4.

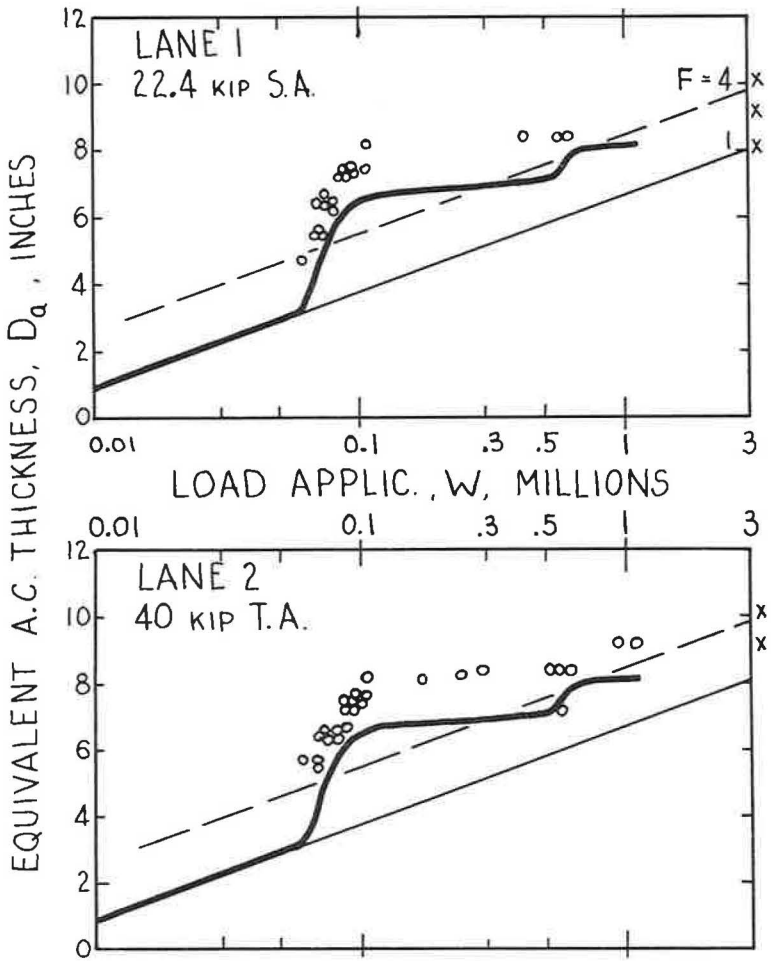

Figure 13. D_a vs actual application for PSIA = 2.5, Loop 5.

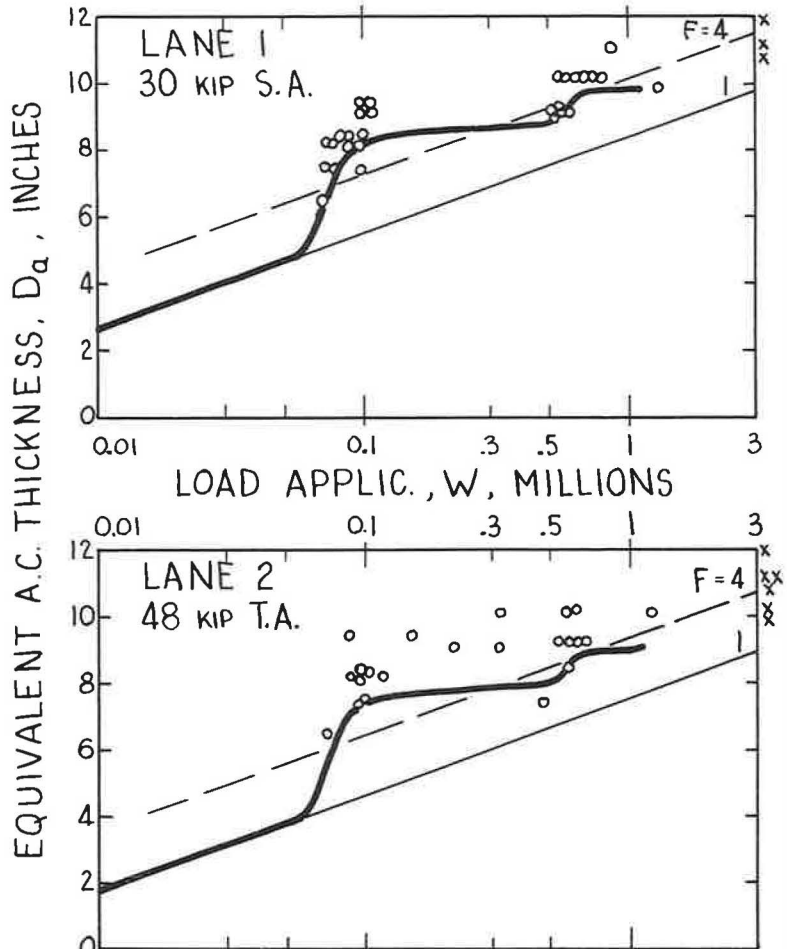

Figure 14. D_a vs actual application for PSIA = 2.5, Loop 6.

defined here. These other analyses of the Road Test data were restricted to average serviceability; hence, no comparisons can be made of the errors for the other performance measures.

Figures 10 through 14 show the PSIA data for each of the traffic lanes, plotted as adjusted actual applications to a terminal serviceability of 2.5, with the equivalent asphalt concrete thickness (D_a) as the ordinate. On each of these plots, straight lines are drawn for F values of 1 (W = weighted applications) and 4.0 (two-year average design value). In addition, a curved line is drawn which represents the conversion of the weighted applications vs D_a (F = 1) line to unweighted (actual) applications. In each graph, this curved line follows the data clusters very closely. We feel that this close fit of the curved lines to the data is a strong point in favor of the models used in this analysis, particularly for our method of weighting the applications.

As can be seen in Figures 10 through 14, quite a few points have large errors in log W because the section reached a 2.5 serviceability level just at the end of the first spring thaw, whereas the fitted actual applications (curved) line indicates the section should have "survived" until the following spring. In our model, a very small difference in pavement strength is decisive in determining whether such a section reaches 2.5 at the end of one spring thaw or the beginning of another. If we delete from the error analysis all points for which this behavior is apparent, we obtain a standard error in log W (for average serviceability) of about 0.12. This is probably a more realistic estimate of error for pavements built for a longer life than the two years of the Road Test.

All other performance measures show similar comparisons of the observed points and fitted lines.

MINIMUM COST DESIGN

The set of design equations which we have developed from the AASHO Road Test data is ideally suited for determining minimum cost structural designs. For a given amount of traffic (service life), each performance measure equation defines a required structural strength (which we call equivalent asphalt surface thickness, D_a; in the Road Test staff analysis, as utilized in the AASHO interim guide, it is called Structural Number) as a function of the amount of deterioration to be permitted at the end of the service life. The problem becomes one of choosing that combination of surface, base, and subbase thicknesses that will satisfy all the desired restraints (terminal values of performance measures) at minimum cost.

It should be apparent that merely specifying a required D_a to meet some performance criterion still permits an infinity of actual designs, i.e., values of D_1, D_2, and D_3, which will give the required D_a. One technique which can be used for selecting the minimum cost design from the large number of possible designs is linear programing. This is a mathematical method for "searching" through a system of linear equations having more than one feasible solution to find the one solution that minimizes (or, if desired, maximizes) an objective equation. Commonly, this objective is an economic one: costs are to be minimized or profits maximized. As a result, the objective has been traditionally called the cost function. This name fits our objective perfectly.

Linear programing is a mathematically rigorous tool for solving our type of problem. Use of this tool requires sound engineering practice to set up the problem, i.e., to decide on the proper restraints and obtain the pertinent economic data. To illustrate the use of this technique for optimum pavement design, we have solved five somewhat simplified problems, using our analysis of the Road Test data to define a design method. Common to all problems are the six performance measure design equations, as shown in Table 4 with D_a replaced by $D_1 + a_2D_2 + a_3D_3$. These are coupled with a cost function equation and ten restraint equations.

The cost function equation was, in all cases,

$$1.0\ D_1 + 0.38\ D_2 + 0.28\ D_3 = \text{Cost} \qquad (45)$$

The coefficients 1.0, 0.38, and 0.28 are costs of an inch of thickness of surface, base, and subbase, respectively, made relative to the per inch cost of a.c. surface. These

figures were obtained from the actual costs reported for a highway project in California's Mendocino County, as tabulated by the Pacific Coast Division of The Asphalt Institute. It is in these cost figures that the major simplification in our examples occurs. The costs are here assumed constant regardless of the layer thickness called for in solving the problem. This is equivalent to assuming that each layer can or will be put down in one lift. Obviously, the time cost per inch is determined both by the number of lifts required and the total thickness of each layer. This type of complication is still amenable to linear programing solution, but was not deemed necessary for these illustrative examples.

The ten restraints imposed on the system in each problem are shown in Table 6, together with the optimum designs which resulted. Certain auxiliary information obtained from the solutions is also included in Table 6; this consists of the range over which the cost figures could vary before the optimum solution would change, the minimum cost arrived at, and the terminal values estimated for all the performance measures for the optimum design. The costs are relative and so do not represent any total number of dollars. In the five problems, only certain of the restraints were changed. The restraints listed in Table 6 are grouped accordingly.

Case 1 may be considered the base case, as the other four problems each involved a change in just one of the four varied restraints away from Case 1. In all cases, the

TABLE 6

OPTIMUM (MINIMUM COST) DESIGNS

Performance Measures	Initial Values	Case 1 (Base)	Case 2	Case 3	Case 4	Case 5
			(a) Restraints			
Fixed						
$F \cdot W_{18}$	-	40×10^6	40×10^6	40×10^6	40×10^6	40×10^6
PSIA	4.2	≥ 2.5	≥ 2.5	≥ 2.5	≥ 2.5	≥ 2.5
PSI, owp	4.2	≤ 2.0	≤ 2.0	≤ 2.0	≤ 2.0	≤ 2.0
SV, owp	1.0	≥ 36.0	≥ 36.0	≥ 36.0	≥ 36.0	≥ 36.0
RI, owp, in./mi	50	≤ 200	≤ 200	≤ 200	≤ 200	≤ 200
D_1, in.	-	≥ 3	≥ 3	≥ 3	≥ 3	≥ 3
Varied						
RD, owp, in.	0	≤ 0.5	≤ 0.5	≤ 0.75	≤ 0.5	≤ 0.5
C+P, owp, %	0	≤ 20	≤ 100	≤ 20	≤ 20	≤ 20
D_2, in.	-	≥ 4	≥ 4	≥ 4	≥ 0	≥ 4
D_3, in.	-	≥ 6	≥ 6	≥ 6	≥ 6	≥ 0
			(b) Solution			
D_1, in.	-	10.0	10.0	8.9	10.6	10.3
D_2, in.	-	4.0	4.0	4.0	0	4.0
D_3, in.	-	6.0	6.0	6.0	6.0	0
Cost ranges D_1	-	0-2.379	0-2.379	0-1.186	0-2.379	0-2.379
D_2	-	0.18-0.38	0.18-0.38	0.33-0.38	0.18-0.38	0.18-0.38
D_3	-	0.05-0.28	0.05-0.28	0.18-0.28	0.05-0.28	0.05-0.28
Minimum relative cost	-	13.07	13.07	11.93	12.27	11.69
Limiting performance measure	-	RD, owp	RD, owp	PSI, owp	RD, owp	RD, owp
Terminal values of						
PSIA	-	3.81	3.81	3.30	3.61	3.40
PSI, owp	-	2.91	2.91	2.00	2.50	2.36
SV, owp	-	5.7	5.7	15.6	10.0	12.7
RD, owp, in.	-	0.50	0.50	0.68	0.50	0.50
RI, owp, in./mi.	-	55	55	64	57	60
C+P, owp, %	-	1.2	1.2	6.9	2.8	6.4

solution calls for the minimum thicknesses of base and subbase. This appears to be related to the fact that the relative cost coefficients of these materials are higher than their "layer substitution" coefficients in any of the performance design equations. If sufficiently different cost figures were used, this pattern would be expected to change. Case 2 gave a solution identical to Case 1 because it involved relaxing the percent cracking tolerated, which was not the variable restricting Case 1.

In Case 3 the rut depth tolerance which was binding on Case 1 was eased in an amount sufficient to make the outer wheelpath serviceability criterion control the optimum solution. This resulted only in decreasing the required surface thickness by 1.1 inches. In Cases 4 and 5, the minimum restrictions were removed on D_2 and D_3, respectively. The maximum ½-in. rut limitation again controlled the optimum designs, which are somewhat lower in relative cost than the base case.

The five cases shown here were calculated in less than one minute on a high speed computer, at a cost of about ten dollars.

These cases are intended merely to indicate what can be done with a set of consistent design equations reflecting different criteria of pavement performance to determine minimum cost designs. The engineer must decide on the design method (equations), the acceptable terminal levels of performance, and must, of course, obtain reliable cost information. This method of finding optimum design should be a great help to the highway engineer.

CONCLUSIONS

In the course of this analysis, deliberate efforts were made to detect and eliminate any biases that might be caused by: (a) changes in the traffic rate during the testing period, (b) differences in the severity of the two spring thaw periods, (c) differences in initial condition of the test sections, (d) times of traffic startup and stopping, and (e) the relatively short (two years plus) testing period.

The need for eliminating any such biases can be stated simply: highways are not designed to last for only two years, rather more like twenty. Unfortunately for the research engineer, projects such as the AASHO Road Test cannot be run for 15 to 20 years; therefore, we must make our way carefully through a very short "data time" in an attempt to discern the long-range trends of real interest. We feel this has been accomplished in our analysis.

Of particular importance is the ability to use this analysis to assist in the minimum cost allocation of structural strength between the several pavement layers. This analysis represents, perhaps, the first use of a consistent set of mathematical models for this purpose.

For full utilization of the results of the AASHO Road Test, whether in economic optimization of pavement design or in more routine structural design, it will be necessary to extend the Road Test findings beyond the engineering limitations of the Road Test. That is, further testing must be done under different climatic conditions, with soils of other strengths, and different methods of construction. The satellite tests being proposed by the various states should help greatly to provide the necessary data.

The equations presented in this paper are not being offered as final results for design purposes. Before this would be possible, it will be necessary to further verify the models used and even then to add on a safety factor to reduce the probability that a pavement will become unserviceable before its design lifespan. (As the equations now stand, there is a 50 percent chance that a pavement falls short of its design life.)

The Asphalt Institute offers these results as an alternative means of evaluating and describing asphalt pavement performance.

REFERENCES

1. Painter, L. J. An Alternate Analysis of the Present Serviceability Index. Proc. Int. Conf. on Structural Design of Asphalt Pavements, Univ. of Michigan, Ann Arbor, Aug. 1962.
2. The AASHO Road Test: Proceedings of a Conference Held May 16-18, 1962, St. Louis, Mo. Highway Research Board Spec. Rept. 73, 1962.

3. Painter, L. J. Analysis of AASHO Road Test Data by The Asphalt Institute. Proc. Int. Conf. on Structural Design of Asphalt Pavement, Univ. of Michigan, Ann Arbor, Aug. 1962.
4. Skok, E. L., Jr., and Finn, F. N. Theoretical Concepts Applied to Asphalt concrete Pavement Design. Proc. Int. Conf. on Structural Design of Asphalt Pavement, Univ. of Michigan, Ann Arbor, Aug. 1962.
5. Skok, E. L., Jr. Use of Elastic Theoretical Deflections for Performance Correlations. Proc. AAPT, Annual Meeting, San Francisco, Calif., Feb. 1963.
6. Housel, W. S. The Michigan Pavement Performance Study for Design Control and Serviceability Rating. Proc. Int. Conf. on Structural Design of Asphalt Pavements, Univ. of Michigan, Ann Arbor, Aug. 1962.
7. The AASHO Road Test: Pavement Research. Highway Research Board Spec. Rept. 61-E, 1962.
8. Carey, W. N., Jr., and Irick, P. E. The Pavement Serviceability-Performance Concept. Highway Research Board Bull. 250, 1960.
9. Chastain, W. E., Sr., and Burke, John E. Experience with a BPR-Type Roadometer in Illinois. Highway Research Board Bull. 328, pp. 52-58, 1962.
10. Shook, J. F., and Finn, F. N. Thickness Design Relationships for Asphalt Pavements. Proc. Int. Conf. on Structural Design of Asphalt Pavements, Univ. of Michigan, Ann Arbor, Aug. 1962.
11. Painter, L. J. Statistical Analysis of AASHO Road Test Asphalt Pavement Data. M. A. Thesis, Univ. of California, Berkeley.

Appendix A

DEVELOPMENT OF PERFORMANCE EQUATIONS

Average serviceability, P, is used here to illustrate the performance equation development. The development of all equations followed the same lines.

The entire analysis is predicated on the assumption that asphalt pavement performance for a particular pavement, p, can be expressed by an equation of the form:

$$\Delta_{t_2 - t_1} f(P)_p = \sum_{t = t_1}^{t_2} \Sigma_1 \zeta_{ltp} \tag{46}$$

This equation states that the change from time t_1 to t_2 in the value of a function of P can be expressed as the sum over that time interval of the effects ζ of all loads l, which effects are dependent also on the time of load application and the pavement considered. The time interval t_1 to t_2 can be considered without loss of generality to be an interval such as the Index Periods used at the Road Test. In this equation we assume that the effects ζ for different loads operate independently of each other.

The object of our analysis was to describe the ζ in terms of design p, time t, and load l. The time dependency of ζ as used here means the seasonal variation of ζ, not something related to the age or condition of the pavement. The parameters ζ_{ltp} are considered to be always positive in value, in the sense that they always contribute to deterioration of the pavement, whether that deterioration be of a form such as a decrease in serviceability index or an increase in slope variance. Actually, the condition $\zeta_{ltp} < 0$ is imposed.

To transform the Eq. 46 into a form consistent with the data from the Road Test, we will consider the change in F(P) from t = 0 to t = t, that is, from the startup of traffic until time t. We assume that the seasonal (t) variations of ζ can be described by the simple function

$$\zeta_{ltp} = \beta_{lp} \mu_t. \tag{47}$$

For the Road Test biweekly Index Periods with their traffic counts N_{lt} in each lane (load), we obtain

$$\sum_{t=t_1}^{t_2} \zeta_{ltp} = \beta_{lp} N_{lt} \bar{\mu}_t \tag{48}$$

in which $\bar{\mu}_t$ is some suitable average value of $\bar{\mu}_t$. It was found in the analysis that the load dependency of β_{lp} was describable by

$$\beta_{lp} = \beta_p e^{\alpha L} \tag{49}$$

Combining these results with Eq. 46 yields the equation

$$f(P)_{pt} - F(P)_{p0} = \beta_p \sum_1 e^{\alpha L} \sum_{t=0}^{t} N_{lt} \bar{\mu}_t \tag{50}$$

in which the summation over t on the right side leads directly to our definition of weighted applications W*. The expression $\sum_1 e^{\alpha L} \sum_t N_{lt} \bar{\mu}_t$ or its equivalent $e^{\alpha L} W_l^*$ immediately defines the equivalencies of different loads in terms of their effects on pavement condition. Two different axle loads, L_1 and L_2, will cause the same deterioration in a pavement if their counts (traffic rates) are related by $e^{\alpha L_1} W_1 = e^{\alpha L_2} W_2$, so that

$$\frac{W_2}{W_1} = e^{(L_2 - L_1)} \tag{51}$$

Choosing L_1 to be some reference load (18 kips), we can relate the effect of W_2 applications of any load to a "deterioration equivalent" number of reference load axle applications by Eq. 51.

Eq. 50 also defines the "mixed-traffic theory" of our analysis. The equation shows clearly the way in which the effects of different loads are to be combined, again through the expression $\sum_1 e^{\alpha L} W_{lt}$. By using 18 kips as a reference axle load we obtain the result

$$\text{total } W_{18} = \sum_1 e^{\alpha (L - 18)} W_l \tag{52}$$

This method of handling mixed-traffic effects is a direct consequence of our basic model (Eq. 46), especially of the assumption of independence of axle application effects. Support for this assumption is obtained from the Road Test data which showed almost independent action of tandem-axle wheels. Theoretical considerations lend support to the idea that heavy axles spaced 20 or more feet apart act independently.

Appendix B

SERVICEABILITY INDEX EQUATION

The development of the equation used to estimate serviceability index for this analysis is described fully in Ref. 1. The equation is

$$\ln \frac{P}{5} = -0.1615 \sqrt{SV} - 0.4967\ RD^2 - 0.00278 \sqrt{C+P} \tag{53}$$

A tabular solution of this equation is also given in Ref. 1.

Results of Oklahoma Flexible Paving Research Project

R. A. HELMER
Research Engineer, Oklahoma State Highway Department

From 1955 to 1962 the Oklahoma Highway Department carried out an extensive investigation of previously constructed pavements. Plate bearing tests and Benkelman beam tests were correlated and the safe load-supporting ability of the pavements was determined. The effects of soils, climate, traffic, and other factors on pavement depreciation and life were studied. A method to design the required thickness of flexible pavement was developed. A Soils Manual was published giving engineering and pedological soil information and the location of the principal soils in Oklahoma. Recently constructed projects giving unsatisfactory service were investigated and studies were made to determine the causes of poor pavement performance.

•THE ACCUMULATION of data for this research project started about twenty years ago when the Oklahoma Highway Department began to design the thickness of flexible pavement to fit the subgrade soils. The Materials Laboratory soon started taking thickness measurements of the base courses and making density tests of completed projects.

At this time a three-phase research program was contemplated: (a) the selection and use of a design method, (b) a period of accumulation of data from service and construction records, and (c) evaluation by the Oklahoma Flexible Paving Research Project of the quality and performance of the pavements and the method used to design them. The project, started in 1955, was conducted by the Oklahoma Highway Department in cooperation with the U. S. Bureau of Public Roads.

Much thought and time were given to planning this project. It was intended to include and evaluate all principal factors affecting paving performance. Because of the volume of data involved, all proposed items were listed and the value of each item was carefully considered. The purpose for which every factor was included was decided in advance. Insofar as possible, tentative procedures were written for assembling the data, analyzing it, and making all tests. There were approximately 40 items in the expanded list. They may be divided into five general classes:

1. Construction Data.—The ten items in this group include information from plans such as paving section, type of construction, quality tests, and information tests made during construction or for the preparation of plans.
2. Other Existing Data.—This group includes eight items including geology, weather, Bureau of Plant Industry and Soil Conservation data, traffic, and maintenance costs.
3. Field Data.—The eight items in this group include such data as a condition survey, geology surveys, and a field check of the original soil survey.
4. Field Tests to Be Made.—The ten items in this group include plate bearing tests, Benkelman beam deflection tests, moisture and density tests, and taking of samples for laboratory testing.
5. Laboratory Tests.—The four classes of items in this group are the usual laboratory tests on materials from surface, base, subbase, and subgrade.

Paper sponsored by Committee on Flexible Pavement Design and presented at the 43rd Annual Meeting.

The actual projects to be evaluated were selected from a list of all paving constructed since adopting a theoretical method of design. This list represented 2,388 mi of paving. For research purposes it was thought preferable to use the older projects when possible. All pavements were two-lane. In selecting the projects no consideration was given to their condition. Five principal types of flexible paving construction were used in Oklahoma and the mileage of the various types selected for research was chosen in proportion to the total mileage of each type constructed.

The soil problem areas of the Soil Conservation Service (SCS) are mapped on the basis of soils, geology, climate, and topography. Because these areas represent many of the factors influencing pavement performance, soil problem areas were used as a second consideration in selecting test projects. There are 16 soil problem areas mapped in Oklahoma. Some of these are subdivisions of primary areas and some are of small extent. It was found that six major areas represented about 80 percent of the area of the state. All projects selected were located in these six major areas. Not all types of paving were represented in each soil problem area, and this method of selection by types of construction and soil areas resulted in 18 groups. All projects in each group were similar in type of paving and were located in the same soil problem area. In selecting the projects to represent these various groups, 321 mi of paving or about a 13 percent sample were designated as test projects. To conform to the existing records, complete construction projects were selected. The list included 42 contract projects.

It was intended to determine the load-supporting value of a limited number of areas by plate bearing tests, then to correlate the load-supporting value of the pavement with Benkelman beam deflection tests, and to use this relationship to determine the load-supporting value of the pavement at all Benkelman beam test locations. A condition survey was made of the selected 321 mi during which 1,486 locations for periodic Benkelman beam deflection tests were painted on the pavement. Deflection tests were made at these locations every four months.

A group of plate bearing tests was made three times a year at 24 plate bearing test locations using 9-, 12-, and 18-in. plates on the surface, base, and subbase, and an 18-in. plate on the subgrade. In addition, one group of tests was to be made at three more locations. The areas for plate bearing tests were selected during the condition survey.

Three trucks were required for deflection testing: one to cover the deflection schedule and two to serve as a reaction load for the plate bearing tests. A 9,000-lb wheel load was established for the beam deflection tests. Tanks and water were used for loading because they could be easily unloaded for crossing substandard structures. To correlate the beam deflection tests with plate bearing tests, the two trucks used for plate bearing tests made beam deflection tests with 7,000-, 9,000- and 12,000-lb wheel loads at the plate bearing test locations.

Personnel required for the field testing was as follows:

1. For plate bearing tests, eight men, including two truck drivers and two flagmen;
2. For deflection tests, six men, including one truck driver, two flagmen, and three men to make tests and record data; and
3. For the office, two men to analyze field data.

The purpose of the research project was to evaluate the pavements that had been constructed and determine whether they were structurally adequate, and to determine whether changes in the design method would result in lowering the rate of depreciation. The total depreciation was considered to be the sum of maintenance costs and the depreciation in the condition of the pavement. To determine this factor, the average cost per mile for the contract construction of the pavement structure was obtained from the construction records and converted to 1950 cost values. A percentage factor representing repaired depreciation was obtained by dividing the average maintenance cost per mile per year by the average contract construction cost per mile in 1950 costs. Unrepaired depreciation was estimated by a condition survey, then expressed as a percentage of the total cost of the pavement structure.

Condition surveys require an estimation founded on the judgment of the individual. Therefore, the personal factor was a major consideration in the survey. For an ob-

server to pass over an extent of pavement and total up mentally and reduce to an exact figure a number of areas of several kinds of defects is an ability that will differ greatly among individuals. For long extents and many items, this ability probably varies greatly in the individual at different times. We found it advisable to divide a test project into a number of small parts, then to evaluate each part separately. The parts could be used to rate the test areas, and the final average condition rating of a project could be determined by averaging the results of all parts in that project.

Reference points were painted on the pavement surface at each 0.2 mi throughout the length of the test project and numbered in consecutive order. The exact station for each of these points was determined from construction plans and used as ties for the condition surveys, soil and geological surveys, Benkelman beam deflection sites, and plate bearing sites. Each extent was evaluated by estimating the percentage of a given defect as compared to the total area of the extent rated.

The terms and values used in making the condition surveys were as follows:

Few-slight	< 5%
Some	5 - 15%
Considerable	15 - 30%
Extensive	> 30%

The six classes used are excellent, superior, good, average, poor, and failure:

1. Excellent.—Percentage rating of 98 to 100 percent, with characteristics: (a) no major or minor defects are apparent; and (b) no maintenance has been performed.
2. Superior.—Percentage rating of 90 to 97 percent, with characteristics: (a) there are no base failures or other major defects; (b) no structural maintenance had yet been necessary, and any one or all of the following characteristics may be present within a 0.2-mi extent: slight surface roughness, slight cracking, and riding quality was impaired, but very slightly.
3. Good.—Percentage rating of 80 to 89 percent, with characteristics: (a) there are no base failures; (b) any one or all of the characteristics listed in this class or the following classes may be present within a 0.2-mi extent: some surface roughness, some cracking, slight raveling, and slight distortion.
4. Average.—Percentage rating of 65 to 79 percent, with characteristics of: few localized base failures; considerable surface roughness; considerable cracking; some raveling, especially in the outer wheel lanes and along the edges; and some distortion.
5. Poor.—Percentage rating of 50 to 64 percent, with characteristics: (a) considerable base failures; (b) extensive surface roughness; (c) extensive cracking; (d) extensive ravel throughout width of surface; and (e) considerable distortion.
6. Failure.—Percentage rating of less than 50 percent, with characteristics: (a) base failures are numerous and extensive; (b) distortion is extensive; (c) traffic hazards are extensive due to failures and distortion; and (d) routine and special maintenance repairs have not been effective.

If maintenance had been performed, the maintained area was rated in one of the preceding classifications as to its effectiveness and a notation was entered in the remarks column of the condition survey form regarding the type of that maintenance, along with any other pertinent comments concerning the general condition of the pavement structure. The final condition rating of each particular project was then obtained by averaging the ratings of each 0.2 mi and dividing by the age of the project to arrive at the average condition depeciation per mile per year.

The repaired depreciation factor taken from existing statistical data and the unrepaired depreciation factor determined by actual condition surveys were combined and together they represented the total depreciation per mile per year as a percent of the contract construction cost based on 1950 cost levels. This depreciation per mile per year of the pavement structure was the dependent variable which was to be evaluated by the research project.

This procedure for making condition surveys was found to give satisfactory results. Condition surveys were made in 1957, 1959, and 1960. It was found that in June 1955, when the average age of the projects was 4.402 yr, the condition depreciation was 1.43 percent and the average condition rating was 91.92 percent. Two years later, in June 1957, when the average age of the projects was 6.285 yr, the condition depreciation percentage was 2.05 percent and the average condition rating had become 87.12 percent. In June 1959, the average age was 8.154 yr, the condition depreciation was 2.00 percent and the average condition rating was 83.73 percent. The last survey, in June 1960, when the average age of the 42 projects was 9.154 yr, the condition depreciation was 2.47 percent and the average condition rating was 77.30 percent.

Because the original condition survey was made in 1955, maintenance consisting of single bituminous surface treatments with required base and surface patching has been placed on 19 of the 42 projects.

The results of the condition surveys indicated that the test pavements were depreciating at a more rapid rate than was anticipated and maintenance performed had not been adequate. A study of the other data indicated that the pavement structure was underdesigned for the poorest type soils. This discovery resulted in the development of an interim design method, adopted in 1958.

The final report of this project was published in two parts, Part One in 1958 and Part Two in 1962.

The subgrade soil on which a pavement is placed is a major factor in the cost of constructing and maintaining a pavement. To evaluate the subgrade throughout a project and to compare subgrades in different extents and different projects, it was necessary to develop a simplified method of rating soils.

In a previous study of the HRB soil classification and their relative California bearing ratio (CBR) values, a noticeable lack of correlation existed. In view of this, the department set out to determine some method of classifying soils so that a higher degree of correlation would occur between the classification and the CBR values.

At the suggestion of the late F. R. Olmstead of the U. S. Bureau of Public Roads, several methods were tried to extend the index numbers of the soils beyond the value of 20. This was accomplished by expanding the upper and lower limiting values of the liquid limit (LL) and the plasticity index (PI) without changing the percent passing the No. 200 screen. This can be justified by the fact that the limiting values of those properties were arbitrarily chosen in the beginning. The limiting values of the LL were changed from the previous 40 or less and 60 or more to 0 and 100 or more with index values increasing from a maximum of 12 to a maximum of 20. The limiting values of the PI were changed from the previous 10 or less and 30 or more to 0 and 50 or more with the index values increasing from a maximum of 8 to a maximum of 20.

In conjunction with these proposed changes, the values of 40 LL and 10 PI were chosen as points where changes in soil performances might occur. Therefore, the conditions were set out that a soil with a LL of 41 or greater could not have an index of less than 8, and a soil with a PI of 11 or more could not have an index of less than 4. (In Part One, the index numbers were called base index numbers, but the name was later changed to Oklahoma subgrade index number.) The soil classes and the limits set by these conditions for their corresponding index numbers are as follows: Class A-1-a, 0; A-1-b, 0-1; A-3, 0; A-2-4, 0-2; A-2-5, 8-10; A-2-6, 4-12; A-2-7, 12-20; A-4, 0-12; A-5, 8-24; A-6, 4-28; A-7-5, 12-40; and A-7-6, 12-40. The charts for determining the index numbers are shown in Figure 1.

To arrive at a method of determining required base thickness, the Oklahoma subgrade index number was converted to the required inches of base by use of CBR values. A study of the standard CBR curves used for design purposes in Oklahoma revealed that the curve was a log-log type curve for CBR values between 3 and 100. Using this information, a linear correlation was made between the index numbers and the CBR values of 472 random samples. The correlation was such that the CBR groupings were made on a linear scale and the index number groupings were made on a logarithmic scale. The mathematical coefficient of correlation was found to be a -0.573, which is a relatively high correlation when the factors used are considered. From this correlation, the relationship between the index number and the CBR values of the soils was

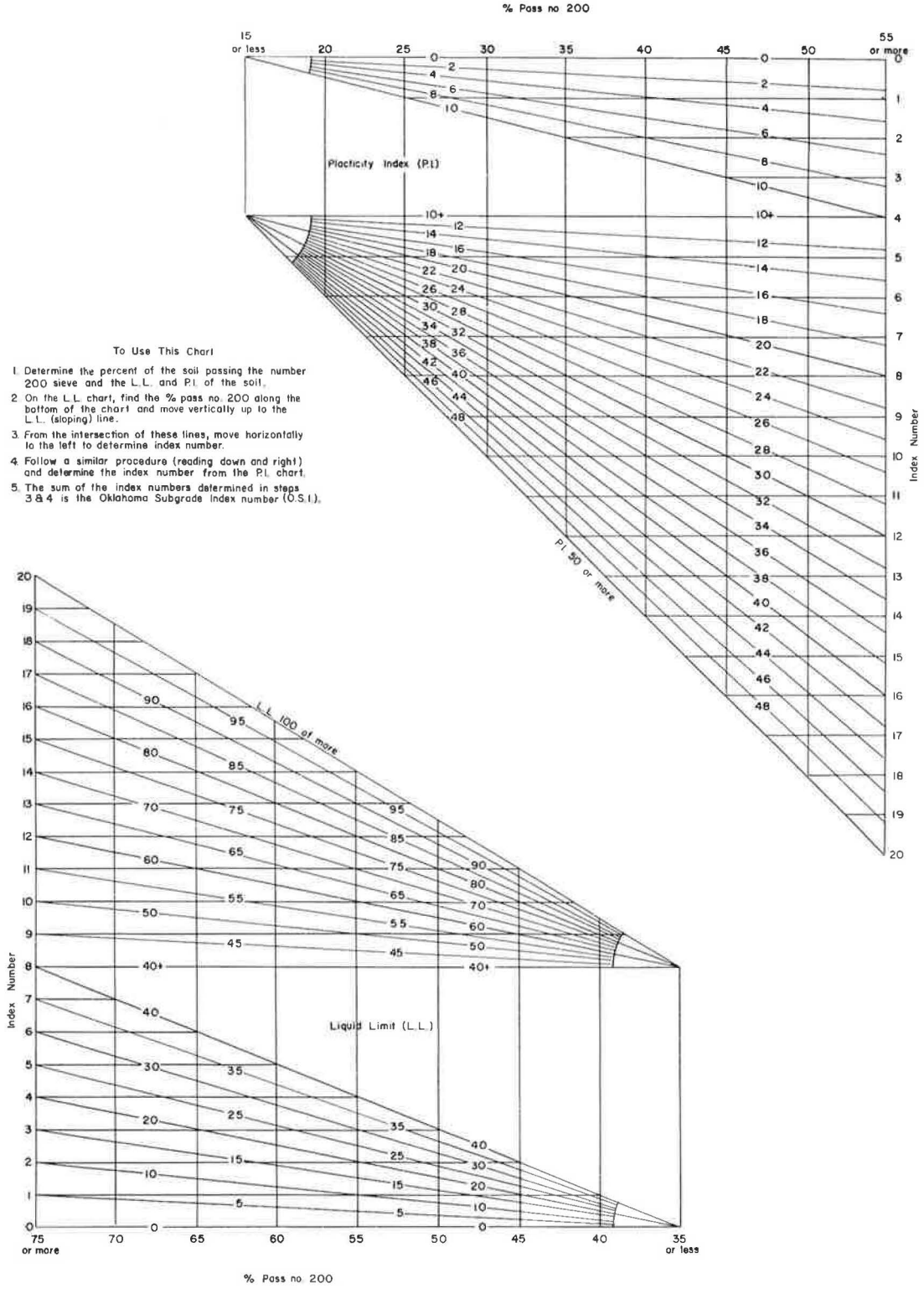

Figure 1. Oklahoma subgrade index numbers chart.

TABLE 1

Index No.	Base (in.)	Index No.	Base (in.)
0	6	21	17
1	6	22	17
2	7	23	19
3	8	24	20
4	8	25	21
5	9	26	22
6	9	27	23
7	10	28	24
8	10	29	25
9	11	30	27
10	11	31	28
11	12	32	30
12	12	33	32
13	13	34	34
14	13	35	36
15	14	36	38
16	14	37	41
17	15	38	44
18	15	39	47
19	16	40	50
20	16		

determined. The CBR values were then converted to inches of required base from the standard CBR curves. This resulted in a relationship between the required inches of base and the index number.

The subgrade index numbers and the required inches of base for a 9,000-lb wheel load are given in Table 1.

To apply these values to lighter or heavier wheel loads, a relation was found between other loads and the 9,000-lb wheel load CBR curve by using the California formula (1):

$$T = \frac{R}{S^n}\left(\frac{P}{S}\right) \qquad (1)$$

in which

- T = thickness of equivalent base (in.),
- R = radius of equivalent circle of contact area (in.),
- S = CBR of subgrade (% of standard),
- P = tire pressure (psi) (for this determination assumed to be 90 psi in all cases),
- n = variable decreasing from 0.43 to 0.20 as S increases from 3 to 60.

The following relations were found:

7,000 lb/9,000 lb = 0.88
12,000 lb/9,000 lb = 1.15
15,000 lb/9,000 lb = 1.29

These factors were applied to the required thickness values for a 9,000-lb wheel load will yield the thickness values for the appropriate wheel load.

Because the climatic, geological, and topographical environments greatly modify the performance of a subgrade soil, and these factors are grouped by the soil problem areas of the SCS, the projects are discussed by problem areas in Part One. The size of the five selected areas range from 4,614,000 to 10,743,000 acres which is from 10 to 24 percent of the area of the state.

In Part One of our final report the selected problem areas are described. As an example of the type of information contained in these descriptions, the following description of the Cherokee Prairies soil problem area is given.

CHEROKEE PRAIRIES SOIL PROBLEM AREA

The Cherokee Prairies have an area of about 5,000,000 acres. These soils occupy about 11 percent of the area of the state. This soil problem area is described as beginning in east central Oklahoma and extending north to the Kansas state line. The elevations range between 600 and 700 ft above sea level. The average annual rainfall is 40 to 43 in. The soils have been developed from the weathering of shale and sandstone under cover of tall grass. Low ridges of outcropping sandstone traverse the area, and here the soils are generally sandy and shallow. The topography varies from gently undulating to rolling. The predominant soils are as follows:

Deep, medium textured, very slowly to slowly permeable	40.5%
Deep, medium textured, permeable to freely permeable	15.8%
Shallow, medium textured, permeable to freely permeable	7.9%

Very shallow, fine textured	3.7%
Bottom lands	13.4%
Minor types and small areas	18.7%

Throughout our report we have used conversion factors to reduce pavements composed of several layers to an equivalent thickness of crushed stone base.

Pavements have been grouped into the following types of construction and the average cost per mile of surface and base (based on 1950 cost figures) are given:

D - Soil asphalt base, single bituminous surface	$18,178
B - Stabilized aggregate base, double bituminous surface	$23,997
A - Stabilized aggregate base, rock asphalt surface	$26,822
C - Stabilized aggregate base, asphaltic concrete surface	$33,015
E - Asphaltic concrete base, asphaltic concrete surface	$44,317

When the sample of roads is grouped by the soils and type of construction, there are 22 groups. Each group has the same type of construction and has soils in the same problem area. The costs per mile for the surface and base on these projects were taken from the final estimates. The projects were constructed in different years and the prevailing unit prices of construction might differ. However, the costs can be compared if they are reduced to a common price index. When the prices have been adjusted to a 1950 price, the cost for each group can be expressed as the weighted average cost per mile of paving.

These large groups can only be considered to be comparable in a general way. Some types of construction have high-type shoulders; others do not. The width of the paving in a group of projects might not be exactly the same. In general, the width of the paving is 24 ft, although six projects out of the 42 have a width of only 22 ft. These differences are particularly important when construction costs are considered. Also, a narrower road or a road without high-type shoulders would probably have a higher maintenance cost.

There is a great difference in the cost of the various types of construction. The types are not evenly distributed in the various soil areas. However, a difference in the average cost of pavement in the soil areas is indicated by the following figures:

Reddish Prairies	$27,392
Rolling Red Plains	$27,485
Cross Timbers	$28,208
Cherokee Prairies	$32,281
Ouachita Highlands	$40,194

The maximum difference in the cost of surface and base due to soils as indicated by the problem areas seems to be $12,802 per mile. This is about one-half of the maximum difference in cost due to type of construction.

In some areas of the state, paving materials must be transported from sources at some distance from the projects. In these areas, freight or transportation costs are a major item in the cost of paving, and freight might have a greater influence on paving cost than either the type of construction or the soils. The required thickness of base would probably be a better indication of the effect of soil areas on the cost of paving. The range in thickness and the average required thickness of base are given in Table 2. The average base thickness shown has been determined from the group index numbers of the subgrade soils as given by the soil survey made to design the paving. Therefore, the difference in thickness of paving which is shown indicates a difference in the soils. If these thicknesses indicate a difference in soils, then the Ouachita Highlands problem area defines soil conditions which require on an average of 3.46 in. of base more than the soils in the Rolling Red Plains.

To eliminate a possible variation in the width of paving or the difference in freight on the cost of paving in the different soil areas we can use the statewide average cost

TABLE 2

REQUIRED BASE THICKNESSES FOR PAVEMENTS IN SOIL PROBLEM AREAS

Area	Range (in.)	Average (in.)
Rolling Red Plains	10.36 - 16.26	12.58
Cross Timbers	11.01 - 14.55	13.07
Reddish Prairies	12.55 - 14.33	13.38
Cherokee Prairies	13.88 - 15.95	15.08
Ouachita Highlands	13.64 - 21.72	16.04

of paving per inch of thickness per mile per foot of width which is $93. For a paving 24 ft wide, the maximum difference in cost per mile because of the average soil conditions in the soil problem areas would be $93 × 3.46 in. × 24 ft = $7,722.72 per mile.

The rather large difference between this amount and the $12,802 found by the first method could be explained by the fact that the high- and low-cost types of paving are not equally distributed in all soil problem areas. A difference in transportation costs could probably be more nearly estimated by comparing the costs of the same type of paving in different soil problem areas.

There are many varieties of climate in Oklahoma. The southeastern corner of the state is in the Red River bottom which has a climate similar to that of the Mississippi River delta. The northwestern corner of the state is on the eastern flank of the Sierra Grande Los Animos arch which is a part of the Rocky Mountain uplift. It is about 700 mi from the southeastern corner to the northwestern corner. In this distance, most of the varieties of climate occurring between the Mississippi River and the Rocky Mountains can be found.

Oklahoma, situated in the southern part of the Great Plains, comprises an area of approximately 70,000 sq mi. The highest point in the state, about 4,500 ft above sea level, is the Black Mesa in the northwestern corner of Cimarron County. From this point the altitude decreases eastward and southward to a minimum level of somewhat less than 350 ft in the extreme southeastern corner of the state. There are elevated regions, ranging from 200 to 1,200 ft higher than the surrounding plains, in the Wichita, Kiamichi, Ouachita, and Arbuckle Mountains, and in the extension of the Ozarks. Considerable timber is found in the mountain districts, especially in the Ouachita Mountains.

There is wide variation in climate throughout Oklahoma. Average annual precipitation varies from more than 50 in. in the southeast to about 17 in. in the northwest. The mean annual temperature ranges from about 64 F in the southeast to about 54 F in the northwest. Summers are long with occasional periods of very high, dry day temperatures of 100 F or more.

TABLE 3

AVERAGE ANNUAL PRECIPITATION

Soil Problem Area	Weather Sta. Avg. (in.)	SCS Avg. (in.)	Diff.[a] (in.)
Rolling Red Plains	28	24	+4
Reddish Prairies	32	32	0
Cross Timbers	36	33	+3
Cherokee Prairies	42	41	+1
Ouachita Highlands	41	48	-7

[a]Above or below SCS average.

Climate is considered to be one of the major factors in the development and modification of soils. The freezing of the ground in winter mellows the soils, and the water which percolates through the soil carries the finer particles and materials in solution to the lower levels. Surface water from the rain transports and sorts the soils and by erosion exposes new material to be weathered. The soil problem areas are large areas of the state and, therefore, can only represent an average climatic condition.

The sample projects were selected without regard to the weather data and it is necessary to know how closely the average rainfall of the projects represents the rainfall of the problem areas as described by SCS. The frost penetration is not given in the SCS description. The average annual rainfall from the two sources is given in Table 3. The two sets of rainfall data indicate that the soil problem areas, in a general way, define areas of average annual rainfall. Unless otherwise mentioned, the climatic data used in this paper will be from the records of the weather stations.

In Table 4 the projects have been grouped by soil problem area and type of construction. The theoretical frost penetration has been calculated from the weather data and the average required base thickness has been calculated from the subgrade index. This table indicates that the average required base thickness is 14.5 in. for the projects with lower than average frost penetration and 12.7 in. for projects having frost penetration above the average. Because the base thickness is determined by the subgrade soil, it is indicated that the better soils are found in the areas of high frost penetration.

In Table 5, the same groups of projects have been listed by average annual rainfall and required base thickness. In this case, the trend is reversed and the poorer soils and thicker base are found in the high rainfall areas, with better soils and lighter bases in the low rainfall area.

These data indicate that the soils and required paving thickness vary inversely with the theoretical depth of frost penetration and directly with the average annual rainfall.

The five soil problem areas can be divided into 32 soil associations which are groups of associated soil series. The previously mentioned trends are similar when the soil associations are used.

Geologic materials are the parent materials of many soils. Because of the greater thickness of the strata, it is probable that there is more geologic material than soils material used in the construction of highways. Not only does the average geologic formation have a greater thickness, but the area occupied by a kind of geological material is much larger.

Many of the rocks in Oklahoma dip toward the west at about 40 ft to the mile. For this reason, there is a tendency for the surface geology and soils to be exposed in bands having a north and south trend. With a dip of 40 ft to the mile, a 20-ft thickness of rock would be exposed in a band about $\frac{1}{2}$ mi wide. In general, soil extents are longer on roads which run north and south than on east and west roads.

A geologic formation may be made up of several members composed of quite different materials, such as shale and sandstone. Each of these materials is the parent material for a different kind of soil, and the geologic members as well as the soils are a different kind of material for engineering purposes. A geologic name does not define a particular kind or type of material as closely as a soil series name. A geologic formation name can be thought of as defining a group of materials in the same way a soil association defines a group of soils; i.e., there are similarities such as climate and topography, although several kinds of rock may be found in an area where the surface geology is of a single geological formation.

When planning the research project, it was found by studying the soil problem areas that a limited number of areas represented a large part of the area of the state. A geologic survey of the 321 mi of highways indicated that there were about 42 geologic formations along these projects. Over 200 samples of the softer material of these formations were taken and tested in our soils laboratory. Because we surveyed a large sample of roads covering the entire state, most of these formations can be considered to be principal geologic formations in Oklahoma for highway building purposes. A soil survey of these roads was also made, and by combining these results with the geologic survey for any place along the road, we can determine the geologic problem area, geologic formation, soil problem area, soil association, and soil series

TABLE 4

PROJECTS GROUPED BY TYPE OF CONSTRUCTION AND SOIL PROBLEM AREA

PROBLEM AREA								TYPE CONSTRUCTION				
ROLLING RED PLAINS	REDDISH PRAIRIES	CROSS TIMBERS	CHEROKEE PRAIRIES	OUACHITA HIGHLANDS	INCHES FROST PENETRATION	GROUP	GROUP INDEX BASE THICKNESS	ROCK ASP. STAB. AG. BS. CS.	DBL. BIT. STAB. AG. BS. CS.	ASP. CONC. STAB. AG. BS. CS.	SING. BIT. ASP. STAB. BS. CS.	ASP. CONC. SURF. & BSE.
I	II	III	IV	V				A	B	C	D	E
				0	12.5	V-E	15.01					0
				0	14.3	V-C	21.72			0		
			0		14.4	IV-A	15.73	0				
	0				14.5	II-C	13.67			0		
		0			14.5	III-C	13.67			0		
				0	14.6	V-B	13.64		0			
0					15.1	I-A	10.72	0				
	0				15.3	II-A	14.33	0				
			0		15.3	IV-B	13.88		0			
			0		15.3	IV-E	15.95					0
				0	15.4	V-A	13.80	0				
			0		15.9	IV-C	14.76			0		
	0				16.3	II-E	13.04					0
		0			16.3	III-E	13.04					0
		0			16.6	III-A	14.55	0				
		0	AVG.		16.6 17.4	III-B	11.01		0			
0					18.9	I-E	10.36					0
0					19.8	I-B	13.30		0			
	0				19.9	II-D	13.33				0	
0					20.8	I-C	16.26			0		
	0				21.0	II-B	12.55		0			
0					21.4	I-D	12.17				0	
20	60	75	100	100	% BELOW AVERAGE		(16.6'')	100	40	80	0	80

AVG. 14.50''

AVG. 12.73''

TABLE 5

PROJECTS GROUPED BY TYPE OF CONSTRUCTION AND SOIL PROBLEM AREA

PROBLEM AREA								TYPE CONSTRUCTION				
ROLLING RED PLAINS	REDDISH PRAIRIES	CROSS TIMBERS	CHEROKEE PRAIRIES	OUACHITA HIGHLANDS	RAINFALL "	GROUP	GROUP BASE INDEX THICKNESS	ROCK ASP. STAB. AG. BS. CS.	DBL. BIT. STAB. AG. BS. CS.	ASP. CONC. STAB. AG. BS. CS.	SING. BIT. ASP. STAB. BSE.	ASP. CONC. SURF. & BSE.
I	II	III	IV	V				A	B	C	D	E
0					24.4	I-A	10.72	0				
0					25.1	I-D	12.27				0	
0					26.6	I-B	13.30		0			
	0				27.4	II-B	12.55		0			
	0				28.0	II-D	13.33 AVG. 12.90"				0	
0					31.4	I-E	10.36					0
0					31.5	I-C	16.26			0		
	0				33.2	II-C	13.67			0		
		0	AVG	35.3	33.2	III-C	13.67			0		
	0				35.4	II-A	14.33	0				
		0			36.4	III-A	14.55	0				
	0				36.9	II-E	13.04					0
		0			36.9	III-E	13.04					0
		0			38.0	III-B	11.01		0			
				0	39.7	V-A	13.80	0	0			
			0		40.4	IV-B	13.88 AVG. 14.65"		0			
				0	40.5	V-B	13.64		0			
				0	40.6	V-C	21.72			0		
			0		41.2	IV-C	14.76			0		
			0		42.3	IV-A	15.73	0				
			0		42.7	IV-E	15.95					0
				0	44.3	V-E	15.01					0
100	60	25	0	0	% BELOW AVERAGE	(35.3")		20	40	60	100	20

for that particular place. Then, from a geologic map, we can determine the geologic formation and soils, and the suitability of the geological and soils material for highway construction. At this time, it is sufficient to show that geologic information may be used as a starting point to arrive at and use the highway soil information. We now have under way a research project to develop an engineering classification of geologic materials.

We made a study of tire pressures and wheel loads to determine whether the 9,000-lb wheel loads used in our design were realistic. The tire contact area for known loads and tire pressures was also investigated. Our data consisted of 7,614 truck wheel loads and 12,896 tire-pressure readings. All vehicles except passenger cars were considered commercial. The study of 7,614 commercial wheel loads showed that 4.2 percent of the truck wheel loads are above the legal limit of 9,000 lb. The size of the tires found on these trucks was smaller than the tire manufacturer's recommendation for a 9,000-lb wheel load on all but 7.3 percent of the wheels. Almost one-third of the wheels on commercial vehicles had single tires. The tires on 21.46 percent of the wheels had pressures above 90 lb and 2.11 percent of the wheels were both overloaded and over-pressured.

It is indicated that the maximum tire contact pressure for a new tire is about 126 percent of the tire pressure. The maximum contact pressure is 132 percent of the average contact pressure for a new tire. For the same tire after 23,500 mi of service, the maximum contact pressure was reduced from 132 to 120 percent of the average contact pressure. The maximum contact pressure for the used tire was found to be 115 percent of the tire pressure.

Calculations indicated that for a 9,000-lb wheel load, a 5-psi increase in tire pressure might be equivalent to a 1,000-lb increase in wheel load if the tire contact area is considered in design. In evaluating the traffic information, it was noted that the higher density traffic is found where the soils are poor, and lighter traffic where soils are good. It is to be expected that with more traffic, higher wheel loads and higher tire pressures will occur more frequently. The four factors (soils, traffic volume, wheel load, and tire pressure) are all adverse conditions which, if considered in paving design, would result in an increase in the required thickness of pavement.

Money spent for highways is an investment in a public utility. It is not a permanent solution for the problem of furnishing highway service to the public. Furnishing continuous service to the public requires a continuous expense. We can judge the worth of an investment for this kind of service by considering the first cost, the upkeep, and how soon a replacement will become necessary.

Roads in time become obsolete. They are subject to damage by traffic, freezing and thawing, floods, and erosion. As with other kinds of property, a continuing depreciation starts as soon as a road is contructed and continues throughout its useful life. This depreciation is a loss of part of the highway investment and must be replaced if the service is to continue.

Money spent for maintenance of highways can be considered as a partial payment for depreciation. It does not necessarily follow that an expenditure for maintenance will repair all depreciation. In fact, it is more than likely that only the most obvious and severe depreciation has been repaired.

The spending of maintenance money is governed not only by highway depreciation but also by many other considerations, such as availability of funds, the importance of the highway, and whether the damage is likely to progress rapidly or slowly.

Figure 2 indicates that the maintenance cost increases as the rainfall increases. In Figure 3, the percent average depreciation for the soil problem areas has been plotted against the percent of permeable to freely permeable soils. It is indicated that the total depreciation increases as the percent of permeable to freely permeable soil decreases. When the percent depreciation used for Figure 3 is reduced to dollars and plotted against the average annual rainfall, the results are as shown in Figure 4.

The sample of highways for each problem area was selected before the pedological soil survey was made. Using the soil surveys, the samples were adjusted to the proper problem area by the logs showing the location of the soil series and the resulting changes reduced the mileage of roads in the Cross Timbers soil area to less than 10 mi. This is not considered to be a large enough sample to represent so large a problem area.

Problem Areas		Rain (in)	Maintenance Cost (dollars)	Theoretical Maintenance	Error
1	RR	28	$ 31.24	$ 50.45	$-19.30
2	RP	32	88.21	59.15	+29.06
3	CT	36	85.90	SEE NOTE*	
4	CP	42	92.50	80.89	+11.16
5	OH	41	57.30	78.71	-21.41

*Note-Cross Timbers omitted due to wide distribution and varied rainfall

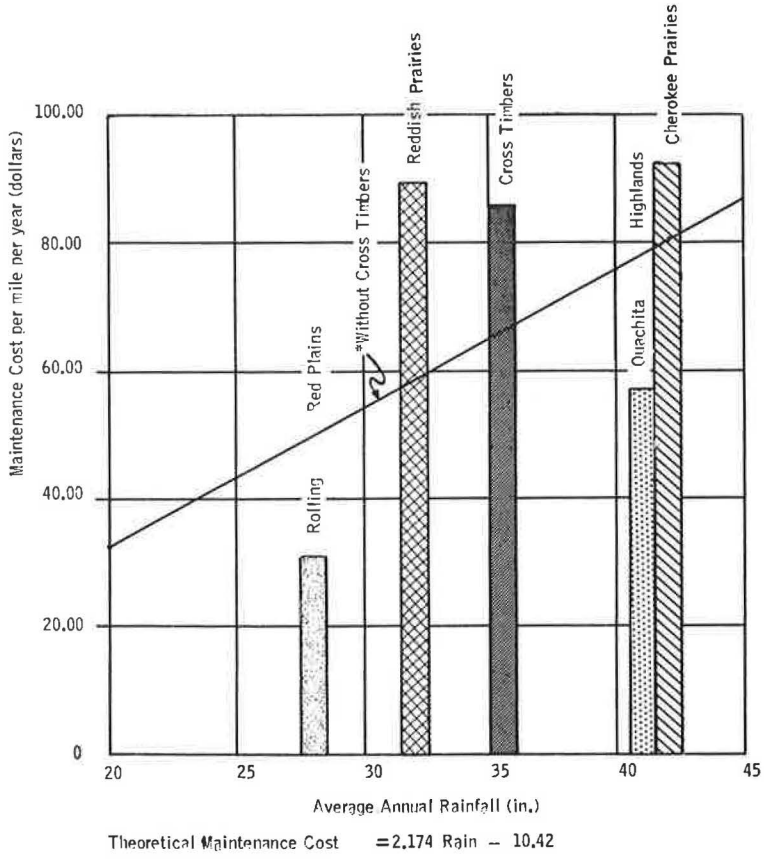

Figure 2. Maintenance cost vs rainfall.

	Problem Areas	% P to FP Soils	% Actual Depreciat.	Theoretical Depreciation	Error
1	Rolling Red Plains	30.1	2.280 %	2.699 %	−.419 %
2	Reddish Prairies	33.7	2.666	2.487	+.179
3	Cross Timbers	58.5	2.011	SEE NOTE *	
4	Cherokee Prairies	23.7	3.402	3.077	+.325
5	Ouachita Highlands	18.6	3.243	3.378	−.135

* Note - Cross Timbers omitted due to wide and varied distribution.

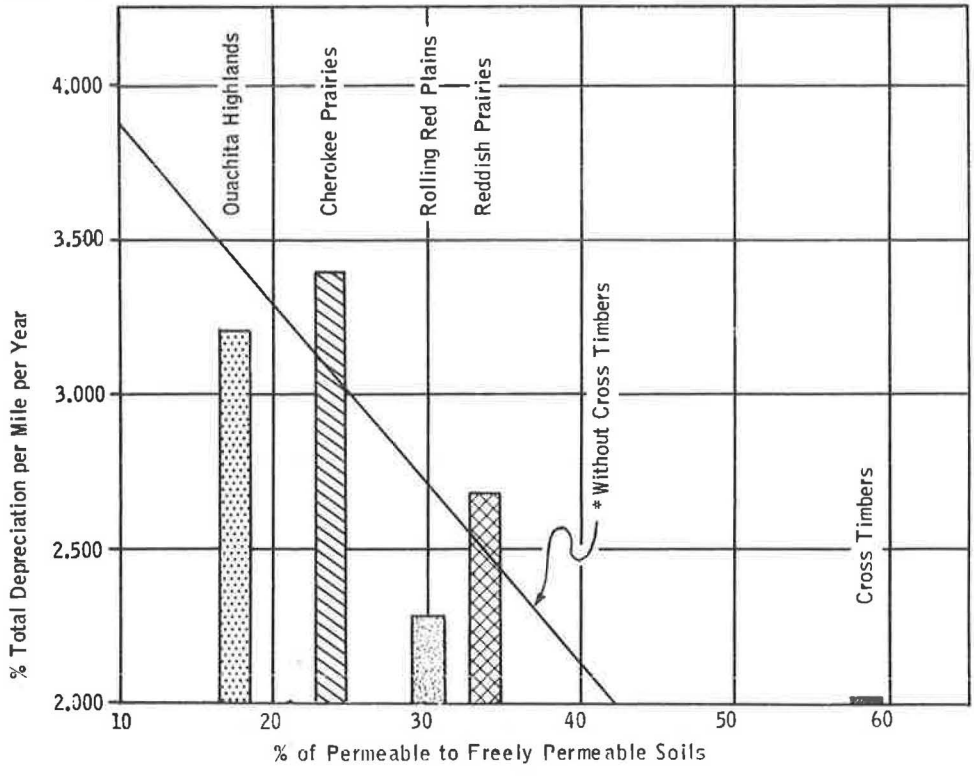

% Total Depreciation per Year = (−.059) P to FP Soils + 4.475

Figure 3. Total depreciation vs percent of permeable to freely permeable soils.

	Problem Areas	Average Annual Rainfall	Depreciation Per Year (Dol)	Theoretical Depreciation	Error
1	Rolling Red Plains	28	$ 582	$ 549	$ + 33
2	Reddish Prairies	32	628	678	− 50
3	Cross Timbers	36	613	SEE NOTE *	
4	Cherokee Prairies	42	908	956	− 48
5	Ouachita Highlands	41	1011	946	+ 65

* Note - Cross Timbers Omitted Due to Wide Distribution and Varied Rainfall

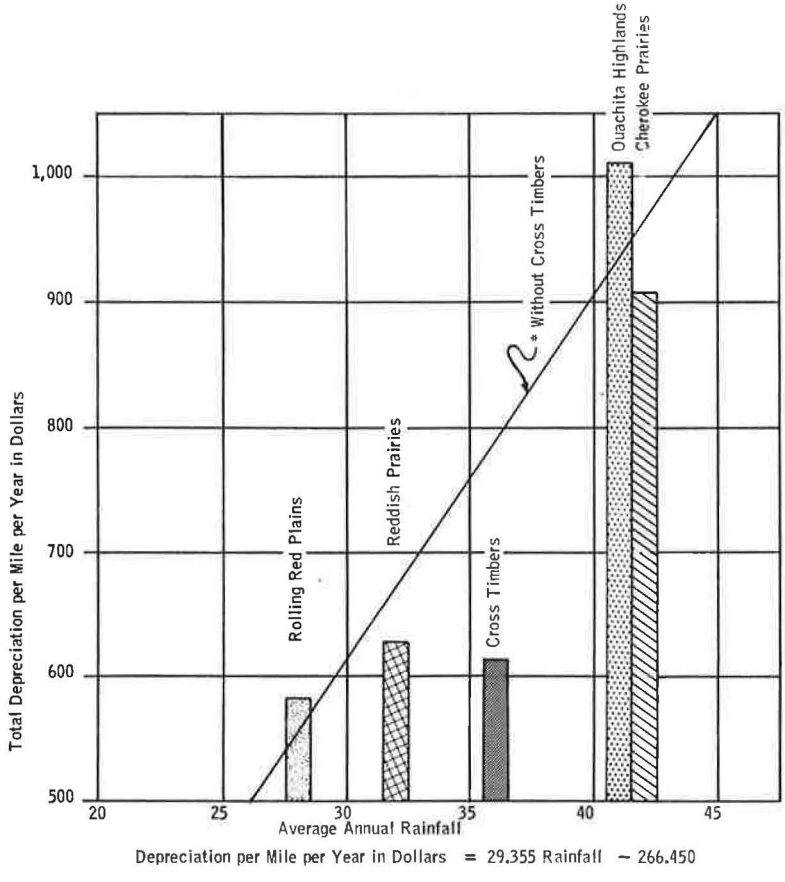

Figure 4. Total depreciation vs average annual rainfall.

TABLE 6

Type of Construction		Cost per Mile per Year[a] ($)					
Surface	Base	10 Yr	20 Yr	30 Yr	40 Yr	50 Yr	60 Yr
Single bitum.	Soil asph.	1,960	1,213	965	840	766	716
Dbl. bitum.	Stab. aggr.	2,487	1,512	1,187	1,024	927	862
Rock asph.	Stab. aggr.	3,700	2,397	1,963	1,745	1,615	1,528
Asph. conc.	Stab. aggr.	3,482	1,962	1,455	1,202	1,050	949
Asph. conc.	Asph. conc.	5,034	3,004	2,328	1,989	1,787	1,651

[a]At indicated life expectancies.

The small size of the sample and the scattered areas of Cross Timbers soils probably account for the fact that there is a lack of correlation for the Cross Timbers area in some of the comparisons.

The Rolling Red Plains soil problem area has an average annual rainfall of 24 in. It could be that for rainfall to become a predominant environment factor, a greater

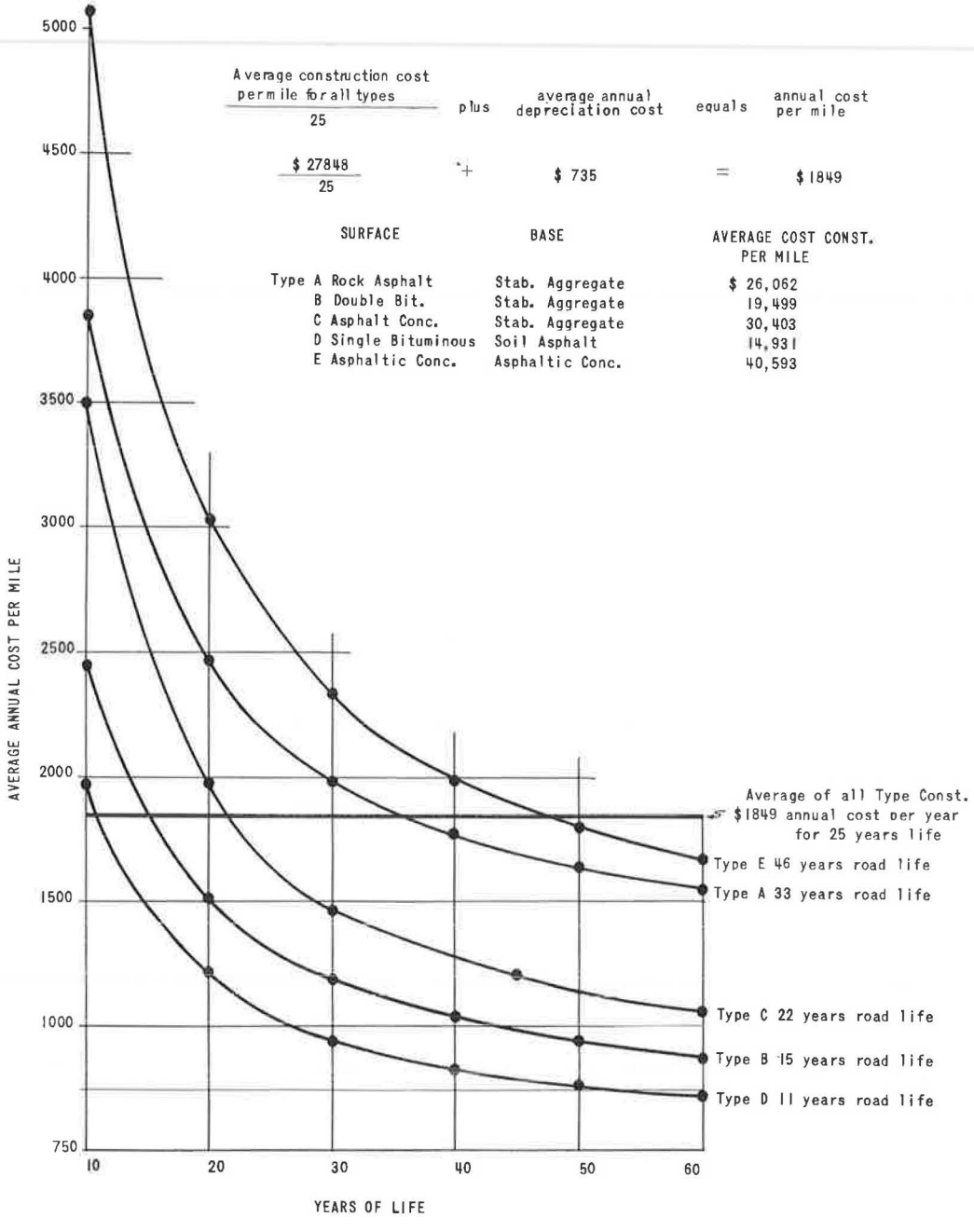

Figure 5. Road life necessary to produce per mile per year cost of average road based on 25 yr life, surface and base only.

amount would be required. About 55 percent of the sample in the Rolling Red Plains is soil asphalt construction which is the least costly type.

By estimating the probable life of the paving and assuming that the condition of the paving represents maintenance that must be done to attain that life, and that the annual maintenance cost would not change with age, the average cost per year of providing the public with a serviceable paving can be calculated:

$$\text{Average cost/mile/year} = \text{Annual depr.} + \frac{\text{Const. cost per mile}}{\text{Assumed years of life}} \qquad (2)$$

The costs per mile per year for different types of pavement and various life expectancies are given in Table 6. In these calculations it has been assumed that the rate of depreciation will not increase during the life of the projects, and therefore, the calculated costs are probably conservative. The data from the calculations have been used to plot the curves in Figure 5 which show the relationship between the costs per mile per year and the estimated life for five types of paving.

For an expected life of 25 yr, the average cost per mile per year is $1,849. All roads which can be paidfor and maintained at this annual cost are equivalent as an investment, disregarding interest.

From the consideration of cost, the curves in Figure 5 seem to indicate that for these roads, a road life longer than 30 yr would not greatly reduce the annual cost. The shape of these curves indicates that as the useful life increases, less and less reduction occurs in the annual cost of providing a serviceable paving. For lives greater than 40 yr, little could be gained by additional expenditure for the construction of a better paving; or if it is assumed that a life greater than 25 yr is unlikely, then a construction cost for surface and base greater than $30,000 per mile will result in a higher than average annual cost.

Strictly speaking, maintenance is not depreciation, although it has been considered as such. In cost accounting, it is sometimes considered an operation cost. In 1958, we found an average total depreciation for the entire research of about 2.4 percent of the construction cost per year. Of this depreciation, about 90 percent was indicated by the condition survey. Therefore, it is thought that the error, due to including maintenance as depreciation, is not great.

The annual rainfall in Oklahoma is an important factor in the cost of maintenance. It is indicated that maintenance costs increase with rainfall. Soil problem areas define areas of environment which are related to maintenance cost. When the maintenance and condition surveys are combined into total depreciation, there is evidence that in Oklahoma the total depreciation might be increased as much as $312 per mile per year by an increase in annual average rainfall of 14 in. The lower the average permeability of the soils in an area, the greater the depreciation.

The strong relationship of pedological soil areas to highway performance and design resulted in the collection of pedological and engineering soils information into a Soils Manual.

As a part of the research project, the SCS made a soil survey and listed the name, location, and extent of each soil series found along each paving project. Each soil series has the same general characteristics wherever found.

Many engineering soil tests of these soils were on file in the laboratory, and additional tests of these soils were made as a part of our research. Each horizon of each soil series and the parent material was tested. These tests were interpreted and given a rating, such as good, fair, or poor and low, medium, or high for various engineering uses.

The soils in the roadway embankment and subgrade are mixed. The structure of the natural soil has been destroyed, and in the cuts, the excavation has been frequently carried far below the soil mantle and into the underlying geology. At first thought, this would seem to destroy the value of the soil series description and the usefulness of the soil series name. However, the mixture of the soil horizons cannot be worse than the

most undersirable horizon of the original soil. Because the source of the parent material is a major factor in determining the kind of soil developed, the name of the soil series will indicate much about the materials that compose the subgrade even though it is comprised of mixtures of soil and geological material.

To identify these soils in the field, a policy has been adopted of dividing the soils of the state into groups of principal soils by location, for example, the soils found in each individual maintenance division. By considering each division separately, the number of principal soils to be recognized is reduced to approximately 30 in each division. With only 30 soils to classify, the problem of classification and identification in the field is greatly simplified. The problem can be simplied further by more closely limiting the location. In this system of classifying soils by location, SCS has divided the soils of the state into problem areas, which have then been divided into soil associations. Maps are available showing the location of the associations. The soil associations are composed of a few related soil series.

A total of 114 soil series was found on the research project. The test data for these soils are listed in the manual. Maps showing the location of the soil associations and the names of the principal soils in the associations are shown. Drawings or block diagrams showing the topographical location of the soil series are included.

The Soils Manual contains much engineering and pedological information about the principal soils found in Oklahoma. To apply this information to soils in the field it is necessary to identify the soil. Before a soil can be mapped, it must have been described. The identification of soils by written description is the usual method of classification. A "key" for mapping soils is a written description of the soils which gives all the characteristics of soils that can be recognized by examination of the soils in the field. The mapping of soils by the use of a key requires many years of experience and a comprehensive knowledge of soils, geology, and the physical and chemical laws of soil development. By using existing information about the location of soils and dealing with a part of the state at a time, the identification of soils can be simplified.

From the description of the problem areas, we could determine the problem area in which a soil was found. From the maps and descriptions of the associations in that problem area we could identify the association, and by using the block diagram for that association and the descriptions of the diagrams and soil series, an unknown soil could be identified by name. All the soils and highway information recorded under the soil series name would then be available for use.

The soil data in the manual include the Oklahoma subgrade index, so by making a pedological survey of the subgrade of a project we can use the recorded data to make a preliminary pavement design for a grading project. This has become our standard practice and we find that only a few tests are necessary to design the paving thickness sufficiently close for a grading project.

There are nine maintenance divisions in Oklahoma and the Soils Manual has been published in separate books for each division. Figure 6 is an example of a block diagram and Table 7 gives the soil series information which can be found in the manual.

The results of the material tests are discussed in Part Two of our final report. The testing program was not intended to evaluate the material specifications of the Highway Department or to investigate the quality of the construction testing. The purpose was to determine the quality of the materials in the pavement. By selecting projects constructed of satisfactory material, the variable of substandard material could be eliminated from the analysis of our plate bearing test data for load-carrying capacity. These selected projects could also be used to develop a thickness design procedure for flexible pavement based on load-carrying capacity and pavement performance.

The tests considered were of two principal kinds: old tests made before and during construction of the pavement, and new tests made during the research program. There are two general classes of research tests which are grouped as field tests and laboratory tests in the testing schedule given in Table 8.

A study of these tests revealed many results that were slightly out of the specifications. There were also some cases so far out that they might seriously affect the quality of the material. The rock asphalt and the hot mix asphaltic concrete surfacing materials were considered to be satisfactory. The asphaltic concrete and soil asphalt

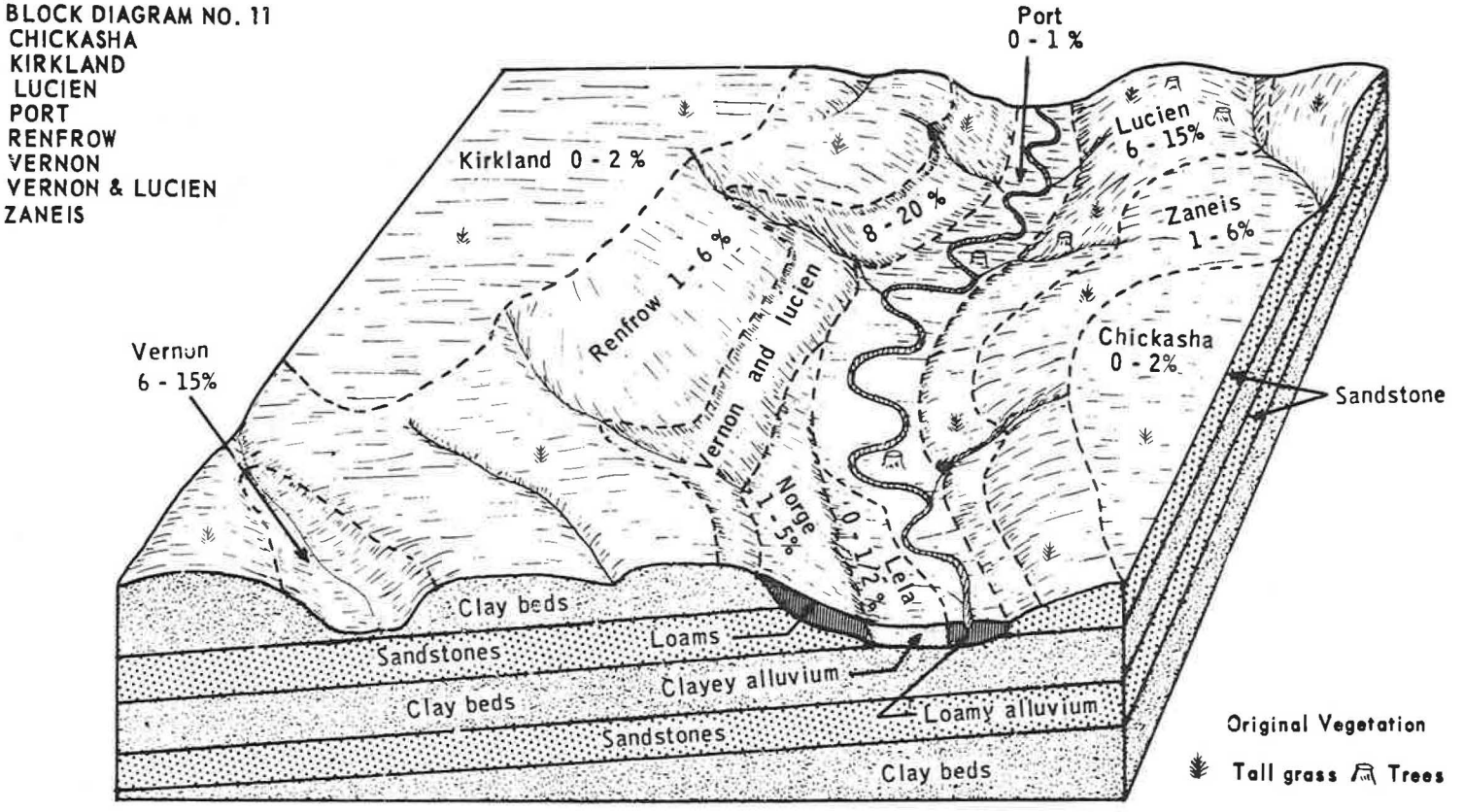

Soils of the Reddish Prairie Area of central Oklahoma on red clays and sandstones of the permian. Principally on Wellington Garber, Hennessey, Flowerpot, Dog Creek and Wichita Formations which dip underground successively toward the West.

Figure 6.

TABLE 7

HIGHWAY ENGINEERING CHARACTERISTICS OF SOIL SERIES

SOIL SERIES and underlying GEOLOGIC DEPOSITS	SOIL ASSOCIATION NUMBERS	SOIL ASSOCIATIONS MAPPED IN DIVISION NO. ___	RATING NUMBER	BASE REQ'D FOR 9000# WHEEL LOAD (By Okla Base Index No)	TEXTURE	PERMEABILITY	COLORS	HIGHWAY RESEARCH BOARD SOIL CLASSIFICATION	LIQUID LIMIT	PLASTIC INDEX	% PASSING No 200 SIEVE	CALIF BEARING RATIO	% ASPHALT FOR STABILIZATION (No = Not Suitable)	% PORTLAND CEMENT FOR STABILIZATION (No = Not Suitable)	SUITABILITY: GOOD SUITABILITY FAIR for SUBGRADE POOR	SUITABILITY: HIGH VOLUMETRIC SHRINKAGE MED LOW	SUITABILITY: SOIL BINDER YES NO	SUITABILITY: SOIL STABILIZATION YES NO	SUITABILITY: GOOD SHOULDER FAIR CONSTRUCTION POOR	SUITABILITY: GOOD EROSION FAIR CONTROL POOR	SUITABILITY: GOOD SEEDING FAIR POOR	SUITABILITY: GOOD SODDING FAIR POOR
EUFAULA "A" 0-30" "C" 30-50" "D" 50"+ Terrace deposits Darby sand Paluxy sand	27	1,2,3,4,7,8	13	6" 6" 6"	C C C	R R R	B B B	A-2-3(0) A-2(0) A-2(0)	NP 25 18	NP 4 1	18 24 21	7 10 9	4.5 4.5 4.5		X X X		X X X	X X X	X X	 X 	 X	 X X	X X	 X X
FORD "A" 0-8" "B" 8-38" "C" 38-78" "D" 78"+ Wichita formation Hennessey shale Dog Creek shale Flowerpot shale	35	5,7	4	10" 14" 14" 12" 16" 14"	MF MF MF 	VS VS VS 	B B TR 	A-4(8) A-6(11) A-6(12) A-6(9) A-7-6(15) A-7-6(11)	26 40 40 33 41 42	7 19 21 13 28 18	68 88 74 96 96 94	6 4 4 5 7 5	No No No No No No		X X X X X X	 	X X X X X X	X X X X X X	X 	 X X X 	 X 	X X X X	 X
GRANT "A" 0-20" "B" 20-48" "C" 48-72" "D" 72"+ Cedar Hills sandstone Hennessey shale Flowerpot shale	31	4,6	9	9" 6" 10" 13" 12"	MF MF MF 	MR MR MR 	B RB,TR TR 	A-4(1) A-4(2) A-4(8) A-6(10) A-4(8)	23 23 29 36 37	3 1 5 14 10	41 45 85 76 92	28 16 12 9 11	5.5 5.5 No No No		X X X X X	 	X X X X X	X X X X X	X 	 X X 	 X 	X X X X X	 X
HECTOR "A" 0-14" "C" 14-28" "D" 28"+ Atoka formation Jackfork sandstone Boggy formation Bluejacket sandstone Savanna formation McAlester formation	11,12	1,2,3,8	11	9" 11" 6" 6"	MC MC 	MR MR 	B B 	A-4(7) A-4(8) A-2(0) A-2-3(0)	22 30 25 NP	1 8 2 NP	70 75 31 12	10 13 17 12	No No 5.0 4.0		X X X X	 	X X X X	X X X X	X 	 X X X	 	X X X X	
KIRKLAND "A" 0-14" "B" 14-38" "C$_{ca}$" 38-70" "C" 70-100" "D" 100"+ Hennessey shale Garber sandstone Wichita formation Wellington formation Flowerpot shale Upper Pontotoc grp	28,29	3,4,5,6,7,8	4	10" 19" 15" 15" 16" 13" 12" 17"	M F F 	VS VS VS 	B B RB 	A-4(8) A-7-6(19) A-7-6(15) A-7-6(13) A-7-6(16) A-6(6) A-6(9) A-7-6(18)	28 53 49 51 47 38 33 50	6 30 23 21 26 13 13 28	94 95 98 70 95 61 96 93	4 9 4 6 7 10 5 4	No No No No No No No No		X X X X X X X X	 	X X X X X X X X	X X X X X X X X	X 	 X X X 	 	X X X X 	 X X X
KIRVIN "A" 0-12" "B" 12-38" "C" 38-60" "D" 60"+ Paluxy sand	13,14	2	4	6" 12" 10"	MC MC MF	M M M	GR B TR	A-2(0) A-6(6) A-4(4)	19 36 29	2 15 9	31 57 58	10 9 16	4.5 7.0 7.0		X X X	 	X X X	X X X	X 	 X X	 	X X X	
LAHETTE "A" 0-10" "B" 10-48" "D" 48"+ Pt. Scott limestone Dologah limestone Pikila limestone Fayetteville shale Hindsville limestone	20	1,8	4	13" 17"	M F	M M	R RB	A-7-6(9) A-7-5(17)	41 56	14 24	93 84	4 -	No No		X X	 	X X	X X	X 	 	 	X X	X
LELA "A" 0-4" "AC" 4-75" "C" 75-90"+ Alluvium	T	All	3	14" 16"	F F F 	VS VS VS 	G RB RB 	A-7-6(13) A-7-6(15)	42 50	20 23	90 90	5 5	No No		X X	 	X X	X X	X X	X 	 	X X	
LIGHTNING "A" 0-10" "AC" 10-28" "C" 28-40"+ Alluvium	3	1,2,3,4,8	2	12" 11" 16" 16"	MF F F 	VS VS VS 	G RB G 	A-4(8) A-4(8) A-7-6(14) A-7-6(15)	35 33 47 50	9 9 23 23	94 86 94 90	9 11 4 5	No No No No		X X X X	 	X X X X	X X X X	 	X X X X	 	X X X X	X X X X
LINCOLN "A" 0-15" "C" 15-50"+ Alluvium	6	All	15	9" 6" 6"	C C 	R R 	B YB 	A-4(5) A-2-3(0) A-2(0)	24 NP 19	4 NP 2	61 17 21	4 13 16	No 4.0 4.0		X X X	 	X X X	X X X	 	X X X	 	X X X	
LIMEX "A" 0-8" "B" 8-40" "C" 40-50" "D" 50"+ Atoka formation Kralestar formation Savanna formation Stanley shale	12	1,2	6	6"	MC MF MC MC	MR MR MR MR	G B B B	A-2-3(0)	NP	NP	21	13	4.5		X	 	X	X	 	X	 	X	
LUCIEN "A" 0-15" "C" 15-30" "D" 30"+ Wellington fm Wichita formation El Reno group Garber sandstone Marlow formation Flowerpot shale	30	2,3,4,7	9	8" 6" 12" 12" 11" 9" 12"	M M 	M M 	RB RB 	A-4(3) A-4(2) A-6(9) A-6(9) A-6(6) A-4(8) A-4(8)	26 22 31 33 38 24 37	3 2 11 13 13 3 10	50 46 98 96 61 94 92	9 17 4 5 10 5 11	6.0 6.0 No No No No No		X X X X X X X	 	X X X X X X X	X X X X X X X	 	X X X X X X X	 	X X X X X X X	

LEGEND

Geologic Abbreviations
fm - formation
fms - formations
grp - group
ss - sandstone

Texture
F - Fine
MF - Moderately fine
M - Medium
MC - Moderately coarse
C - Coarse

Permeability
VS - Very slow
S - Slow
M - Moderate
MR - Moderately rapid
R - Rapid

Colors
B = Brown
G = Gray
O = Olive
P = Pink
R = Red
W = White
Y = Yellow

TABLE 8

SCHEDULE OF LABORATORY AND FIELD RESEARCH TESTS

FIELD TESTS	SURFACE: ASPHALTIC CONCRETE	SURFACE: ROCK ASPHALT	SURFACE: DOUBLE BITUMINOUS	SURFACE: SINGLE BITUMINOUS	BASE: SOIL ASPHALT	BASE: STABILIZED AGGREGATE	SUBBASE	SUBGRADE	TEST PROCEDURE	
Moisture						X	X	X	Oklahoma	
Plate Bearing	X	X	X	X	X	X	X		Research	(a)
Plate Bearing								X	Research	(a)
Split Tube Drive								X	Research	(b)
Benkelman Beam Deflection	X	X	X	X					Research	(a)
Field C.B.R.					X	X	X	X	Research	(b)
Thickness Measurement	X	X			X	X	X		Oklahoma	
Field Density					X	X	X	X	A.A.S.H.O.	T-147
LABORATORY TESTS										
Extraction	X	X	X		X				A.A.S.H.O.	T-58 Mod
Gradation	X	X	X		X	X			A.A.S.H.O.	T-27
Hveem Stability	X	X							Hveem, Oklahoma	(b)
Asphalt Penetration	X	X	X		X				A.A.S.H.O.	T-49
Asphalt Ductility	X	X	X		X				A.A.S.H.O.	T-51
Asphalt Softening Point	X	X	X		X				A.A.S.H.O.	T-53
Aggregate per square yard			X						Oklahoma	(c)
Asphalt per square yard		X	X						Oklahoma	(c)
Soil Classification					X	X	X	X	A.A.S.H.O.	T-88
Los Angeles Abrasion						X			A.A.S.H.O.	T-96
Laboratory C.B.R.						X	X	X	Oklahoma	(b)
Standard Density						X	X	X	For Base (corrected) A.A.S.H.O.	T-99
Optimum Moisture						X	X	X	A.A.S.H.O.	T-89

base courses were also considered to be composed of satisfactory materials and of the required thickness. The density of the asphaltic concrete surfaces and bases showed an average increase of 4 percent. The tests of the selected soil subbase material indicated so many variations that it would probably be better to use select grading or higher type subbase material.

Material tests were made on 26 projects and in selecting projects having material essentially meeting the requirements of the specifications, half of them were eliminated. Only the selected projects were used for the remainder of the study. All of the data for these selected projects were punched on cards for computer analysis. Several trial analyses by statistical methods gave results that indicated the need to develop new methods of evaluating some of the factors. For example, climate which had been expressed as annual average precipitation did not give satisfactory results until it was expressed as wet and dry cycles.

From the weather bureau records, the 3-mo moving averages of the recorded rainfall were calculated for the 10-yr period from January 1950 through December 1959. The average monthly rainfall for the same period was also calculated. These values were plotted and the lines inspected. Each time a moving average line crossed above or below the average monthly rainfall line, it was considered as a change in moisture content and as a potential volumetric change in the subgrade. The total number of cycle changes for the 10-yr period was used as the rainfall factor.

In Part One a traffic index was used. This index was based on the estimated percent of commercial vehicles having wheel loads and tire pressures greater than 9,000 and 90 lb, respectively. The same percentage was applied to the traffic count on all projects. The results were not satisfactory using this index. This factor was revised by using the average number of heavy commercial vehicles per day for each project and the overloaded axle percentage for the appropriate area. This figure was found to give satisfactory results when used as the traffic factor.

Processing complete sets of data with the computer indicated the need of a factor to evaluate the variations in shoulder width and the type of shoulders on the road. The factors used were arrived at by inspection of the projects and review of the condition survey data. From this study, numerical ratings for the protection provided by the shoulders were developed. The ratings given ranged from zero for the lowest support to 20 for the best. The type of material and surfacing, and width of shoulders were considered.

At the beginning of this research project it was assumed that it would be necessary for the state to furnish roads to the public for a longer period of time than the expected life of any pavement. Economically, the best pavement was not necessarily the one that had the longest life, but the pavement that could be paid for and maintained at the lowest cost per mile per year. This cost was used as the dependent variable to evaluate all factors and for the development of a pavement design method.

Because the annual cost or rate of depreciation of a pavement changes from year to year, it is necessary to relate depreciation to time. Using the data from our condition surveys for 457 deflection sites on 13 projects, a satisfactory relationship between depreciation and time was obtained by using a Pearl - Reed curve of the form

$$\text{Depreciation} = \frac{100}{1 + Ce^{rt}} \tag{3}$$

in which

C = depreciation constant,
r = rate of depreciation,
t = age, and
e = base of natural logarithms.

This equation in log form is

$$\log_e \frac{100 - \text{Depr.}}{\text{Depr.}} = rt + \log_e C \tag{4}$$

For all types of construction taken together it was found that

$$\text{Depreciation} = \frac{100}{1 + 99e^{-0.3776t}} \tag{5}$$

A simplified method of calculating the plots for this type of curve was developed. This method of computing depreciation curves allowed the determination of depreciation at any given time for each deflection site. The depreciation at 10 yr of age was calculated for each deflection site.

Depreciation, as defined in this report, correlated better with the Pearl-Reed curve than with any other mathematical model, so this curve was accepted as representing the relationship between depreciation and time. The depreciation curves for Type "D" construction and for an average of all types of construction are shown in Figure 7.

The method used to design the thickness of the pavements tested in this study was essentially the CBR method as given in the 1946 Highway Research Board Proceedings. To determine whether this method produced a design of the expected strength and to evaluate the comparative strength of the materials, a program of deflection testing was carried out. These pavement strengths were determined by plate bearing tests. The

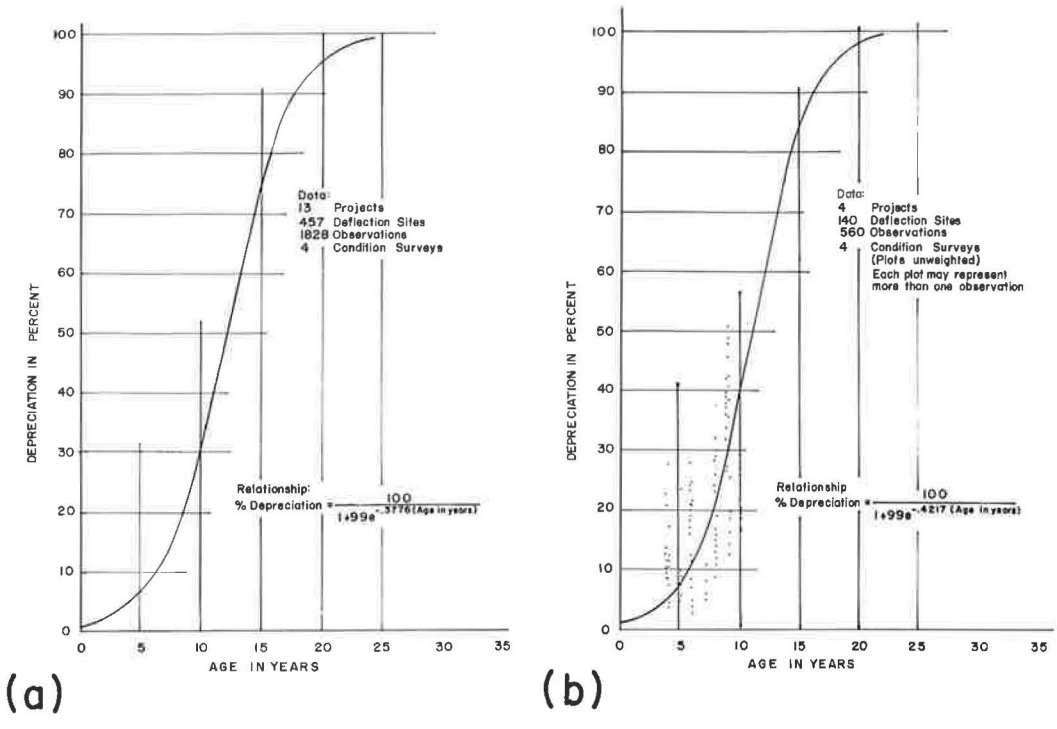

Figure 7. Depreciation curves: (a) all types of construction; and (b) Type "D" construction.

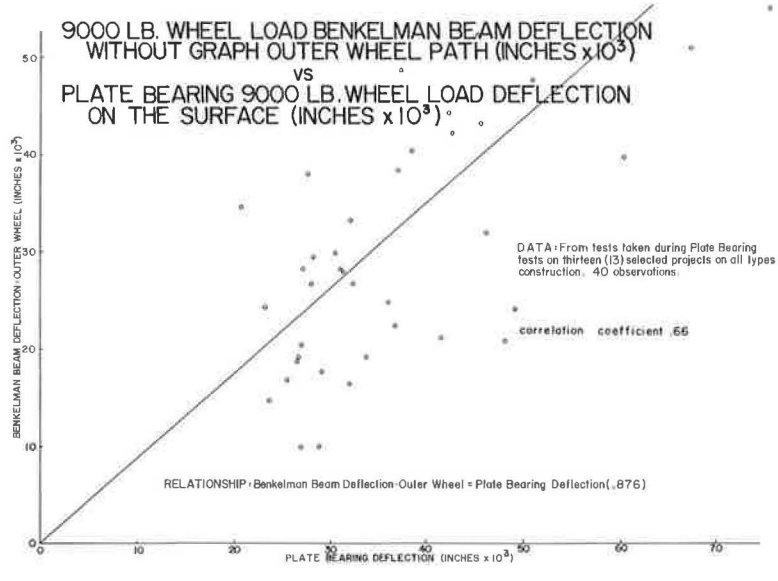

Figure 8.

TABLE 9

BENKELMAN BEAM DEFLECTIONS AND DEPRECIATIONS FROM BENKELMAN BEAM DEFLECTIONS SITES

Benkelman Beam Deflection (in. × 10^3)	% Deprec. at 10 Yr (Avg.)	Benkelman Beam Deflection (in. × 10^3)	% Deprec. at 10 Yr (Avg.)
0	11.27	26	35.51
3	17.77	27	35.14
6	15.42	28	44.16
7	27.50	29	36.64
8	17.70	30	29.42
9	21.56	31	43.38
10	31.52	32	45.65
11	18.62	33	44.01
12	28.94	34	55.70
13	25.31	35	38.96
14	29.14	36	40.11
15	32.73	37	41.31
16	24.91	38	41.09
17	40.06	39	45.98
18	30.14	40	50.54
19	20.98	41	67.11
20	28.64	42	63.01
21	29.67	43	55.94
22	34.09	44	62.43
23	36.03	50	59.72
24	35.01	52	69.42
25	39.25		

strength of a pavement when determined by plate bearing tests depends on the location of the test transversely and the allowable deflection to control depreciation.

The plate bearing deflections were correlated with the Benkelman beam deflections (Fig. 8). Benkelman beam deflections were related to the total depreciation at 10 yr of age. This information (Table 9) was taken from 452 deflection sites on 13 selected projects on all types construction. This information was compiled by electronic computer using the deflection as the controlling factor. The depreciation values were averaged for each deflection. The deflection values for each deflection site are an average of five readings. The frequency of each deflection occurrence is not shown and is variable. The depreciation values are from life curves calculated for each deflection site.

Plate bearing tests taken at the top and bottom of each layer were used to evaluate the load-supporting ability of the layer. This load-supporting ability divided by the thickness of the layer gave a load-supporting value per inch of material. To evaluate the materials in relation to each other, the strength of stabilized aggregate base course material (SABC) was selected as the standard. The values determined for the strength of the various materials at allowable deflections of 0.03, 0.04 and 0.05 in. are given in Table 10. These results indicate that at the least deflection, subbase material and soil asphalt material have more supporting value than at higher deflections when compared to SABC. This seems to be a result of either or both of two factors:

1. The soil asphalt is unrestrained by overburden; and
2. The rigid plates used in the plate bearing tests tend to shear the soil-type materials at the plate perimeter with relative light loads due to the small grain size of the material (i.e., little or no material retained on the No. 4 sieve).

TABLE 10

LOAD SUPPORT AT INDICATED DEFLECTION[a]

Materials & Type Construction	0.03 In.		0.04 In.		0.05 In.	
	Lb/In.	% SABC	Lb/In.	% SABC	Lb/In.	% SABC
Stab. aggregate, Type "B"	528	100	746	100	895	100
Blended rock asph., Type "A"	972	184	1,692	227	2,724	302
Asph. concrete, Type "E"	599	113	939	126	1,321	147
Soil asphalt, Type "D"	359	68	445	60	603	67
Subbase, Types "B", "D" and "E"	40	64	413	55	447	50

[a]SABC = stabilized aggregate base course material.

Because soil asphalt bases had a double bituminous surface which was considered to have no load-supporting value, Benkelman beam tests could be used to evaluate the load-supporting value and eliminate the shearings of the rigid plates. This procedure gave the following values which were considered to be more realistic:

Deflection (in.)	Lb	% of SABC
0.03	818	155
0.04	916	123
0.05	1,172	131

Many comparisons of deflection with other factors were made. Table 11 gives an index of most of them.

To record the movement of the pavement during a Benkelman beam test, the Research Branch developed a graphing attachment for the Benkelman beam. This attachment draws a continuous curve recording the movement of the pavement under the probe of the beam as the wheel approaches and travels past the test point. These curves were used to check the dial readings, to determine whether the fixed legs of the beam had moved during the test, and to determine whether the curvature of the deflection area had a closer relationship to depreciation than the total deflection. There is some difference in the deflection taken with and without the graphing attachment. The relationship between the deflections is shown in Figure 9.

To determine the relationship of curvature to depreciation, the Benkelman beam deflection curves were analyzed in three parts: (a) by total deflection, (b) by the compressive or deflection portion of the curve, and (c) by the recovery portion of the curve. Figure 10 illustrates a typical deflection curve and its elements.

In the computer analysis of the deflection data and depreciation of the deflection sites of the 13 selected projects, statistical correlations were made of the depreciation and the elements of the deflection curve. The ratio of the chord to total deflection is a measurement of curvature. The elements and the resulting correlation coefficients were as follows:

TABLE 11

INDEX TO FIGURES AND TABLES

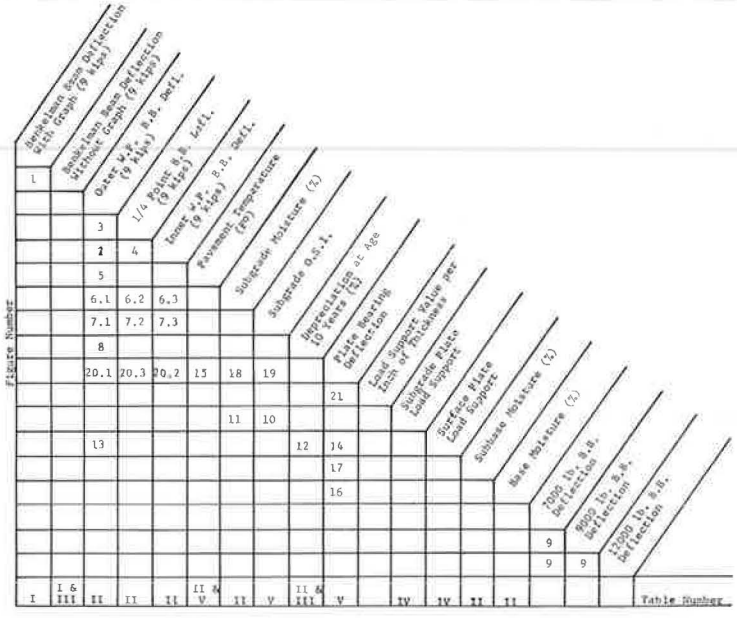

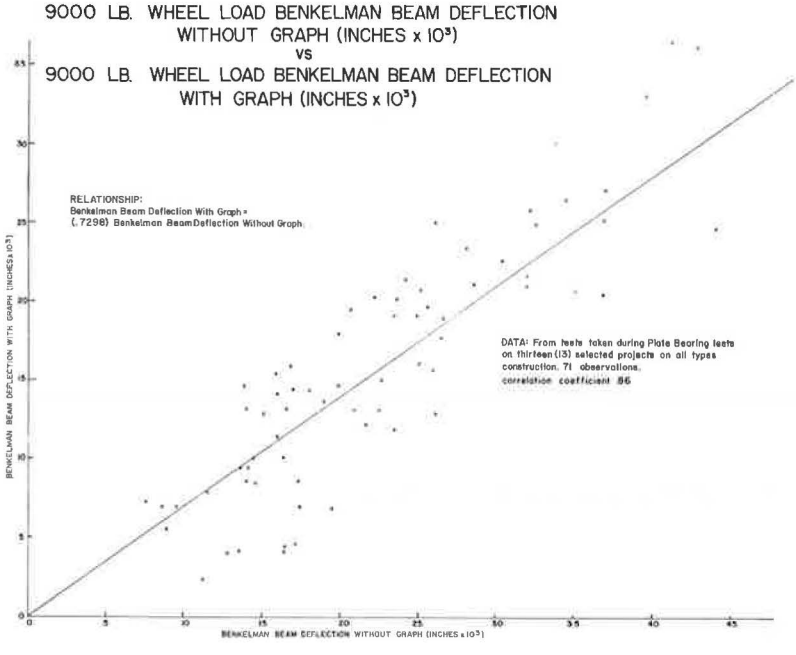

Figure 9.

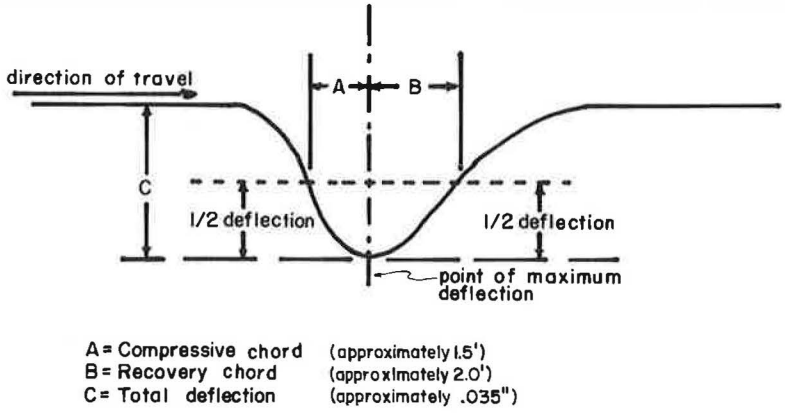

Figure 10. Typical deflection curve and its elements.

Total deflection vs depreciation	r = 0.404
Ratio of compressive chord to total deflection vs depreciation	r = 0.399
Ratio of recovery chord to total deflection vs depreciation	r = 0.382

Because the total deflection is the easiest to measure and correlates as well with depreciation, the total deflection was used in our analysis.

From a study of the depreciation of the pavements, it was found that about $\frac{1}{8}$ of the roads constructed to our design requirements were unsatisfactory. A special study of unsatisfactory projects was undertaken to determine the reasons for poor performance. The study involved 250 mi of pavement in 33 construction projects. Most of the projects had several defects. The frequency with which these defects occurred in the 33 projects was as follows:

57% of projects, underdesigned for the load assumed;
48% of projects, base materials were defective;
33% of projects, overloaded above design load;
30% of projects, poor subbase material;
21% of projects, shrinkage of subgrade soil; and
21% of projects, water entering through surface.

As a result of this special study and our research project, it was indicated that our method of flexible paving design should be revised. It was decided to develop a new method by combining the old method with additional factors to reflect the findings of our research. A design equation was developed by a multiple regression analysis of the data.

In the final analysis, the following factors with letter and number designations for ease of expression were used:

- Tb = required equivalent base thickness, determined from the Oklahoma subgrade index number of the subgrade and wheel load;
- Tp = adjusted equivalent base thickness, determined from the constructed thicknesses of the pavement courses and the equivalence factors of materials;
- X_0 = depreciation at age 10 yr (%);
- X_1 = Log_e (Tb + 20 - Tp) (20 arbitrarily chosen to provide a positive result in each case to permit the use of logarithms);
- X_2 = (Tb - Tp) multiplied by shoulder factor;
- X_3 = Benkelman beam deflection;

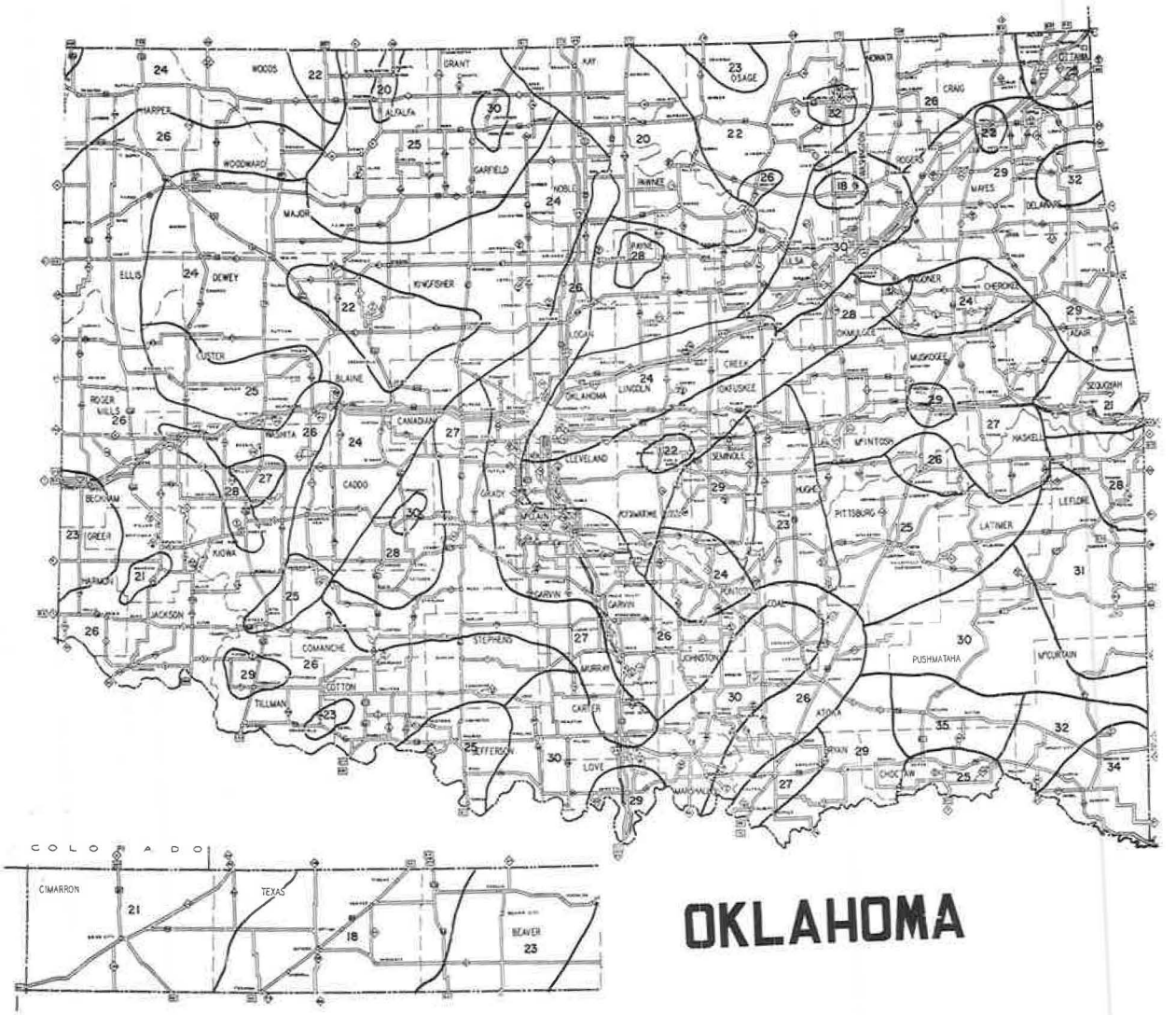

Figure 11. Weather (wet-dry) cycles, 10-yr period.

X_4 = square root of shoulder factor;
X_5 = square root of number of overloaded axles per day; and
X_6 = square root of wet-dry climatic cycles in 10-yr period 1950 through 1959.

In the analysis of this regression equation, approximately 50 different mathematical models were tried and discarded. The result is a linear equation involving the seven factors described and designated as X_0 through X_6:

$$X_0 = 48.37940\ X_1 - 0.09505\ X_2 + 445.95413\ X_3 - 4.58581\ X_4 + 1.70678\ X_5 + 14.86333\ X_6 - 186.76322 \quad (6)$$

The variance ratio for this equation is 1.816. This was considered satisfactory because we did not have a controlled research project and all the unknown influencing factors which are a part of normal highway construction were present. Only projects having satisfactory materials were included in the variance ratio of 1.816. For projects with substandard materials, the ratio was 8.073.

A nomograph was constructed for the solution of the design equation. Tables, graphs, and maps have been developed from which the values of the necessary factors can be obtained. The map in Figure 11, showing the wet and dry cycles, is an example of the recording of the weather information used in our flexible pavement design method.

Work was carried out on this project continuously for almost 8 yr and much has been learned about highways and the performance of pavements in Oklahoma. The results of this research have been put to use. It is not considered that the final report is the end of the project. We feel that the data collected contain much additional information of value.

One evident fact, frequently lost sight of, is that it is much easier to collect data than it is to determine what truths are indicated by the data. It is also well to remember that much data have been collected and many years later their true value has been demonstrated after many men had failed to find a method to determine their meaning. There is also in existence a vast store of carefully collected data which has not been interpreted even after a long period of time and many attempts to analyze it.

FUTURE RESEARCH

The work we have done and the work of other people seems to point out clearly that there are two major parts to flexible pavement design; the pavement itself and the subgrade on which the pavement is placed. The development of methods to design the pavement has received the lion's share of attention.

Common practice is to design the pavement to fit the subgrade, but it would be equally possible to design the subgrade to fit a specified thickness of pavement. In an area where 50 percent of the soils required a base 12 in. or less in thickness, we could use selected grading to eliminate the poorest soils from the top of the subgrade. This would result in the elimination of the thickest bases and would produce a more uniform base thickness for a project. Shrinkage and swell of subgrade soils is a cause of pavement depreciation in this state. Thicker pavements are not a corrective remedy for this condition, but placing better soils in the top of the subgrade would extend the life of a pavement.

The design of subgrades has been largely confined to specifying density and providing drainage. Indirectly, we are aware of the fact that the drainage of free water and density at the time of construction does not accomplish everything assumed in the pavement design.

Time may change the density and moisture of a subgrade, yet if we expect a road to last 20 yr, we should make some provision in the design of the subgrade to guard against detrimental changes for the next 20 yr. Such things as frost susceptibility, capillary water, climatic environment, internal drainage, and volumetric change are problems of subgrade design. Selected grading, modification with line or cement, membranes and blankets of other material might be used as a protection of the subgrade. Other

methods to secure uniformity, strength, and protection from change in the subgrade are needed.

The comparison of our thickness with the AASHO guide and comparisons made by others using different methods seem to indicate that the design of flexible paving thickness is rather well standardized.

We are of the opinion that the field of rational subgrade design is wide open and future research in the design of subgrades and the protection of them from the environment might yield a greater return than further research directed toward the design of pavement.

REFERENCE

1. McLeod, Norman W. Jour. Asphalt Tech., Vol. 2, No. 2, p. 7, March-June 1943.

Discussion

O. L. STOKSTAD, Design & Development Engineer, Michigan State Highway Department.—Mr. Helmer is to be congratulated on the thoroughness of his testing program, on the significance of the results which he has obtained, and on the forthright discussion of lessons learned.

With respect to the question of designing pavements to fit subgrade conditions or of designing the subgrade to fit the pavement design selected, Michigan's practice involves a median procedure. As a matter of general policy, it has long been accepted that traffic needs should be the major factor in pavement selection and that the subgrade should be modified to support properly the pavement selected. This policy is tempered by a modification which states that either flexible or rigid type pavements can be designed for any traffic load and that the type selected can be based on the cost of construction as dictated by existing foundation conditions. Normally in Michigan a flexible design enjoys an economic advantage when building over well-drained granular soils which need only compaction and confinement to supply adequate support for any normal axle load. Over cohesive soils, on the other hand, where granular materials must be imported, rigid designs become competitive. Once the general pavement type has been determined, the details of pavement design will be dictated by the traffic load to be carried. The details of foundation design will be influenced first by the needs of the pavement to be built and secondly by the drainage, soil and climatic conditions involved. The final effort in tailoring the foundation to satisfy pavement needs is accomplished on construction as details of foundation conditions become exposed during grading operations. Comprehensive soil survey and geologic information is, therefore, the first need in selecting pavement type, not only to learn of the soils over which the road is to be built but also to acquire an inventory of construction materials which are going to be available in the construction area.

It is gratifying to read of Mr. Helmer's conclusions concerning climate as an influence on subgrade conditions when dealing with the period of time involved in a normal pavement life span. Each soil and soil material under these conditions will have developed its own moisture and density range which will have been determined more by climatic environment than by design requirements accomplished at the time of foundation construction. This is one important reason why the existing highway pavements in service form such a fruitful source of information concerning design and construction requirements. It was 38 years ago that the Michigan State Highway Department stated in its Eleventh Biennial Report, "The continued expenditure of large sums of money for highway improvement makes it imperative to study the roads which have been built during the past few years, it benefit is to be derived from past experience."

Design Curves for Flexible Pavements Based on Layered System Theory

G. M. DORMON and C. T. METCALF
Respectively, Shell International Petroleum Company Ltd. and Martinez Research Laboratory, Shell Oil Company

Use of the recently developed theoretical three-layer elastic theory has aided the development of a method for design of flexible pavements. A series of design curves is presented which show the relationship between the combined thickness of granular base and asphalt surface necessary to support heavy truck loading (18,000-lb axle load). Development of the theoretical curves is based on the use of the three-layer elastic theory. The curves have been created by methods similar to those described in a paper for the International Conference on the Structural Design of Asphalt Pavements. The provisional curves of the previous paper have been modified slightly and also expanded to include a fatigue factor. Principal assumptions of the design method are outlined.

Adequate design according to the present method is based on the prevention of failure at critical locations in the pavement structure. Consideration is given to extent of displacement (strain) in the subgrade, and magnitude of tensile strain at the base of the asphalt surface. The relative severity of these conditions governs the design of the pavement. Within calculable limits, surface and base can be replaced by each other. Examples are given which demonstrate the use of these principles in the design of pavements for "weak" (CBR = 2.5) and "strong" (CBR = 20) subgrades.

•UNTIL RECENTLY, solutions to the equations for the behavior of layered systems have been limited to those for two layers. Acum and Fox (1) investigated three-layer systems within limited conditions. Jones (2) expanded the equations and tabulated stress and strain factors for three-layer structures over a wider range of values. Peattie (3) demonstrated the use of these three-layer tables in stress investigations. He also proposed a method for utilizing the data to design pavements (4). This method was recently applied in the preparation of a series of pavement design curves presented at the International Conference on the Structural Design of Asphalt Pavements (5).

The basic principle in the development of the theoretical design method is the prevention of excessive stress or strain in a pavement or in the underlying soil. This is accomplished by investigating the strain conditions at certain critical locations in the pavement and then designing to maintain strains within safe limits. The design curves presented at Ann Arbor (5) are based on limiting the vertical compressive strain in the subgrade and the tensile stress in the asphalt-bound layer. These limitations are aimed at prevention of deformation in the pavement and cracking of the asphalt surface.

Design curves prepared on the basis of these principles show many different combinations of asphalt surface and granular base which will fulfill the strain limitations. An appropriate design—depending on economic or other considerations—can be selected from several different choices.

In the previous design curves presented at Ann Arbor, no specific allowance was made for different intensities of traffic loading. Thus, there was no quantitative basis for differentiation between light and heavily traveled roads. Correlations developed

Paper sponsored by Committee on Flexible Pavement Design and presented at the 43rd Annual Meeting.

from published results of the AASHO test, however, have aided in the development of a series of fatigue criteria. These have been added to the theoretical design method and a new series of design curves have been prepared to incorporate these principles. Thus, the method is expanded to include design for different amounts of traffic, as well as for different wheel loads.

DESIGN FACTORS

Development of the theoretical design curves has required certain assumptions to be made concerning factors influencing design. Assumptions are necessary because of uncertainties in current information relating to design. The adopted assumptions appear to be reasonable and in line with existing experience. As additional information is accumulated, changes in these criteria might be suggested which would be more realistic.

Wheel Loading

Although calculations may be made for any wheel loading, the basic load selected for these design calculations is a 9,000-lb wheel load (18,000-lb axle load). In practice this load is applied by a dual wheel. For subgrade strain calculations, however, the load is assumed to be applied by an 80-psi contact pressure acting on a single area of 6-in. radius. This is considered the most reasonable basis for design within the limitations of stress distribution data currently available.

At relatively shallow depths in the pavement, general stress analysis made by Fox (6) indicates that the maximum stress (or strain) occurs under the center of either individual wheel of the dual-wheel pair (6). Stress under the wheel is produced almost entirely by the contribution of one wheel alone. In accordance with this principle, the calculation of the tensile strain in the asphalt layer is based on the use of a single wheel

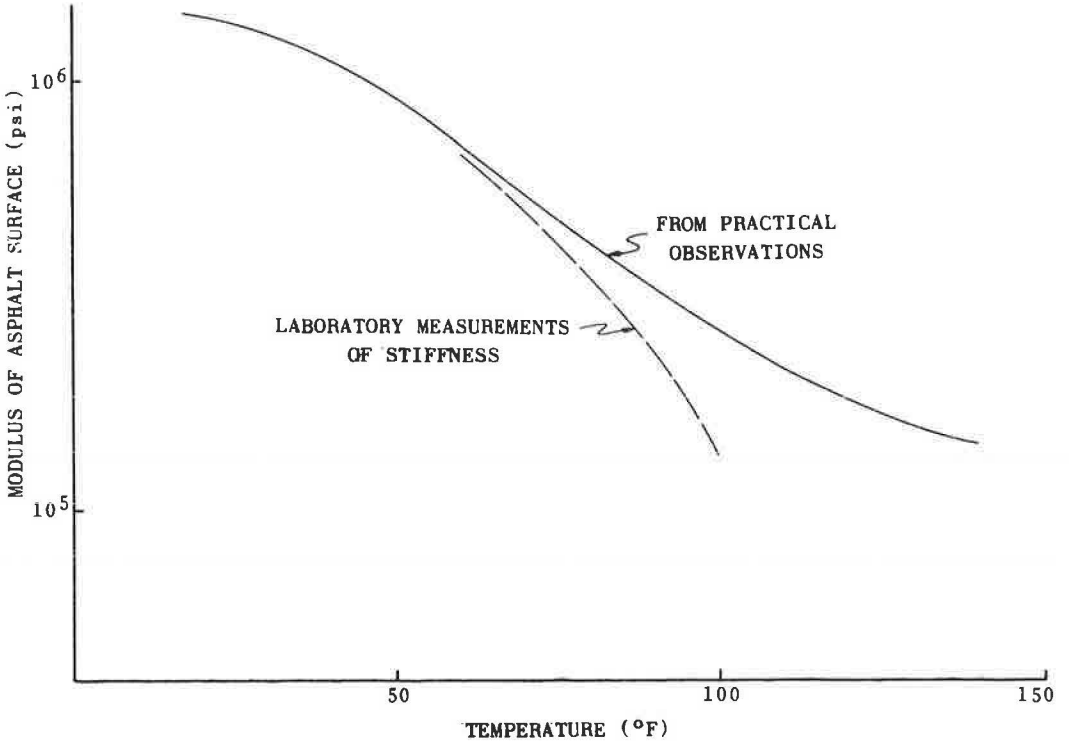

Figure 1. Relation of modulus of asphalt layer to temperature.

in a dual pair. This is represented by the 80-psi contact pressure acting on an area of 4.2-in. radius.

In all calculations for strain in the subgrade or in the asphalt surface, impact effects are considered to be negligible, especially in view of the conservative nature of the basic wheel loading assumption.

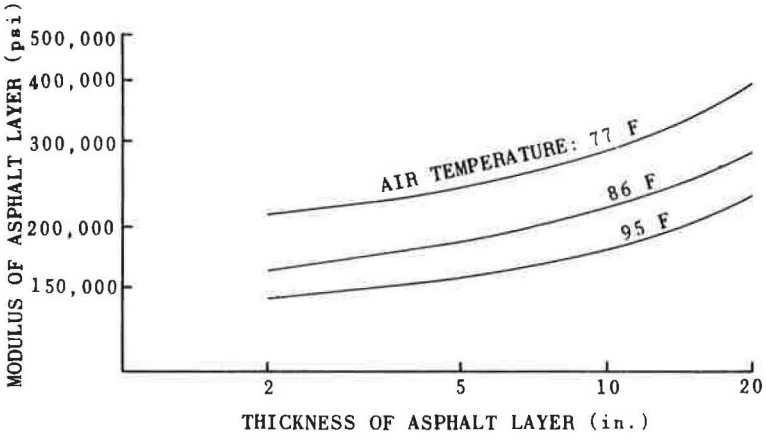

Figure 2. Relation of asphalt modulus to thickness of layer.

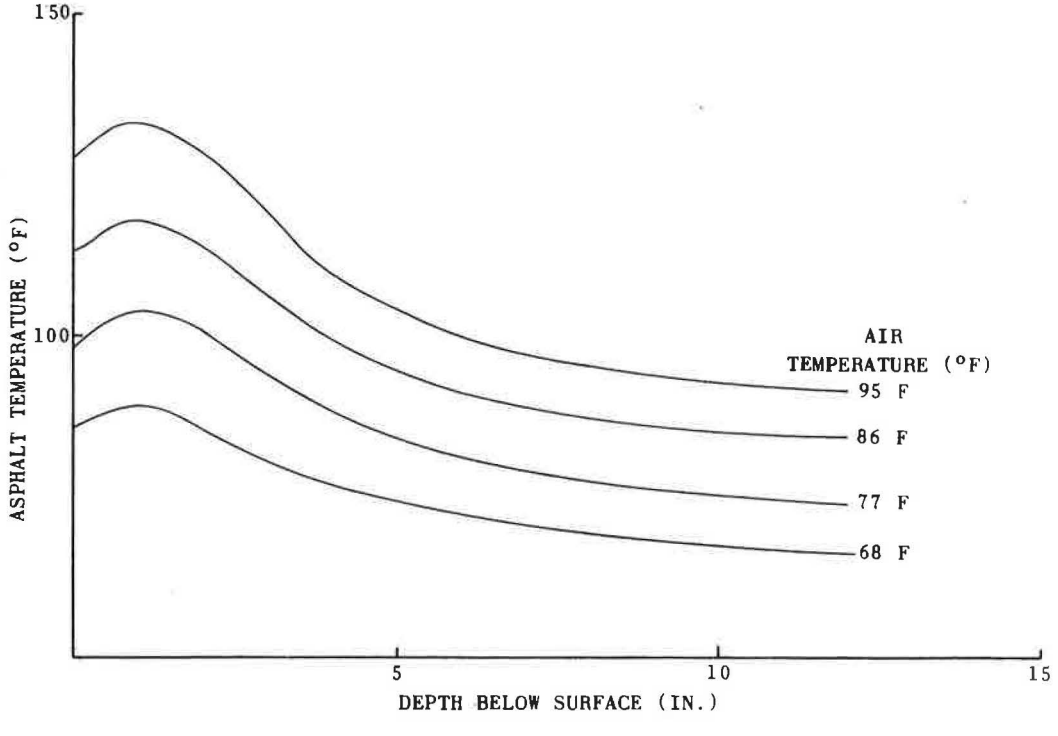

Figure 3. Relation of temperature of asphalt surface to depth below surface.

Properties of Pavement Components

Modulus of Asphalt-Bound Layer. —A curve illustrating the influence of temperature on the elastic modulus of the asphalt layer is shown in Figure 1. The graph depicts information obtained from two separate sources. The dashed line traces the relation between modulus and temperature for a series of laboratory stiffness measurements at a loading time of 0.02 sec. The solid line was prepared by use of the results of subgrade stress measurements at different pavement temperatures reported by Whiffin and Lister (7) of the Road Research Laboratory.

Critical strain in the subgrade occurs when the effective modulus of the asphalt-bound layer is at a minimum. This takes place as the asphalt becomes warm and the asphalt layer affords less protection to the subgrade. Figure 2 shows a plot of the asphalt layer moduli corresponding to selected air temperatures. Moduli used in strain calculations are those pertaining to a maximum air temperature of 95 F. It is evident in this figure that an allowance is also made for a reduction in the effective temperature of thicker asphalt layers. This is reflected by an increase in the effective modulus of the layer. Typical maximum temperature/depth relationships deduced for asphalt-bound materials are shown in Figure 3. These provide the basis for the preparation of the curves in Figure 2. The effective modulus of the asphalt-bound layer is associated with the temperature at a depth equal to one-third of the layer.

Modular Ratio of Base Subgrade. —Investigations by Heukelom and Klomp (8) have indicated that the effective modulus developed by a granular base tends to be related to the modulus of the subgrade. Theoretical design curves in the Ann Arbor paper (5) assumed the effective modulus of a combined thickness of base and subbase course to be in a range of 2 to 4 times greater than the subgrade modulus.

To make allowance for the surcharge effect on modular ratio, the ratio $E_2/E_3(K_2)$ is varied according to the thickness of the granular layer as shown in Figure 4. This relation is arbitrarily chosen to give designs which correlate reasonably well with empirically developed CBR curves.

PERMISSIBLE STRAIN VALUES

Development of the design curves is based on the principle of limiting the magnitude of strains produced at certain critical locations in the pavement structure. The pres-

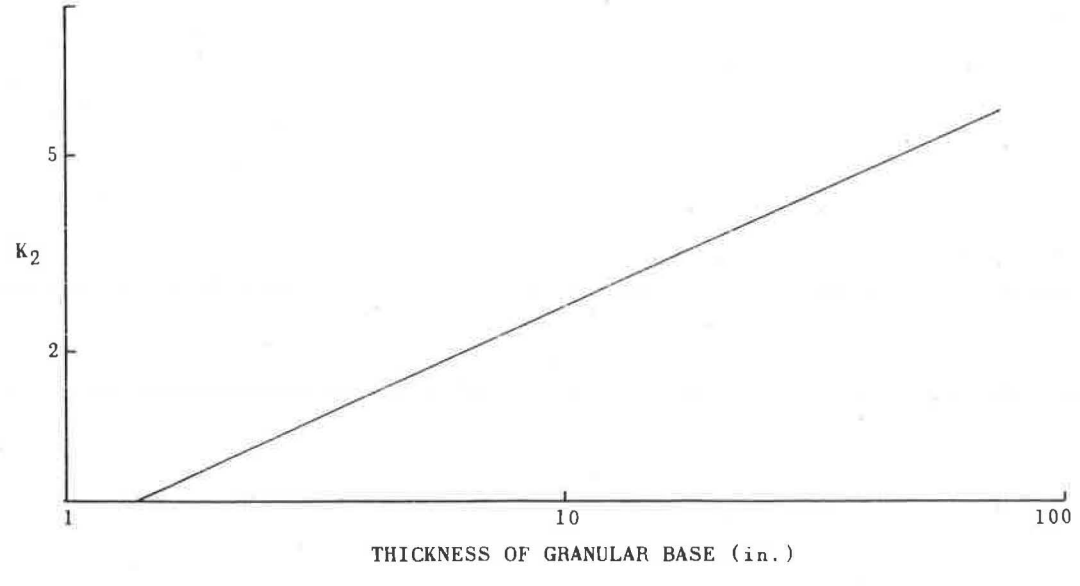

Figure 4. Relation of modular ratio, K_2, to thickness of granular base.

ent method places emphasis on consideration of the vertical compressive strain on the subgrade and the tensile strain at the base of the asphalt-bound layer. Control of the strain at these places contributes to the control of important elements in pavement performance. Compressive strain on the subgrade has an influence on pavement deformation. Tensile strain in the asphalt layer influences the tendency for cracks to develop.

Compressive Strain on Subgrade

Design curves previously presented (5) were based on the use of a single critical strain value representing one condition of heavy traffic loading. By empirical correlation with AASHO results, the relation between compressive strain and number of load applications shown in Figure 5 was established. Use of this relationship permits the introduction of fatigue criteria into the theoretical method.

Several different procedures were coordinated to produce the load application curve in Figure 5. First, calculation of vertical compressive strain in the subgrade for several different sections in the AASHO test indicated that a compressive strain of 6.5×10^{-4} was associated with 10^6 applications (5).

The AASHO results (9) also provided information by which the effects of different wheel loads of mixed traffic could be weighted. This relationship, shown in Figure 6 led to the development of the wheel load weighting curve in Figure 7. Subsequently, the compressive strain values previously assigned to different wheel loads (5) were plotted according to their equivalent numbers as shown in Figure 5. Table 1 lists the permissible strains obtained for use in design calculations.

Tensile Strain in Asphalt-Bound Layer

The provisional laboratory fatigue data for asphalt-bound materials (Fig. 8) employed by Heukelom and Klomp (8) were used to provide information on strain/load-repetition

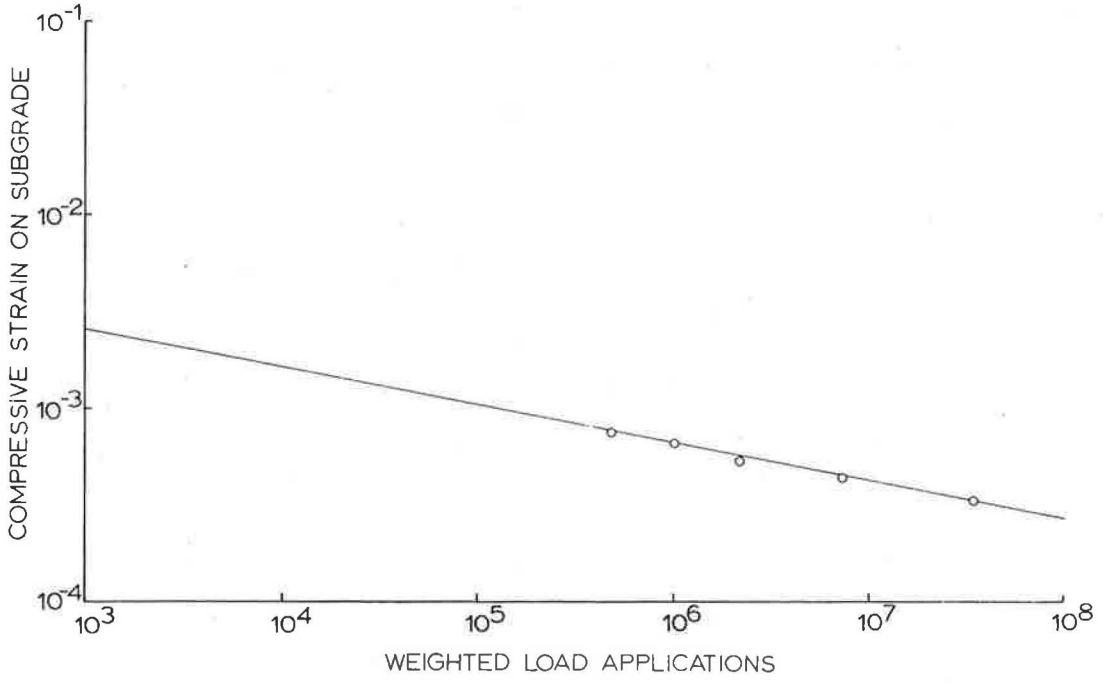

Figure 5. Relation of compressive strain to number of load applications, 18,000-lb axle load.

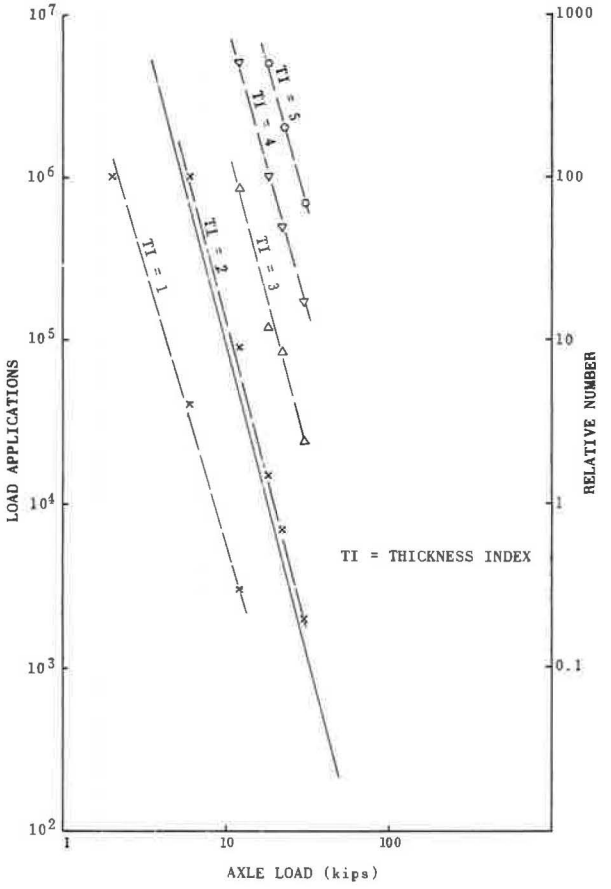

Figure 6.

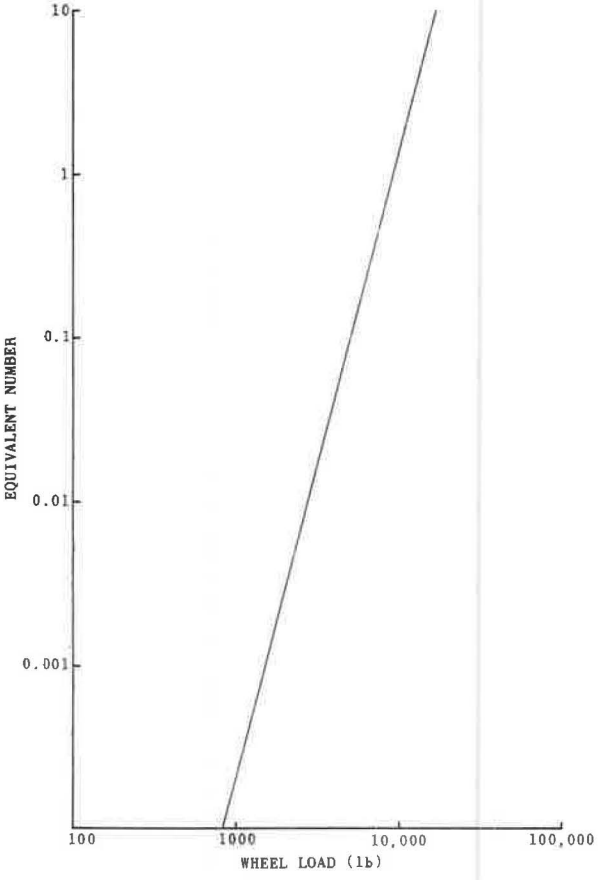

Figure 7. Wheel load weighting.

TABLE 1

SUBGRADE COMPRESSIVE STRAIN VALUES CORRESPONDING TO DIFFERENT LOAD APPLICATIONS

Load	Strain
10^5	1.05×10^{-3}
10^6	6.5×10^{-4}
10^7	4.2×10^{-4}
10^8	2.6×10^{-4}

TABLE 2

TENSILE STRAIN IN ASPHALT-BOUND LAYER CORRESPONDING TO DIFFERENT LOAD APPLICATIONS

Load	Strain
10^5	2.3×10^{-4}
10^6	1.45×10^{-4}
10^7	9.2×10^{-5}
10^8	5.8×10^{-5}

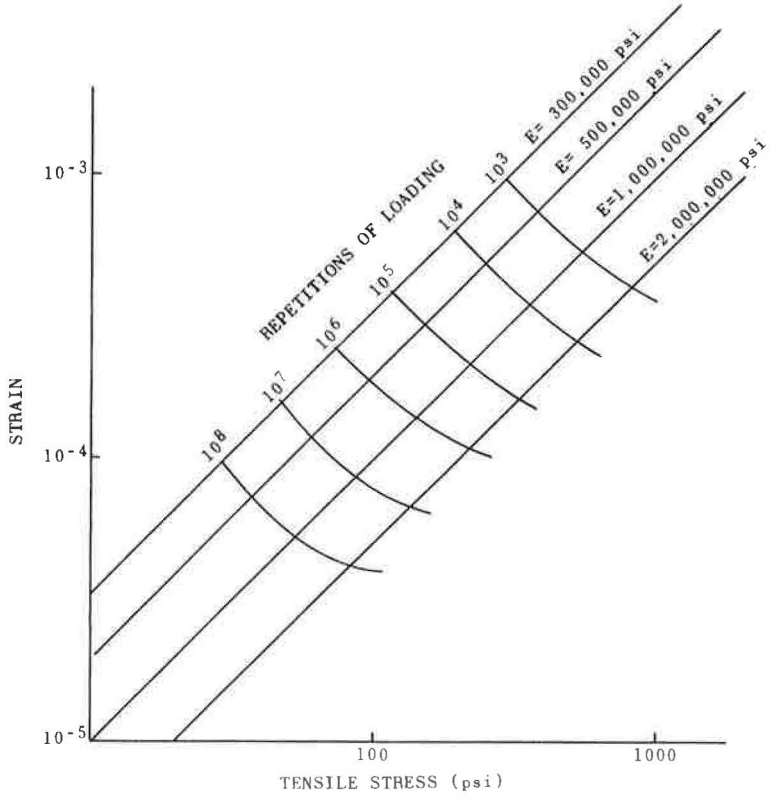

Figure 8. Provisional fatigue data for asphalt base course materials.

relationships at different temperatures. Meiner's law was then applied to integrate the effect on fatigue life of yearly temperature variations. A number of hypothetical constructions were investigated to determine an equivalent temperature for design purposes. It was found that a temperature between 50 and 60 F was suitable, and 50 F was selected for calculations. Figure 1 indicates that the effective modulus of a typical asphalt layer at this temperature is 900,000 psi. Fatigue data for tensile strain relationships for an elastic modulus of 900,000 psi are contained in Figure 9. Table 2 lists the critical strain values obtained by the method for use in design calculations.

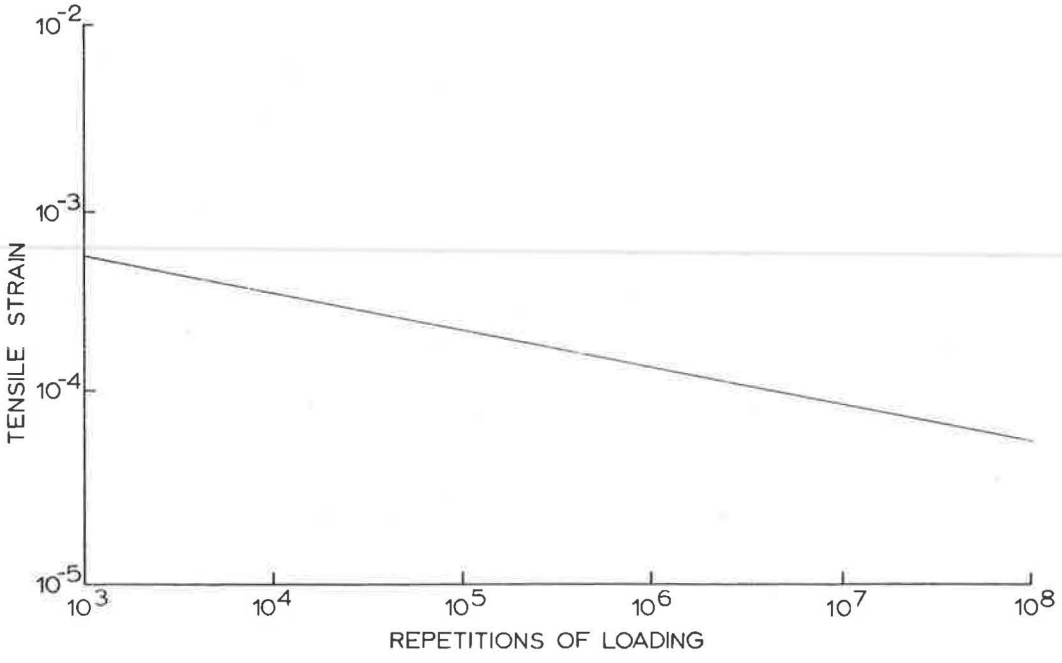

Figure 9. Fatigue curve tensile strain of asphalt base material.

The influence of different wheel loads on the tensile strain in the asphalt can be calculated directly for any particular construction. The wheel load weighting obtained depends on the construction. Because it is similar to that derived on the basis of the compressive strain in the subgrade (Fig. 7), the latter has been adopted for general use.

PAVEMENT DESIGN CURVES

Interpretation and Significance

On the basis of the foregoing criteria, pavement design curves have been prepared to show the relationship between thickness of asphalt surface and thickness of granular base for the representative 18,000-lb axle loading. Typical design curves in Figure 10 represent conditions of equal strain produced by the design load in the subgrade and in the asphalt surface. The subgrade compressive strain curve shows the combinations of asphalt surface and granular base at which the subgrade strain is 6.5×10^{-4} (10^6 load applications). The tensile strain curve shows the combination of surface and base at which the strain in the asphalt layer is limited to 14.5×10^{-5}. Each curve represents equivalent designs for the respective critical strains. Sample calculations for the construction of these curves are shown in the Appendix.

In this example, for thicknesses of granular base less than 21 in., compressive strain in the subgrade controls the design. This means that a greater thickness of asphalt-bound material is required to prevent damage to the subgrade than is required to prevent cracking in the asphalt layer. For granular bases thicker than 21 in., the situation is reversed. A thicker surface is required to prevent cracking than to prevent excessive subgrade strain. This demonstrates that a specific minimum thickness of asphalt surface is required for protection against cracking, even though a thinner surface combined with a thick base might otherwise offer ample protection to the subgrade. Thus, the design takes into consideration two separate limitations.

Comparison of the separate design requirements reveals that tensile strain is not influenced greatly by the thickness of the base. The tensile strain curve is nearly horizontal and, thus, the susceptibility to cracking does not change to any large degree on

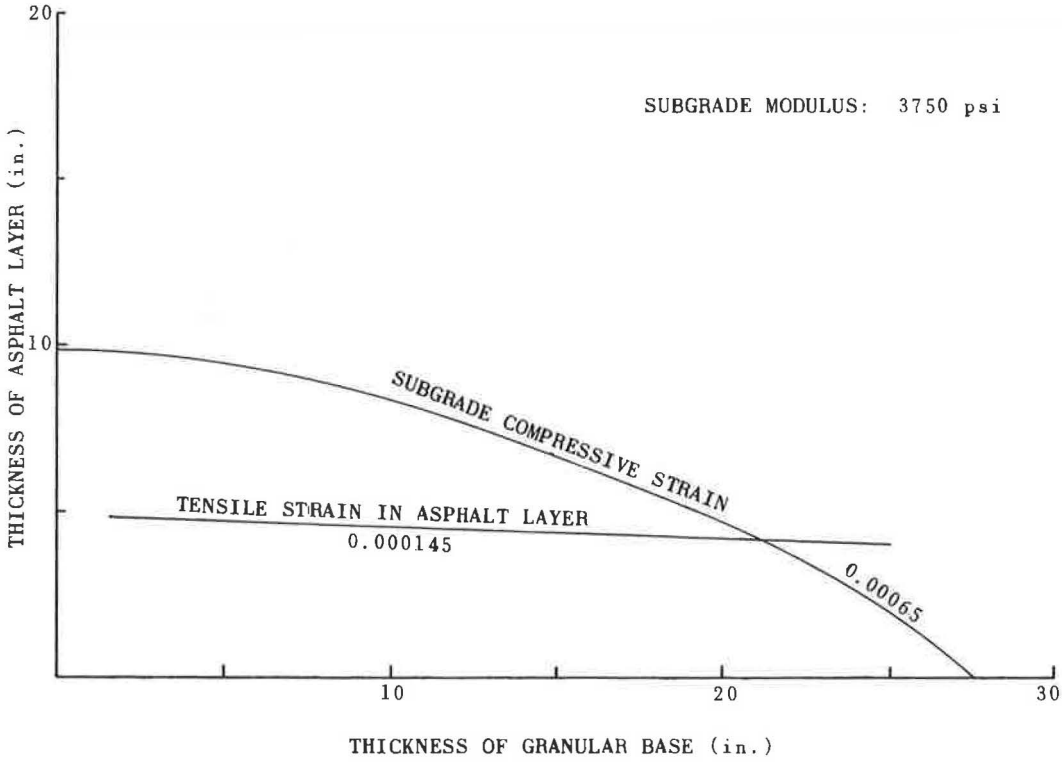

Figure 10. Typical design curves, 18,000-lb axle load (10^6 repetitions).

either thin or thick bases. The subgrade strain curve, however, is more strongly influenced by surface and base thicknesses.

It should be noted that the reciprocal of the slope at any point on the design curve is equal to the equivalency ratio between granular base and asphalt surface. The design curve is essentially dominated by the subgrade strain line which is curvilinear. Thus, the equivalency ratio does not have a constant value in this region. As the thickness of the base approaches zero, the equivalency ratio becomes very large (reflecting the flat slope of the curve). As base thickness increases, the ratio gradually decreases. A pavement with a 21-in. base has an equivalency ratio approximately equal to 2.1 (i.e., 1 in. of asphalt surface equals 2.1 in. of granular base). An average equivalency ratio representing a wider range of designs yields a higher value. If a pavement with no base (9.9-in. surface) is compared to the pavement with a 21-in. base (4.1-in. surface), the equivalency ratio is 3.6, i.e., 21/(9.9 - 4.1). Similar comparisons can be made for other combinations of surface and base.

TABLE 3

EQUIVALENT PAVEMENT DESIGNS[a]

Design	Thickness (in.)		
	Surface	Base	Total
1	9.9	0.0	9.9
2	8.4	10.0	18.4
3	6.7	15.0	21.7
4	4.1	21.0	25.1

[a]Subgrade modulus; 3,750 psi; 18,000-lb axle load, 10^6 applications.

Points on the design curves define strain contours and, therefore, they represent equivalent designs. This offers an opportunity to interchange thicknesses of asphalt surface and granular base to meet economic necessities. The data in Table 3 describe several equivalent designs taken from the curve in Figure 10.

Application of Fatigue Criteria to Design Curves

Individual design curves in Figures 11 through 14 have been prepared for subgrade moduli of 3,750, 7,500, 15,000 and 30,000 psi, respectively. These moduli correspond to CBR values of 2.5, 5, 10 and 20 according to an approximate relationship between modulus and CBR (Dynamic Modulus = 1,500 CBR) (10). In each figure separate curves are plotted for different numbers of load applications from 10^5 to 10^8. These are based on the application of the fatigue criteria outlined previously. The same calculation method is employed in the construction of each curve, but separate values of the limiting strain are used for each magnitude of loading.

Similar trends can be found in all curves. It is important to note, however, that design for larger volumes of traffic involves consideration of more than an increase in the thickness of granular base. The minimum thickness of asphalt-bound layer needed to prevent cracking also increases as traffic becomes greater.

CORRELATION WITH PRACTICE

A description has been given here of the way in which the results of the AASHO Road Test were used to establish subgrade strain criteria. In addition, it is shown in the Ann Arbor paper (5) that reasonable agreement exists between the behavior of the AASHO test sections and the theoretical trends of the design curves. It might be expected that some agreement also exists between the theoretical design curves and the empirical design criteria developed by the AASHO tests.

In Figure 15, the AASHO design criteria as proposed by Liddle (11) are superimposed on the theoretical design curves for the designated number of load applications. The AASHO lines correspond to the equation:

$$D = 0.44\ D_1 + 0.14\ D_2 \qquad (1)$$

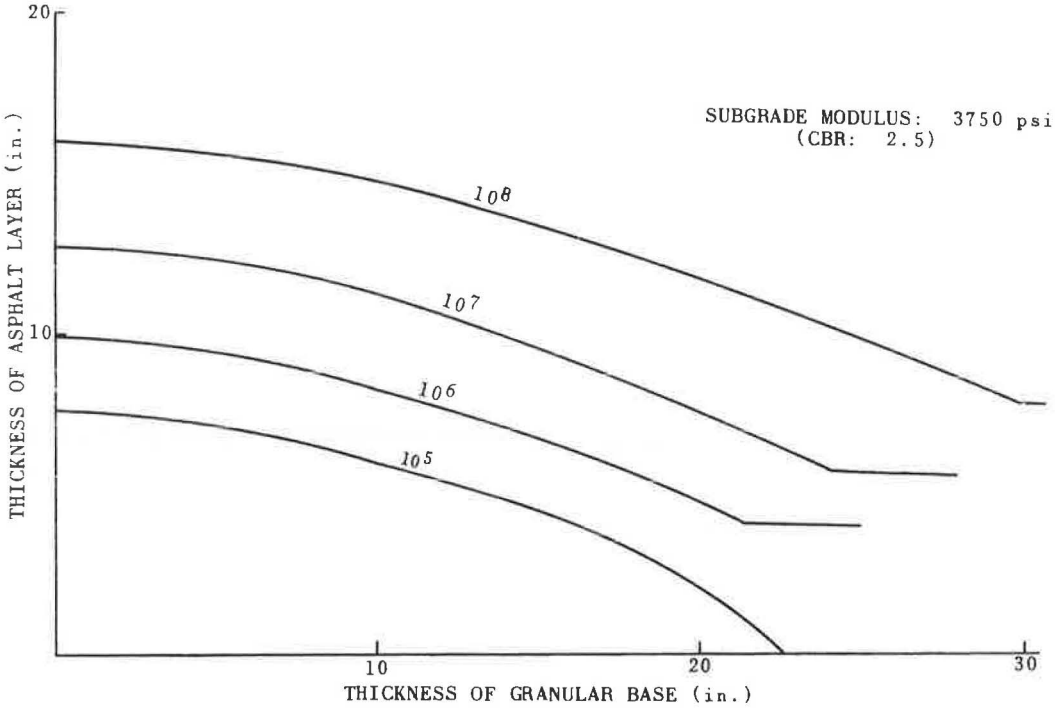

Figure 11. Design curves, 18,000-lb axle load.

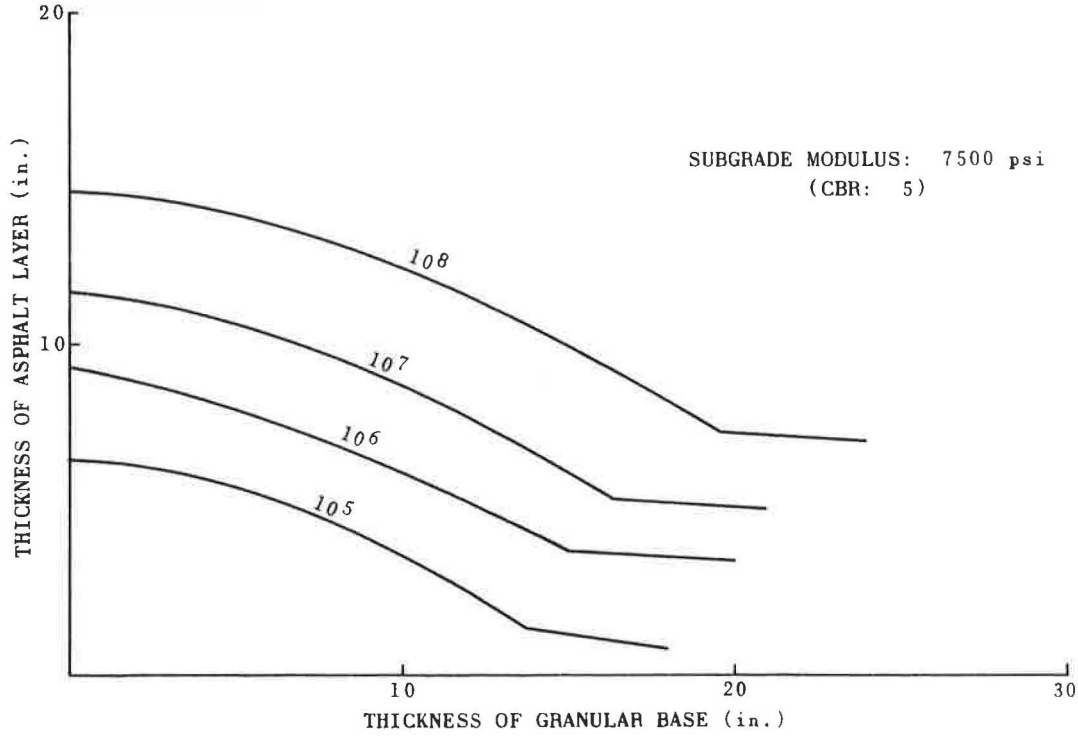

Figure 12. Design curves, 18,000-lb axle load.

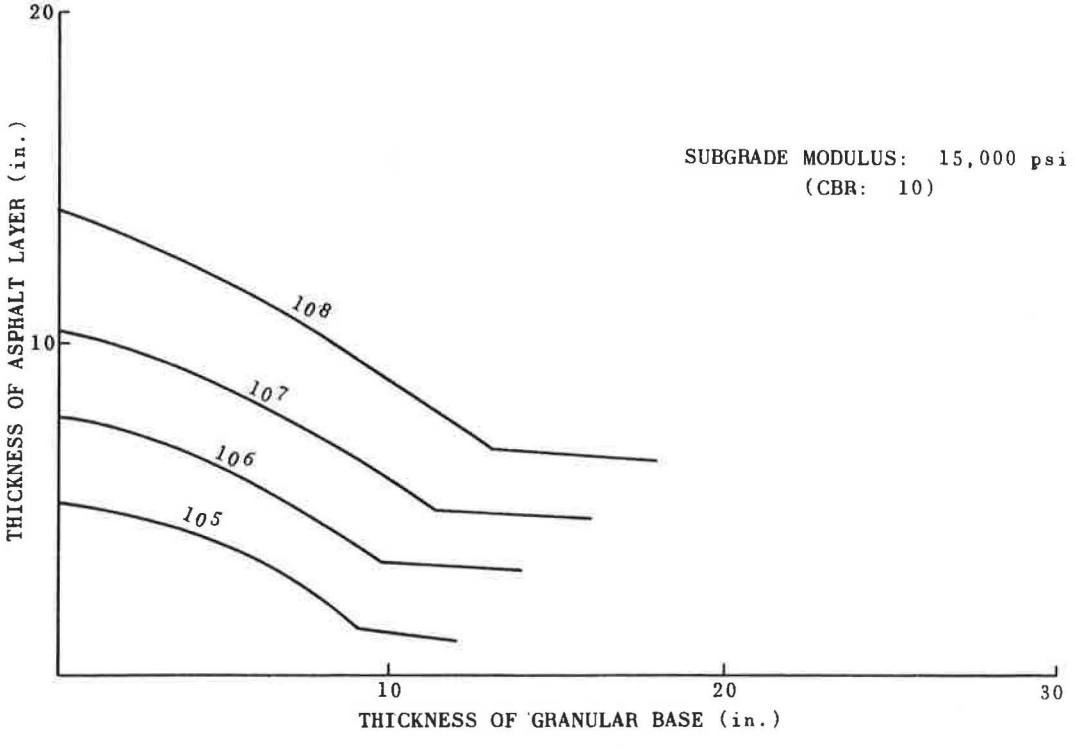

Figure 13. Design curves, 18,000-lb axle load.

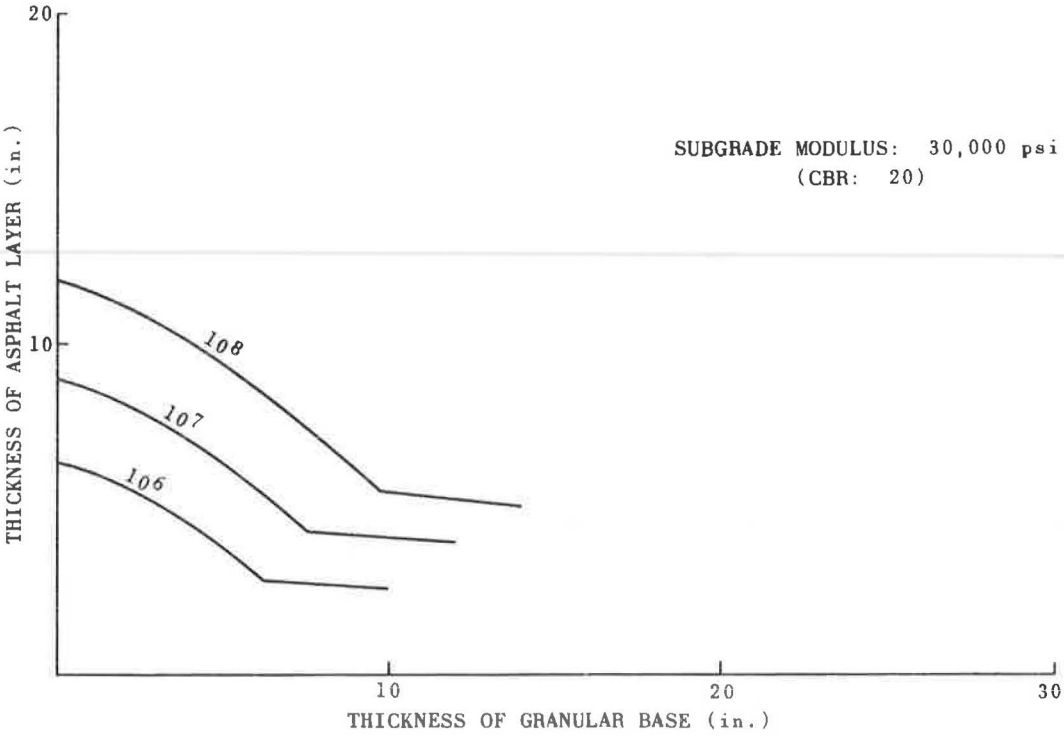

Figure 14. Design curves, 18,000-lb axle load.

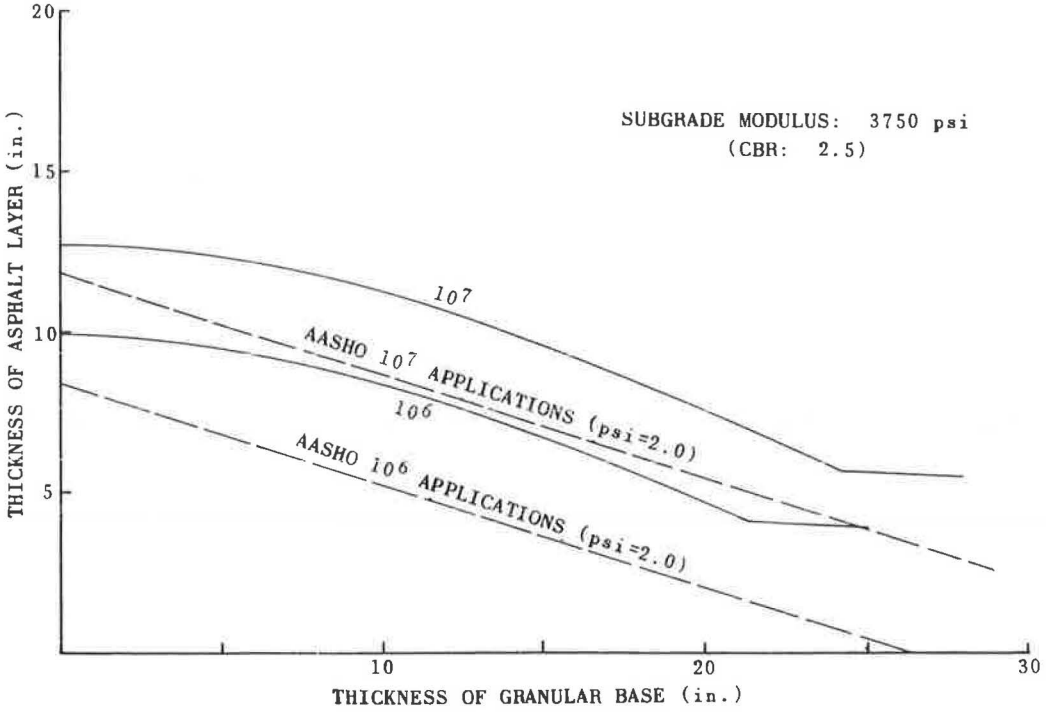

Figure 15. Design curves, 18,000-lb axle load.

in which D represents the structural number for the pavement, and D_1 and D_2 are the thicknesses of the surface and base course, respectively. The strength coefficients, 0.44 and 0.14, are selected from those listed by Liddle for "plant mix surface" and "crushed stone base." These are considered the most representative values for use in the equation. Carey and Irick (12) found that structural numbers of 3.7 and 5.2 correspond to 10^6 and 10^7 load applications for a terminal serviceability index of 2.0. These values are used in plotting the AASHO design lines.

Although the AASHO lines are somewhat below the theoretical curves, it must be noted that the AASHO designs shown here are based on a relatively low serviceability index of 2.0. The development of the theoretical designs depends on a relatively higher serviceability of 3.0 or higher.

The slope of the AASHO designs is roughly equal to the average trend of the theoretical curves. The AASHO designs, however, which plot as straight lines, have a constant equivalency ratio between surface and base of 3.1. No allowance is made for the change in equivalency ratio of different thicknesses of base shown by the theoretical designs. Otherwise, the distance separating the AASHO lines for the different magnitudes of load application is approximately the same as for the theoretical curves. This lends support to the belief that fatigue criteria developed for the theoretical method are reasonable.

CONCLUSION

A series of pavement design curves has been prepared on the basis of the principles of theoretical layered system analysis. The results demonstrate how theoretical methods can be utilized in the design of pavement for different subgrade strengths. Introduction of fatigue criteria to the method permits pavement design to be adjusted to different traffic intensities.

The guiding principle in the design method is to provide pavements in which the strains at critical locations within the structure do not exceed certain permissible values. In the present analysis, the different combinations of asphalt-bound surface and granular base are calculated to prevent excessive deformation of the subgrade and cracking of the asphalt surface. The method provides a series of design curves which represent equivalent designs for a given subgrade strength and magnitude of traffic. These offer a convenient basis for interchanging thicknesses of surface and base to meet economic requirements.

In the development of the method, it has been necessary to make certain assumptions concerning properties and strengths of materials. This need arises because precise information on these factors is frequently lacking. In these cases, assumptions are made on the basis of existing experience and results of laboratory tests. Use of these assumptions leads to designs that appear to be in reasonable agreement with practice. As additional information is accumulated in the future, specific values for design factors can be more thoroughly investigated. Any needed modifications can be made in accordance with these studies.

An example of this is the effect of climatic conditions. Because the design curves are drawn up on the basis of severe conditions (i.e., low soil strength and low dynamic modulus of the asphalt layer), it is probable that constructions will tend to be overdesigned, particularly for the thicker asphalt layers in temperate areas. It is felt undesirable, however, to apply a theoretical correction for such conditions until there is more confirmation from experience.

For the present, it is believed that the theoretical method provides a reliable basis for design and accurately reflects the influence of important design variables. It should be clear that work on the method is not concluded and modification of the proposals is a continuing process.

REFERENCES

1. Acum, W. E. A., and Fox, L. Geotechnique, Vol. 2, pp. 293-300, 1951.
2. Jones, A. Tables of Stresses in Three-Layer Elastic Systems. Highway Research Board Bull. 342, pp. 176-214, 1962.

3. Peattie, K. R. Stress and Strain Factors for Three-Layer Elastic Systems. Highway Research Board Bull. 342, pp. 215-253, 1962.
4. Peattie, K. R. Proc. Int. Conf. on the Structural Design of Asphalt Pavements, p. 403, 1962.
5. Dormon, G. M. Proc. Int. Conf. on the Structural Design of Asphalt Pavements, p. 785, 1962.
6. Fox, L. Road Res. Tech. Paper No. 9, D. S. I. R., H. M. S. O., 1948.
7. Whiffin, A. C., and Lister, N. W. Proc. Int. Conf. on the Structural Design of Asphalt Pavements, p. 499, 1962.
8. Heukelom, W., and Klomp, A. J. G. Proc. Int. Conf. on the Structural Design of Asphalt Pavements, p. 667, 1962.
9. The AASHO Road Test, Highway Research Board Spec. Rept. 61E, 1962.
10. Heukelom, W., and Foster, C. R. Proceedings, ASCE, Vol. 86, 1960.
11. Liddle, W. J. Proc. Int. Conf. on the Structural Design of Asphalt Pavements, p. 42, 1962.
12. Carey, W. N., and Irick, P. E. Proc. Int. Conf. on the Structural Design of Asphalt Pavements, p. 22, 1962.

Appendix

NOMENCLATURE

E_1 = elastic modulus of top (surface) layer,

E_2 = elastic modulus of second (base) layer,

E_3 = elastic modulus of third (subgrade) layer,

K_1 = modular ratio E_1/E_2,

K_2 = modular ratio E_2/E_3,

h_1 = thickness of top layer (in.),

h_2 = thickness of second layer (in.),

a = radius of loaded area (in.),

A = thickness ratio a/h_2,

H = thickness ratio h_1/h_2,

σ = unit contact pressure (psi),

ZZ1 = vertical stress at bottom of top layer,

ZZ2 = vertical stress at bottom of second layer,

RR1 = radial stress at bottom of top (surface) layer, and

RR3 = radial stress at top of third (subgrade) layer.

SAMPLE CALCULATIONS FOR DESIGN CURVES

Calculations apply to curves in Figure 10, i.e., E_3 = 3,750 psi, with 10^6 load applications of an 18,000-lb wheel load.

Subgrade Strain

Wheel Load.—Total load = 9,000 lb; contact pressure = 80 psi (σ); and radius of loaded area (a) = 6.0 in.

Permissible Strain. —6.5×10^{-4} (Fig. 5). Strain factor (ZZ2 - RR3) = strain $\times$ $E/\sigma = (6.5 \times 10^{-4})\ (3,735/80) = 0.0305$.

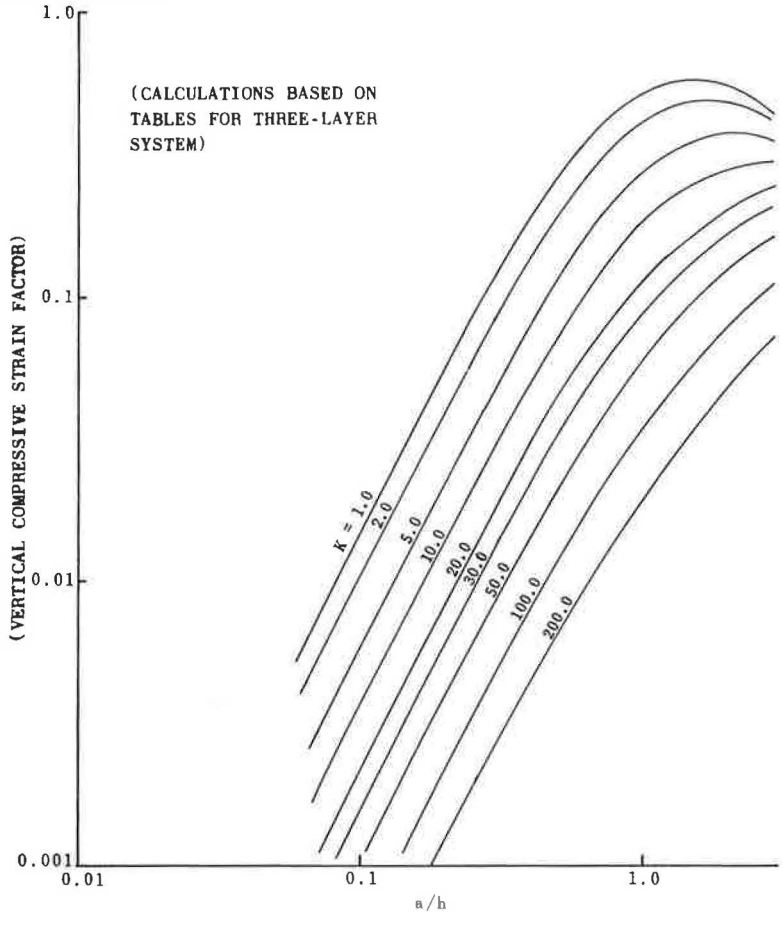

Figure 16. Vertical compressive strain on subgrade two-layer system.

No Granular Layer (Two-Layer Theory, Fig. 16). —Assume h = 10 in.; then E_1 = 180,000 psi (Fig. 2), and K_1 = 180,000/3,750 = 48.

By interpolation from chart for two-layer theory (Fig. 16) a/h = 0.61 and h = a/0.61 = 6.0/0.61 = 9.9 in. This is an agreement with assumed value; thus, provisional assumptions are satisfactory.

No Asphalt Layer (Two-Layer Theory, Fig. 16). —Assume h_2 = 28 in.; then K_2 = 4.0 (Fig. 4).

By interpolation from chart for two-layer theory (Fig. 16), a/h = 0.217, and h_2 = 6.0/0.217 = 27.5 in. Therefore, the provisional assumptions are satisfactory.

Intermediate Points. —When h_2 = 6 in. (A = 1.0), K_2 = 2 (Fig. 4). Assume h_1 = 9.0 in., then E_1 = 175,000 psi (Fig. 2), and K_1 = 175,000/7,500 = 23.4. By interpolation from three-layer data (2), H = h_1/h_2 = 1.55, and h_1 = 1.55 × 6.0 = 9.3 in.

When h_2 = 15 in. (A = 0.4), K_2 = 3 (Fig. 4). Assume h_1 = 7.0 in.; then E_1 = 165,000 psi (Fig. 2), and K_1 = 165,000/11,250 = 14.7. By interpolation from three-layer data (2), H = h_1/h_2 = 0.45, and h_1 = 0.45 × 15 = 6.75. Therefore, the provisional assumptions are satisfactory.

Tensile Strain in Asphalt Layer

Wheel Load. —Load is assumed to consist of one wheel of a dual-wheel pair. Total load = 9,000/2 = 4,500 lb; contact pressure = 80 psi; contact area = 56.2 sq in.; and radius of area = 4.2 in.

Permissible Strain. —1.45×10^{-4}. Strain factor $\frac{1}{2}$ (RR1 - ZZ1) = strain × E/σ = (1.45×10^{-4}) (900,000/80) = 1.63. A graphical representation of strain factors is contained in Ref. 3.

Tensile Strain Curve. —Points are determined by interpolation from three-layer data (2, 3). Calculations are made for several different thicknesses of granular base:

When h_2 = 5.25 in. (A = 0.8), K_2 = 1.9 (Fig. 4), E_1 = 900,000 psi, and K_1 = 126. By interpolation from tensile strain charts, H = 0.92, and h_1 = 4.8 in.

When h_2 = 10.5 in. (A = 0.4), K_2 = 2.6 (Fig. 4), E_1 = 900,000 psi, and K_1 = 92. By interpolation from tensile strain charts, H = 0.43, and h_1 = 4.5 in.

Discussion

K. R. PEATTIE, Esso Petroleum Co. Ltd., England. —The writer would like to comment on the use by Dormon and Metcalf of results from the AASHO Road Test in order to introduce the effects of repeated loads on the subgrade into a design method for flexible pavements.

The AASHO Road Test curves (9) showing the effect of numbers of axle loads on the thickness index were obtained by taking into account all the factors that reduced the serviceability indexes to the approporiate level. That is, they include the effect of repeated loads on the subgrade, the base courses, and the bituminous layers. However, Dormon and Metcalf have apparently used these curves as a basis for introducing the effect of repeated loads on subgrades alone because they treat the effect on the bituminous layers separately as a question of fatigue of bituminous materials.

Data relating to the effect of repeated applications of axle loads on the subgrade could be obtained from the results of the AASHO Road Test by calculating the stress or strain developed in the subgrade under the design load in pavement sections that were known to have failed by excessive deformation of the subgrade. These stresses or strains may then be plotted against the number of axle loads corresponding to the end value of the serviceability index. This has been done to a very limited extent by the writer (4). The main difficulty in extending this is the lack of knowledge of the mode of failure of the individual sections.

Furthermore, there are perhaps some doubts about the wisdom of applying the results of the AASHO Road Test in this way. In the first place, the climate and the types of construction used at the Road Test are not necessarily typical of those occurring in other regions. Secondly, the incidence of failures at the AASHO Road Test was not regular throughout the duration of the test. Most of the failures in the flexible sections occurred during the spring periods of 1959 and 1960, although the number of axle load applications increased smoothly throughout the test. There was no smooth relationship between axle applications and damage to the subgrade.

There is an urgent need to introduce the effect of repeated loads on the subgrade into design methods for flexible pavements. This may be done by using the results of laboratory tests on soils in conjunction with road trials in which damage is known to have increased smoothly with the buildup of axle loads.

Some Notes on Pavement Structural Design—Part 2

NORMAN W. McLEOD
Asphalt Consultant, Imperial Oil Ltd., Toronto, Ontario, Canada

This continuation of the paper of the same title presented at the 1963 Annual Meeting of the Highway Research Board is concerned with the elastic layered system method of pavement design proposed by Burmister in 1943. It is shown that for subgrades with CBR ratings from about 4 to 20, the Burmister equation can provide thickness requirements that are practically identical with those of the Corps of Engineers. Over the same range of subgrade support, the design curve provided by the Burmister equation practically coincides with the thickness requirements given by the Canadian Department of Transport's design equation, $T = K \log P/S$, when using empirically determined values for K. The reason for the good agreement in the latter case is investigated. It is shown that the approximate method of analysis for a multilayered pavement system referred to in last year's paper can lead to underdesign for a small number of pavement layers and to overdesign for a larger number of layers. Reference is made to the development of the method of pavement design in which all materials above the subgrade are treated with an asphalt binder. The urgent need for a simple laboratory method for accurately measuring the modulus of elasticity or some other rational strength value of subgrades and different pavement materials is emphasized.

•THIS paper, like last year's (1), is concerned primarily with the elastic layered system approach to pavement design (Fig. 1) that was originally published by Burmister (2) in 1943.

It is reasonable to ask how closely the thicknesses of flexible pavements provided by the elastic layered system approximate the thickness requirements of some of the empirical methods in current use. The Corps of Engineers' design curves, based on CBR ratings of subgrade strength, are well known and are supported by results from extensive full-scale field tests.

In Figure 2, the solid line represents the Corps of Engineers' design curve for an airplane single wheel load of 60,000 lb at 100-psi tire inflation pressure. The broken line curve represents the Burmister equation, assuming that the granular base material has an elastic modulus E_1 of 15,000 psi. The use of the Burmister equation to obtain the thicknesses indicated by the broken line curve of Figure 2 is illustrated by Table 1. The relationship between Burmister's deflection factor F_W, pavement thickness expressed as T/r, and the ratio of pavement elastic modulus to subgrade elastic modulus E_1/E_2 was shown previously (1, Fig. 1). The relationship between CBR and plate bearing values (1, Fig. 15) provides a common basis of comparison for the two designs.

From Figure 2, it is apparent that for subgrade CBR values ranging from about 4 to 20, the range of subgrade strengths most frequently encountered in practice, the pavement thickness requirements given by the Burmister equation are practically identical with those of the Corps of Engineers. For subgrade CBR values lower than 4 and greater

Paper sponsored by Committee on Flexible Pavement Design and presented at the 43rd Annual Meeting.

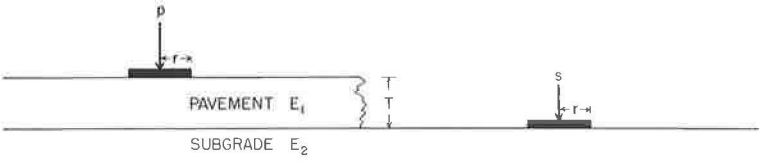

$T = K \log \frac{p}{s}$ CANADIAN D.O.T. (1)

$W_p = \frac{1{\cdot}18\,pr}{E_2} \times F_w$ PAVEMENT *(BURMISTER)*

$W_s = \frac{1{\cdot}18sr}{E_2}$ SUBGRADE *(BOUSSINESQ)*

WHERE T = THICKNESS OF PAVEMENT
p = WHEEL LOAD
s = SUBGRADE SUPPORT
K = PAVEMENT FACTOR

WHERE W_p = PAVEMENT DEFLECTION
W_s = SUBGRADE DEFLECTION
r = RADIUS OF LOADED AREA
E_2 = ELASTIC MODULUS OF SUBGRADE
F_w = DEFLECTION FACTOR

WHEN $W_p = W_s$

$F_w = \frac{s}{p}$

SUBSTITUTING IN EQUATION (I)

$K = \frac{T}{-\log F_w}$ (2)

Figure 1. Relationship between Canadian Department of Transport and Burmister equations for pavement design.

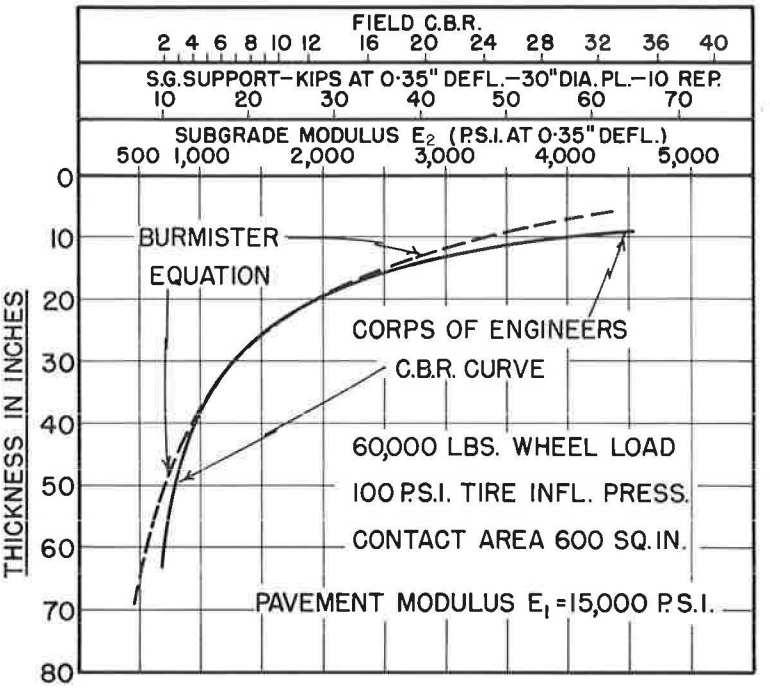

Figure 2. Comparison of Corps of Engineers and Burmister design curves for 60,000-lb wheel load.

TABLE 1

DATA FOR CONSTRUCTION DESIGN CURVE FOR AN AIRPLANE SINGLE WHEEL LOAD BURMISTER EQUATION[a]

$\frac{E_1}{E_2}$	Subgrade Elastic Modulus, E_2 (psi)	Subgrade Support, S[b] (lb)	$F_w = \frac{S}{P}$	$\frac{T}{r}$	Pavement Thickness, T (in.)
4	3,750	48,240	0.804	0.60	8.3
5	3,000	38,590	0.643	0.88	12.1
6	2,500	32,160	0.536	1.16	16.0
8	1,875	24,120	0.402	1.56	20.1
10	1,500	19,290	0.322	1.87	25.8
15	1,000	12,860	0.214	2.70	37.2
20	750	9,650	0.161	3.46	47.8
30	500	6,430	0.107	4.70	65.0

[a]Single wheel load, P = 60,000 lb,
Tire inflation pressure = 100 psi,
Pavement deflection = 0.35 in.,
Tire contact area = equiv. to 27.64-in. diam. bearing plate,
Radius of contact area, r = 13.82 in., and
Elastic modulus of pavement material, E_1 = 15,000 psi.

[b]$S = \frac{E_2 w r}{0.376} = \frac{E_2 (0.35)(13.82)}{0.376} = 12.86\ E_2$

than 20, the Burmister curve calls for slightly less thickness than the Corps of Engineers' curve. However, Foster (3) has pointed out that for the higher subgrade CBR values, the Corps of Engineers' design curves are probably conservative. In addition, the compaction of granular base over very soft subgrades to a specified density is very difficult, and the normal value of the elastic modulus E_1 of the granular material may not be achieved throughout the full depth. This lower E_1 value would have to be compensated for by a somewhat greater thickness to attain the same load-carrying capacity, which in this case is a single wheel load of 60,000 lb.

CANADIAN DEPARTMENT OF TRANSPORT VS BURMISTER DESIGN CURVES

The design equation

$$T = K \log \frac{P}{S} \tag{1}$$

(Fig. 1) was developed from the analysis of hundreds of plate bearing tests on flexible pavements on airport runways in Canada (4), and has been used successfully by the Canadian Department of Transport for the design of flexible pavements at more than 100 airports during the past fifteen years. The pavement factor K in Eq. 1 was evaluated empirically by substituting measured values for P, S, and T and solving for K. This resulted in an empirical relationship between K and the diameter of the loaded area (circular steel plates) (1, Fig. 5).

By employing Eq. 1, and the value of K = 35 indicated (1, Fig. 5) for a 12-in. diameter bearing plate, the solid line thickness design curve of Figure 3 is obtained for a wheel load of 9,000 lb at a tire inflation pressure of 80 psi for very heavy traffic. The

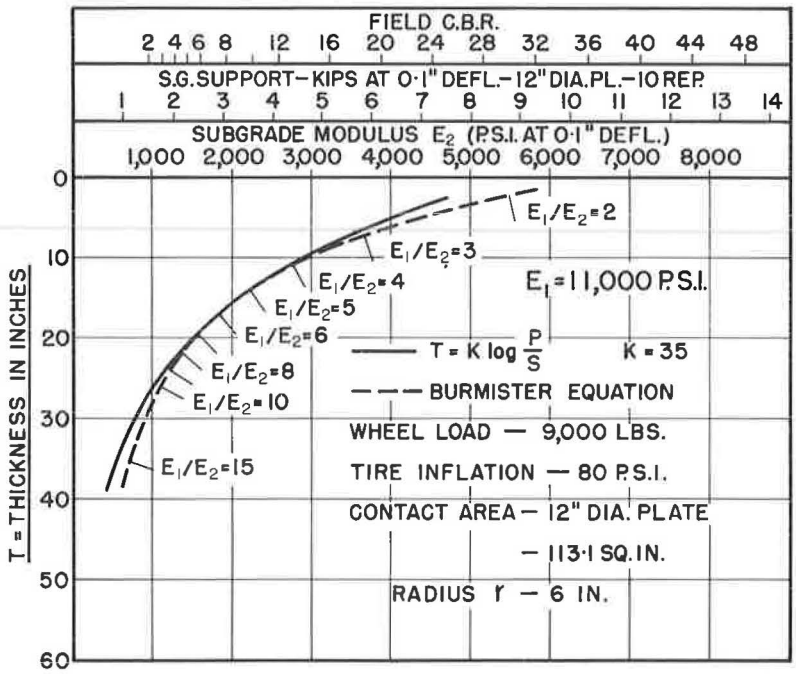

Figure 3. Comparison of Canadian Department of Transport and Burmister design curves for 9,000-lb wheel load.

TABLE 2

EVALUATION OF PAVEMENT CONSTANT K BY BURMISTER EQUATION[a]

$\frac{E_1}{E_2}$	Subgrade Elastic Modulus, E_2 (psi)	Subgrade Support, S[b] (lb)	$F_W = \frac{P}{S}$	$\frac{T}{r}$	Pavement Thickness, T (in.)	$\frac{P}{S}$	$\text{Log}\frac{P}{S}$	$K = \frac{T}{\log \frac{P}{S}}$
3	3,667	5,865	0.652	1.30	7.8	1.535	0.1860	41.9
4	2,750	4,400	0.490	1.85	11.1	2.046	0.3108	35.7
5	2,200	3,520	0.391	2.35	14.1	2.557	0.4077	34.5
6	1,833	2,930	0.326	2.82	16.9	3.070	0.4871	34.7
7	1,571	2,510	0.279	3.22	19.3	3.586	0.5546	34.8
8	1,375	2,200	0.244	3.65	21.9	4.091	0.6118	35.8
10	1,100	1,760	0.196	4.30	25.8	5.114	0.7087	36.4
15	733	1,170	0.130	5.95	35.7	7.679	0.8853	40.0

[a]Single wheel load, P = 9,000 lb;
Tire inflation pressure = 80 psi;
Pavement deflection = 0.1 in.;
Tire contact area = equiv. to 12-in. diam. bearing plate;
Radius of contact area, r = 6 in.;
Elastic modulus of pavement material, E_1 = 11,000 psi.

[b]$S = \frac{E_2 \, w \, r}{0.376} = \frac{E_2 (0.1)(6)}{0.376} = 1.6 \, E_2$

tire contact area is assumed to be equal to that of a 12-in. diameter circular steel plate. The broken line curve in Figure 3 is given by the Burmister equation for the same wheel load and tire inflation pressure (Table 2) if it is assumed that the elastic modulus E_1 of the pavement material has a value of 11,000 psi. It is clear from Figure 3 that for the range of CBR subgrade strength ratings from about 3 to 20, the flexible pavement thickness requirements indicated by Eq. 1 and by the Burmister equation are practically identical. For subgrade CBR strength values less than 3 and more than 20, the use of Eq. 1 in conjunction with a value of 35 for the pavement factor K indicates slightly less pavement thickness than the Burmister equation calls for.

Consequently, for the most commonly occurring range of subgrade CBR strength ratings (3 to 20), the Burmister equation derived from a purely theoretical study of the elastic properties of a layered pavement system is capable of providing flexible pavement thickness requirements practically identical with those indicated by the entirely empirical Corps of Engineers and Canadian Department of Transport methods of design.

DISCUSSION OF THE PAVEMENT FACTOR K

It was shown (1) that Eq. 1, derived empirically from the analysis of data from plate bearing tests, is closely related mathematically to the design equation developed by Burmister from a theoretical study of the elastic properties of a two-layer pavement system. As illustrated by Figure 1, the mathematical bridge between these two design equations is provided by

$$K = \frac{T}{-\log F_W} \tag{2}$$

Previously provided values (1, Fig. 10) for Burmister's deflection factor F_W are seen to depend on pavement thickness T and the ratio E_1/E_2, in which E_1 and E_2 are elastic moduli of the pavement and subgrade, respectively. Therefore, it follows from this and Eq. 2 that the value of the pavement factor K in Eq. 1 also depends on the pavement thickness T and the ratio of E_1/E_2. This is illustrated in Figure 4. Consequently, since Eq. 1 and the Burmister equation appear to be mathematically identical, it is clear that if the values of K provided by Figure 4 were employed for Eq. 1, the design curve provided by Eq. 1 would coincide at all points with the broken line curve in Figure 3 given by the Burmister equation. The difference between the solid and broken line curves in Figure 3, therefore, is due to the use of the empirical value of 35 for the pavement factor K in Eq. 1.

From Figure 3 it can be seen that the value of the ratio of E_1/E_2 ranges from 2 to 15 for different points on the broken line Burmister design curve. It would be expected from an examination of Figure 4 that a range of values from 2 to 15 for E_1/E_2 would result in a corresponding substantial range of values for the pavement factor K. Nevertheless, Figure 3 demonstrates that when K has the constant empirical value of 35, the solid line design curve provided by Eq. 1 practically coincides with the broken line design curve given by the theoretical Burmister equation for a wide range of subgrade strength ratings. It is worthwhile investigating the reason for this apparent inconsistency.

Figure 5 illustrates a typical plot of load test data obtained by a 30-in. diameter bearing plate at 0.5-in. deflection on the subgrade and on the surface of 12 in. of granular base at a number of Canadian airports. Figure 6 provides similar information for a granular base thickness of 21 in. Similar graphs of plate bearing test data have been published elsewhere (4, 5). The plots of data in Figures 5 and 6, and in other similar graphs, led to the development of Eq. 1 and to the empirical values for the pavement factor K (1, Fig. 5).

In Figure 7, Line (1), K = 35, represents the straight line relationship between the load-supporting values at the surface of 15 in. of normal granular base and the corresponding load-supporting values of underlying subgrades of different strengths, both measured with a 12-in. diameter bearing plate at 0.1-in. deflection, that would be expected on the basis of Eq. 1 if the pavement factor K had a constant empirical value of

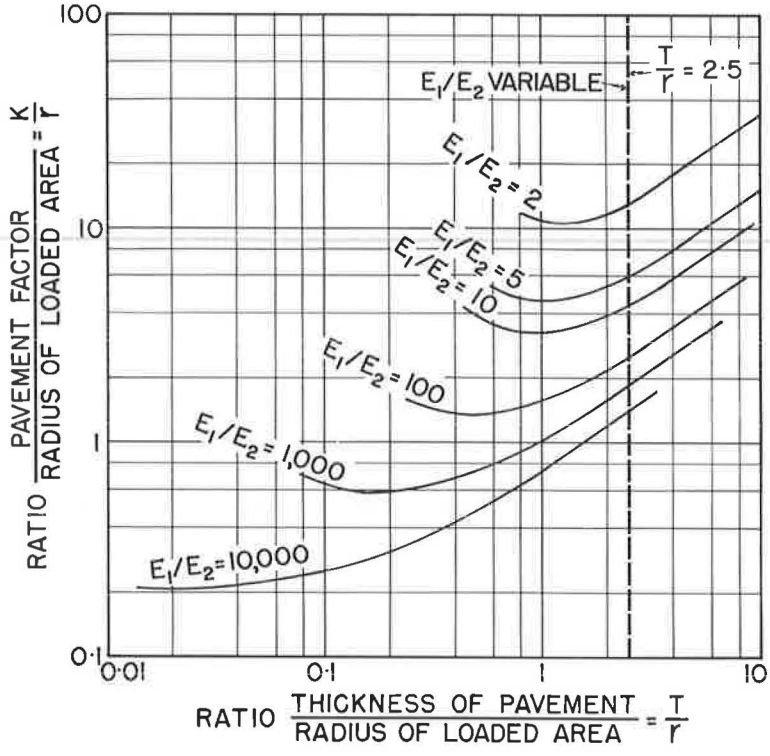

Figure 4. Theoretical relationships between pavement factor K, E_1/E_2, and pavement thickness T.

35, regardless of the strength of the subgrade. On the other hand, Lines (2), (3), and (4) indicate, for a 12-in. diameter bearing plate at 0.1-in. deflection, the curved line relationships between loads on subgrades of different strengths vs the corresponding loads on 15-in. thicknesses of granular bases having elastic moduli of 10,000, 15,000, and 20,000 psi, respectively, given by the Burmister equation. Consequently, the problem arises as to whether the relationship between load on the subgrade and the corresponding load on 15 in. of granular base is provided more accurately by the straight line relationship of Line (1) or by the curved line relationship of Lines (2), (3), and (4). The straight line relationship of Line (1) appears to be supported empirically by actual plate bearing test data such as those of Figures 5 and 6. On the other hand, the curved line relationship of Lines (2), (3), and (4) is indicated by the theoretically derived Burmister equation for an elastic two-layer pavement system.

It was realized at the time Eq. 1 was originally developed that a constant value of K for any given granular material, on which the straight line relationship of Figures 5 and 6 and Line (1) of Figure 7 depends, could apply to only a limited range of subgrade support and of thickness of granular base. Quite obviously, if a layer of granular material were placed on a subgrade as strong as itself, it would provide no increase in load-carrying capacity. In this case, because the value of P/S in Eq. 1 would be unity, the value of the pavement factor K would become infinite. Figure 8 demonstrates that according to the Burmister strength curve, when 15 in. of granular base having an elastic modulus E_1 of 10,000 psi is placed on subgrades of increasing strength, as the values of the ratio of P/S in Eq. 1 approach unity, the corresponding values of K increase from 35 to 50, 75, 100, and 200, and finally become infinite when the strength of the subgrade becomes equal to that of the base course material, that is, when the value of P/S becomes unity.

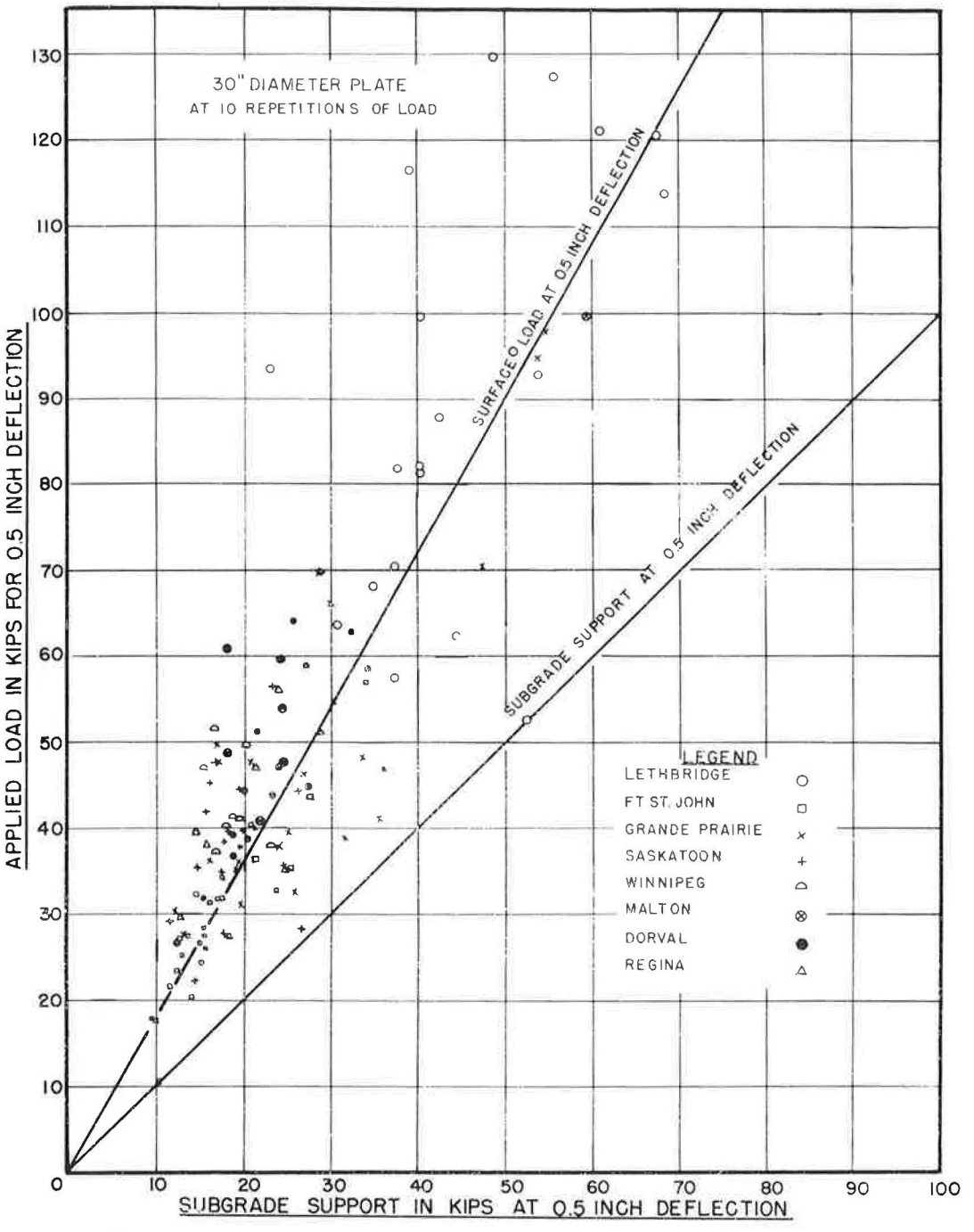

Figure 5. Applied load on 12-in. pavement vs subgrade support.

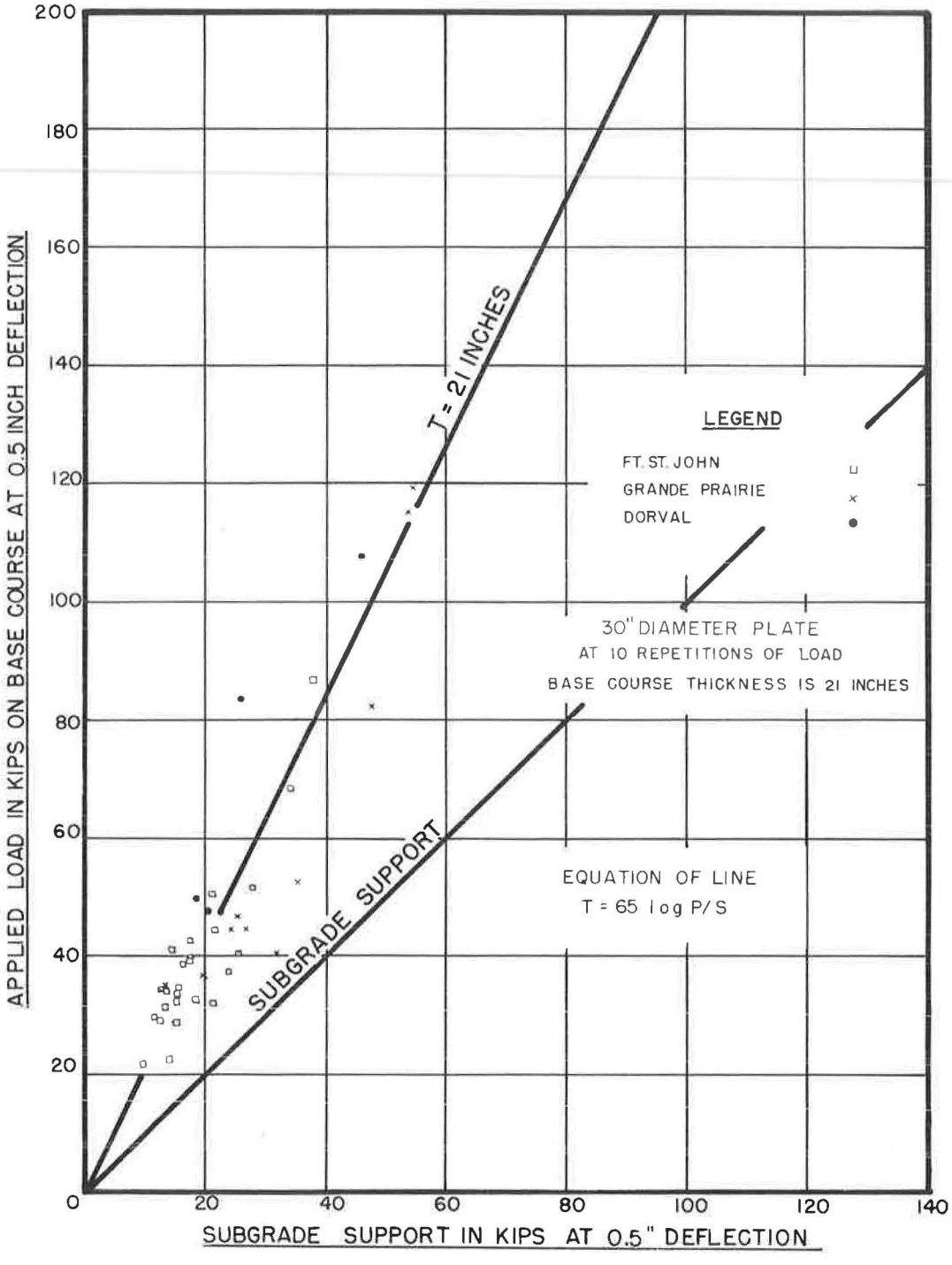

Figure 6. Applied load on 21-in. pavement vs subgrade support.

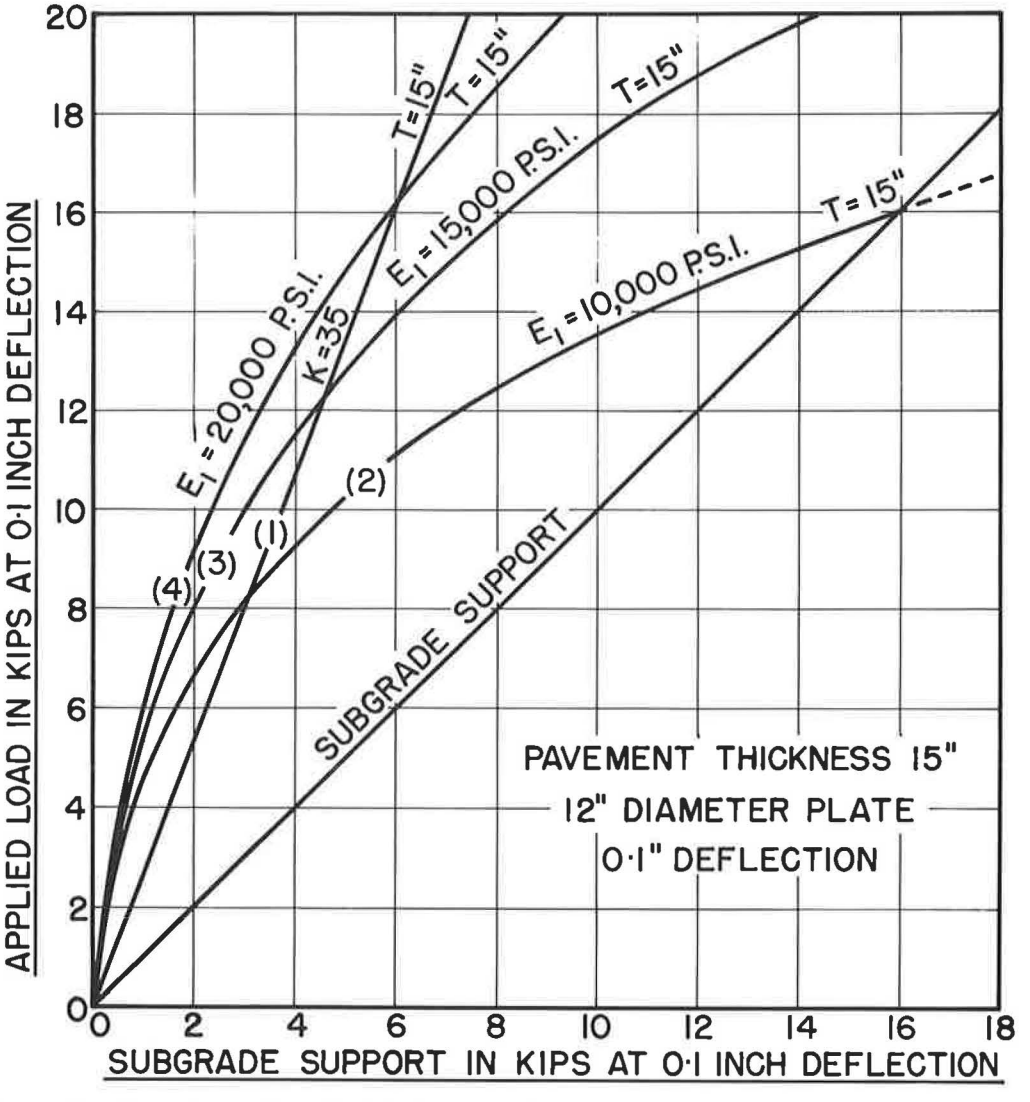

Figure 7. Comparison of applied loads on 15-in. pavement indicated by Canadian Department of Transport empirical design and Burmister theoretical design.

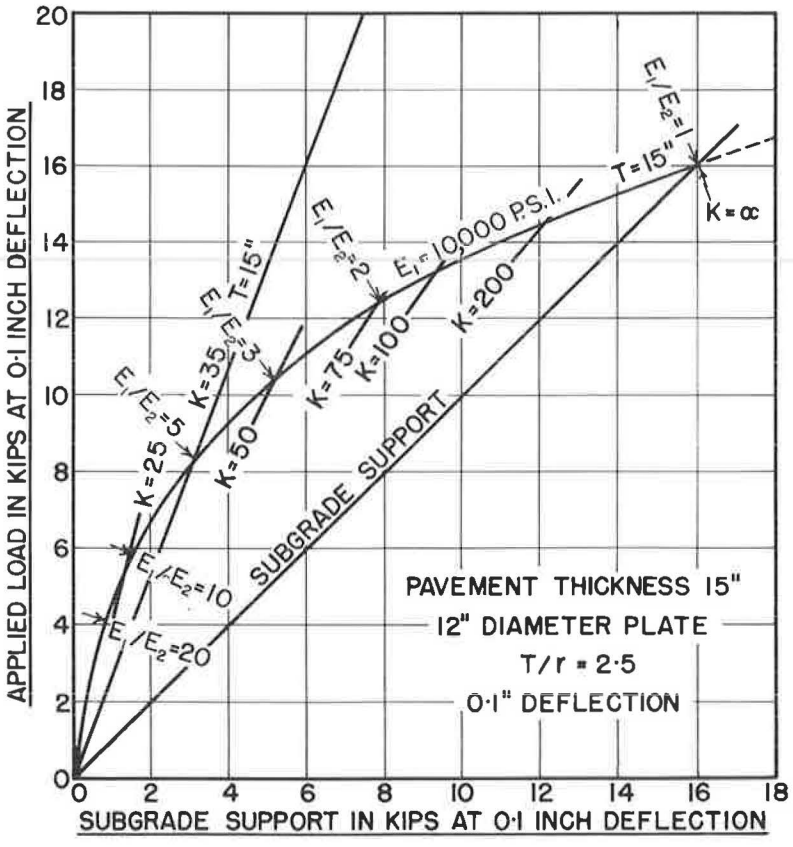

Figure 8. Relationship between empirical and theoretical values of pavement factor K for a given 15-in. pavement.

The Burmister strength curve of Figure 8 also shows that for stronger and stronger subgrades the value of the ratio E_1/E_2 decreases (the elastic modulus of the granular base E_1 = 10,000 psi and is constant, whereas the elastic modulus of the subgrade E_2 increases as the strength of the subgrade is increased) and becomes unity when the elastic modulus of the subgrade E_2 becomes equal to the elastic modulus of the base course material E_1. Therefore, the curved line of Figure 8 represents the case in which the values of E_1 and T/r are constant, but the ratio E_1/E_2 changes with a change in subgrade strength (subgrade elastic modulus E_2), and the applied load P increases as the value of the ratio E_1/E_2 decreases. This set of conditions is also illustrated by the heavy vertical line in Figure 4, which represents a constant value for T/r of 2.5 but a wide range of values for the ratio of E_1/E_2.

If the relationship between load on the subgrade and load on a superimposed specified thickness of any given granular base material should be represented by curved lines such as Lines (2), (3), and (4) in Figure 7, how is the straight line relationship in Figures 5 and 6, that appears to be indicated by plotting actual load test data, to be explained? There would appear to be several possible explanations. One, of course, is the certain scatter of data inevitably associated with plate bearing tests on pavements, which makes it difficult to plot relationship trends with complete confidence.

Another reason is that the load test data were obtained at eight different airports for Figure 5 and at three different airports for Figure 6. The E_1 or elastic modulus values of the granular materials at the different airports are not likely to have been identical. Figure 7 indicates that for the same range of subgrade strengths, a given thickness of

granular materials with different E_1 values could provide load test values that would seem to cluster along Line (1), when instead they could actually belong to a series of curved lines representing different E_1 values, such as Lines (2), (3) and (4).

A third possible reason is that it is difficult to compact granular materials to high density on weak subgrades, but this can be achieved readily on strong subgrades. It is known that the elastic modulus E_1 of any given granular material will be low if it is poorly compacted and higher if it is thoroughly compacted. Consequently, even if under certain standard conditions, all base course materials at the airports represented by the data of Figures 5 and 6 had approximately the same E_1 value, the E_1 value actually developed in the field could be lower than this on weak subgrades due to poor compaction and could be higher on stronger subgrades because of compaction to higher density. This gradual increase in the E_1 values of any given granular base when placed on stronger and stronger subgrades would also make the load test data seem to cluster along Line (1) of Figure 7, rather than along curved lines like Lines (2), (3), and (4) where they might actually belong because of the different E_1 values developed in the field.

It would seem on the basis of this discussion, therefore, that the load test data for subgrades and for given thicknesses of superimposed granular base, which appear to support a straight line relationship in Figures 5 and 6, would in each case probably be more accurately represented by either a single curved line or by a series of curved lines similar to Lines (2), (3) and (4) in Figure 7 where each curved line corresponds to a different value of elastic modulus E_1 for the granular base material.

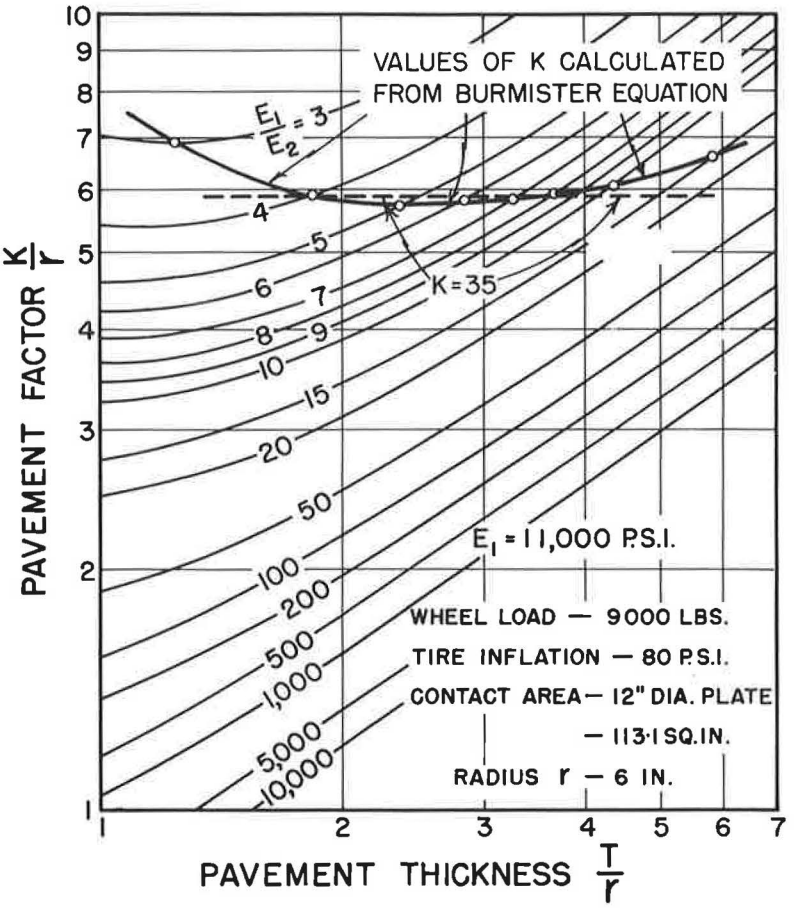

Figure 9. Relationship between theoretical and empirical values of pavement factor K.

This discussion has shown that for any given base course material, it seems quite unlikely that the pavement factor K in Eq. 1 can have a constant value that depends only on the diameter of the loaded area (1, Fig. 5) and that it cannot, therefore, be represented by a straight line relationship like that of Line (1) in Figure 7. Instead, it appears that the value of K also depends on the thickness of granular base and on the strength of the subgrade on which it is placed. It is of interest, therefore, to determine why in Figure 3 the use of a constant value of 35 for the pavement factor K in Eq. 1 provides a design curve (solid line) for a wheel load of 9,000 pounds that for the range of CBR subgrade strength ratings between about 3 and 20 practically coincides with the design curve (broken line) given by the Burmister equation for the same wheel load.

For the Burmister design curve in Figure 3, the elastic modulus of the granular base E_1 has the constant value of 11,000 psi and the applied load of 9,000 pounds is also constant, but both the thickness of base T and the value of the ratio E_1/E_2 increase as the subgrade strength decreases, and vice versa. Table 2 provides corresponding values of subgrade elastic modulus E_2 and pavement thickness T obtained by the Burmister equation, from which the Burmister design curve (broken line curve) of Figure 3 is plotted. Table 2 also gives data obtained by the Burmister equation that enable values for the pavement factor K of Eq. 1 to be calculated for various points along the Burmister design curve.

Values of the pavement factor K associated with the Burmister design curve of Figure 3, expressed in terms of K/r and corresponding values of E_1/E_2 (Table 2), are plotted as the curved solid line in Figure 9. The straight horizontal broken line in Figure 9 represents the value of 35 for the pavement factor K that was employed with Eq. 1 to obtain the solid line design curve of Figure 3.

It is clear from Figure 9 that the corresponding values for T/r and E_1/E_2 change in such a way over a wide range that the values of the pavement factor K obtained from the Burmister equation are practically equal to the empirically derived value of 35. Stated more completely, Figure 9 demonstrates that for the design conditions of Figure 3, the values of the pavement factor K that can be calculated from the Burmister equation are almost identical to the empirically determined value of 35 for the pavement factor K for the range of subgrade strength ratings ordinarily encountered in pavement design (CBR 3 to 20). It is for this reason also that Eq. 1, together with the simple empirical values for the pavement factor K (1, Fig. 5), provides thickness requirements for conventional flexible pavements that are in good agreement with other empirical methods of structural design.

ACCURACY OF APPROXIMATE METHOD OF DESIGN FOR MULTILAYERED PAVEMENTS

During the past decade or so, studies based on the elastic properties of a three-layer pavement have been made to evaluate the stresses and strains at all points in a loaded three-layer pavement system, and rational methods of pavement design employing the values obtained have been proposed (6, 7, 8, 9). It should be noted, however, that the accuracy of these rational methods of design depends on how nearly the pavement materials actually employed on each project are represented by such assumptions as those of elasticity, isotropy, and values of Poisson's ratio employed when applying the rational method, and on the ability of currently available test methods to make the necessary strength measurements on the various pavement materials and on the subgrade soil with the degree of precision required.

Until the influence of these uncertainties on the pavement design requirements provided by these rational methods has been established, there would appear to be room for simpler methods of design that might also be considered to be rational, or at least quasi-rational if they can be devised. It was for this reason that an approximate rational method for the design and evaluation of multilayered pavements was suggested in the final section of last year's paper. For this approximate method it was assumed that a multilayer pavement could be converted step by step to an equivalent two-layer pavement by employing Burmister's analysis for an elastic two-layer pavement system.

It is worthwhile to examine the degree of accuracy that this approximate method provides. Figure 10 illustrates the method of analysis to be employed for this purpose.

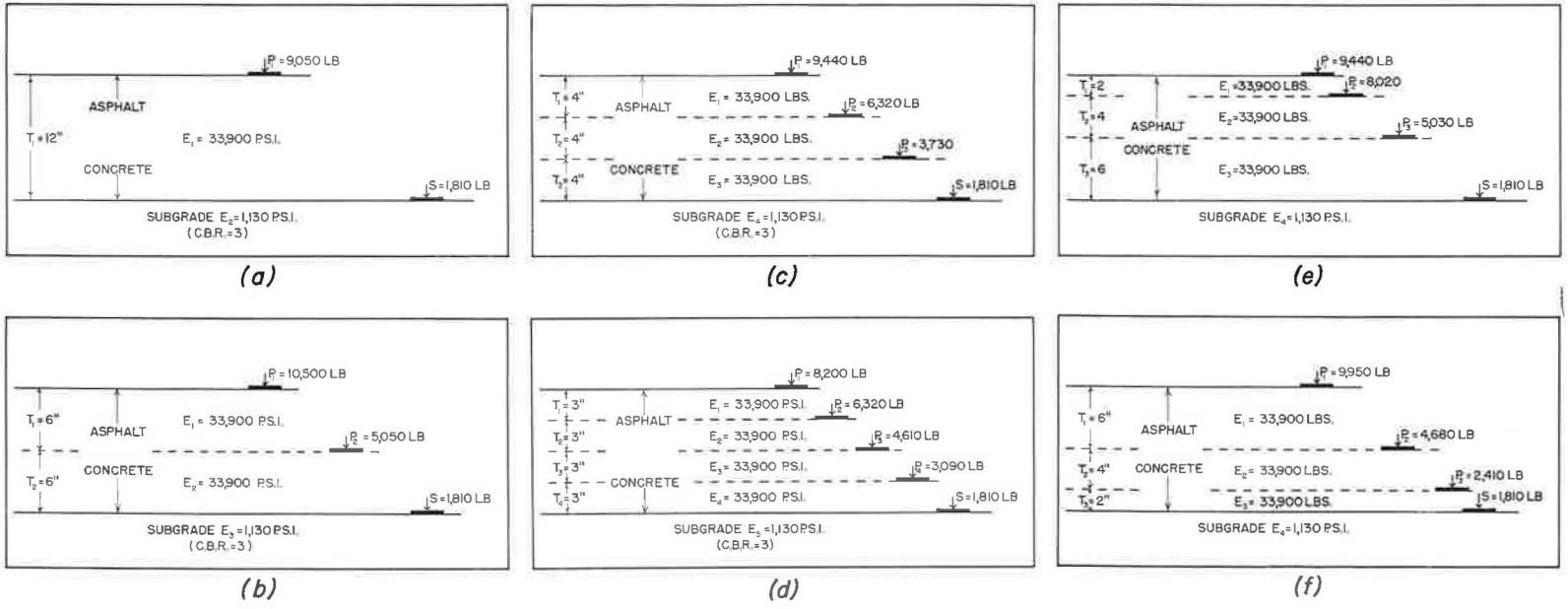

Figure 10. Limitations of approximate method of analysis for multilayer pavement system.

First, Figure 10a, a two-layer pavement system consisting of 12-in. of given pavement material on a specified subgrade, is analyzed by Burmister's method to determine the load it will support on a 12-in. diameter bearing plate at 0.1-in. deflection. It is then assumed (Figs. 10b to 10f) that this 12-in. layer of given pavement material consists of two 6-in. layers, or three 4-in. layers, or four 3-in. layers, etc., and the approximate method of analysis referred to in the last section of the 1963 paper is employed to calculate the load-carrying capacity of each of these multilayer pavement systems. In all cases, the strength of the subgrade (elastic modulus = 1,130 psi), the thickness (12 in.), and strength (elastic modulus = 33,900 psi) of the pavement material remain the same. The calculations for the cases represented by Figures 10a and 10b are illustrated below:

Case 1. Two-Layer Pavement (Fig. 10a)

Given: $E_1 = 33,900$ psi, $E_2 = 1,130$ psi, $T_1 = 12$ in., r = radius of loaded area = 6 in., and pavement deflection = 0.1 in.

Problem: What load will this two-layer pavement support?

Solution:

$$\frac{E_1}{E_2} = \frac{33,900}{1,130} = 30,$$

$$\frac{T_1}{r} = \frac{12}{6} = 2,$$

$$F_W = 0.2 \text{ (1, Fig. 10)},$$

$$S = \frac{E_2 wr}{0.376} = \frac{(1130)(0.1)(6)}{0.376} = 1,810 \text{ lb, and}$$

$$P_1 = \frac{S}{F_W} = \frac{1,810}{0.2} = 9,050 \text{ lb.}$$

Therefore, the two-layer pavement structure illustrated in Figure 10a will support heavy traffic by a wheel load of 9,050 pounds or equivalent.

Case 2. Three-Layer Pavement (Fig. 10b)

Given: E_1 and $E_2 = 33,900$ psi, $E_3 = 1,130$ psi, T_1 and $T_2 = 6$ in., r = radius of loaded area = 6 in., and pavement deflection = 0.1 in.

Problem: What load will this three-layer pavement support?

Solution:

$$\frac{E_2}{E_3} = \frac{33,900}{1,130} = 30,$$

$$\frac{T_2}{r} = \frac{6}{6} = 1,$$

$$F_W = 0.36 \text{ (1, Fig. 10)},$$

$$S = 1,810 \text{ lb (from Case 1), and}$$

$$P_2 = \frac{S}{F_W} = \frac{1,810}{0.36} = 5,050 \text{ lb.}$$

The assumption is now made that an equivalent homogeneous soil of elastic modulus E_{23} will also support a load $P_2 = 5,050$ lb at 0.1-in. deflection, from which

$$E_{23} = \frac{0.376\, P_2}{wr} = \frac{(0.376)(5,050)}{(0.1)(6)} = 3,170 \text{ psi},$$

$$\frac{E_1}{E_{23}} = \frac{33,900}{3,170} = 107.7,$$

$$\frac{T_1}{r} = \frac{6}{6} = 1,$$

$F_W = 0.48$ (1, Fig. 10), and

$$P_1 = \frac{P_2}{F_W} = \frac{5,050}{0.48} = 10,500 \text{ lb.}$$

Therefore, according to this approximate method of analysis, the three-layer pavement of Figure 10b will support heavy traffic by a wheel load of 10,500 lb or equivalent.

However, the pavement system of Figure 10b is identical with that of Figure 10a. In both cases it consists of 12 in. of pavement material with an elastic modulus of 33,900 psi on a subgrade with an elastic modulus of 1,130 psi. Therefore, the difference in wheel load supporting values, 10,500 pounds for Case 2 vs 9,050 pounds for Case 1, represents in this instance the degree of accuracy provided by the approximate method for analyzing the three-layer pavement system. In this particular example, the use of the approximate method would lead to 16 percent underdesign because it indicates a supporting capacity of 10,500 lb for a pavement that will actually support only 9,050 lb.

Figure 10c shows that a similar analysis on the basis of three 4-in. pavement layers on the same subgrade results in a load-carrying capacity of 9,440 lb, which represents 4.3 percent underdesign. On the other hand, as demonstrated by Figure 10d, the load-supporting value of 8,200 lb indicated by an analysis based on four 3-in. pavement layers represents 9.4 percent overdesign. Figures 10e and 10f show that the same analysis applied to three pavement layers of unequal thickness (6, 4, and 2 in.), placed in two different sequences results in overestimating the load-carrying capacity of the pavement structure, and, therefore, in underdesign.

The results of a similar set of calculations, summarized in Table 3 for 24 in. of pavement material having an elastic modulus of 12,430 psi on a subgrade with an elastic modulus of 1,130 psi (CBR 3), also indicate a load-supporting value of 9,050 lb on a 12-in. diameter bearing plate at 0.1-in. deflection when analyzed as a two-layer pavement system. However, when the pavement layer itself is divided into two, three, and four layers and analyzed on this basis by the approximate method, the load-carrying capacity of the pavement structure is overestimated by nearly 30 percent.

TABLE 3

LOAD SUPPORTING VALUES CALULATED BY APPROXIMATE METHOD OF ANALYSIS[a]

No. of Pavement Layers	Load (lb)
1	9,050
2	11,500
3	11,800
4	11,200

[a]Diameter of bearing plate = 12 in.;
Radius of loaded area = 6 in.;
Pavement of deflection = 0.1 in.;
Pavement thickness = 24 in.;
Elastic modulus of pavement material, E_1 = 12,430 psi; and
Elastic modulus of subgrade, E_2 = 1,130 psi (CBR = 3)

Figure 10 and the results summarized in Table 3 indicate, therefore, that for the number of layers of pavement ordinarily employed, which seldom exceeds three pavement layers on top of the subgrade, the use of the approximate method referred to in the final section of the 1963 paper for analyzing a multilayer pavement system would lead to overestimating the load-supporting value of a pavement structure by up to 30 percent. In some cases it might be more than this. It should be noted again that the results for all cases covered by Figure 10 are for a homogeneous pavement material, 12 in. thick, with an elastic modulus of 33,900 psi throughout. It is possible that for a typical flexible pavement, which normally consists of three layers of different pavement materials over the subgrade, the tendency of the approximate method to lead to underdesign might be even greater.

EVOLUTION OF FLEXIBLE PAVEMENT STRUCTURAL DESIGN

One of the most important contributions of the AASHO Road Test to highway engineering is an authoritative new approach it has brought to the structural design of asphalt pavements. This new approach involves the incorporation of an asphalt binder into all material above the subgrade. This in turn introduces the need for recognizing the concept of slab action (Fig. 11a), when designing flexible pavements that are to contain these asphalt treated aggregates. Although this type of construction has been employed on a minor scale in the past, previous to the AASHO Road Test there had been no general agreement, and only very limited evidence, that its ability to support load is superior to that of untreated granular materials.

The conventional method of flexible pavement design, which has been employed since the time of MacAdam, is illustrated in Figure 11b. Whereas on most modern highways it has an asphalt surface of some type, a conventional flexible pavement structure consists primarily of sufficient thickness of granular material to carry the anticipated wheel loads and traffic volumes without overstressing or overstraining the subgrade at any point. Because the granular materials employed consist of discrete particles, they have limited load-distributing capacity (Fig. 11b), and substantial thicknesses of granular bases must, therefore, be provided, particularly over poor subgrades.

The principal advantage of conventional flexible pavements in the past has been their relatively low cost due to the wide distribution of abundant deposits of good natural gravels. However, their use also has several serious disadvantages. Their principal fault is the huge volume of granular material required per mile of heavy duty highway, especially on weaker subgrades. This is due to the usual practice of carrying the full depth of granular base and subbase from shoulder to shoulder to provide natural drainage for the granular material. In addition, depths of granular base approaching and exceeding 30 in. are required over poorer subgrade soils on major highways carrying high traffic volumes which include many heavy trucks.

Figure 43 from the 1963 paper (1) demonstrates that the load-carrying capacity of granular materials per inch of thickness decreases quite rapidly after reaching a maximum at a thickness approximately equal to the diameter of the loaded area, which is about 12 in. for heavy highway vehicles. For the conditions illustrated, it can be determined from this figure that the 5-in. increment in pavement thickness from 30 to 35 in. adds load-supporting value at an average rate of about only 120 lb/in. of thickness, vs an average increase in load support of about 340 lb/in. of thickness for the first 10.5 in. of pavement, which is the optimum thickness in this particular case. Consequently, the use of great thicknesses of granular bases is a very inefficient way to employ granular materials to obtain increased wheel load supporting capacity.

Another rapidly developing major disadvantage of conventional flexible pavement design was stressed in a recent report by (10). This report emphasizes that the natural

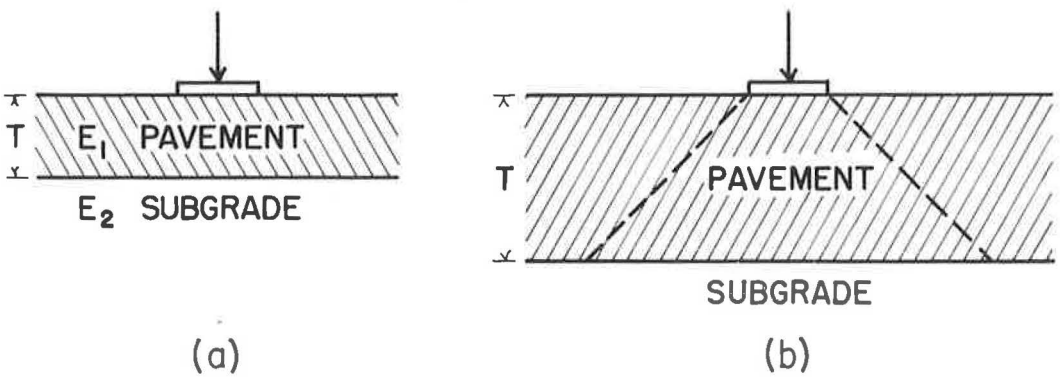

Figure 11. Evolution of flexible pavement structural design: (a) layered system slab action, and (b) conventional flexible pavement.

deposits of readily available good aggregates are becoming exhausted in many regions, and that one of the most serious problems facing highway engineers in North America is the conservation of the remaining good natural aggregates by learning how to upgrade the quality of the relatively undeveloped large deposits of inferior granular materials.

In view of the developing scarcity of good natural aggregates, which has already been eliminating consideration of conventional flexible pavements for major roads in some areas, the published result (11) concerning the special base sections at the AASHO Road Test have become available at a most opportune moment in the development of highway technology. These results have opened the door to a whole new field of opportunity in flexible pavement design.

Analysis of data from the special base sections at the AASHO Road Test (11) showed that a layer of pavement material made by incorporating about five percent of 85/100 penetration asphalt cement into a relatively unstable sandy gravel in a hot mix plant had the same load-carrying capacity as a layer of untreated sandy gravel four times as thick, and as a layer of good quality crushed stone three times as thick. Because the asphalt-treated aggregate is waterproof when well designed, the width of base required is only slightly more than the width of the main pavement. Consequently, where it can be economically justified, the use of asphalt-treated aggregates for the full depth above the subgrade decreases the thickness and width of base courses and results in large reductions in the quantities of aggregates required by conventional flexible pavement design. In addition, by improving their quality and increasing their load-supporting capacity, this treatment enables the huge volumes of inferior aggregates in natural deposits to be utilized for flexible pavement construction. Therefore, full depth asphalt-treated base provides a practical answer to the two major disadvantages of conventional flexible pavement design, namely, the very large volume of granular base materials it requires and the developing scarcity of good natural aggregates.

A recent survey has shown that 38 states have now started to employ either "deep strength" (use of an asphalt binder in at least the top 6 in. of the pavement structure or the treatment of all material above the subgrade with asphalt when designing flexible pavements for their highway construction programs.

Because of the economy of granular materials and other advantages it provides, the evolution of flexible pavement design in the immediate future can be expected to be away from the conventional approach shown in Figure 11b and in the direction of full depth treatment with asphalt binders. Most of these benefits result directly from the slab action provided by these binders (Fig. 11a).

NEEDED RESEARCH ON FLEXIBLE PAVEMENT DESIGN

The previous section referred to the important advantages of the recently developed flexible pavement design procedure requiring treatment of all materials above the subgrade with asphalt. One of the principal benefits of this design procedure is the slab action it achieves (Fig. 11a).

Two major questions that still remain to be answered, however, are how this slab action is to be measured, and how it is to be utilized in the structural design of asphalt pavements. Initial theoretical solutions to these questions have been available since the publication of Burmister's analysis of an elastic two-layer pavement system in 1943 (2) (Fig. 1), and they have been supplemented substantially by further studies since that time (6, 7, 8, 9). These answers are illustrated in Figure 30 from the 1963 paper (1). This figure demonstrates the relationship between the elastic modulus E_1 of the pavement material and the pavement thickness T required to support heavy traffic by a 9,000-lb wheel load or equivalent over a CBR 3 subgrade. The elastic modulus E_1 provides a measure of the slab action of the pavement.

This figure also illustrates the very important influence that the value of the elastic modulus E_1 of the pavement material (the magnitude of the slab action of the pavement) can have on the pavement thickness requirement. It indicates that 36 in. of granular material with an elastic modulus E_1 of 9,000 psi would be needed. If sufficient asphalt binder were incorporated into this granular material to increase its elastic modulus E_1 to 12,500 psi, the thickness requirement would be reduced to 24 in. If by some other

treatment of the granular material with an asphalt binder, its elastic modulus E_1 were increased to 32,500 psi, the thickness requirement would be only 12 in. For the example illustrated by Figure 30 of Ref. (1), therefore, by increasing the slab action of the pavement in terms of its elastic modulus E_1 from 9,000 to 32,500 psi through the incorporation of the required amount and type of asphalt binder, the pavement thickness T can be reduced from 36 to 12 in., that is, to one-third. In this case, the layer equivalency value achieved by treating the granular material with an asphalt binder would be three.

At the AASHO Road Test, the layer equivalency values obtained by treating the sandy gravel subbase material with asphalt cement were three in terms of the good quality crushed stone base employed at the Road Test, and four in terms of the untreated sandy gravel. These layer equivalency values, however, were obtained empirically by the relative performance of the special base sections under the test traffic. No systematic large-scale attempt was made to determine the relative strengths of these three materials in terms of elastic modulus E_1 values or other fundamental strength units because this was outside of the scheduled scope of the Road Test.

Among the most serious mistakes that could be made would be failure to keep the layer equivalency values of the AASHO Road Test in their proper perspective, and to expect a great deal more from them than they are actually able to provide. It needs to be clearly realized that the layer equivalency values established by AASHO Road Test data apply essentially to the particular materials employed for the Road Test. They are not necessarily applicable to similarly treated and untreated aggregates available for ordinary paving projects elsewhere nor for treatments different from those selected for the special base sections at the AASHO Road Test. Consequently, the question that highway engineers everywhere ask themselves are: "What layer equivalencies can I obtain if I treat the aggregates available for this particular paving project with a given asphalt binder?" and "What asphalt treatment do I have to apply to the aggregates available for this particular paving project, to obtain the required layer equivalency of two, three, etc., that is needed to make such treatment economically attractive?" Furthermore, highway engineers want to be able to obtain this information during the design stage for each paving project, not after it has been built.

Because, apart from the findings of the AASHO Road Test, equally authoritative information on layer equivalencies does not exist, the development of a method that can be employed to obtain specific answers to these questions is the most pressing research problem in flexible pavement structural design at the present time. To have to build small full-scale test sections incorporating various treatments of the granular or soil materials available for each paving project and to evaluate them by traffic or other field tests to establish layer equivalencies before the paving project could be designed is too costly and time consuming. Therefore, a research program is urgently needed to develop a suitable laboratory test for this purpose. This program of research might be conducted as follows:

1. The ultimate objective of the research program would be the development of a simple, reliable, rapid laboratory test that would enable layer equivalencies to be established when different types and quantities of asphalt binders are incorporated into the particular aggregates (and in some cases soils) that are available for each proposed paving project.
2. It seems unlikely that this objective can be achieved by working solely with laboratory tests. It appears to require a closely coordinated program of field and laboratory tests. As it exists in a pavement, the material in each layer, subbase, base course, and asphalt surface (and the subgrade also) is subjected to definite restraints. Each layer is restrained because it is either sandwiched between, or in firm contact with, other layers. Because of these restraints, the strength value developed by the material in each layer in a pavement in service may be quite different from the strength value measured for an isolated sample of the same material by a simple test in the laboratory, where there may be no restraints on the sample or where the restraints applied to the sample are not representative of those exerted in the field. A good example of this would be a simple laboratory compression test in which no restraints were applied to the sample.

3. It would be the principal function of the field testing crew to develop or perfect suitable simple field tests for measuring the strengths of the materials in the subgrade, subbase, base course, and asphalt surface, as each of these materials exists within its respective layer in a pavement in the field. The equipment developed and employed for field testing should enable both static and dynamic strength tests to be made. The field testing crew would also obtain a representative sample of the material from the subgrade and from each pavement layer at each test site in the field, together with other pertinent field data, and would forward the samples and a copy of the complete field information to the laboratory.

4. It would be the principal function of the laboratory staff to develop the simplest, most reliable, and rapid laboratory procedure that would duplicate for these samples of materials in the laboratory, the strength values measured for them in-place in the field.

5. It is assumed that the procedures employed for all strength tests conducted in the field and in the laboratory would enable basic characteristics such as elastic modulus, and stress and strain to be determined in fundamental units of measurement.

6. This research program could utilize existing paved highways to develop and perfect the required field and laboratory testing procedures. At the same time, however, specially constructed test sections in which granular materials are treated with various types and quantities of asphalt binders should be incorporated into new highway paving projects and investigated over a period of time under in-service conditions to establish the potential range of layer equivalencies made possible by these treatments and the conditions under which they are most effective.

Representative values of stress and strain, elastic modulus, shear strength, and other fundamental characteristics measured for the subgrade and each of the pavement materials available for a paving project are useful for design purposes only if a rational method of design exists that is capable of utilizing this fundamental information. Theoretical rational methods of pavement design have been developed on the basis of the elastic properties of two- and three-layer pavement systems. However, the degree of accuracy of these methods still remains to be established. Assuming that the laboratory procedure developed is able to duplicate the elastic moduli, stress and strain, and other fundamental characteristics of the subgrade and pavement materials as they exist in a pavement in the field, an adequate rational method of design must be capable of achieving the following:

1. It must be able to utilize these fundamental laboratory determined values to calculate the thickness requirements for the proposed component layers to provide a pavement having the overall structural strength needed for the design wheel load.

2. It must provide calculated values for load vs deflection for this overall pavement design that will agree with measured values for load vs deflection obtained for the overall pavement structure after it has been built in accordance with the design requirements.

Consequently, the research program outlined previously should provide data that will indicate whether any of the existing rational methods of design are sufficiently accurate for practical use, or whether some new more precise rational method of design still remains to be developed.

SUMMARY

Results presented indicate that for subgrades with CBR ratings from 4 to 20, the thickness requirements for a 60,000-lb airplane wheel load given by Burmister's design equation for an elastic two-layer pavement system are practically identical with those of the Corps of Engineers. For subgrade CBR values from 3 to 20, the thickness requirements for a 9,000-lb highway wheel load provided by Burmister's design equation for an elastic two-layer pavement system are practically identical with those given by the Canadian Department of Transport's design equation, $T = K \log P/S$, when using an empirically determined value for the pavement factor K. A discussion of values of the pavement factor K in the design equation, $T = K \log P/S$, calculated theoretically from the Burmister equation, vs experimentally determined values of K is included.

Because of the slab action and other advantages it possesses, it is pointed out that the evolution of flexible pavement design in the immediate future is likely to be toward the adoption of the treatment of all materials above the subgrade with asphalt. A research program is outlined for the purpose of providing urgently needed information on the range of layer equivalency values to be obtained by treating granular materials with different types and quantities of asphalt binders.

ACKNOWLEDGMENTS

C. L. Perkins's competent drafting of the figures and his able assistance with the calculations for the charts and tables is gratefully acknowledged.

REFERENCES

1. McLeod, N. W. Some Notes on Pavement Structural Design. Highway Research Record No. 13, pp. 66-141, 1963.
2. Burmister, D. M. The Theory of Stresses and Displacements in Layered Systems and Applications to the Design of Airports. Highway Research Board Proc., Vol. 38, pp. 126-148, 1943.
3. Foster, C. R. Design Curves for Single Wheel Loads. Proc. ASCE, Vol. 25, No. 1, p. 83, 1949.
4. McLeod, N. W. Airport Runway Evaluation in Canada. HRB Research Rept 4B, Oct. 1947.
5. McLeod, N. W. Airport Runway Evaluation in Canada, Part 2. HRB Research Rept 4B-1948 Suppl., Dec. 1948.
6. Acum, W. E. A., and Fox, L. Geotechnique, Vol. 2, pp. 293-300, 1951.
7. Jones, A. Tables of Stresses in Three-Layer Elastic Systems. Highway Research Board Bull. 342, pp. 176-214, 1962.
8. Whiffen, A. C., and Lister, N. W. The Application of Elastic Theory to Flexible Pavements. Proc. Int. Conf. on the Structural Design of Asphalt Pavements, pp. 499-521, 1962.
9. Dormon, G. M., and Metcalf, C. T. Design Curves for Flexible Pavements Based on Layered System Theory. Highway Research Record 71, pp. 69-84, 1964.
10. Highway Research in the United States. Highway Research Board Spec. Rept. 55, 1959.
11. Benkelman, A. C., Kingham, R. I., and Schmitt, H. M. Performance of Treated and Untreated Aggregate Bases. Proc. Int. Conf. on the Structural Design of Asphalt Pavements, pp. 29-41, 1962.

A Critical Review of Present Knowledge of the Problem of Rational Thickness Design of Flexible Pavements

S. THENN DE BARROS
Consulting Engineer, São Paulo, Brasil

A study of theoretical knowledge of the structural behavior of flexible pavements is reported. The limitations of present concepts of the elastic layer theory are discussed and means for developing better theoretical relationships are suggested. Several concepts of elastic models including two- and three-layer systems were studied. The hypothesis that flexible pavements are perfectly elastic appears to be valid for limited numbers of safe loads of short duration. However, for slow-moving or static loads large enough to nearly overstress the pavement, a rheologic model is more applicable. It was also determined that pavement layers lacking tensile strength may account for a large part of the difference between calculated and measured deflections and stresses. Also, there may be merit to an approach using an equivalent modulus of elasticity, E, for the system. In a discussion of Poisson's ratio it is concluded that although this parameter has little effect on calculated stresses, a value of 0.5 seems to be most appropriate for soils and pavements. A discussion of the effect of pavement rigidity on pavement deflections indicated that the deflection factor is most important. The layered system model of flexible pavements should be expanded to include the condition of zero tensile modulus of the component materials.

A well-documented history of the development of theoretical solutions for the design of flexible pavements for the period 1906 through 1962 is presented. At least five different theoretical approaches to the design of flexible pavements have been developed.

•FOR THE LAST two years the São Paulo State Highway Department has been engaged in a research study of pavement deflections in several state highways, employing Benkelman beams and load bearing tests. The research program is still under way at this time. Some 12,000 individual measurements have already been made covering 1,200 km (750 mi) of roads. The test results obtained so far have been statistically analyzed and reported (1), but final conclusions are not yet available. In a parallel project a bibliography survey was made of present knowledge on the structural behavior of flexible pavements, seeking to provide a theoretical framework to be used in the analysis and interpretation of experimental data. This survey has been already completed (2), and includes in unified and comprehensive form, a critical review of most of the proposed theories on the problem and of experimental studies published by several authors. It was later felt that this report might be of enough interest to other engineers engaged in pavement research to warrant its publication as a separate study. This paper is an abridgment of the latter report.

Paper sponsored by Committee on Flexible Pavement Design and presented at the 43rd Annual Meeting.

BACKGROUND

A quarter of a century has elapsed since the development of the CBR method, the first correlation-based empirical method of thickness design of flexible pavements (3). Twenty years have passed since the presentation of the elastic layered theory, the first wholly theoretical analysis of the flexible pavement (4). These two opposite but converging approaches to the same problem still stand today, though much improved. In the meantime, more than three dozen different methods have been proposed, both of semiempirical and semitheoretical conception. The problem is still far from solved, but a few definite trends can be recognized, at least on a worldwide scale.

The CBR method has gained an increasing reputation and has won the confidence of design engineers the world over. Its advance and improvement have been continuous and steady, largely due to the remarkable contribution of the U.S. Army Corps of Engineers (5). A review of the technical literature of several countries and of several organizations in the U. S. indicates that the use of the CBR method and its modifications far exceeds the use of all the other non-CBR methods combined. Starting as a purely empirical method, the CBR has evolved, due to experience, research, and theoretical analysis of the correlation curves, into what could be very properly called a rational method. It is rational in the sense of having reason and understanding, of properly relating causes and effects, of being suitable for intelligent use, and providing sound and trustworthy design. It is not entirely "scientific"—but then very few, if any, engineering design methods are.

The elastic layered theory, however, has lagged far behind. Its advance and development have been slow, hampered by the tremendous mathematical complexity of its equations in analytical form (6). Nevertheless, many research engineers have retained hope in this theory as the best scientific approach to the design problem. A good advance was made by several authors in the numerical computation of influence coefficients for stresses and deflections by the layered theory. The calculation of most of these coefficients required the use of modern electronic computers. The first numerical coefficients for deflections for a two-layer system were computed by Burmister himself in 1943 (4). Coefficients for two-layer stresses were published by Hank and Scrivner (7) and Fox (8) five years later. However, the two-layer elastic system is a grossly oversimplified model of the flexible pavement. Stress coefficients for the three-layer system were published in 1951 by Acum and Fox (9), and were extended to a wider range of parameters by Jones in 1962 (10). Coefficients for three-layer deflections are still unavailable, except for a particular case computed by Shiffman (11), and an approximate process by Jeuffroy and Bachelez (32). The three-layer elastic system is still a simplified model of the multilayer pavement, but a more complex model would hardly be susceptable to calculation.

The numerical computation of influence coefficients made possible the experimental testing of the elastic layered theory. With the works of Sowers and Vesic (13) and other researchers, the layered theory was put through a severe trial. The available results show a reasonable agreement between measured stresses and deflections and theoretic computed values, but only for pavements possessing some tensile strength, such as soil-cement bases. These results tend somewhat to confirm the theory. Unfortunately, for flexible pavements which do not have tensile strength, that is, for truly flexible pavements, the measured and computed values show a disagreement great enough to overrule the physical analogy between the theoretical elastic model and the real pavement.

It is not likely that the application of rheologic principles could bring much improvement to the present concept of the layered theory. The rheological analysis must include elastic components in the complex rheological model. The influence of the elastic components would still be solely governed by the elastic layered theory—and this theory has proven to be not entirely correct.

The need is apparent for a better theoretical analysis than the present layered theory. It is hoped that such improved theoretical analysis can evolve in time to meet halfway the steadily improving empirically originated CBR analysis. Both systems of knowledge would then be encompassed by one larger branch of applied science, pavement mechanics. This seems to be the discernible trend.

This paper reviews the logical foundations of the elastic layered theory, discusses some of its inconsistencies, and points out possible ways of improvement.

THEORY OF ELASTICITY APPLIED TO FLEXIBLE PAVEMENTS

The first question that arises in trying to apply the elastic theory to pavement structures is whether a flexible pavement is an elastic body, at least approximately following Hooke's law. Considerable research and theoretical studies have been done on this point by several authors. One of the best approaches to the problem is the one proposed by Ruiz (14) and Baker and Papazian (29). The flexible pavement structural behavior normally falls in one of the two following patterns:

1. Case A.—Under a finite number of repetitions of loads of short duration (of the same order of duration as moving wheel loads) with intensity of loading well below breaking strength, the behavior of pavements of adequate design and construction is predominantly elastic, especially at low temperatures. The AASHO Road Test (15) for instance, determined that "deflections of flexible pavement surfacing increased almost linearly with load . . . ." The pavement in this case can be adequately represented by an elastic model whose most important characteristic is its modulus of elasticity. The elastic modulus of pavements in Case A should be determined under conditions typical of this case.
2. Case B.—For slow-moving or static loads, close to the breaking strength, especially at high temperature and for new pavements, the behavior is predominantly viscous or plastic. The pavement in this case is best represented by a rheologic viscoelastic model, such as the Voigt model. Peltier (12) suggests that the behavior of pavements in Case B is elastic delayed. The final deflection, given time, depends on the final modulus of elasticity but not on the viscosity of the pavement. The viscous components of the pavement structure affect the immediate deformation but not the final deflection if enough time is allowed for the time-dependent part of the deflection to take place. The elastic model would also apply, within certain limitations, to Case B if the final modulus of elasticity is chosen as the working modulus.

These considerations justify the conclusion that an elastic model is adequate to represent the pavement in Case A, and to a lesser extent in Case B. A rheologic model would better represent the pavement in Case B. However, the rheologic model must include elastic components. The influence of the elastic components would necessarily follow the elastic theory. Therefore, the theory of elasticity is the governing law in Case A, and also plays an important role in Case B.

Elastic Model of Pavement--Elastic Constants

The term "pavement" here refers to the whole structure built above the subgrade, including all existing layers of subbase, base, binder course and surface course. The term "subgrade" means the soil mass resulting from earthmoving operations and is located below the pavement.

The simplest elastic model of a pavement is the two-layer elastic system depicted in Figure 1. The subgrade soil and the pavement materials are supposed to be homogeneous, isotropic and perfectly elastic. The subgrade is considered to be a layer of infinite depth, limited in its upper boundary by the subgrade surface and unlimited in the vertical downward direction and the horizontal direction. The pavement is considered to be a layer of finite thickness, h, unlimited horizontally, lying over the subgrade. The dividing surface between the two layers is the interface. The wheel load, Q, is represented by a contact pressure, p, uniformly distributed over a circular contact area of radius, r. The wheel load is initially considered a vertical static load. The effects of dynamic impact, horizontal forces and repetition of loads are later incorporated into the analysis, usually as corrective coefficients. The dead load due to the weight of the materials is usually considered to be negligible as compared to the live loads.

It is known from the theory of elasticity that a homogeneous, isotropic and elastic material is characterized by two independent elastic constants. These constants can

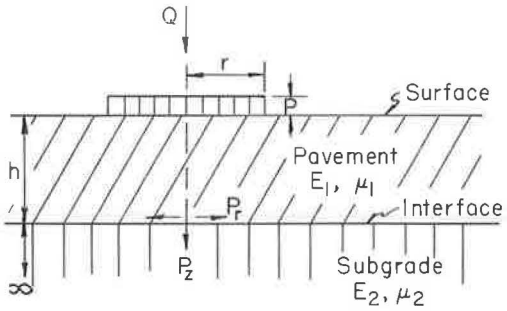

Figure 1. Two-layer system.

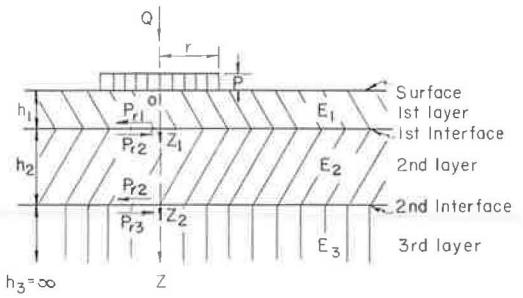

Figure 2. Three-layer system.

be taken as the modulus of elasticity or Young's modulus, E, and the Poisson's ratio, μ. A nonisotropic material has up to 15 independent elastic constants, according to the degree of anisotropy. A nonhomogeneous material has variable physical characteristics. A nonelastic material obviously has no elastic constants. In the two-layer elastic model, there are then four constants, namely E_1, μ_1 for the upper layer and E_2, μ_2 for the lower layer.

A further improvement of the elastic model is the three-layer elastic system indicated in Figure 2. In this system are six elastic constants, two for each layer. The remaining assumptions apply as for the two-layer system. A still better analogy to the real pavement would be a multilayer elastic system. However, the solution of an elastic model with more than three layers would present an exceedingly complex mathematical problem.

Of all simplifying assumptions made in the construction of the elastic model of the pavement, the hypothesis of perfect elasticity is the one which most departs from reality. The stress-strain relationship of real materials is not exactly linear; moreover, it depends on the material conditions. In other words, the elastic "constants" of real materials are not really constants, but depend on factors such as load, state of stress, rate of loading, temperature, compaction, and moisture. However, if we choose adequate average values for the elastic constants, valid for the particular conditions of the problem under study, the elastic theory should provide a reasonably accurate framework for the solution of many problems.

The main difficulty is then of an experimental nature: the determination of adequate values for the elastic constants. The determination of elastic modulus of soils and pavement materials can be made by experimental methods such as triaxial tests, load bearing tests, drop impact, and pulse velocity. Each of these methods has its merits and shortcomings, its limitations and range of application. This subject has been widely studied by several authors. For our purposes it is enough to recognize that the elastic modulus is a physical characteristic of materials that can be measured experimentally for a given set of conditions. The experimental methods of measurement will not be further discussed in this paper, which is directed to the discussion of the conceptual or philosophical foundations of the theories.

The determination of Poisson's ratio for soils and flexible pavement materials poses a different problem, generally overlooked by most authors. For soils, Poisson's ratio is a very tenuous property which has never been satisfactorily determined. It is usually supposed to be near 0.5, the value for an incompressible engineering material (16). Because saturated nondraining soils can be assumed to be incompressible within the range of practical loads, this value appears to be reasonable. It has the additional advantage of simplifying theoretical equations, in which the term $2\,\mu$ is frequently found. There is no reliable test to measure Poisson's ratio for soils and pavement materials, and no sound criterion to chose a value different from 0.5. The author suggests that the difficulty of measuring Poisson's ratio may go deeper than testing complexities. It is possible that the Poisson's ratio as such—a relation of radial and axial unit elongations—may have no physical significance for soils and pavement materials. The concept of Poisson's ratio, according to the elastic theory, is based on

the assumption that the deformations are small and the corresponding small displacements do not substantially affect the action of the external forces. These conditions are not generally met for soils. Consequently, the elastic principle of superposition of effects is not exactly valid for the stresses and strains acting on the elemental volume within the soil mass. The principle of superposition may eventually give acceptable results for the effects of external macro loads, as a sort of gross average blanketing the interrelated effects of several micro phenomena, but it is not strictly valid for the point stresses and strains. Therefore, the elastic Poisson's ratio becomes meaningless—and it is small wonder that it could never be satisfactorily determined. But according to theory, a second elastic constant, in addition to the modulus of elasticity, is necessary to define the elastic material. For practical applications, a coefficient related to the volumetric change, such as the elastic modulus of compression, would be more reliable as the second elastic constant. The condition most likely to prevail in actual subgrades is the permanence of volume, corresponding to a coefficient of volumetric change equal to zero. It can be demonstrated that this zero coefficient corresponds to a theoretical value of Poisson's ratio equal to 0.5. Therefore, this value of $\mu = 0.5$ seems to be well justified from a theoretical standpoint.

In the Vicksburg tests (17), the value of $\mu = 0.5$ was found to be adequate for the clayey-silt soil test section. For the air-dry pure sand test section (18), the most probable value was considered to be 0.3. However, the result for the pure sand is not as convincing as the one for the clayey-silt soil. Closely examining the sand section data presented (18, Plate 96), one can see that the agreement between measured and computed horizontal stresses is very poor, both for 0.3 and 0.5 values of μ, the former being only a little better than the latter. The pure sand section test results deviate in several respects from the elastic theory, much more than the clayey-silt soil section. There are several reasons to believe that most actual subgrades are closer to the clayey-silt soil than to the pure sand and, therefore, closer to $\mu = 0.5$.

In the absence of more experimental work, we have to rely on the theoretical analysis. It is fortunate that the theoretical influence of Poisson's ratio on the vertical stresses and deflections is small, for both homogeneous and layered systems. Shiffman (11) computed the vertical stresses and deflections for a three-layer system with Poisson's ratio of 0.4, 0.2 and 0.4, respectively. The author compared the vertical stresses from Shiffman with the values for Poisson's ratio of 0.5 interpolated from the tables of Jones (10) and found differences less than 5 percent, below experimental accuracy. The author also compared the vertical deflections from Shiffman to the deflections of a corresponding two-layer system with Poisson's ratio of 0.5 given by the Burmister graph (4). This comparison is valid because the two upper layers of the Shiffman case have the same modulus of elasticity, being different only in Poisson's ratios. The two upper layers of the Shiffman three-layer case correspond to the upper layer of the Burmister two-layer case. The comparison shows that the influence of Poisson's ratios of the upper layers is entirely negligible. The influence of the lower layer is sensible but less than 15 percent. This difference is of little significance because the lower layer of real pavements, that is the moist subgrade, is most likely to have a Poisson's ratio of 0.5.

Available experimental and theoretical evidence indicates that a Poisson's ratio of 0.5 seems to be the most adequate for general use. The discussion of alternative values for Poisson's ratio belongs to the realm of theoretical hypothesis. Practical graphs or formulas for deflection analysis including values of Poisson's ratio other than 0.5 are utterly unwarranted. This inclusion is misleading because it presupposes the wrong notion that Poisson's ratio is a parameter that can be varied to suit particular project conditions. Actually there is no such thing as the selection of a μ value in practical problems of deflection analysis, at least in the light of present knowledge.

This adoption of a fixed value for one of the two independent elastic constants somewhat simplifed the elastic model. We have now just one elastic constant, the modulus of elasticity, for each layer. As stated before, it is most important for the validity of the elastic model that the actual values of the modulus be measured under conditions similar to the service conditions of the real pavement. The elastic modulus is the

physical parameter that binds the theory to the ground—and so to say, it is the clay foot of many theoretic giants.

The elastic model of the pavement will be completely defined by the following conditions and parameters (6):

1. Elasticity condition.—The subgrade soil and pavement materials are supposed to be homogeneous, isotropic and perfectly elastic, obeying Hooke's law. The modulus of elasticity is supposed constant, and usually assumed to be the same for tension and compression.
2. Geometric parameters.—These are radius, r, and layer thicknesses, h_1, h_2, h_3, ... It is convenient to express all thicknesses as nondimensional multiples of the radius, which is the same as to consider r = 1. The radius is thus eliminated as an independent parameter. There is one independent geometric parameter for each layer: h_1/r, h_2/r, h_3/r, ...
3. Loading parameter.—The applied contact pressure, p, is usually assumed to be normal to the surface, that is, of vertical direction. It is convenient to adopt the value, p = 100 percent and express all induced stresses in the model as a percentage of p. The contact pressure is then also eliminated as an independent parameter. The dead weight of the layers is usually neglected.
4. Physical parameters.—There is a modulus of elasticity for each layer, E_1, E_2, E_3, ... It is convenient to adopt as independent parameters the nondimensional ratios between successive modulus, plus the lowest modulus: E_1/E_2, E_2/E_3 and E_3. Sometimes it is useful to express the combined effects of all different moduli as an equivalent modulus E_e.
5. Boundary conditions.—The top surface of the layer is assumed to be free of any stresses outside the contact area and of shearing stresses inside the contact area. The lower boundary at infinite depth is supposed to be free of any stresses and strains.
6. Continuity conditions.--The interfaces between the layers are assumed to fall within one of the two limiting cases: Case 1 (Rough interfaces)—with perfect continuity and the layers in continuous contact, acting together with no slippage at the interfaces; or Case 2 (Smooth interfaces)—with no friction and the layers in continuous contact but perfectly free to move horizontally relative to each other. In reality, the actual conditions at the interface are intermediate between these two extremes, but probably closer to the first case than to the second.

The mathematical problem posed by the elastic model consists in expressing all induced stresses and strains within the model as functions of the independent parameters, for the given conditions.

Relative Rigidity of Flexible Pavement

Because the pavement modulus is greater than the subgrade modulus, there is a relative rigidity of the flexible pavement with respect to the subgrade. The relative rigidity improves the pavement performance in two ways: (a) it reduces the vertical downward pressure transmitted to the subgrade beneath the loaded area, and (b) it increases the ultimate shearing strength opposing the upward movement of the subgrade soil around the loaded area. According to Hveem (19), the second effect is more important than the first one. Certainly, the most important effect of the rigidity is a reduction of the total deflection for a given load. A convenient form of indicating the effect of the pavement rigidity is to compare the total deflection of the layered system with the corresponding deflection of a uniform medium of the same modulus of elasticity as the subgrade modulus. The ratio between the two deflections is the deflection factor. The most important problem to be solved in the elastic model is the calculation of the deflection factor.

PREVIOUS STUDIES

Almost all mathematical solutions of the layered system are based on the classical Boussinesq-Love solution for the semi-infinite uniform medium presented by Love (20). There were a few partial solutions of the layered system problem before the Burmister

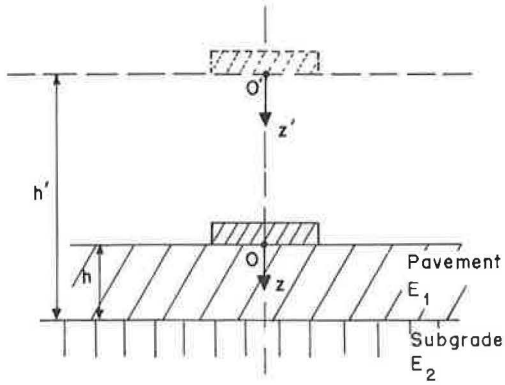

Figure 3. Equivalent thickness.

analysis. One of the most widely known is the solution presented by Hogg (21) of the problem of a thin rigid slab supported by a semi-infinite elastic foundation. Hogg's solution introduces an additional condition in the elastic model previously defined. It supposes that the thin slab deflects according to Navier hypothesis; that is, top and bottom faces and median plane deflect along parallel curves. This hypothesis causes a considerable simplification in the calculus, but it covers only approximately Case 2 of the continuity condition. Hogg's solution was numerically computed and presented in graphical form by Odemark (22). An extension of Hogg's solution to the three-layer problem was recently presented by Jeuffroy and Bachelez (32).

For the two-layer system, the deflection factor and vertical stress computed by Hogg and Odemark are practically equal to the corresponding values given by the Burmister analysis. The radial and shear stresses in the top layer are slightly different in the two solutions, but the radial and shear stresses in the lower layer cannot be correctly calculated with Hogg's solution. For the three-layer system the agreement is not as good.

Semi-Empricial Solutions

Palmer and Barber (23) presented an approximate process for calculation of deflections of the two-layer system which gave results close to the Burmister analysis. Palmer and Barber start from the hypothesis that, for deflection computation, the pavement thickness, h, could be replaced by an equivalent thickness, h', of subgrade soil (Fig. 3), satisfying the condition:

$$\frac{h'}{h} = \left(\frac{E_1}{E_2}\right)^{1/3} \qquad \left(\mu_1 = \mu_2 = \frac{1}{2}\right) \tag{1}$$

The factor $(E_1/E_2)^{1/3}$ had been previously proposed by Marguerre as the relative rigidity factor for slabs. It should be noted that the replacement of h by h' corresponds to a transformation of coordinates, displacing the origin 0 to 0' but keeping the interface unchanged.

By combining the equivalent thickness hypothesis of Palmer and Barber with the Boussinesq-Love analysis of the uniform medium and neglecting the deformations within the pavement itself, the subgrade deflection may be substituted for the total deflection, and expressed by:

$$W = \frac{1.5\ pr^2}{E_2\sqrt{r^2 + h^2\left(\frac{E_1}{E_2}\right)^{2/3}}} \tag{2}$$

This equation may be rewritten in another form by calling W_0 the total deflection of the uniform medium and F' the Palmer and Barber deflection factor:

$$W_o = \frac{1.5\ pr}{E_2} \tag{3}$$

$$F' = \frac{1}{\sqrt{1 + \left(\frac{h}{r}\right)^2 \left(\frac{E_1}{E_2}\right)^{2/3}}} \tag{4}$$

therefore

$$W = W_o\ F' \tag{5}$$

Eqs. 2 or 5 will give the total deflection if the pavement deflection is neglected. If the ratio E_1/E_2 is greater than 100, the pavement deflection is much smaller than the subgrade deflection and can be safely neglected. But if the modular ratio is smaller than 100, this cannot be done. In actual practice, the modular ratio of flexible pavement is seldom greater than 100 and the pavement deflection should be taken into consideration. By an extension of the Palmer-Barber analysis (4, Discussion), it can be demonstrated that the total deflection may be expressed by the following equation:

$$W_t = W_o \left[F' \left(1 - \frac{E_2}{E_1} \right) + \frac{E_2}{E_1} \right] \tag{6}$$

By making:

$$F = F' \left(1 - \frac{E_2}{E_1} \right) + \frac{E_2}{E_1} \tag{7}$$

we have:

$$W_t = W_o F \tag{8}$$

Eq. 8 will give values for the total deflection practically equal to the values given by the Burmister analysis. This final agreement justifies the initial hypothesis of substituting h' for h, according to Eq. 1.

The vertical stress in any point of the vertical axis passing through the center of the contact area, within the pavement or the subgrade, can be calculated by the equivalent thickness hypothesis combined with the Boussinesq-Love equation. However, the Palmer-Barber analysis is less correct for stresses than for deflections. The vertical stress values given by the Palmer-Barber analysis are smaller than the corresponding values computed by the Burmister analysis. Moreover, the radial and shear stresses cannot be calculated by the Palmer-Barber analysis.

From Eq. 2 comes the well-known semi-empirical Kansas formula (25):

$$h = \sqrt{\left(\frac{1.5\ Q}{\pi E_2 W_a} \right)^2 - r^2} \quad \sqrt[3]{\frac{E_2}{E_1}} \tag{9}$$

in which

h = required thickness of pavement (in.),
Q = design wheel load (lb),
r = radius of contact area (in.),
E_1 = elastic modulus of pavement (psi),
E_2 = elastic modulus of subgrade (psi), and
W_a = allowable deflection of subgrade (usually assumed to be 0.1 in.).

For practical use, the wheel load, Q, is affected by two empirical factors related to traffic and rainfall, as follows:

$$Q = Pmn \tag{10}$$

in which

P = maximum wheel load, usually 9,000 lb;
m = traffic coefficient, between 0.5 and 1; and
n = rainfall coefficient, between 0.6 and 1.

The subgrade modulus E_2 is determined by the triaxial test, with the use of a graphical process that takes into consideration the variation of the vertical and radial stresses with depth. The pavement modulus, E_1, can be determined by the triaxial test, or a value for E_1 is assumed from previous experience. The thickness of each component layer of the pavement is also calculated with the help of the rigidity factor; that is, the thickness is inversely proportional to the cube root of the modulus.

The Kansas method, however useful in actual practice, has several shortcomings when viewed from a theoretical standpoint. To begin with, it neglects the pavement deflection. Actual tests, such as the AASHO Road Test (15), show that the pavement deflection often amounts to 30 percent or more of the total deflection. Furthermore, the determination of the elastic modulus by the triaxial test is, at best, a delicate operation and does not take into consideration the rate of loading in the two patterns of structural behavior previously discussed. But the weakest point of the method is the assumption of a fixed and arbitrary value for the allowable deflection, regardless of the pavement type. The assumed allowable deflection is very critical because it has a great influence on the resulting thickness. The usual value of 0.1 in. is rather large. Several performance studies, including the AASHO Road Test, indicate that 0.04 in. would be a more realistic value to prevent the early deterioration of the pavement. However, if this is introduced in the Kansas formula, unrealistically high thicknesses will result. Many authors have shown the difficulty of designing for an arbitrary allowable deflection. McLeod (26) points out that a given deflection under a specified wheel load does not indicate the same ability to carry traffic if the strengths of the underlying subgrades are different. In spite of its theoretical inconsistencies, the Kansas design method has been reportedly used with success (25). This might be explained by the experience and "engineering judgment" of Kansas engineers in supplementing their method.

Another semi-empirical method employing the triaxial test in a modified form is the Texas method (27) which uses a correlation-based classification chart rather than a design formula. The subgrade soil and pavement materials are classified by the position of their Mohr's envelopes in the classification chart, and the required thickness is taken from a design chart using the classification of materials and the design wheel load. The Texas method employs the triaxial test in a rather dependable manner. Instead of using just one numerical value for the modulus of elasticity of each material, it relies on several points of the shear envelope, each point being determined by stressing the material until failure at various lateral pressures. The theoretical justification of the method is based on the Burmister analysis, making use of the Hank-Scrivner solution (7). The Texas method represents definite progress towards the development of a scientific design method, but because it does not properly present a new solution for the mathematical problem of the elastic model, it will not be further discussed here.

Ivanov (28) presented a semi-empricial thickness design method that is said to have been the official Russian method for many years. The Ivanov method has some re-

semblance to the Palmer-Barber analysis. It is essentially based on the assumption of an arbitrary allowable deflection and the calculation of stresses and deflection with approximate formulas. The rigidity factor of the pavement is assumed to be the following:

$$n = \frac{h'}{h} = \left(\frac{E_1}{E_2}\right)^{1/2.5} \tag{11}$$

Comparing Eqs. 1 and 11, we can see that Ivanov attributes greater rigidity to the pavement than do Palmer and Barber. On the other hand, Ivanov permits smaller allowable deflection, of the order of 0.04 in.

Ivanov proposes an approximate formula for the vertical stresses but gives no formulas for the radial and shear stresses. The vertical stresses computed by the Ivanov formula for the uniform medium are very close to the values given by the classical Boussinesq-Love equation. For the two-layer system, Ivanov's formula gives vertical stresses well below the values given by the Burmister analysis. For the deflections, the two theories present a reasonable agreement.

The final deflection equation of Ivanov is:

$$W = \frac{2pr}{E_2} \quad \frac{\pi}{2\sqrt{a}} \left[1 - \frac{2}{\pi}\left(1 - \frac{1}{n^{3.5}}\right) \text{ arc tan } \frac{nh\sqrt{a}}{2r}\right] \tag{12}$$

in which

- p = contact pressure,
- r = radius of contact area,
- a = empirical constant,
- E_2 = subgrade modulus of elasticity,
- n = rigidity factor, and
- h = pavement thickness.

The elastic modulus is determined by load bearing tests or dynamic tests. The proposed values for the constant a are as follows: for a uniform medium a = 2.5; for a two-layer system a = 2; and for a three-layer or greater system, a = 1.

Implied in the analytical derivation of Ivanov's equation, though not clearly stated, is the assumption of $\mu = 0$ because the effect of the radial stress on the deflection is neglected. Ivanov's deflection equation for a uniform medium is:

$$W_o = \frac{2pr}{E} \tag{13}$$

The same expression would be given by the Boussinesq-Love analysis for $\mu = 0$. This condition should be borne in mind when using Eqs. 12 and 13. Of course, if the elasticity modulus is determined with load bearing tests by Eq. 13 and the resulting value is introduced in Eq. 12, the difference is canceled out. But if the modulus is determined in the usual way, for $\mu = 0.5$, it should be multiplied by a factor of 1.33 before entering it into Eqs. 12 and 13. Eq. 12 may be somewhat simplified for the two-layer system by using the values a = 2, $n = (E_1/E_2)^{1/2.5}$, and $W_o = 2\,pr/E_2$:

$$F = \frac{W}{W_o} = 0.7\left[\text{arc tan } \frac{1}{\left(0.7\,n\,\frac{h}{r}\right)} + \frac{1}{n^{3.5}} \text{ arc tan}\left(0.7\,n\,\frac{h}{r}\right)\right] \tag{14}$$

and, therefore,

$$W = W_o F \tag{15}$$

From Eq. 14 Ivanov defines a uniform medium of equivalent modulus, E_e, which would have the same deflection of the layered system. It is possible to calculate the equivalent modulus of a multilayered system, considering the layers two by two, from the lowest to the top. This concept of an equivalent modulus, based on equality of deflections, is the most outstanding feature of Ivanov's method. From Eqs. 13 and 14, the equivalent modulus is:

$$E_e = \frac{E_2}{F} \tag{16}$$

Burmister Analysis

Burmister presented in 1943 the first rigorous and complete theoretical solution of the problem of stresses and strains in the elastic model of the pavement (4, 6). The Burmister solution follows exactly all conditions of the elastic model previously defined. In his first paper (4), Burmister extended the Boussinesq-Love equations to the two-layer system, determining the parameters by the boundary and continuity conditions, and checking the compatibility of the equations. The Burmister solution, with the use of Bessel auxiliary functions, gives the stresses and displacements in any point of the two-layer system for the two cases of interfaces. In his second paper (6), Burmister extended his analysis to the three-layer system with rough interfaces, but derived only the equation for total deflection at the surface. The Burmister equations in analytical form are exceedingly complex and not suitable for immediate application. For practical use, they require the computation of numerical influence coefficients for stresses and deflections.

The first numerical coefficients were computed by Burmister (4) for the total deflection at the surface beneath the center of the contact area of a two-layer system with rough interface and with 0.5 Poisson's ratio in both layers. The Burmister equation for deflection is:

$$W = \frac{1.5\ pr}{E_2} \quad F \tag{17}$$

$$F = f\ (E_1/E_2,\ h/r)$$

in which

- W = total deflection,
- p = contact pressure,
- r = radius of contact area,
- h = pavement thickness,
- E_1 = pavement modulus of elasticity,
- E_2 = subgrade modulus of elasticity, and
- F = deflection factor, function of the ratios E_1/E_2 and h/r.

In the Boussinesq-Love analysis, the total deflection of a uniform medium of modulus, E_2, loaded with a uniform pressure is:

$$W_o = \frac{1.5\ pr}{E_2} \tag{18}$$

Therefore,

$$W = W_o F \tag{19}$$

for $F = 1$ and $W = W_o$.

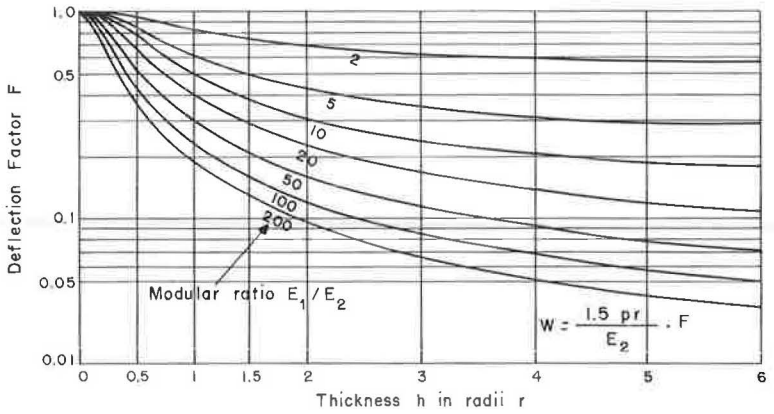

Figure 4. Two-layer deflection factor.

The total deflection of a uniform medium loaded with a rigid plate is:

$$W_o = \frac{1.18\ pr}{E_2} \qquad (20)$$

Eq. 19 is valid with the substitution of the value given by Eq. 20 for W_o. The theoretical analysis shows the influence of the two parameters E_1/E_2 and h/r on the deflection. Burmister computed numerically the deflection factor, F, for usual values of the parameters, and presented the results in graphical form (Fig. 4).

Burmister Design Method

Burmister also suggested (4) a semi-empirical thickness design method based on his analysis. It consists essentially of fixing an arbitrary value for the allowable deflection and calculating the required thickness by the deflection graph. The subgrade modulus is determined by load bearing tests, and the pavement modulus is assumed from experience. The total deflection is then checked in a trial section of the pavement. This method has the same weakness already discussed in the Kansas method, namely the difficulty and inconsistency of assuming an arbitrary value for the allowable deflection. The required thickness is very sensitive to the chosen value of the allowable deflection. Burmister's design method has not encountered the same acceptance as has his theoretical analysis of stresses and deflections.

TABLE 1

INFLUENCE COEFFICIENTS FOR TWO-LAYER STRESSES[a]

E_1/E_2	h/r	Vertical Stress (Compression), p_z/p (%)	Radial Stress[b] p_r/p (%)	Shear Stress, p_s/p (%)
		(a) Rough Interface		
100	1	8.1	352	180
	2	2.4	122	62
	5	0.4	23	12
	10	0.1	6.0	3.0
20	1	20.5	218	119
	2	6.6	84	45
	5	1.2	16	8.7
	10	0.3	4.0	2.1
10	1	29.2	158	94
	2	10.1	66	38
	5	1.8	13	7.4
	10	0.5	3.3	1.9
2	1	54.7	30	42
	2	22.4	18	20
	5	4.4	3.9	4.2
	10	1.1	1.0	1.1
		(b) Smooth Interface		
10	1	30.5	106	108
	2	10.5	76	43
	5	1.9	15	8.5
	10	0.5	3.8	2.2
2	1	59.8	81	70
	2	24.0	41	33
	5	4.7	8.7	6.7
	10	1.2	2.2	1.7

[a] At interface on vertical axis, as percentage of contact pressure (7).
[b] In top layer (tension).

Extensions of the Burmister Analysis

Hank and Scrivner (7) published numerical coefficients for two-layer stresses and some three-layer stresses at the interfaces, in the vertical axis for rough and smooth interfaces. Some of these values are given in Table 1. The vertical stresses

are very similar in both types of interfaces, but the radial and shear stresses at the base of first layer are greater for the smooth interface, particularly for the lower modular ratios. The radial stress at the top of the second layer (not shown in Table 1) is always smaller than the radial stress at the base of first layer. There is always a discontinuity of radial stresses, even in the case of rough interfaces, induced by an equal strain under different moduli of elasticity.

Fox (8) presented numerical values for the two-layer stresses in the vertical axis and also in points off-set from the axis, computed with the help of the relaxation method of Southwell. The Road Research Laboratory (24) published some of Fox results in graphical form, comparing the two-layer stresses with the corresponding stresses for a uniform medium (Fig. 5). This comparison indicates that the two-layer vertical stresses are considerably lower than the uniform medium stresses. For example, at a depth $z/r = 1$, the uniform medium vertical stress is 65 percent of p, whereas in the two-layer system it is reduced to 29 percent of p. This result indicates that the pavement rigidity reduced the vertical stress at that particular point to less than half. However, at greater depths, i.e., for z/r greater than 3, the stresses in the two systems are very similar.

The reduction of the vertical stresses in the layered system is accompanied by a considerable increase in the radial and shear stresses and the appearance of tensile stresses in the top layer. The greatest values of the layered system tensile stress are located beneath the center, in the lower face of the top layer. The tensile stress depends on the same parameters E_1/E_2 and h/r. The uniform medium ($E_1/E_2 = 1$) with $\mu = 0.5$ has no tensile stress in the vertical axis. When the modular ratio exceeds 1.5,

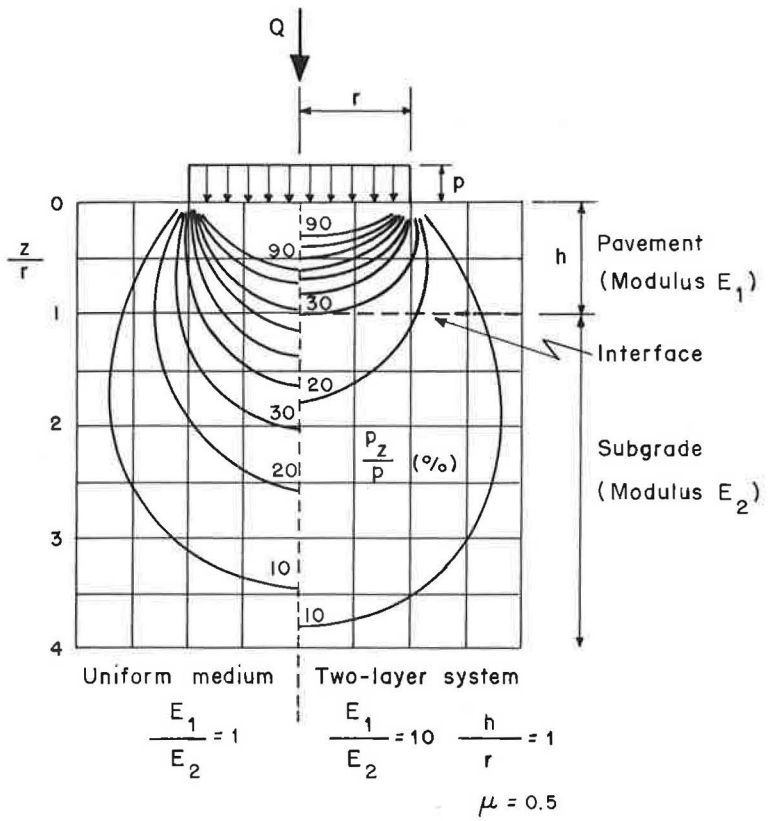

Figure 5. Pressure bulb for the two-layer system (Burmister) compared to a uniform medium (Boussinesq-Love).

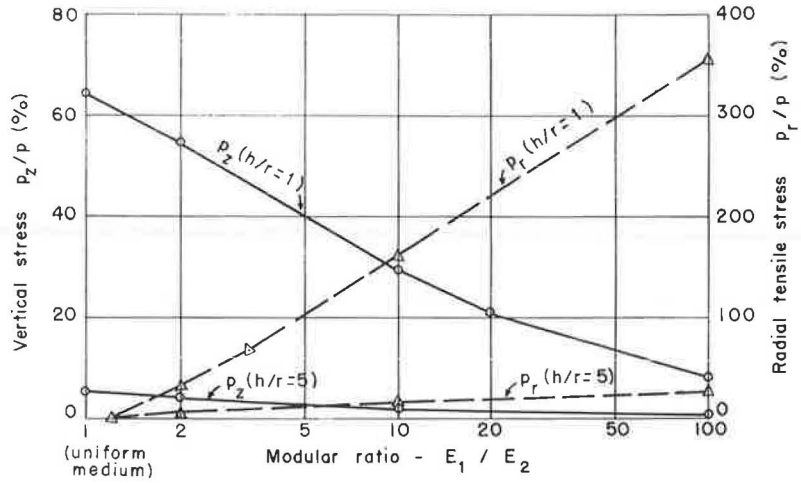

Figure 6. Variation of vertical stress and radial tensile stress in a two-layer system with h/r = 1 and h/r = 5, as functions of the modular ratio, E_1/E_2.

tensile stresses begin to appear. Figure 6, based on Hank-Scrivner values, indicates the reduction of vertical stresses and the increase of radial stresses in a two-layer system, with the increase of the modular ratio. For h/r = 1 and $E_1/E_2 = 2$, the tensile stress already reaches one-third of the contact pressure. For $E_1/E_2 = 100$, which is the greatest modular ratio normally occurring in flexible pavements, the tensile stress exceeds three times the contact pressure. In the last case, the flexible pavement has a stress distribution similar to a rigid slab in flexure, with top and lower face stresses almost equal in absolute value but opposite in signal, and middle plane stresses almost zero. Baker and Papazian (29) also noted this basic similarity in the structural design of rigid and flexible pavements. They computed tensile stresses of flexible pavements by the Burmister analysis, and the correspondent rigid slab stresses by the Westergaard analysis, and found comparable stresses, particularly for the thicker pavements. As for the influence of thickness, the tensile stress reaches a maximum for a certain critical thickness (of the order of half the radius) and then decreases with an increase in the thickness of the top layer. This theoretical finding explains the recognized fact that thin surfaces are more prone to tensile cracking and, therefore, should be more flexible.

The three-layer stress coefficients were computed by Acum and Fox (9) for points at the interfaces in the vertical axis. The relaxation method was found to be unsuitable for off-set points in the three-layer system. Jones (10) extended the Acum-Fox computation to a wide range of the parameters for the three-layer system with rough interfaces and Poisson's ratio of 0.5. The Jones tables were computed by the electronic computer at Shell Laboratorium, Amsterdam. Table 2 gives some of the Jones coefficients, expressed as a percentage of contact pressure. Peattie (30) organized a series of charts based on the Jones tables giving the stress and strain factors in graphical form for convenience of interpolation. The Jones-Peattie works are the most extensive set of numerical data now available on the elastic layered system. They give the stress and strain coefficients (but not the deflection factor) for the three-layer system for any combination of parameters within the following range (Fig. 2):

$$E_1/E_2 = K_1 = 0.2 \text{ to } 200$$
$$E_2/E_3 = K_2 = 0.2 \text{ to } 200$$
$$h_1/h_2 = H = 0.125 \text{ to } 8$$
$$r/h_2 = A = 0.1 \text{ to } 3.2$$

TABLE 2

INFLUENCE COEFFICIENTS FOR THREE-LAYER STRESSES[a]

$E_1/E_2 = K_1$	$E_2/E_3 = K_2$	$h_1/h_2 = H$	$h_2/r = \frac{1}{A}$	A	p_{z2}/p (%)	p_{r1}/p (%)	p_{s1}/p (%)
20	20	0.25	1.25	0.8	6.7	580.1	324.5
			2.5	0.4	1.9	378.3	207.0
			5	0.2	0.5	177.0	95.3
20	20	1	1.25	0.8	1.5	251.7	129.8
			2.5	0.4	0.4	79.7	41.2
			5	0.2	0.1	21.6	11.2
20	2	0.25	1.25	0.8	26.3	474.9	275.4
			2.5	0.4	7.9	348.9	193.4
			5	0.2	2.1	169.5	91.9
20	2	1	1.25	0.8	5.9	185.2	98.7
			2.5	0.4	1.6	62.9	33.3
			5	0.2	0.4	17.5	9.2
2	20	0.25	1.25	0.8	9.3	-70.8	11.0
			2.5	0.4	2.7	7.9	42.2
			5	0.2	0.7	24.6	33.5
2	20	1	1.25	0.8	3.6	43.0	38.1
			2.5	0.4	0.9	16.8	14.8
			5	0.2	0.2	4.9	4.3

[a] At interfaces (rough interfaces) on the vertical axis as percentage of contact pressure; symbols used are as follows:

p_{z2} = vertical stress at 2nd interface (pressure on subgrade),

p_{r1} = radial stress at 1st interface (tension at base of top layer), and

p_{s1} = shear stress at 1st interface (at base of top layer).

(Interpolation between given values of K_1 and K_2 can be performed graphically on log-log paper.)

The last parameter is the reciprocal of the usual one, that is:

$$h_2/r = 0.32 \text{ to } 10$$

Shiffman (11) computed the stresses and also the deflection factor for a particular case of a three-layer system having $E_1/E_2 = 1$ and $E_2/E_3 = 10$; that is, the same modulus in the two top layers, but different Poisson's ratios for each layer: $\mu_1 = 0.4$, $\mu_2 = 0.2$ and $\mu_3 = 0.4$. Except for this specific case, which is of little practical interest, there are no published values for the three-layer deflection factor determined by the rigorous Burmister analysis.

Shiffman has also presented (31) a general analysis of stresses and displacements in layered systems, developing analytical procedures for the consideration of normal and tangential loads and axisymmetric and inclined plates. Numerical coefficients were not presented.

Jeuffroy and Bachelez (32) proposed an approximate solution for the three-layer system to which we have already referred. The Jeuffroy-Bachelez solution is an extension of Hogg's solution. The top layer is supposed to follow Navier's hypothesis. The first interface is assumed to be smooth and free of shear stresses. The second interface is assumed to be rough, but having all stresses and strains equal in both layers. This is a further simplification because, according to the rigorous Burmister analysis, the radial stresses at the interfaces are different in both layers, even for the rough interfaces. Jeuffroy and Bachelez presented a series of charts giving the stresses and deflection factor for the three-layer system, for single and dual wheel loads. The stresses computed by Jeuffroy and Bachelez are higher than the correspondent values in the Jones tables. The radial and shear stresses in the two lower layers cannot be computed by the Jeuffroy-Bachelez solution.

EXAMPLES OF APPLICATION

A few simple practical applications of the theories discussed are in order, to try the engineering "feeling" of so many tables, graphs and formulas. For example, if

the wheel load is Q = 7,800 lb, p = 100 psi, and r = 5 in. and we assume a uniform medium of modulus E = 1,000 psi, the deflection at surface is:

$$W_o = \frac{1.5 \times 100 \times 5}{1,000} = 0.75 \text{ in.}$$

Calculation of vertical and radial stresses at an arbitrary depth of 10 in., according to the Boussinesq-Love analysis (35) yields $p_z = 28.4\% \times 100 = 28.4$ psi and $p_r = 1.6\% \times 100 = 1.6$ psi (compression) because $z/r = 10/5 = 2$. If over this subgrade we build a 10 in. base of modulus 20,000 psi, we have a two-layer system, whose parameters are $h/r = 10/5 = 2$ and $E_1/E_2 = 20,000/1,000 = 20$. The two-layer deflection, by the Burmister graph (Fig. 4), is F = 0.22 and W = 0.75 x 0.22 = 0.17 in. If the two-layer deflection is calculated by some of the other referred methods, the following results will be found:

1. By the Hogg-Odemark graph, W = 0.75 x 0.23 = 0.17 in.
2. By the Palmer-Barber approximated formula

$$F' = \frac{1}{\sqrt{1 + 2^2 \times 20^{2/3}}} = 0.182$$

and W = 0.75 x 0.18 = 0.14 in.

3. By the Palmer-Barber corrected formula, F = 0.182 (1 - 1/20) + 1/20 = 0.223 and W = 0.75 x 0.22 = 0.17 in.

4. By the Ivanov formula, $n = 20^{1/2.5} = 3.31$, $h/r = 2$, $1/n^{1/3.5} = 1/3.31^{1/3.5} = 0.015$, $0.7\, n\, h/r = 4.65$ which yield F = 0.7 (arc tan 1/4.65 + 0.015 arc tan 4.65) = 0.164 and W = 0.75 x 0.16 = 0.12 in.

In calculating the stresses at the interface by the Hank-Scrivner table, because p = 100 psi, the percentages of p correspond to psi. The vertical and radial stresses are $p_z = 6.6$ psi and $p_r = 84.4$ psi (tension). Comparison of the two-layer system with the uniform medium indicates that the deflection was reduced from 0.75 to 0.17 in., and the vertical pressure on the subgrade from 28.4 to 6.6 psi, but at the same time the radial stress passed from a compression of 1.6 psi to a tension of 84.4 psi. The shear stress, not computed in this example, also increased. It should be noted that the computed values of radial and shear stresses are very high.

If we cap this base with a 2½-in. asphaltic surface course of modulus 400,000 psi, we have a three-layer system with the following parameters:

$$\frac{h_1}{h_2} = H = \frac{2.5}{10} = 0.25$$

$$\frac{h_2}{r} = \frac{1}{A} = \frac{10}{5} = 2 \qquad (A = 0.5)$$

$$\frac{E_1}{E_2} = \frac{400,000}{20,000} = 20$$

$$\frac{E_2}{E_3} = \frac{20,000}{1,000} = 20$$

The three-layer deflection, by the Jeuffroy-Bachelez method, is W = 0.75 x 0.18 = 0.14 in. This value is very close to the two-layer deflection.

The stresses at the interfaces, by the Jones tables, are as follows:

1. Radial stress at the base of first layer, p_{r1} = 428 psi (tension);
2. Radial stress at the base of second layer; p_{r2} = 43 psi (tension); and
3. Vertical stress at second interface, p_{z2} = 3.1 psi.

The vertical pressure on the subgrade was further reduced from 6.6 to 3.1 psi, and the radial tensile stress at the second interface was also reduced from 84 to 43 psi with respect to the two-layer system, but for this the surface course should resist a very high tensile stress of 428 psi. The shear stress would also be very high.

The high values of the theoretically computed tensile stresses in the base, and particularly in the surface course, seem to be very unrealistic. It is unlikely that common flexible pavement materials would withstand such high stresses, unless at very low temperatures. And according to the Jones tables the theoretical tensile stresses in the three-layer system can go even higher than those in this example, surpassing six times the contact pressure, i.e., to over 600 psi. It is curious to note that few authors have shown much concern for this apparent unrealism of the layered theory.

The stress values included in Table 2 allow another interesting comparison. It is known that at low temperatures asphaltic surface courses have high elastic moduli and relatively high tensile strength. When the temperature rises, the surface modulus is reduced, but the base and subgrade modulus are practically unaffected. As the ratio E_1/E_2 decreases, the tensile stress is drastically reduced, while the vertical stress increases just a little. Consequently, the "slab effect" of the flexible pavement is considerably reduced and the structural behavior changes from elastic to plastic. We should investigate, for example, what would theoretically happen in a thin pavement when the modular ratio E_1/E_2 changes from 20 to 2, without alteration in the other modulus. For the parameters E_1/E_2 = 20, E_2/E_3 = 20, h_1/h_2 = 0.25, h_2/r = 1.25, and p = 100 psi, we have p_{z2} = 7 psi and p_{r1} = 580 psi (tension). For E_1/E_2 = 2 with the other parameters remaining the same, we now have p_{z2} = 9 psi and p_{r1} = 71 psi (compression). In this particular case, simply because of a temperature change, the radial stress changed from a tension of 580 psi to a compression of 71 psi, while the vertical stress was only slightly affected.

EXPERIMENTAL TESTING OF THE ELASTIC LAYERED THEORY

The numerical computation of influence coefficients made possible the experimental testing of the elastic layered theory. In his original paper, Burmister (4) proposed a graphical solution of his multiple equations system to calculate the deflection of the two-layered system. The graphical process consists in drawing trial curves of the deflection factor, F, on Burmister's graph (Fig. 4) and selecting the best fitting curve. Later Burmister (33) presented an evaluation of pavement systems of the WASHO Road Test by this method. Yet, under close examination the results seem to be somewhat disappointing. It is apparent that the sole criterion of the shape of the trial curves is not reliable enough to permit an evaluation of the acting modulus of elasticity.

There have been several experimental studies that have attempted to interpret measured stresses and deflections through the layered theory and to correlate measured and theoretic values. The prevailing trend in many technical reports has been to underestimate observed discrepancies, explaining the deviation between measured and computed values as inconsistencies of the measured data. However, a close check on the comparison often shows that the differences are not to be disregarded.

Sowers and Vesic (13) presented an experimental study which factually compared and reported measured and computed vertical stresses in the subgrade beneath statically loaded flexible pavements. In a recent paper (34), Vesic widened the range of his conclusions, showing on a graph, besides his own findings, data from other researchers such as Griffith, McMahon and Yoder, the Road Research Laboratory and the AASHO Road Test. The general conclusion of these studies indicates a reasonable agreement between measured and computed values only for pavements possessing some tensile strength, like soil-cement and tar-macadam bases. For flexible pavements devoid of tensile strength, the measured and computed values show a considerable dis-

agreement. The vertical stresses beneath the latter type of pavement are much higher than the values computed by the layered theory, being closer to the values given by the Boussinesq-Love analysis for a uniform medium. The vertical stresses in a homogeneous soil measured by the U. S. Corps of Engineers in the Vicksburg tests (17) are close to the distribution predicted by the Boussinesq-Love analysis.

The mass of experience available from several sources is not yet large enough to warrant a final conclusion, but it strongly indicates a serious deficiency of the layered theory. At least there is not one experimental study showing a good and general agreement between measured and computed stresses. The consistency of results among different researchers utilizing different procedures rules out the possibility of a systematic error in the measuring system. The inadequacy of the layered theory appears to be so great that the discussion of the degree of physical analogy between the theoretic elastic model and the real pavement would be meaningless. The tentative conclusion would be that the theory simply does not apply to the non-tension-resisting pavements.

It cannot be said, however, that pavements without tensile strength follow the Boussinesq-Love analysis. This would be a mathematical absurdity because the Boussinesq-Love analysis starts from the assumption of a uniform medium with constant modulus of elasticity, and is not valid for a layered system. What can be said is that such pavements, for unknown reasons, present a stress distribution that happens to be similar to the Boussinesq-Love curve for a uniform medium.

INTERPRETATION OF EXPERIMENTAL RESULTS

Several factors could be pointed out as possible causes of the disagreement between theory and practice. The most important factor seems to be the lack of tensile strength of the pavement materials. The layered theory assumes equal moduli of elasticity for tension and compression, but most actual flexible pavement materials have practically no tensile strength, that is, a zero tensile modulus. A new layered theory for zero tensile modulus would be helpful to test this hypothesis, but it is not avialable. Another important factor is the nonlinearity of the stress-strain relationship. The compressive modulus depends on the load and the lateral pressure, hence on the depth. This latter factor should be less important because it is also present in the uniform medium and it does not affect the validity of the theory for that medium.

There are some other disturbing factors that the theoretical analysis shows to be of lesser importance: anisotropy of layered systems, adhesive restraint between the tire and the pavement, etc. Of course, the lack of homogeneity of the materials would also be of a disturbing factor, but its effect would be a scattering of the data and not a definite trend as shown by the test data.

If more experimental testing supports the tentative conclusions based on the data now available, the final conclusion will be warranted that the pavement rigidity has practically no effect on the stress distribution and on the reduction of the pressure transmitted to the subgrade. Semirigid pavements, like soil-cement, consitute an exception and should be designed by proper methods that take into account its tensile strength. But truly flexible pavement, devoid of tensile strength, does not contribute strength by the slab effect. It resists applied forces only by lateral distribution of stresses in depth, like a uniform medium. If this conclusion is proved true, as it seems to be, the Burmister analysis will have lost its usefulness. On the other hand, the usual CBR method that fixes the required total thickness based on subgrade strength, without much regard for quality of pavement materials, will be proved scientifically correct, at least in what concerns the pressure reduction. The shear strength of the system will be the determining factor of the pavement bearing capacity. Shear strength computations will be very much simplified by the hypothesis of Boussinesq-Love stress distribution.

The problem of deflection computation remains unsolved, however. The CBR method bypasses the deflection problem through the use of correlation curves, but this is a limited method. The correlation is strictly valid only for the conditions previously experienced. The deflection calculation is essential to any scientific design method because the maximum deflection has a large bearing on the fatigue resistance of pavement layers subject to repeated loadings. It is a recognized fact that the pavement

rigidity has an important influence on the reduction of the maximum deflection of the layered system, as compared to a uniform medium. If the layered system, according to Sowers and Vesic, has a stress distribution similar to the uniform medium but the deflections are different, this difference in behavior could be interpreted as a difference in the respective elasticity moduli. The problem could be approached by the computation of an effective or equivalent modulus of the system, as a function of the layer modulus and thicknesses, so as to make the computed deflections agree with the experience. Presently there is no entirely valid theoretical analysis of this problem.

VESIC'S PROCESS OF DEFLECTION COMPUTATION

As a first solution to this problem, Vesic (34) proposed an approximate method of deflection computation based on the assumption that the layered system has a stress distribution similar to the Boussinesq-Love curve, but with a different modulus of elasticity for each layer. A slight mofidication of the Vesic process is shown in Figure 7. The modification consists in using the well-known deflection factor for a uniform medium computed by Foster and Ahlvin (35) instead of a new definition of the deflection factor as proposed by Vesic, and suppressing the curves for Poisson's ratios other than 0.5, for the reasons previously mentioned. Also a correction was made in the curve for rigid plate.

The deflection for a uniform medium subjected to a flexible load is (23, 25):

$$W = \frac{pr}{E} \quad F \tag{21}$$

$$F = \frac{1.5}{\sqrt{1 + Z^2}} \qquad (Z = z/r,\ \mu = 0.5) \tag{22}$$

For $z = 0$ and $F_0 = 1.5$, in which

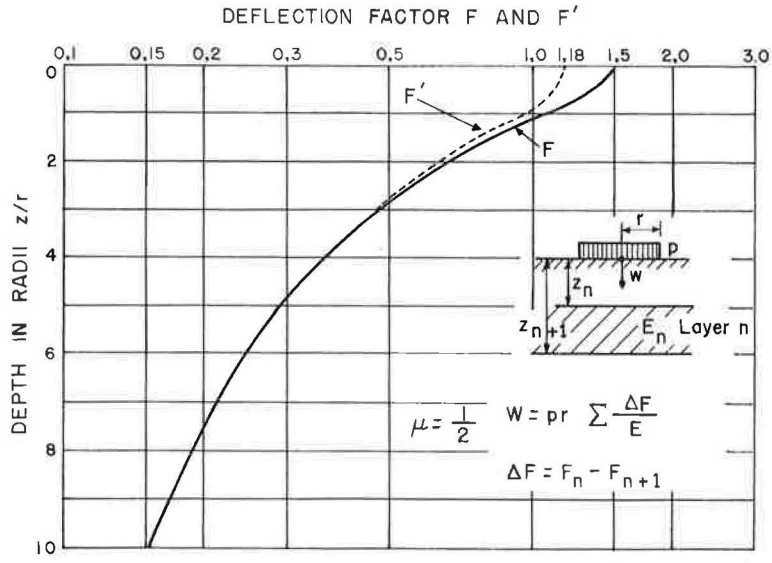

Figure 7. Vertical deflection factor for uniform load, F, and for rigid plate, F'.

W = deflection for flexible load,
p = contact pressure,
z = depth,
E = modulus of elasticity,
F = deflection factor,
r = radius of contact area,
Z = depth in radius, and
μ = Poisson's ratio.

The deflection equation for a uniform medium loaded with a rigid plate, not generally found in the technical literature, is the following:

$$W' = \frac{pr}{E} \quad F' \tag{23}$$

$$F' = \frac{1.5}{2}\left[\frac{Z}{1 + Z^2} + \arctan\frac{1}{Z}\right] \tag{24}$$

For $z = 0$ and $F'_0 = 1.18$, in which

W' = deflection for rigid plate, and
F' = deflection factor.

For Z equal to or greater than 0.5, F' may be computed by the following approximate formula:

$$F' = \frac{1.5}{\sqrt{1.5 + Z^2}} \tag{25}$$

For Z greater than 3, F' is practically equal to F. This is a predictable conclusion because at greater depths the difference between the two cases of loading becomes less important. This fact is apparent in Figure 7. For Z greater than 6, both F and F' may be computed by the following approximate formula:

$$F = F' = \frac{1.5}{Z} \tag{26}$$

When Z is infinite, $F = F' = 0$. Factors F and F' are shown in Figure 7.

Starting from the premises assumed by Vesic, and from the differential deflection equation:

$$dW = \left(p_z - p_r\right) dz \qquad (\mu = 0.5) \tag{27}$$

it can be demonstrated that the total deflection of the layered system is given by the following equation (Fig. 7):

$$W = pr \sum \frac{\Delta F}{E} \tag{28}$$

$$\Delta F = F_n - F_{n+1}$$

For the rigid plate F' is substituted for F, and 1.18 for 1.50.

For the two-layer system, Eq. 28 becomes:

$$W = pr\left(\frac{1.5 - F_1}{E_1} + \frac{F_1}{E_2}\right) \qquad (F_2 = 0) \tag{29}$$

and for the three-layer system the deflection is:

$$W = pr\left(\frac{1.5 - F_1}{E_1} + \frac{F_1 - F_2}{E_2} + \frac{F_2}{E_3}\right) \qquad (F_3 = 0) \tag{30}$$

and so on.

Vesic presented an evaluation of the deflection of the WASHO and AASHO Road Tests by his process. Deflections computed by the Vesic process are much higher than those given by the Burmister analysis. Deflections of the two- and three-layer systems of the previous example determined by the Vesic process are as follows:

1. For the two-layer system ($h/r = 2$ and $F_1 = 0.67$):

$$W = 100 \times 5\left[\frac{1.5 - 0.67}{20,000} + \frac{0.67}{1,000}\right] = 0.35 \text{ in.}$$

The deflection found by the Burmister analysis was 0.17 in.

2. For the three-layer system:

$$W = 100 \times 5\left[\frac{1.5 - 1.34}{400,000} + \frac{1.34 - 0.56}{20,000} + \frac{0.56}{1,000}\right] = 0.30 \text{ in.}$$

The deflection computed by the Jeuffroy-Bachelez method was 0.14 in.

The equivalent modulus of a layered system by Vesic's process is given by the equation:

$$\frac{1.5}{E_2} = \frac{1.5 - F_1}{E_1} + \frac{F_1 - F_2}{E_2} + \frac{F_3 - F_4}{E_3} + \ldots \tag{31}$$

$$W = \frac{1.5\,pr}{E_e} \tag{32}$$

SUMMARY AND CONCLUSIONS

The structural behavior of the flexible pavement may be described as elastic or viscoelastic. An elastic model is adequate to represent the flexible pavement in the first case, and also to a lesser extent in the second case if the final modulus of elasticity is adopted as the effective modulus. The theory of elasticity is the governing law in the first case, and also plays an important role in the second.

The layered system model of the flexible pavements, with the usual assumptions of perfect elasticity, boundary and continuity conditions, is adequate for the development of valid theoretical analysis. However, this model should be expanded to include the condition of zero tensile modulus of the component materials. The elastic model is characterized by two elastic constants for each layer, the modulus of elasticity and Poisson's ratio.

The 0.5 value for Poisson's ratio seems to be the most adequate, in the light of the

available experimental and theoretical evidence. Practical graphs of formulas for deflection analysis should not include other values for Poisson's ratio, for this inclusion would be unwarranted and misleading. The discussion of alternative values for Poisson's ratio belongs to the realm of theoretical hypothesis. A coefficient related to the volumetric change would be more reliable as the second elastic constant, besides the elasticity modulus.

Starting from the elastic model and known values of the model parameters and chosing adequate average values for the elastic constants, valid for the particular conditions of the problem under study, the elastic layered theory should provide a reasonably accurate framework for the solution of many problems. One of the main problems of the layered system is the calculation of the deflection factor.

The most important layered system analyses and theories were reviewed and discussed. Examples of application were computed. The available experimental data from many sources were used to test the validity of the layered system analysis. It is apparent from the available testing data that the present layered system theory is inadequate to explain the structural behavior of flexible pavements lacking tensile strength. However, more research is needed to confirm this statement.

It has been suggested that the most important cause of disagreement between theory and practice is the lack of tensile strength of common flexible pavement materials. The nonlinearity of stress-strain relationship is a secondary cause. Other disturbing factors exist but are of lesser importance.

The need is apparent for a better theoretical analysis than the present layered system theory. It is suggested that the layered theory should be corrected to apply to zero tensile modulus materials.

The deflection computation of layered systems could be profitably approached by the theoretical calculation of an equivalent modulus of the system as a function of moduli and thicknesses of the layers, so as to make the computed deflections agree with experience.

The CBR in its actual improved form is considered to be one of the most dependable methods of thickness design now available.

ACKNOWLEDGMENTS

In a paper of this kind, the author owes almost everthing to writers of original papers in the field. His personal task was to review, organize and discuss, and to a certain extent to evaluate, other authors' works. The author has endeavored to keep track of the sources of the most important theories and studies, which are acknowledged in the list of references. However, in the process of reading and utilizing a large number of books, papers and articles, comprising almost all available technical literature on the subject, it is possible that the author involuntarily missed making some reference. This is almost unavoidable when one tries to present a comprehensive and integrated picture of the subject, and not a mere catalog of papers.

Professor J. Washington Oliveira's encouragement and help in the mathematical analysis is greatly appreciated.

REFERENCES

1. Aratangy, N. Medida de Deformacão de Pavimentos. Rel. IV Reunião Anual de Pavimentacão, 1963.
2. de Barros, S. Thenn. O Cálculo das Tensões e dos Recalques do Pavimento Flexivel. 1963.
3. Porter, O. J. The Preparation of Subgrades. Highway Research Board Proc., Vol. 18, pp. 324-335, 1938.
4. Burmister, D. M. The Theory of Stresses and Displacements in Layered Systems and Applications to the Design of Airport Runways. Highway Research Board Proc., Vol. 23, pp. 126-148, 1943.
5. Revised Method of Thickness Design for Flexible Highway Pavements at Military Installations. U. S. Army Corps of Engineers Tech. Rept. No. 3-582, 1961.

6. Burmister, D. M. The General Theory of Stresses and Displacements in Layered Systems. Journal of Applied Physics, 1945.
7. Hank, R. J., and Scrivner, F. H. Some Numerical Solutions of Stresses in Two- and Three-Layered Systems. Highway Research Board Proc., Vol. 28, pp. 457-468, 1948.
8. Fox, L. Computation of Traffic Stresses in a Simple Road Structure. Proc. 2nd Int. Conf. on Soil Mech. and Found. Eng., 1948.
9. Acum, W. E. A., and Fox, L. Computation of Load Stresses in a Three-Layer Elastic System. Geotechnique, 1951.
10. Jones, A. Tables of Stresses in Three-Layer Elastic Systems. Highway Research Board Bull. 342, pp. 176-214, 1962.
11. Shiffman, R. L. The Numerical Solution for Stresses and Displacements in a Three-Layer Soil System. Proc. 4th Int. Conf. on Soil Mech. and Found. Eng., 1957.
12. Peltier, R. Evolution des Methodes de Calcul des Chaussees Souples. Routes, 1962.
13. Sowers, G. F., and Vesic, A. B. Vertical Stresses in Subgrades Beneath Statically Loaded Flexible Pavements. Highway Research Board Bull. 342, pp. 90-123, 1962.
14. Ruiz, C. L. Flexibilidad de las Capas Asfalticas de Tipo Superior. XII Reunion Anual del Asfalto, 1962.
15. The AASHO Road Test, Report 7, Summary Report. Highway Research Board Spec. Rept. 61G, 1962.
16. Spangler, M. G. Engineering Characteristics of Soils and Soil Testing. In Highway Engineering Handbook, ed. by K. B. Woods, Pt. 2, Sect. 8, pp. 8-3–8-63. New York, McGraw-Hill, 1960.
17. Investigations of Pressures and Deflections for Flexible Pavement. U. S. Army Corps of Engineers, Tech. Memo. No. 3-323, Rept. 1, 1951.
18. Investigations of Pressures and Deflections for Flexible Pavement. U. S. Army Corps of Engineers, Tech. Memo. No. 3-323, Rept. 4, 1954.
19. Hveem, F. N., and Carmany, R. The Factors Underlying the Rational Design of Pavements. Highway Research Board Proc., Vol. 28, pp. 101-136, 1948.
20. Love, A. E. H. The Stress Produced in a Semi-Infinite Body by Pressure on Part of the Boundary. Philosophical Trans. of the Royal Society, 1928.
21. Hogg, A. H. A. Equilibrium of a Thin Plate Symmetrically Load Resting on an Elastic Foundation of Infinite Depth. Philosophical Magazine, pp. 576-582, 1938.
22. Odemark, N. Investigations as to the Elastic Properties of Soils and Design of Pavements According to the Theory of Elasticity. Statens Väginstitut, Meddelande No. 77, 1949.
23. Palmer, L. A., and Barber, E. S. Soil Displacement Under a Circular Loaded Area. Highway Research Board Proc., Vol. 20, pp. 279-286, 1940.
24. Pavement Design for Roads and Airfields. Road Research Laboratory, Tech. Paper No. 20, 1951.
25. Kansas State Highway Commission. Design of Flexible Pavements Using the Triaxial Compression Test. Highway Research Board Bull. No. 8, 1947. 63 pp.
26. McLeod, N. W. Relationships Between Applied Loads, Surface Deflection, Traffic Volumes and Thickness of Flexible Pavements. Proc. 5th Int. Conf. on Soil Mech. and Found. Eng., 1961.
27. McDowell, C. Wheel Load Stress Computations Related to Flexible Pavement Design. Highway Research Board Bull. 114, pp. 1-20, 1955.
28. Ivanov, N. N. Calcul des Chaussees Souples Soumises a des Charges Repetees de Courte Duree. Routes, 1962.
29. Baker, R. F., and Papazian, H. S. The Effect of Stiffness Ratio on Pavement Stress Analysis. Highway Research Board Proc., Vol. 39, pp. 61-85, 1960.
30. Peattie, K. R. Stress and Strain Factors for Three-Layer Elastic Systems. Highway Research Board Bull. 342, pp. 215-253, 1962.

31. Shiffman, R. L. General Analysis of Stresses and Displacements in Layered Elastic Systems. Proc. Ann Arbor Conf., 1962.
32. Jeuffroy, G., and Bachelez, J. Note on a Method of Analysis for Pavements. Proc. Ann Arbor Conf., 1962.
33. Burmister, D. M. Evaluation of Pavement Systems of the WASHO Road Test by Layered System Methods. Highway Research Board Bull. 177, pp. 26-54, 1958.
34. Vesic, A. B. Discussion at the Ann Arbor Conference. Proc. Ann Arbor Conf., 1962.
35. Foster, C. R., and Ahlvin, R. G. Stresses and Deflections Induced by a Uniform Circular Load. Highway Research Board Proc., Vol. 33, pp. 467-470, 1954.

An Investigation of the Destructive Effect of Flotation Tires on Flexible Pavement

ERNEST ZUBE and RAYMOND FORSYTH
Respectively, Assistant Materials and Research Engineer and Senior Materials and Research Engineer, California Division of Highways, Sacramento

As a result of the increased usage of flotation or "wide base" tires in lieu of the normal dual-wheel configuration during the last three years, an investigation has been completed to compare the relative destructive effect or to determine the single-axle loading which would produce the same destructive effect as that resulting from the dual-wheel single-axle legal loading of 18,000 lb. The two criteria of destructive effect selected for this investigation were pavement deflection and strain. Deflection measurements were made using linear variable differential transformer gage installations and the Benkelman beam. Pavement strain measurements were made using SR-4 strain gages attached to the top and bottom of the AC surfacing. Test sites with widely varying structural sections were selected for this study. Analysis of strain and deflection data indicates that the destructive effect of a flotation tire with a single-axle loading of 12,000 lb equals or exceeds that of the dual-wheel configuration at an axle loading of 18,000 lb. Relationships between tire pressure, pavement temperature, axle loading, pavement deflection, surface tensile strain, and type of wheel loading are presented.

•IN THE LAST two years, the use of flotation or "wide base" tires in lieu of the normal dual-wheel configuration has become increasingly commonplace, particularly on transit mix concrete trucks. The reasons advanced by the tire manufacturers for the increased popularity of these tires include lower rolling resistance, reduced dead weight, improved riding qualities, off-the-road mobility, and a high-load front axle capacity. With the increased usage of these tires, it was apparent that a comparison should be made of the destructive effect of trucks utilizing this type of tire with that induced by the normal single-axle dual-wheel configuration at its maximum legal load limit of 18,000 lb.

An investigation of a similar nature was included and reported on during the AASHO Road Test (1). In this investigation, various test sections of Loop 2 were subjected to 32,000 lb tandem-axle loads with conventional and low-pressure low-silhouette (LPLS) tires. The results of this study indicated that loss of pavement serviceability was slightly less over those sections on which the LPLS tires were utilized. However, it is believed that these results are not significant to this investigation because the tires involved were of a military type. An examination of the contact prints shown in the report of the test (1, Fig. 9) reveals an entirely different dual and flotation tire configuration than that resulting from standard commercial truck tires of both types. In fact, the overall width of the two military duals is equal to or less than that of the military LPLS tire. The reverse holds true in the case of the commercial flotation and dual truck tires used in this investigation.

Paper sponsored by Committee on Flexible Pavement Design and presented at the 44th Annual Meeting.

CRITERIA OF DESTRUCTIVE EFFECT

To compare the destructive effects of two types of truck tire configuration, criteria on which rational judgments may be based must first be selected. Certainly destructive effect of wheel loads on flexible pavements may be evaluated in many different ways. In this particular case, however, the difference between the wheel configurations is relatively minor so that a valid appraisal requires sensitive criteria. In addition, these criteria must be related to flexible pavement performance. It is believed these requirements are effectively fulfilled by measurements of AC surfacing tensile strain and transient pavement deflection.

The choice of AC surfacing tensile strain was based on the preliminary findings of Pell (2) and others, who observed that the fatigue life of an AC surfacing is primarily a function of tensile strain and independent of surfacing temperature or speed of loading. Application of the layer theory and of the limited data available indicates that tensile strain at the bottom of the AC surfacing is substantially greater than that which occurs on the surface.

Unfortunately, the time available for this investigation did not permit the installation of strain gages at the bottom of the AC surfacing, except for the one project installation at the Shell Avenue test road. It is reasonable to assume, however, that surface tensile strain measurements, if not as large in an absolute sense as the bottom strain measurements, are at least directly proportional so that for the purpose of comparison they may be considered valid criteria.

The selection of pavement deflection was made with considerable confidence in view of the amounts of very productive pavement deflection research of the last twenty years. In addition to the extensive deflection work done on the two major test roads (AASHO and WASHO), the California Division of Highways and other agencies have, with some success, related allowable levels of transient pavement deflection to fatigue cracking of AC surfacing. The California Division of Highways has, in fact, for some years utilized deflection measurements in the design of reconstruction of distressed roadways. There can be little doubt that transient pavement deflection provides an excellent indicator of the in-place strength of an existing roadway and a reasonably accurate forecast of future fatigue cracking.

Considerations of plastic deformation or lateral displacement have not been taken into consideration because for a given axle load the pressures induced by both wheel configurations at depths greater than 6 in. are, for all practical purposes, the same.

TEST EQUIPMENT AND INSTRUMENTATION

This study, undertaken in April 1963 was accomplished using pavement deflection and strain measurements taken over several different structural sections in Northern California. Two trucks, both with single rear axles, were used as test vehicles. In one case, the axle was loaded to California's legal limit of 18,000 lb and supported with dual wheels using 10.00-20 truck tires with the 12-ply casings inflated to a pressure of 70 psi. The rear axle of the other truck carried a variable load and was supported by 18.00-19.5 flotation tires with 16-ply wide-base casings inflated to 75 psi (Fig. 1).

Pavement deflection measurements were obtained with a Benkelman beam and, at three locations, with linear variable differential transformer (LVDT) gages. Strain measurements were taken at varying distances from the outside edge of the loaded tires utilizing surface set SR-4 strain gages attached to the pavement surface (Figs. 2 and 3). At the Shell Avenue test road in Martinez, instrumentation installed previously in support of the test road project sponsored jointly by the University of California and Contra Costa County made it possible to obtain pavement strain measurements at the bottom of the AC surfacing layer.

After grinding the surface to remove large irregularities, two transversely oriented SR-4 strain gages were placed at each test location. These gages, placed at 6-in. intervals, were cemented into place with Duco cement and then covered with Gagekoat No. 5 for physical protection. During the early trials, it was noted that actual contact between the strain gage and the tire resulted in extremely erratic and obviously incorrect readings. Because unprotected gages were prone to damage by tire contact, this protective coating was necessary.

Figure 1. Truck with single-axle flotation tire configuration.

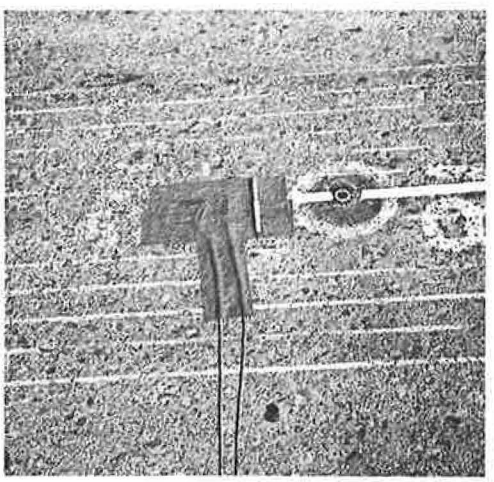

Figure 2. SR-4 pavement strain and LVDT deflection gage installations at Shell Ave. test road at Martinez.

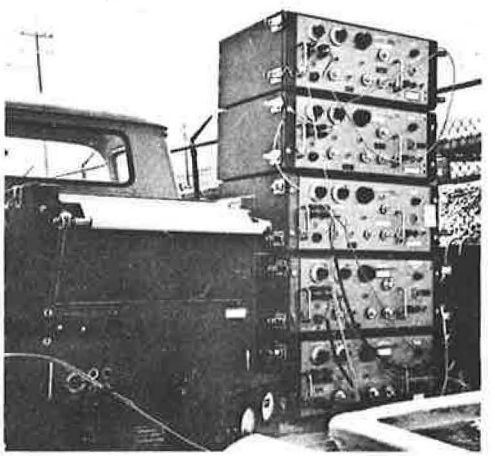

Figure 3. Strain recording equipment operated by personnel of University of California at Shell Ave. test road.

TEST SECTIONS

It was apparent from the beginning of the investigation that a study involving the variables of load, tire configuration, structural section, pavement deflection, and pavement strain could, unless limited in scope, become extremely unwieldy, time consuming, and expensive. The relatively few test sections were chosen, therefore, to represent the most common types of AC surfaced structural sections, and in addition, to present a large range of pavement deflection for increased sensitivity. The sites selected for this study are given in Table 1.

TABLE 1

TABULATION OF PEAK VALUES OF TRANSVERSE SURFACE TENSILE STRAIN

Location	Structural Section	Pav. Temp (° F)	Flotation Tire Axle Loading (lb)	Max Surface Tensile Strain (Flotation) (μ in./in.)	Max Surface Tensile Strain (Dual Wheel) (μ in./in.)
III-Sac-232-A	3¾-in. AC	110 - 118	11,000	28[a]	36[a]
Sta. 304+04	8-in. CTB(C1"A")	94 - 98	12,000	48[a]	42[a]
	Exist. Pav.				
III-Sac-232-A	3¾-in. AC	93 - 94	11,000	112	108
Sta. 405+90	3-in. AC (Base)	92 - 99	11,000	170	185
	6-in. AB	85 - 90	12,000	170	170
	Exist. Pav.	87 - 92	12,000	175	163
III-Sac-232-A	3¾-in. AC	75 - 77	10,000	90	125
Sta. 354+00	12-in. AB	130 - 132	12,000	62	49
	Exist. Pav.	68 - 71	12,000	105	116
Service & Supply	3-in. AC	105 - 115	10,000	314	352
Yard (60th St.	9-in. AB	85 - 95	11,000	257	277
& Folsom Blvd.)		118 - 128	12,000	352	310
City of Woodland	3-in. AC	100 - 110	10,000	385	468
(Pendergast St.)	6-in. AB	70 - 75	11,000	473	588
		61 - 64	12,000	427	463
Shell Ave.	3-in. AC (new)				
test road	2-in. AC (old)				
	Var. AB	70 - 71	12,000	795[b]	800[b]
State Fair Grounds	2-in. AC				
(Women's Bldg.)	4-in. AB				
Gage 1		40 - 42	10,000	145	190
		42	12,000	167	205
		46	15,000	253	228
		43 - 46	18,000	283	188
Gage 2		40 - 42	10,000	80	122
		42	12,000	100	125
		46	15,000	148	140
		43 - 46	18,000	160	119
Gage 3		40 - 42	10,000	110	150
		42	12,000	124	162
		46	15,000	190	177
		43 - 46	18,000	215	155
Gage 4		40 - 42	10,000	110	158
		42	12,000	135	167
		46	15,000	205	198
			18,000	232	155

[a]Point of stress reversal not determined.
[b]Transverse tensile strain at bottom of AC layer.

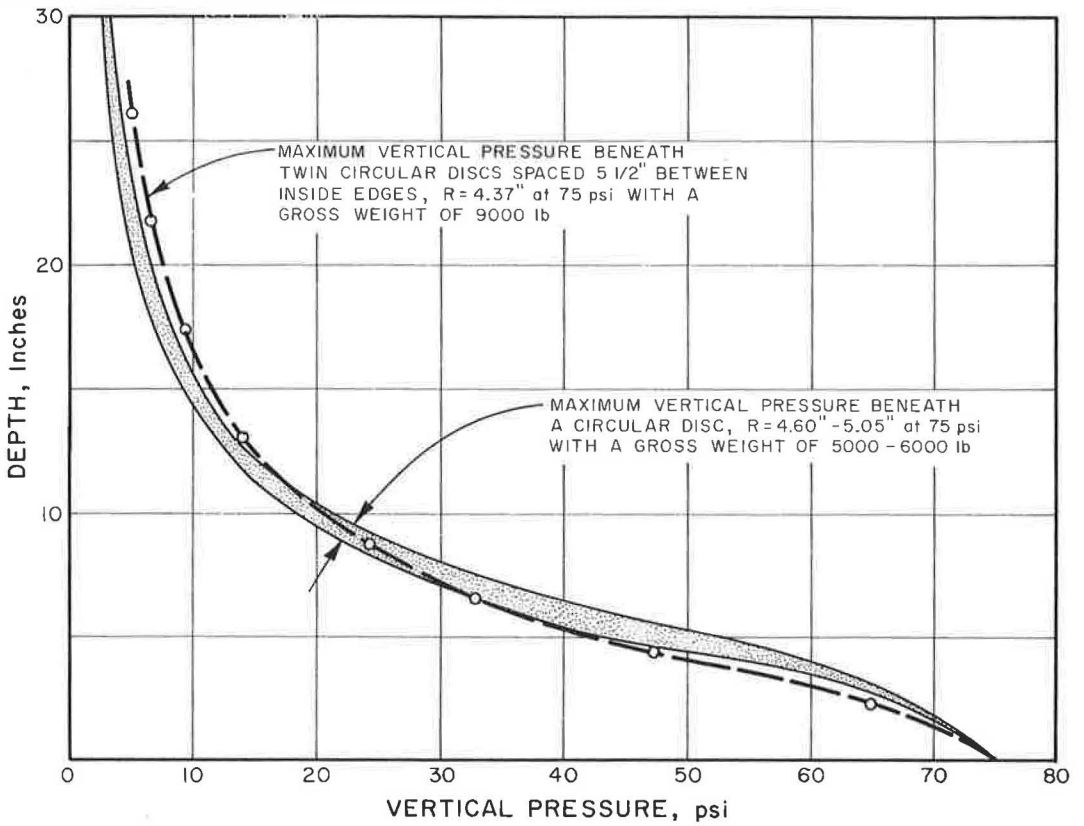

Figure 4. Vertical pressure vs depth (Boussinesq equation).

The initial range of flotation tire loading was determined by utilizing the theoretical Boussinesq equation. With this analysis, a comparison of vertical pressure induced by twin circular discs at 75 psi carrying a gross weight of 9,000 lb was compared to that induced by a single circular disc at 75 psi loaded from 5,000 to 6,000 lb. The results of this analysis (Fig. 4) correspond to calculations made earlier by personnel of the Washington State Highway Department. Examination of Figure 4 shows that at depths of from 0 to 6 in., the vertical pressure induced by the single circular disc would exceed that of the twin circular discs. Beyond approximately 11-in., the vertical pressure induced by the twin discs exceeds that of the single circular disc. Although the Boussinesq equation is purely a mathematical development of the elastic theory for an isotropic, elastic, homogenous, and infinite mass, it has been shown to be reasonably accurate for flexible sections as demonstrated by Herner (3) and Sowers (4) and the results by the Stockton test track (5). It was decided, based on this analysis, that a single flotation tire loading range of 5,000 to 6,000 lb would provide a good starting point for the comparison of the two types of tire and wheel configuration.

It was also decided to confine both deflection and pavement strain measurements to the axis normal to the direction of travel at each test point. This selection is based on long experience in California in which it has often been observed that the initial manifestation of alligator cracking is, in almost every case, longitudinal cracking in or close to the wheelpath. The fact that transverse bending is generally more pronounced is obvious from examination of deflection contour maps resulting from the WASHO (6) and AASHO (7) test roads. The test program for each test section, therefore, consisted of applying SR-4 strain gages oriented transversely and, on completion of instrumentation, measuring pavement surface strain at varying distances from the edge of the

loaded wheel. At each location, strain gage measurements were determined for a dual-wheel loading of 9,000 lb and single flotation tire loaded at 5,000, 5,500, and 6,000 lb. Where these installations were available, LVDT deflection measurements were also obtained for the aforementioned wheel loadings. At those locations where LVDT gages were not available, however, Benkelman beam deflection measurements were obtained.

During the final phase of the investigation, a series of surface strain and LVDT deflection measurements were obtained at a roadway immediately in front of the Women's Building of the California State Fair Grounds. This site offered advantages not available elsewhere, including (a) complete freedom from traffic interference, (b) a high range of pavement deflection, (c) availability of electric power for instrumentation, and (d) close proximity to the Headquarters Laboratory. Because of these advantages, a more comprehensive instrumentation was accomplished and the scope of the investigation increased to study the effects of two more variables: (a) a wider range of flotation tire single-axle loadings, and (b) the effect on pavement deflection and surface tensile strain of lowered flotation tire pressures.

ANALYSIS OF DATA

During the first few trials it was observed that even relatively minor variations in pavement surface temperature resulted in very significant differences in the strain measurement induced by a given wheel load. Because the principal objective of this program was a comparison of destructive effect induced by two different vehicles with differing wheel configurations and loadings, it became apparent that the variable of pavement surface temperature had to be eliminated or minimized. This was accomplished by continuously alternating the two different trucks during every test series. Thus, for each balloon tire strain measurement, a corresponding dual-wheel measurement was obtained to provide the basis of the comparison (Fig. 5).

The effect of variations in temperature on surface tensile strain is shown by Figure 6, which is a plot of surface strain vs distance to edge of loaded tire for three different pavement temperatures at one test location. Examination of these plots reveals that maximum tensile strain for the dual-wheel configuration varied from 460 to 585 μ in./in. These plots also show the very definite reversal of a surface stress from tension to compression, which generally occurs at from 2 to 5 in. from the edge of the loaded wheel.

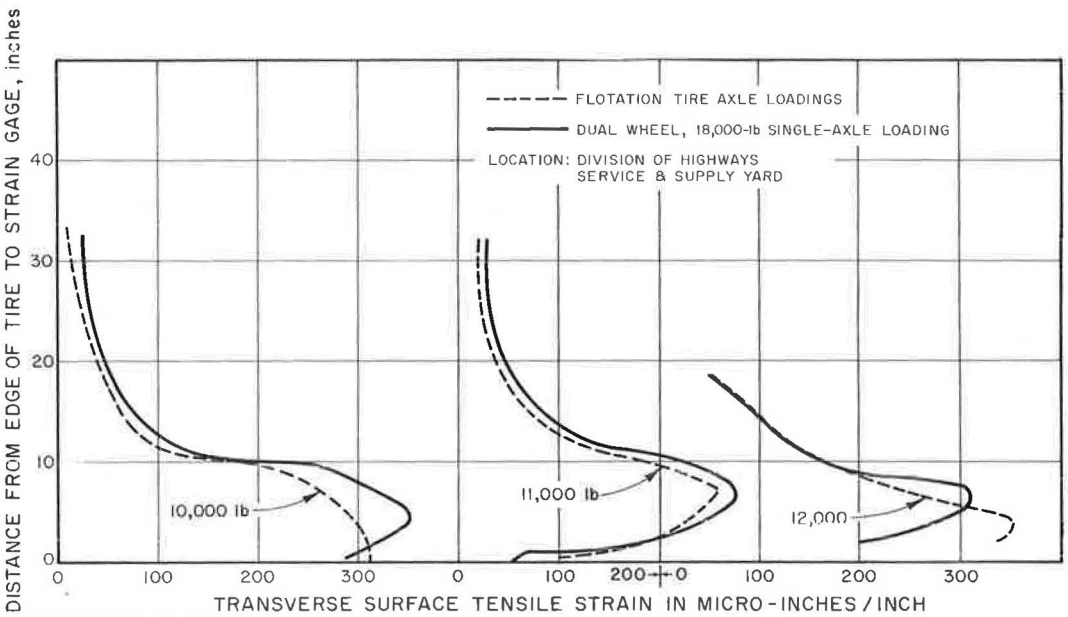

Figure 5. Pavement surface tensile strain.

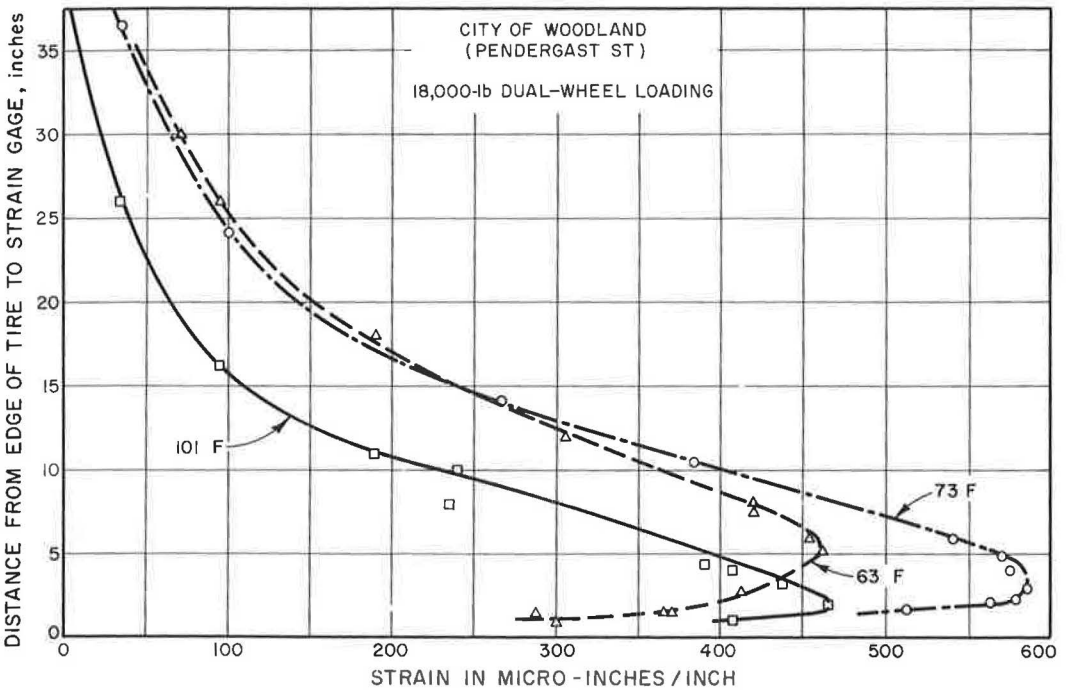

Figure 6. Variation in transverse surface strain induced by change of pavement temperature.

Another interesting aspect of Figure 6 is that maximum tensile strain occurred, for this gage installation, at the middle pavement temperature (73 F) with the strains at 63 and 101 F being about equal. This may indicate the existence of an optimum value of pavement temperature for a given AC surfacing insofar as surface strain is concerned. It is possible that increased cohesion at low temperatures and strain attenuation over a relatively large area due to plastic flow at high temperatures results in low strains at temperature extremes.

Over the cement-treated base section on III-Sac-232-A, the data did not reveal any peaking out of tensile strain. It is possible that inability to attain the critical distance to the edge of the tire due to the strain gage insulation precluded the determination of this peak value. This section, however, produced extremely low strain values, so there is some doubt as to the relative importance of this section to the study.

The relationship between strains induced by both wheel configurations for all sections revealed a very noticeable lack of consistency insofar as type of structural section is concerned. This is shown by the relatively weak structural section of Pendergast Street in the City of Woodland. Here, it was found that the equivalent flotation tire axle loading, insofar as destructive effect was concerned, was 12,300 lb as compared to the 11,000 lb equivalency for the cement-treated base overlay section at El Centro Road. Further examination of the data revealed that relative surface tensile strain can be related more directly to pavement temperature than to structural section. This is shown by Figure 7, a plot of the ratio of surface tensile strain induced by 11,000- and 12,000-lb flotation tire axle loadings and an 18,000-lb dual-wheel single-axle loading vs pavement temperature. A relatively good correlation exists for the ratio involving a flotation tire axle loading of 12,000 lb and pavement temperature. The beginning of a trend is also apparent for the 11,000-lb flotation tire axle loading. These data would indicate that, regardless of the structural section, the surface tensile strain induced by the flotation tire with a 12,000-lb single-axle loading is equivalent to a dual-wheel axle loading of 18,000 lb at a pavement temperature of approximately 80 F. At lower tempera-

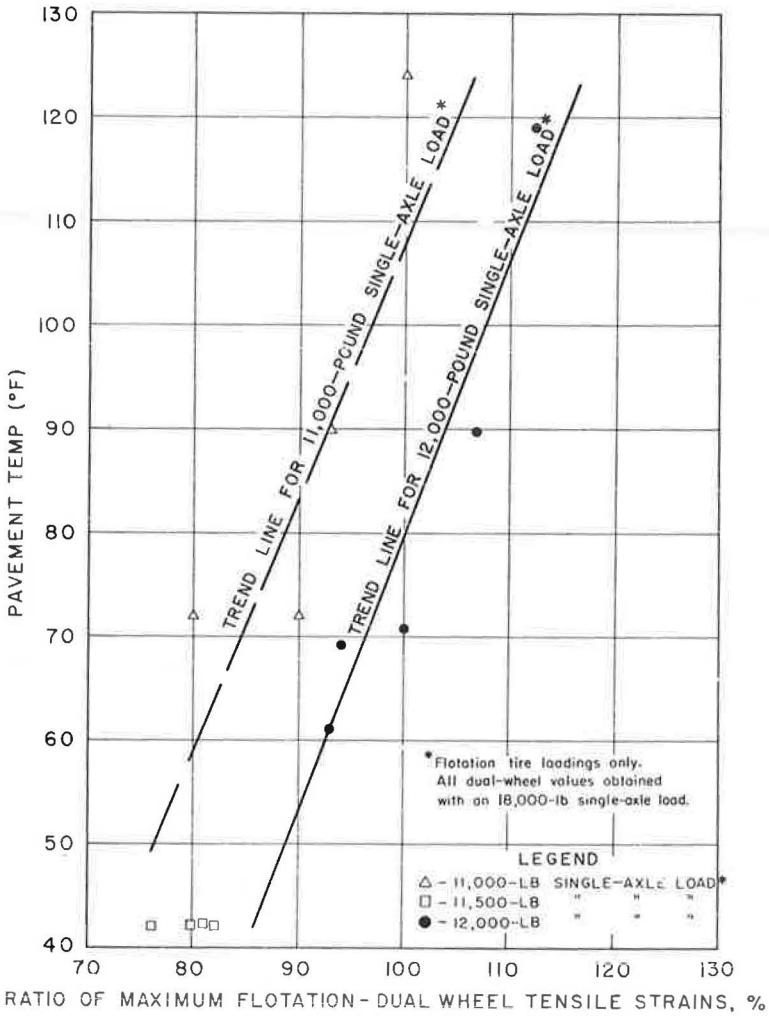

Figure 7. Flotation-dual tire surface tensile strain ratios vs pavement temperature.

tures the strain induced by the flotation tire is less and at higher temperatures the strain is greater. This general trend is also apparent for the flotation tire at an 11,000-lb axle loading, which is equivalent in surface strain to the dual-wheel loading at approximately 105 F.

Table 1 presents peak values of surface tensile strains for varying flotation tire axle loadings and the dual-wheel loading at 18,000 lb for varying structural sections and temperatures. These data show that the heavier structural sections tested on Road III-Sac-232-A produce substantially lower surface tensile strains than were obtained on the relatively weak sections at the Shell Avenue test road, City of Woodland, and the State of California Service and Supply Yard. It is also interesting to note that the maximum surface tensile strains induced by the dual wheels did not occur at the maximum test temperature at any of the test sections except the asphalt-treated base section on Road III-Sac-232-A. A comparison at this location was somewhat difficult, however, because of the limited range of pavement temperature.

At the Shell Avenue test section, it was possible to determine both transverse and longitudinal strain measurements from the bottom of the surfacing. These results are shown by Figures 8 and 9. Because the strain gage involved was fully protected from direct approach of the loaded tire, the full range of tensile and compressive strain

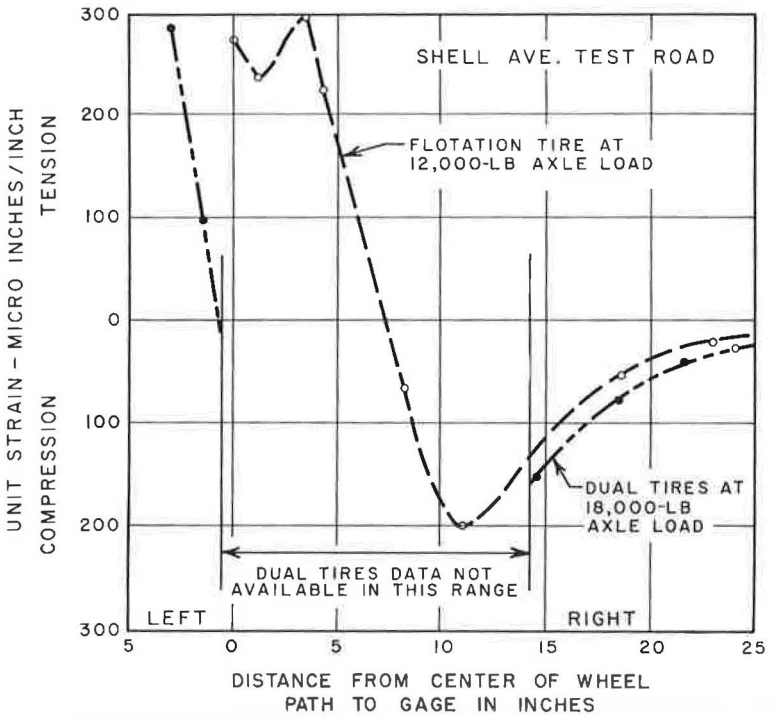

Figure 8. Bottom transverse strain.

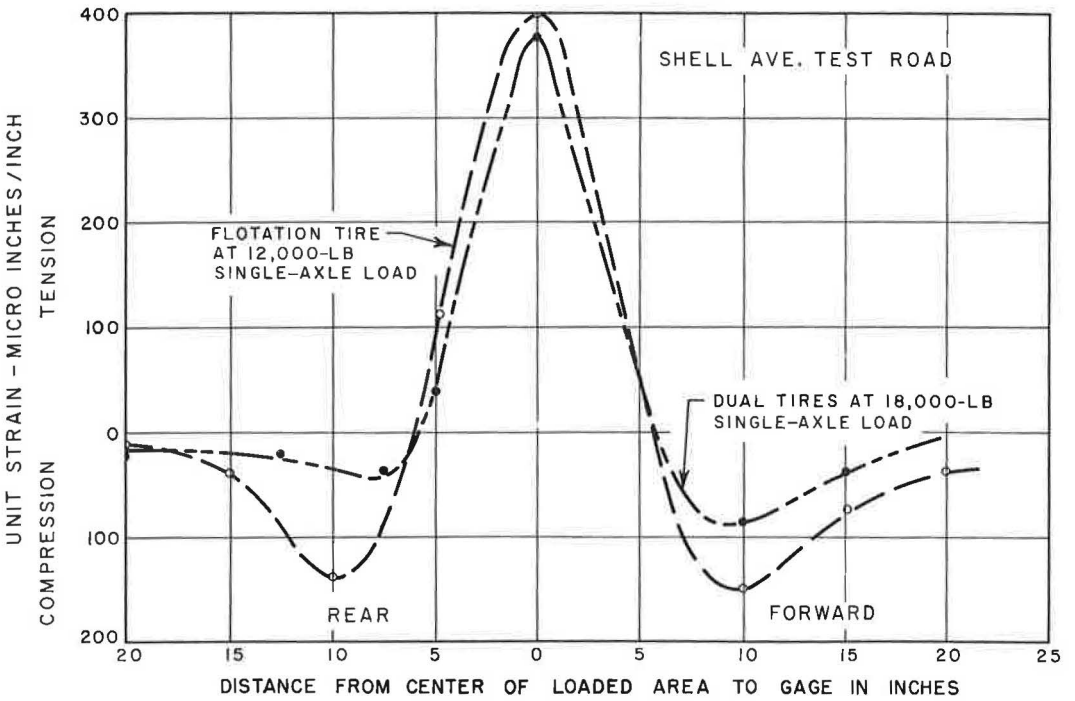

Figure 9. Bottom longitudinal strain.

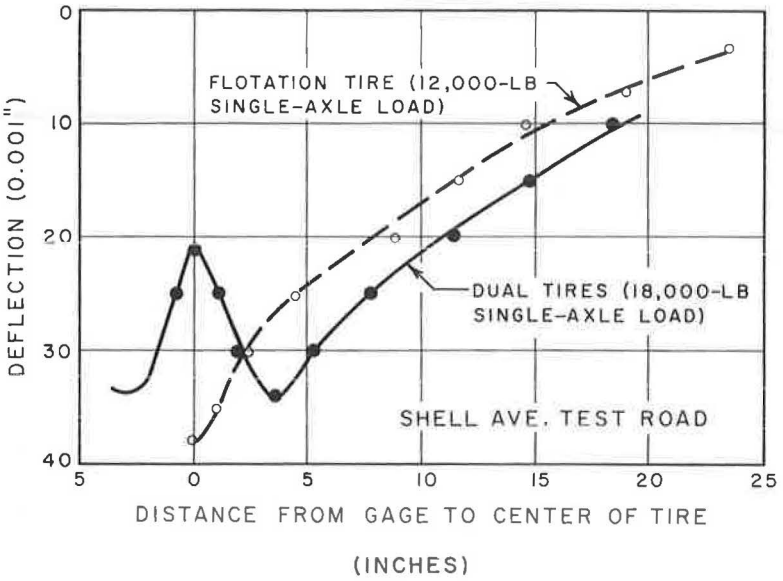

Figure 10. Transverse deflection profile LVDT gage unit.

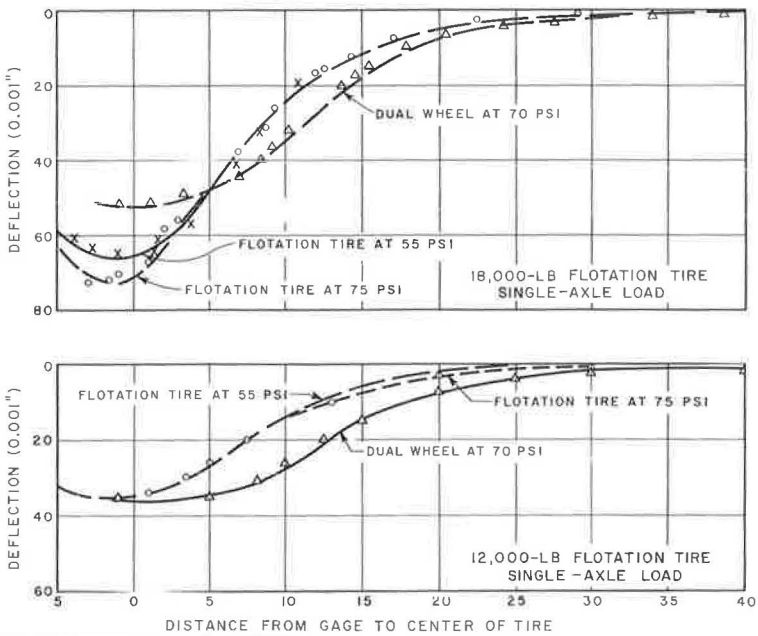

Figure 11. Effect of lowering flotation tire pressure on transverse deflection profile LVDT gage unit.

measurements could be determined for the dual-wheel configuration with an axle load of 18,000 lb and a flotation tire single-axle configuration loaded to 12,000 lb. It was found that longitudinal strain is higher at the bottom of this pavement than is the transverse strain. Figure 8 reveals that the bottom transverse strain of the flotation tire with an axle loading of 12,000 lb is almost equal to that induced by the dual tires. The bottom longitudinal strain induced by the flotation tire (Fig. 9), however, was well in excess of that for the dual tires.

At three locations it was possible to compare pavement deflection values for both balloon and dual wheels with LVDT gage installations. The data from two of these in-

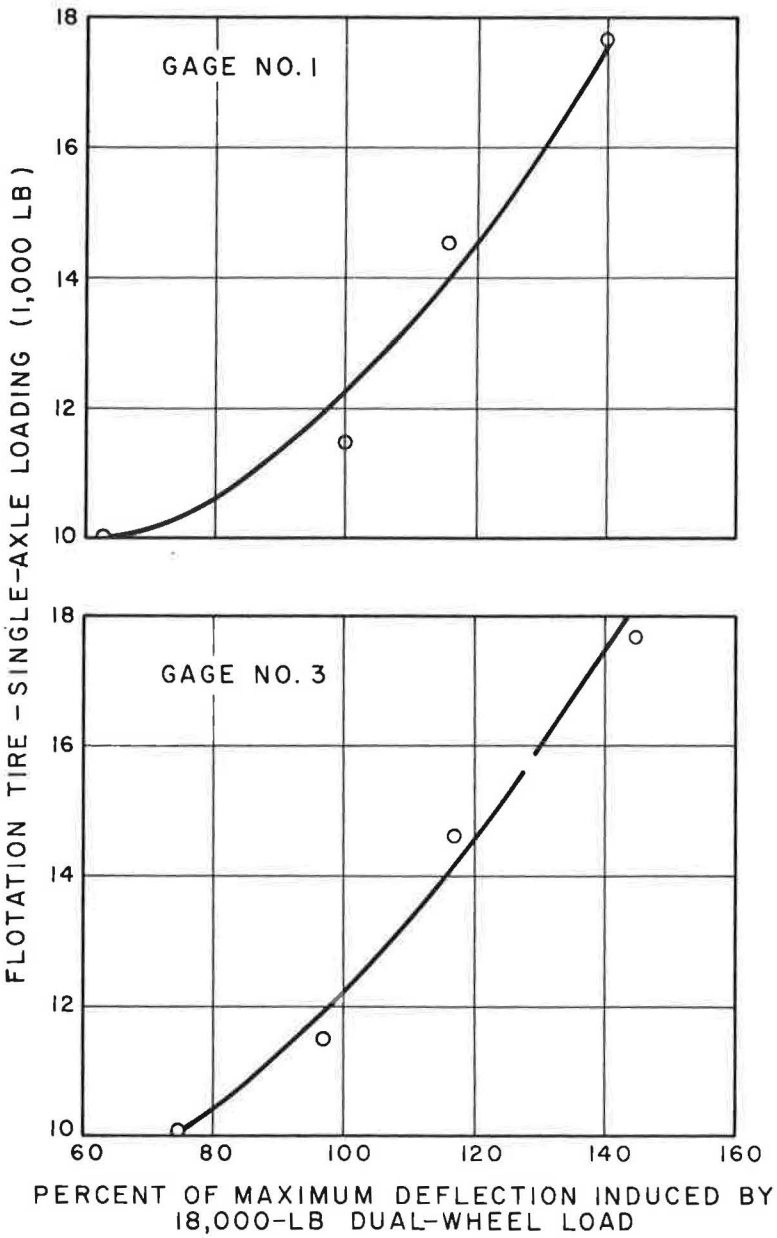

Figure 12. Flotation-dual tire deflection ratios vs flotation single-axle loading.

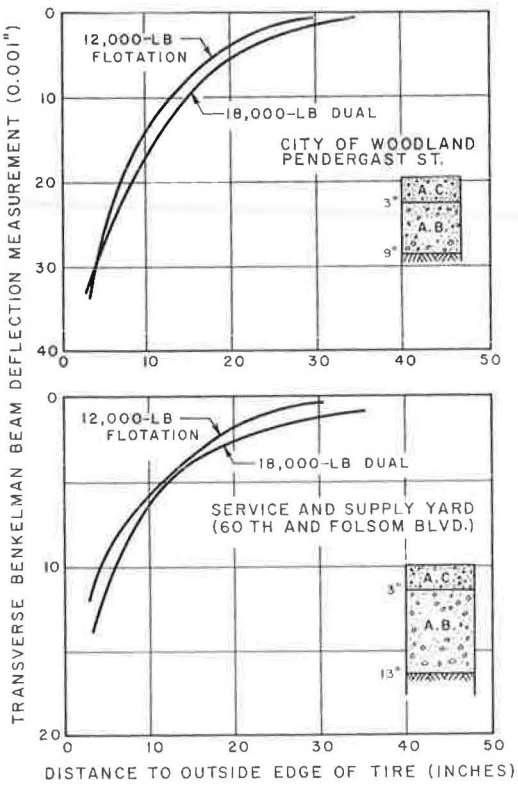

Figure 13. Transverse deflection profile.

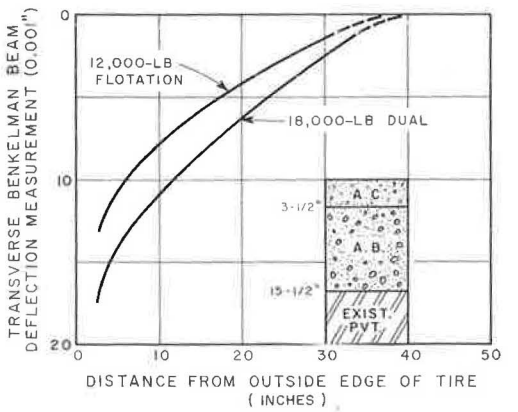

Figure 14. Transverse deflection profile, Road III-Sac-232-A, Sta.354+00.

stallations are shown in Figures 10 and 11. In Figure 10, the transverse deflection profile obtained at Shell Avenue reveals a higher maximum deflection value for the flotation tire axle loaded to 12,000 lb (0.038 in.) than the dual-wheel axle configuration at 18,000 lb (0.034 in.).

At all three locations, however, the maximum value of pavement deflection for the flotation tire with an axle loading of 12,000 lb exceeded that of the dual-wheel axle configuration loaded to 18,000 lb. The flotation tire axle loading at 11,000 lb was less, however, than that of the dual-wheel axle configuration at 18,000 lb.

A plot of flotation-dual tire deflection ratios for varying flotation tire loads is presented in Figure 12 for two gage locations at the State Fair Grounds. These data are considered significant because of the very minor temperature differential during the test period. At both gage locations, an equivalence in pavement deflections is attained at a flotation tire single-axle loading of 12,200 lb, which is in accordance with the earlier data.

Although it was impossible to compare maximum pavement deflections at those installations where LVDT gage installations were not available, the Benkelman beam data did provide an opportunity to compare the shapes of the transverse deflection profiles from the outside tire edge for each wheel configuration. These plots are shown in Figures 13 through 15. They indicate, in every case, a smaller area of influence and, hence, sharper bending of the pavement by the flotation tire.

As previously mentioned, a final portion of the program at the State Fair Grounds was devoted to a determination of the effect of lowered flotation tire pressures on transverse tensile strain and deflection. In addition to the strain and deflection measurements obtained at flotation tire single-axle loadings of 10,000, 12,000, 15,000, and 18,000 lb, additional data were obtained at the 12,000- and 18,000-lb flotation tire single-axle loadings for a flotation tire pressure of 55 psi. This tire pressure was selected as the minimum at which the flotation tires could be operated without incurring tire damage. Deflection and strain data resulting from the lowered flotation tire pressures are presented by Figures 11, 16, and 17. Figure 11 indicates that pavement deflection at the flotation tire single-axle loading of 12,000 lb was not significantly reduced by lowering the tire pressure. At the

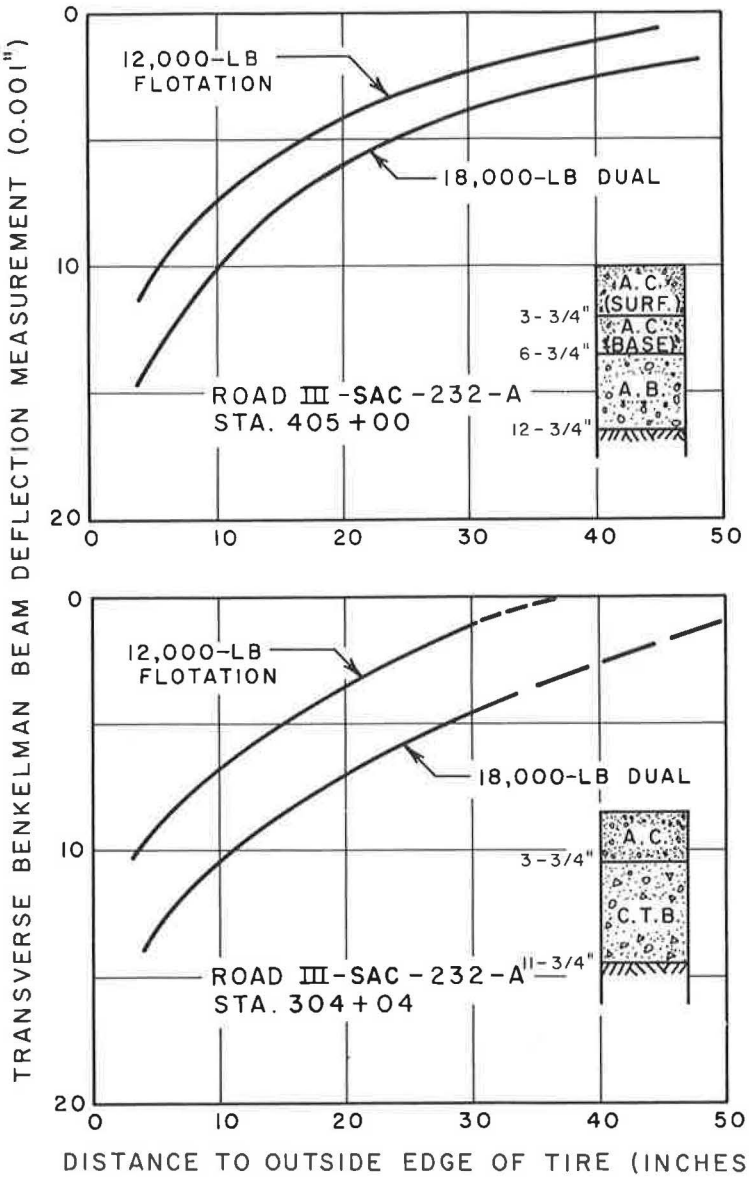

Figure 15. Transverse deflection profile.

18,000-lb flotation tire single-axle loading, however, the lowered flotation tire pressure induces a 10 percent reduction in pavement deflection. Figures 16 and 17 indicate that lateral surface tensile strain was actually increased by 13 percent at both the 12,000- and 18,000-lb flotation tire single-axle loadings, with a reduction in flotation tire pressure. This phenomenon is apparently the result of an increased pressure concentration at the side walls due to the reduction of pressure. This conclusion tends to be borne out by the work of Freitag and Green, who show vertical stress contours under an 11.00-20, 12-ply smooth tire loaded to 3,000 lb for three inflation pressures (8, Fig. 4). Here, side wall vertical stress remains relatively high for all three inflation pressures, with interior vertical stresses increasing in approximate proportion to increased inflation pressure. It is interesting to note that maximum edge or side wall stress was attained at the median inflation pressure rather

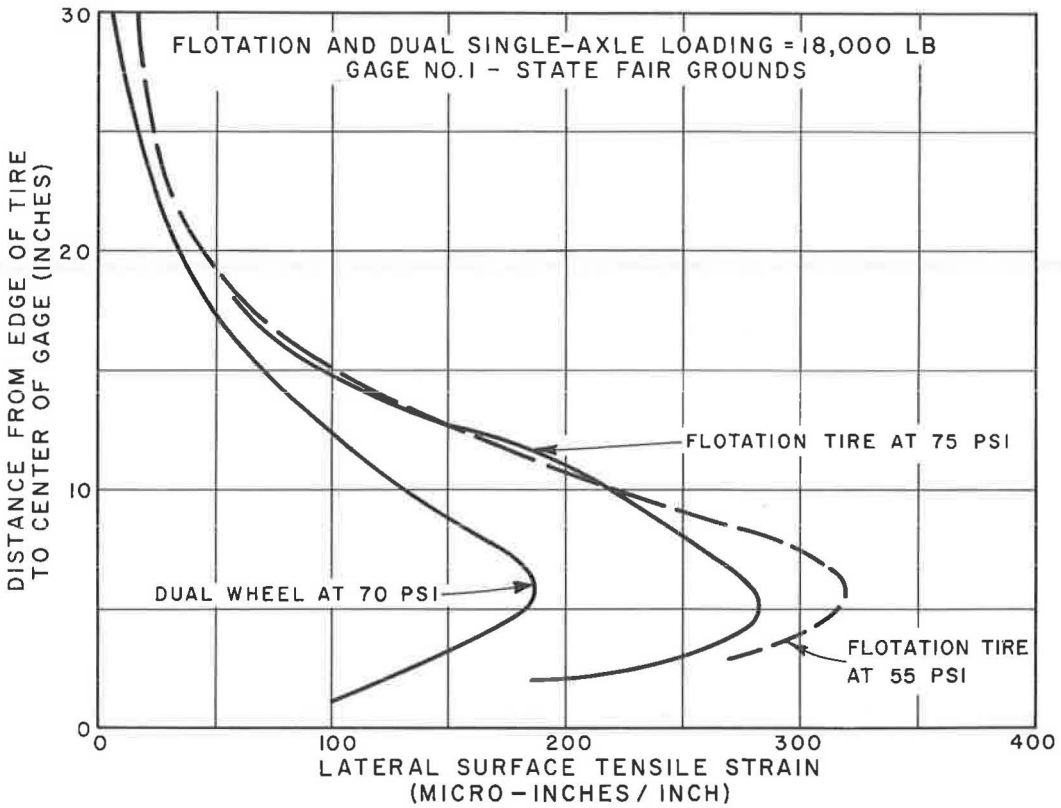

Figure 16. Effect of lowering flotation tire pressure on lateral surface tensile strain.

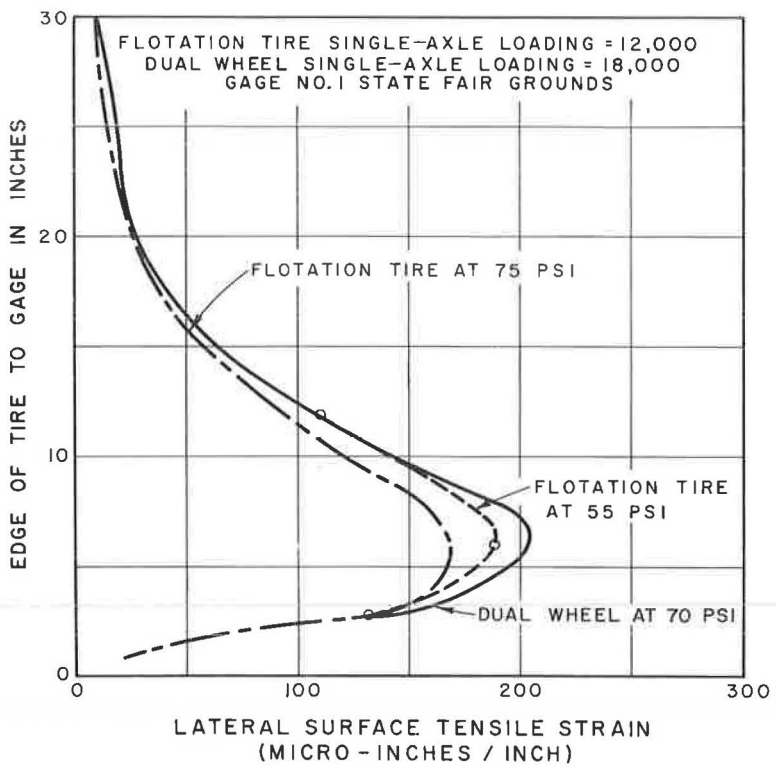

Figure 17. Effect of lowering flotation tire pressure on lateral surface tensile strain.

than at the highest or design inflation pressure. The data presented in the paper also indicate that vertical stress is very much a function of the construction or ply of the tire; i.e., the lower the ply, the more closely the contact pressure approximates air pressure. Therefore, a tangible reduction in surface tensile strain through lowered air pressure could be accomplished only by a tire specifically designed for the lower pressure and as low a ply rating as possible, consistent with the operational demands of the truck.

SUMMARY

From April until November 1963, an investigation for the purpose of comparing the destructive effect of wide-base flotation tires and the standard dual-wheel configuration on pavement was completed by the Pavement Section of the Materials and Research Laboratory. Transient pavement deflection and surface tensile strain were selected as the two criteria for evaluating destructive effect. Pavement deflection and strain measurements were obtained over eight roadways, representing a relatively wide range of flexible and composite structural section. Sufficient data were accumulated to evaluate the effect of pavement temperature, single-axle load, and tire inflation pressure on pavement deflection and surface tensile strain. With the cooperation of the University of California, it was possible to obtain bottom longitudinal and transverse strain measurements at the Shell Avenue test road.

Analysis of the data resulting from this investigation indicates that:

1. Using maximum pavement deflection as a criterion, the destructive effect of a flotation tire with a single-axle loading of 12,000 lb equals or exceeds that of a dual-wheel configuration at an axle loading of 18,000 lb.
2. The relationship between the maximum transverse tensile surface strains induced by flotation tires at various axle loadings and the dual wheel at an 18,000-lb single-axle loading relates directly to pavement temperature.
3. At a pavement temperature of 80 F, a 12,000-lb flotation tire axle loading is equivalent to the dual-wheel axle configuration at 18,000 lb. Balloon tire strains are less at lower temperatures and are greater at higher temperatures than those induced by the dual-wheel configuration.
4. At 105 F, the flotation tire axle loading at 11,000 lb is approximately equivalent to the dual-wheel axle configuration at 18,000 lb.
5. Absolute surface strain values are significantly greater for weaker structural sections for both wheel configurations than those resulting from relatively strong structural sections.
6. The data available indicate surface tensile strain is relatively low at extremes of temperature and approaches a definite peak at an intermediate temperature range. The temperature for peak tensile strain is probably a function of the type of structural section. Therefore, it is probable that even though the ratio of flotation to dual wheel strain increases with temperature, absolute values of strain for both types of wheel configuration decrease at higher temperatures.
7. At a flotation tire single-axle loading of 18,000 lb, pavement deflection decreased by 10 percent with a reduction in inflation pressure from 75 to 55 psi. At a flotation tire single-axle loading of 12,000 lb, the reduction in deflection due to fluctuations of inflation pressures was not significant.
8. Lateral surface tensile strain increased by 13 percent at both the 12,000- and 18,000-lb flotation tire single-axle loadings with a reduction in tire pressure of from 75 to 55 psi. This is believed to be the result of a greater concentration of contact stress at the side walls resulting from a decrease in tire pressure.

CONCLUSION

A standard flotation tire with a 12,000-lb single-axle loading is, insofar as relative destructive effect on a flexible or composite pavement is concerned, the equal to a standard dual-wheel configuration with an 18,000-lb single-axle loading. This equivalency, however, is subject to a certain degree of variation with pavement temperature.

Also, it appears that variations in flotation tire pressure will have a beneficial effect on this equivalency only with an accompanying change in the tire structure. In terms of absolute destructive effect, both tire and wheel configurations induce greater destructive effect on a relatively thin or weak structural section than a thick or composite pavement section.

ACKNOWLEDGMENTS

We wish to acknowledge the advice and assistance of James Barton, William Chow, and Albert Sequeira of the Structural Materials Section in the instrumentation of the LVDT deflection and pavement strain gages. We also wish to express our appreciation to Carl Monismith and the University of California for their assistance in obtaining and evaluating the strain and deflection data from the Shell Avenue test road. The work of Harold Munday, Carl Johnson, and Orvis Box in taking and tabulating the test data is acknowledged and appreciated. J. L. Beaton is Materials and Research Engineer.

REFERENCES

1. The AASHO Road Test, Report 6: Special Studies. Highway Research Board Spec. Rept. 61F, pp. 8-34, 1962.
2. Pell, P. S. Fatigue Characteristics of Bitumen and Bituminous Mixes. Proc. Int. Conf. on the Structural Design of Asphalt Pavements, Univ. of Michigan, Aug. 20-24, 1962.
3. Herner, Raymond C. Progress Report on Load-Transmission Characteristics of Flexible Paving and Base Courses. Highway Research Board Proc., Vol. 31, pp. 101-120, 1952.
4. Sowers, George F., and Vesic, Aleksandar B. Vertical Stresses in Subgrades Beneath Statically Loaded Flexible Pavements. Highway Research Board Bull. 342, pp. 90-123, 1962.
5. Accelerated Traffic Test at Stockton Airfield, Stockton, California. O. J. Porter & Co., Consulting Engineers, 1948.
6. The WASHO Road Test, Part 2: Data, Analyses and Findings. p. 105, 1955.
7. The AASHO Road Test, Report 5: Pavement Research. Highway Research Board Spec. Rept. 61E, 1962.
8. Freitag, D. R., and Green, A. J. Distribution of Stresses on an Unyielding Surface Beneath a Pneumatic Tire. Highway Research Board Bull. 342, pp. 14-23, 1962.

Discussion

J. B. DONALDSON, Truck Tire Engineering, The Goodyear Tire and Rubber Company, Akron, Ohio. —Interest in all factors affecting highway durability is evident from the support obtained for research and development studies directed toward safer and more efficient highway use. On occasion, comments may prove useful towards relating new information to existing highway use, concepts and practices.

Zube and Forsyth relate surface tensile strain and transient pavement deflection to final fatigue failure in asphaltic concrete surfaces of flexible road structures. Their study concludes that the destructive effect of flotation tires, at a single-axle loading of 12,000 lb, equals or exceeds that of a dual-wheel configuration at a single-axle loading of 18,000 lb. The scope of this investigation, however, does not include an analysis of all axle positions and characteristics to establish critical axle location with regard to pavement fatigue.

Surface tensile strain and pavement deflection developed by an 18-19.5 tire at 75-psi inflation, having approximately 130-sq in. contact area and a tread width of 12 in., are compared to a dual-wheel configuration at 70-psi inflation, having approximately 130 sq

in. of contact area and 20 in. effective tread width in the dual mounting. It is apparent that the dual-tire configuration benefits substantially from the separation of the load areas and the corresponding increase in effective contact width.

The study assumes that all single axles loaded to 18,000 lb would utilize a dual-wheel configuration or, conversely, that a single axle utilizing only one conventional tire at each axle hub would have an axle loading of approximately 9,000 lb. A large, and increasing, segment of the transportation industry utilizes vehicles which develop steering axle loads of between 12,000 and 18,000 lb. This vehicle characteristic has developed over the past decade and many vehicle concepts are committed to steering axle loads of 15,000 lb or more. The development of this vehicle class incorporated the use of conventional tires on the steering axle.

An evaluation of a single axle loaded to 12,000 lb and utilizing single 10.00-20 tires at 100 psi indicates that pavement deflection is substantially higher than for the same axle load on 18-19.5 flotation tires. A comparison of the relative tire contact areas, 72 sq in. vs 130 sq in., and tread widths, 7.5 in. vs 12 in., indicates that directionally the use of the conventional 10.00-20 tire must develop substantially higher pavement deflection and surface strain. A similar parallel exists where a single axle loaded to 18,000 lb and utilizing 14.00-20 conventional tires at 85 psi is compared to the same axle load using 18-19.5 flotation tires at 75 psi. In this service, the 14.00-20 tire develops approximately 110-sq in. contact area over a 10-in. tread width compared to an 18-19.5 contact area of 130 sq in. and tread width of 12 in.

As stated previously, these examples represent substantial segments of current transport industry practice and conditions which have prevailed for a number of years. To develop an accurate perspective of the destructive effect of flotation tires on flexible pavement it is necessary that the entire vehicle be studied. Such studies should incorporate conditions currently existing in the transport industry and justified through long use and experience. An expansion of this investigation into this area appears justified.

R. P. POWERS and W. E. MOORE, Respectively, Manager, Testing and Advanced Tire Engineering, and Manager, Truck and Mileage Tire Engineering, Firestone Tire and Rubber Company. —The paper by Messrs. Zube and Forsyth is well written and documented with much test data which have no doubt been carefully acquired. However, we do not agree with their basic conclusions and respectfully take issue with the following:

1. The choice of title is unfortunate; it states a conclusion of damaging and far-reaching significance based on a specific series of tests, ignoring other facets.
2. We question whether measurements taken at creep speeds under ideal conditions are representative of what happens under dynamic conditions, where admittedly most road damage must occur.
3. No mention is made of any surface strain measurements taken between the duals. Undoubtedly, there must be a significant reversal of stress in this area and such an action is known to be more detrimental to flexible materials than higher stress without a reversal.

Based on our own tests and those of others with which we are acquainted, we suggest that the flotation or wide-base single tire under comparable loads and inflation will actually be easier on the pavement than will duals. This is primarily because of the inherent lower spring rate of the wide-base single tire and secondarily because dual tires are subject to the effects of mismating, unequal inflation, and road crown. These conditions are almost impossible to avoid (except with single tires) and must produce stresses far different than those measured under ideal circumstances by Zube and Forsyth. Also, the fact that roads are not smooth but irregular suggests that the dynamic factors cannot be ignored.

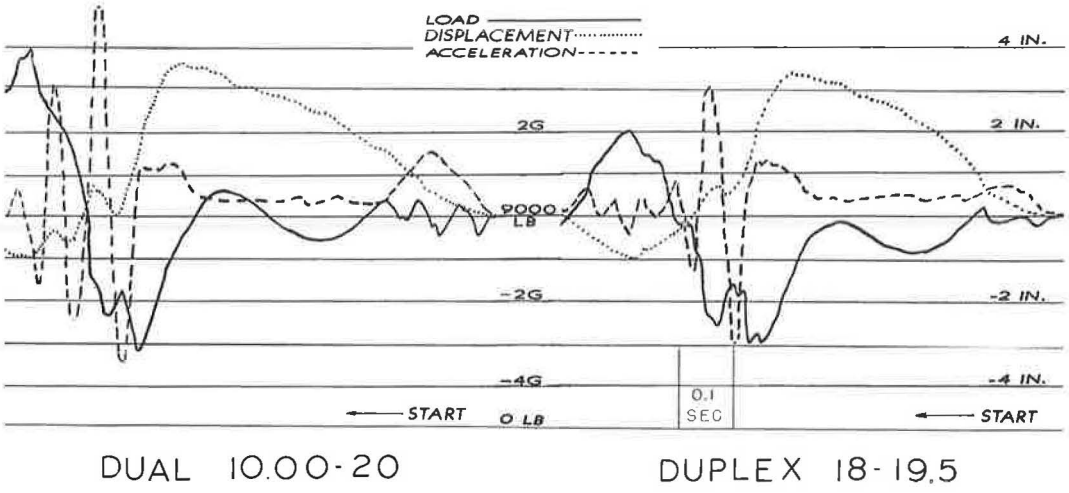

Figure 18. Impact loading, axle acceleration, and axle displacement for 18,000-lb axle load, 75 psi, 10 mph, no springs, up and over 4-in. ramp.

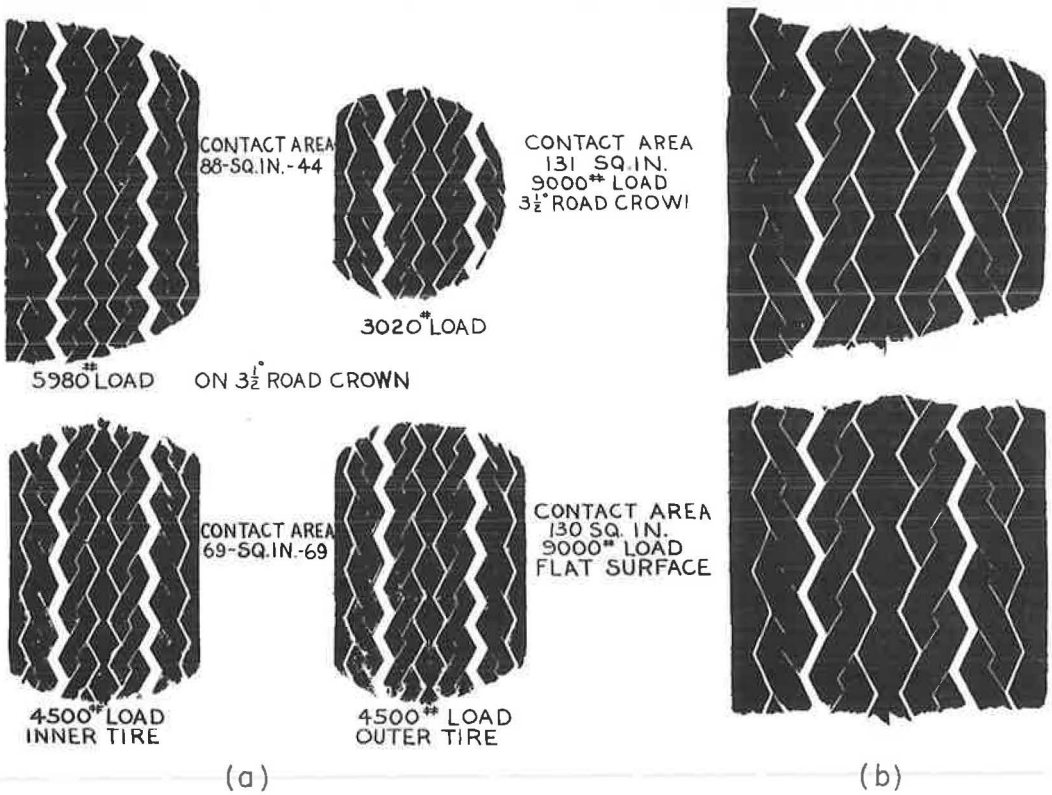

Figure 19. Effect of road crown: (a) on dual-tire loading, 11-22.5 duals, 18,000-lb axle; and (b) on single tire, 18-19.5, 18,000-lb axle.

6070# LOAD

CONTACT AREA

91 - SQ. IN. - 44

ON 3½° ROAD CROWN

2930# LOAD

4875# LOAD

INNER 90 PSI

CONTACT AREA

78 - SQ. IN. - 66

4125# LOAD

OUTER 65 PSI

Figure 20. Effect of inflation differences, 11-22.5 duals, 18,000-lb axle.

In a previous paper (9), Moore presented test data on dual tires vs wide-base single tires obtained under dynamic conditions. These data, shown in Figure 18, were obtained by running a truck up and over a 4-in. ramp with the springs blocked out. Measurements were recorded for axle load, axle acceleration, and axle displacement. The axle load was determined by measuring the amount of axle bending. Analysis of the curves show that under dynamic shock load conditions, less load and acceleration are imparted to the axle by the wide-base single tire than by the dual tires. For example, the peak load with the wide-base single tire was 12,600 lb, and with the duals was 16,200 lb. In addition, the magnitude of the axle acceleration was also considerably less for the single tire. Other tests, under less exaggerated conditions and with the springs allowed to function normally, were also run and in every comparison the single tire transmitted less shock and acceleration to the truck. Although these data indicate only the effect of the dynamic impact on the truck (in particular, the axle), to say that the pavement does not feel the same load would be a violation of Newton's Third Law. Such data indicate an advantage in the wide-base single tire insofar as the truck is concerned, and we fail to see why the pavement would not be similarly affected.

Along the same lines as these tests, missile transporters were evaluated by a manufacturer on both single and dual tires, and here again, the wide-base single tires transmitted much less shock to the vehicle than did the duals.

Preliminary unofficial results of a road test being conducted by the Forestry Service and the University of Washington are reported to show less road deterioration with the wide-base singles than with dual-tired trucks. This test also shows less shock transmitted to the road base by vehicle travel with single than with dual tires.

Among data illustrating some of the inherent disadvantages of duals, Figure 19 shows how dual tires are affected by a crowned road. In this case, the inflation in all tires is 75 psi. As the tires pass over a 3½° crowned road, the inside tire on the dual assembly is loaded more than the outside tire, 5,980 lb (⅔ of the 9,000-lb dual load) vs 3,020 lb for the outside tire. The condition is further exaggerated when the outer dual drops off the edge of the pavement, leaving the full 9,000-lb load on one narrow tread.

Figure 20 shows the effect of inflation differences on dual tires. On a flat road the tire at 90 psi is carrying 4,895 lb of the 9,000-lb dual load, and the tire at 65 psi is carrying 4,125 lb or 46 percent. On a crowned road, the effect of inflation is even more important. Here the inside tire is carrying 67 percent of the load.

In addition to the points mentioned previously, there are other factors to consider in evaluating the effect of flotation tires on flexible pavement. In many instances, wide-base single tires at normal or lower inflation are being used to replace conventional tires at high inflation on front axles. In this case, a tire with a large contact area is replacing a tire with a much smaller contact area, which should result in less pavement strain and deflection.

With all due respect to Mr. Zube and Mr. Forsyth, their study appears to us to be incomplete and certainly in conflict with vehicle test data and ride reports from users everywhere. It is recommended that they be encouraged to extend their investigation to include the dynamic effect of these same tires on pavements.

Reference

9. Powers, R. P., and Moore, W. E. Ride Characteristics of the Wide Base Tire. Paper prepared for Society of Automotive Engineers.

ERNEST ZUBE and RAYMOND FORSYTH, Closure. —We have read with a great deal of interest the discussion by R. P. Powers and W. E. Moore of the Firestone Tire and Rubber Company. It is surprising to the authors that at this late date (the results of this investigation have been available to representatives of the tire industry for over a year) there is still a basic misconception as to the reason for this study and the selection of the criteria utilized.

As stated in our original presentation, we have no opinions or comments on the relative merits of dual vs flotation tires with respect to vehicle riding characteristics and wear rate and, thus, vehicle maintenance. Certainly there is every reason to believe that the use of flotation tires has a very beneficial effect on the dynamic characteristics of trucks and would very likely, therefore, offer significant economic benefits for truckers. Our primary concern is the effect of this product on the highway itself.

We must take issue with several specific points in the discussion of Messrs. Powers and Moore. The choice of the title of the paper was not intended to criticize or cast a shadow on flotation tires. At the time, it appeared to be an adequate and succinct description of the study because an evaluation of the detrimental effect of any new product on highways is of primary concern to our agency, whether this product be less or more damaging than the standard of comparison.

We must take strong exception to Item No. 2. It is a well-known fact that pavement deflection is highest at creep speed and diminishes lineally as the speed increases. Work to this effect has been published by innumerable investigators and most recently was presented in the findings of the AASHO Road Test (7). Visual evidence of this is many times apparent on highways in mountainous or hilly country subject to heavy truck traffic, in which we often note distress first appearing on the upgrades near the peaks of hills where trucks are moving at their lowest speeds. Another commonly observed example of this is the preponderance of cracking on any street at intersections where the vehicles come to rest.

With respect to Item No. 3, we will admit to a very limited amount of strain data in the zone between dual tires. Some readings were obtained in the very successful installations at our State Fair Grounds. However, during that phase of the study (involving reduction of tire pressure), strain values between the duals were relatively low, with some being in tension and others in compression (Table 2). As Messrs. Powers and Moore point out, there is definitely stress reversal in this zone. In terms of absolute tensile strain, however, maximum readings were obtained at from 5 to 8 in. from the outside edge of the tire, then rapidly reversing and going into compression as the edge of the tire came closer to the gage. There can be little doubt that highest tensile strain and, hence, the most critical reversal, occurs in this outside zone. This is also borne out be examination of transverse deflection profiles at the LVDT locations with the single exception from the plot of the Shell Avenue test road. These profiles show sharper bending and thus indicate higher tensile strains from the edge of the tire outward. This seems reasonable in view of the restraint afforded by the tires in the zone between the duals. We must, therefore, adhere to our original position that maximum tensile strain occurs near the outside edge of the loaded tire until evidence to the contrary is presented.

TABLE 2

COMPARISON OF PAVEMENT STRAINS AT VARIOUS CRITICAL DUAL WHEEL LOCATIONS
(State Fair Grounds)

Run No.	Gage No.	Temperature (° F)	Strain (μ in./in.)[a]		
			Gage Centered Under 1 Wheel	Gage Centered Between Wheels	Max Tensile Strain Recorded[b]
1	1	45	-570	+180	+186
	2	45	-330	-84	+119
	3	45	-450	-120	+155
	4	45	-430	+60	+157
	5	45	-570	+30	+200
2	1	46	-770	+208	+228
	2	46	-400	+6	+138
	3	46	-500	+40	+182
	4	46	-500	+80	+200
	5	46	-700	-95	+280
3	1	42	-600	+155	+190
	2	42	-430	-80	+120
	3	42	-450	-125	+150
	4	42	-440	+30	+165

[a] Minus sign indicates compressive strain; plus sign indicates tensile strain.
[b] At 5 to 8 in. from outside edge of tire.

At this point Messrs. Powers and Moore proceed with what is believed to be their principal argument with regard to this paper; that is, their contention that the factor of truck dynamics has been neglected. There can be little argument, based on the results of various impact tests, that the use of flotation tires offers real advantages for truckers with respect to the shock or impact. Recently there has been evidence presented to the effect that the use of flotation tires on unimproved or unsurfaced roads is beneficial to the road itself. For this type of road, dynamic considerations have a significant effect on the tendency of a road to rut or "washboard." A report recently com-

pleted by the University of Washington and the U. S. Forest Service on this subject presents convincing evidence to this effect (10).

Our prime concern, however, was a comparison of the destructive effects of flotation and standard dual tires on improved highways (surfaced with asphalt concrete) in California. Because, in general, our pavements are quite smooth, measurements involved in truck dynamics or impact effects on the roadway were not considered to be a factor in this investigation. We, therefore, concerned ourselves only with AC pavement flexure as indicated by measurements of strain and deflection because these criteria, and particularly that of pavement deflection, have been successfully related to pavement performance by many past investigations. We fail to see how impact data resulting from trucks dropping from a 4-in. ramp are applicable to our problem.

At the other extreme, our study indicates that for highways which we would consider primary (that is, those utilizing heavy AC surfacing and/or cement-treated bases), even though flotation tires are relatively more destructive, the difference in absolute units of strain or deflection are minimal. We would, therefore, anticipate no real detrimental effect in the use of these tires. This is also undoubtedly the case with respect to PCC pavements. Our prime concern is, therefore, roads with relatively thin AC surfacings and a flexible structural section which can be subject to early deterioration by way of fatigue failure of the surfacing if exposed to unusually high pavement strains and deflections. It appears that the critical zone in this evaluation is the possible detrimental effect of flotation tires on secondary roads and city streets.

We would agree that one dual may be more heavily loaded than the other due to crown slopes. This variable is, we believe, automatically introduced into this investigation because our data were obtained on roadways with widely varying crown slopes. The matter of variation in tread wear was of some concern early in this investigation. At one gage site, a worn and a new dual were purposely matched so that the strain measurements for this pair could be compared with those from two evenly worn duals on the opposite wheel. No significant difference in absolute transverse tensile strain was noted. These results and those from that phase of the investigation involving reduction in tire pressure lead us to believe that tire structure is a much more important variable with regard to surface strain than degree of tread wear.

With respect to the concluding paragraph of the discussion, we fail to see how any of the data presented in this investigation conflict with the results of any other study. In fact, to the best of our knowledge, this is the first time that an evaluation of flotation tires, based on pavement strain deflection measurement, has been undertaken. Because our primary concern is the design, construction, and maintenance of highways, we must, of necessity, leave investigations involving truck dynamics and wear rates to representatives of the tire and trucking industry.

Reference

10. University of Washington and U. S. Forest Service. Logging Road Test. Univ. of Washington College of Engineering, Dept. of Civil Engineering, Suppl. No. 7, Nov. 1964.

Georgia Satellite Flexible Pavement Evaluation And Its Application to Design

GEORGE F. SOWERS
Professor of Civil Engineering, Georgia Institute of Technology, and Vice President, Law Engineering Testing Co.

A study was made of the deterioration or failure of flexible pavements in all the geologic provinces of Georgia. The pavement serviceability was estimated visually and from measured rut depth. Total traffic was estimated from short-term counts and from data of nearby traffic stations. Laboratory tests were made of undisturbed samples of subgrade. The serviceability rating of the pavement was found to be a function of the computed safety factor of the subgrade against shear failure beneath the pavement and the amount of traffic. A similar analysis of the AASHO Road Test flexible pavement failures found a comparable relationship. The bearing capacity of the AASHO subgrade compared to those of the Georgia subgrades furnished the quantitative tie between the proposed AASHO design charts and Georgia materials and environment, and makes it possible to utilize the AASHO interim design for Georgia pavements. Alternatively, a direct design method can be derived for pavements from the traffic-soil bearing-serviceability relationship.

•THE DESIGN of flexible pavements in Georgia has been largely based on experience expressed in the form of correlations between soil class, traffic, and base course thickness and character. Although this method has been reasonably successful in the past, the rapid increases in the number of heavy axle loads and in the variety of subgrades that must support the heaviest loads have outrun past experience.

Design criteria resulting from the AASHO Road Test, although furnishing quantitative information on the relationship between traffic, pavement thickness, and pavement performance, are limited to the conditions of the test road.

> Generalizations and extrapolations of these findings to conditions other than those that existed at the Road Test should be based on experimental evidence of ... the effects on pavement performance of the variations in climate, soil type, materials, construction practices and traffic. (1, p. 3)

It is the object of this research to provide a rational background for extending both Georgia experience and the results of the AASHO Road Test program to the design of new pavements in the state. This required an evaluation of the performance of pavements throughout Georgia, particularly in terms of subgrade capacity. It also involved a correlation of the AASHO Interim Guide for the Design of Flexible Pavements (2) with the properties of Georgia highway construction materials.

The evaluation of the Georgia pavements began with a field examination of typical examples exhibiting both satisfactory and unsatisfactory performance. Samples of the subgrade from each type of pavement were secured and tested to determine the subgrade's elasticity and strength. Computations were made to determine the subgrade's elastic deflection and safety against shear failure. The results were then correlated

Paper sponsored by Committee on Flexible Pavement Design and presented at the 44th Annual Meeting.

with the pavement performance to establish the requirements for a safe design. The correlation with the AASHO Road Test data was centered on tests of four undisturbed samples from the test road subgrade. Deflection and bearing capacity were correlated with the serviceability index or rating in the same way as the data for the Georgia pavements. A comparison of the correlations permits a comparison of the supporting qualities of the Georgia subgrades with those of the AASHO subgrade. Finally, the Georgia performance and soil support data were utilized independently to develop a semirational design method for Georgia pavements. Although this method is incomplete and requires further development, it appears to have some advantages that cannot be realized from the AASHO-derived design method.

PAVEMENT PERFORMANCE AND FAILURE

The term failure can easily be applied to a pavement that has ruptured or broken sufficiently so that it is no longer usable. However, pavements may be deficient long before rupture is reached. In such cases, failure of a pavement must be defined in terms of pavement function and the degree of impairment of that function. A modern pavement is a multi-purpose structure. It includes as its functions spreading the concentrated wheel load to match the supporting power of the subgrade, providing traction and a smooth riding surface, and protecting subgrade from deterioration by weather. The relative importance of these depends on the vehicle and its physical requirements, and on the person using the vehicle, including his physical and psychological needs. Therefore, the relative importance would not be the same for a jeep as for a heavily loaded inter-city truck, nor for an inter-city traveler and a man visiting his neighbor on the next block. The relative importance would also be different for a person who had been accustomed all his life to muddy rural roads and one who was accustomed only to paved city streets.

It is impossible, therefore, to define pavement failure precisely; it must be considered to be a deficiency in any one or more of the required functions. It cannot be defined as an absolute quantity or point; rather, it is a matter of degree. Finally, failure cannot be defined objectively but depends on the needs and whims of the users.

Performance-Serviceability

A new concept of pavement performance was developed in the AASHO Road Test in an attempt to express all the functions of the pavement in terms of the needs and demands of the using public. This is the Present Serviceability Rating, PSR (3), which is a subjective evaluation of the ability of the pavement to serve high-speed high-volume mixed truck and automobile traffic in its existing condition in terms of a numerical grade from 0 (or no quality) to 5 (the maximum). The rating was established as a composite of the individual ratings by a cross-section of users: highway administrators, maintenance men, materials suppliers, truckers, highway educators, designers, automotive manufacturers, and researchers.

The Present Serviceability Index, PSI, is a synthesis of the PSR from measurements of the shape of the pavement surface and its physical condition, based on empirical correlations between the PSR established from the opinions of the group of individuals and measurements of the same pavements. The major factors in the PSI were found to be the longitudinal profile of the surface and the mean depth of the ruts. The amount of cracking and patching were also factors, but not to the same degree. The longitudinal profile is expressed by the slope variance, $\overline{SV}$, which is the mean variance of the pavement surface slope (measured between two points 9 in. apart and the horizontal). The deterioration in PSI due to this factor was found to be $1.9 \log (1 + \overline{SV})$. The deterioration in rating due to rutting was found to be $1.38\ \overline{RD}^2$, where $\overline{RD}$ is the mean rut depth in inches. Of these two, mean rut depth appears the more significant when structural failure is near.

A simple approximation for the serviceability index based only on rut depth was derived by the author from the same data on which the AASHO PSI was based (1, p. 304):

$$PSI = 4.5 - 7\,\overline{RD}^2 \qquad (1)$$

Georgia Satellite Flexible Pavement Evaluation And Its Application to Design

GEORGE F. SOWERS
Professor of Civil Engineering, Georgia Institute of Technology, and Vice President, Law Engineering Testing Co.

A study was made of the deterioration or failure of flexible pavements in all the geologic provinces of Georgia. The pavement serviceability was estimated visually and from measured rut depth. Total traffic was estimated from short-term counts and from data of nearby traffic stations. Laboratory tests were made of undisturbed samples of subgrade. The serviceability rating of the pavement was found to be a function of the computed safety factor of the subgrade against shear failure beneath the pavement and the amount of traffic. A similar analysis of the AASHO Road Test flexible pavement failures found a comparable relationship. The bearing capacity of the AASHO subgrade compared to those of the Georgia subgrades furnished the quantitative tie between the proposed AASHO design charts and Georgia materials and environment, and makes it possible to utilize the AASHO interim design for Georgia pavements. Alternatively, a direct design method can be derived for pavements from the traffic-soil bearing-serviceability relationship.

•THE DESIGN of flexible pavements in Georgia has been largely based on experience expressed in the form of correlations between soil class, traffic, and base course thickness and character. Although this method has been reasonably successful in the past, the rapid increases in the number of heavy axle loads and in the variety of subgrades that must support the heaviest loads have outrun past experience.

Design criteria resulting from the AASHO Road Test, although furnishing quantitative information on the relationship between traffic, pavement thickness, and pavement performance, are limited to the conditions of the test road.

> Generalizations and extrapolations of these findings to conditions other than those that existed at the Road Test should be based on experimental evidence of ... the effects on pavement performance of the variations in climate, soil type, materials, construction practices and traffic. (1, p. 3)

It is the object of this research to provide a rational background for extending both Georgia experience and the results of the AASHO Road Test program to the design of new pavements in the state. This required an evaluation of the performance of pavements throughout Georgia, particularly in terms of subgrade capacity. It also involved a correlation of the AASHO Interim Guide for the Design of Flexible Pavements (2) with the properties of Georgia highway construction materials.

The evaluation of the Georgia pavements began with a field examination of typical examples exhibiting both satisfactory and unsatisfactory performance. Samples of the subgrade from each type of pavement were secured and tested to determine the subgrade's elasticity and strength. Computations were made to determine the subgrade's elastic deflection and safety against shear failure. The results were then correlated

Paper sponsored by Committee on Flexible Pavement Design and presented at the 44th Annual Meeting.

with the pavement performance to establish the requirements for a safe design. The correlation with the AASHO Road Test data was centered on tests of four undisturbed samples from the test road subgrade. Deflection and bearing capacity were correlated with the serviceability index or rating in the same way as the data for the Georgia pavements. A comparison of the correlations permits a comparison of the supporting qualities of the Georgia subgrades with those of the AASHO subgrade. Finally, the Georgia performance and soil support data were utilized independently to develop a semirational design method for Georgia pavements. Although this method is incomplete and requires further development, it appears to have some advantages that cannot be realized from the AASHO-derived design method.

PAVEMENT PERFORMANCE AND FAILURE

The term failure can easily be applied to a pavement that has ruptured or broken sufficiently so that it is no longer usable. However, pavements may be deficient long before rupture is reached. In such cases, failure of a pavement must be defined in terms of pavement function and the degree of impairment of that function. A modern pavement is a multi-purpose structure. It includes as its functions spreading the concentrated wheel load to match the supporting power of the subgrade, providing traction and a smooth riding surface, and protecting subgrade from deterioration by weather. The relative importance of these depends on the vehicle and its physical requirements, and on the person using the vehicle, including his physical and psychological needs. Therefore, the relative importance would not be the same for a jeep as for a heavily loaded inter-city truck, nor for an inter-city traveler and a man visiting his neighbor on the next block. The relative importance would also be different for a person who had been accustomed all his life to muddy rural roads and one who was accustomed only to paved city streets.

It is impossible, therefore, to define pavement failure precisely; it must be considered to be a deficiency in any one or more of the required functions. It cannot be defined as an absolute quantity or point; rather, it is a matter of degree. Finally, failure cannot be defined objectively but depends on the needs and whims of the users.

Performance-Serviceability

A new concept of pavement performance was developed in the AASHO Road Test in an attempt to express all the functions of the pavement in terms of the needs and demands of the using public. This is the Present Serviceability Rating, PSR (3), which is a subjective evaluation of the ability of the pavement to serve high-speed high-volume mixed truck and automobile traffic in its existing condition in terms of a numerical grade from 0 (or no quality) to 5 (the maximum). The rating was established as a composite of the individual ratings by a cross-section of users: highway administrators, maintenance men, materials suppliers, truckers, highway educators, designers, automotive manufacturers, and researchers.

The Present Serviceability Index, PSI, is a synthesis of the PSR from measurements of the shape of the pavement surface and its physical condition, based on empirical correlations between the PSR established from the opinions of the group of individuals and measurements of the same pavements. The major factors in the PSI were found to be the longitudinal profile of the surface and the mean depth of the ruts. The amount of cracking and patching were also factors, but not to the same degree. The longitudinal profile is expressed by the slope variance, $\overline{SV}$, which is the mean variance of the pavement surface slope (measured between two points 9 in. apart and the horizontal). The deterioration in PSI due to this factor was found to be $1.9 \log (1 + \overline{SV})$. The deterioration in rating due to rutting was found to be $1.38\ \overline{RD}^2$, where $\overline{RD}$ is the mean rut depth in inches. Of these two, mean rut depth appears the more significant when structural failure is near.

A simple approximation for the serviceability index based only on rut depth was derived by the author from the same data on which the AASHO PSI was based (1, p. 304):

$$PSI = 4.5 - 7\ \overline{RD}^2 \qquad (1)$$

Although the scatter of the data from this simplified relation is great, the equation agrees reasonably well with the observation that many of the test road pavements reached a PSI rating of 1.5 when the mean rut depth reached 0.6 to 0.7 in. (virtual structural failure).

Causes of Pavement Deterioration and Failure

The subjective PSR gives no clue as to the cause of the deterioration of a pavement from the high value it presumably possessed when it was built. The empirical PSI indicates the major and minor factors in the loss of the initial serviceability, but does not define the mechanism by which they develop. In addition, the scatter of the data suggests that there are additional factors in the PSI.

Although deterioration or failure of the pavement to perform its function may be reflected in the surface condition, the seat of the trouble can be in any of the layers which make up the flexible pavement system: the surface course, the base course, the subbase (if any), and the subgrade or embankment. Furthermore, the initial failure of one may lead to a failure, often in a different form, in another. For example, cracking of the asphaltic surface may let surface water into the subgrade and cause its softening and eventual shear.

The mechanisms for pavement deterioration are suggested in Table 1. Some are primarily related to traffic load, whereas others are either independent of the traffic load or are related to the load only in that the failure is intensified or aggravated by the load rather than caused by it. Deterioration and failure in the surface were not within the scope of this investigation. The causes are listed because they had to be considered in diagnosing the mechanism of deterioration of existing pavements and deciding which failures were the result of inadequate pavement thickness. Deterioration and failure of the base and subbase were similarly beyond the scope of this study, except when the base was so similar to the subgrade in its properties that the base and subgrade had to be considered as a unit, as with topsoil and sand bases. The failure of the higher types such as sand-asphalt and soil-cement was not investigated.

A major, and possibly the most important, function of the pavement is to distribute the concentrated wheel load so that the stress does not exceed the supporting capabilities of the subgrade. Of course, the deformation and failure of the subgrade are reflected in the surface condition and thereby in the PSR or PSI. The elastic deformation, consolidation (densification) and shear (bearing capacity) failure of the subgrade are directly related to the wheel load and the resulting stress distributed through the surface and base courses.

TABLE 1

MECHANISMS FOR PAVEMENT DETERIORATION

Surface	Base and Subbase	Subgrade
Elastic deformation--rebound[a]	Elastic deformation[a]	Elastic deformation[a]
Densification (consolidation)[a]	Densification (consolidation)[a]	Densification (consolidation)[a]
Thermal expansion and contraction	Shear failure (bearing capacity)[a]	Shear failure (bearing capacity)[a]
Longitudinal shear failure (shoving)[a]	Deterioration of aggregate	Swell-shrink
Curvilinear shear (bearing failure)[a]	Deterioration of cementing agent	Pumping
Deterioration of bitumen	Swell-shrink	Settlement of deep strata
Separation of courses	Pumping	Mass shear failure (landslide)
Bleeding		Local mass shear (due to weak culverts, trenches)

[a]Primarily related to traffic loads.

The remaining mechanisms are not directly caused by the wheel loads. Swelling and shrinking of the subgrade depend on the moisture changes as well as the mineralogy of the soil. The effect may be bumps and hollows at irregular intervals not related to the traffic or load pattern. Swelling may have a secondary effect in that softening or weakening of the subgrade can lead to deflection or shear failure that is load related. Similarly, shrinkage has a secondary effect in producing tension and shear cracks in the pavement courses above. Although these are not necessarily load related, they may be aggravated by the load. Therefore, it is difficult to isolate the effects of deterioration due to swelling and shrinking, although the basic mechanism is different from the others.

Pumping is a complex phenomenon indirectly related to load; it arises from the effect of free available moisture on a susceptible subgrade or base. The load of the moving wheel causes the pavement components to deflect. After the load passes, the components rebound. If the upper layers rebound faster or more than the lower layers (which is likely because in the typical flexible pavement system, the upper layers are more rigid and possibly more nearly elastic), a temporary void is formed between the layers. If free water is available, it is sucked into the void, only to be expelled at the next loading. If the base or subgrade is easily softened or eroded, the pumping of water in and out creates an erosion cavity and eventually a structural failure.

Settlement of the roadway (ordinarily an embankment), because of consolidation of deeper strata, landslides and localized shear failures caused by weak culverts or improperly compacted backfills behind bridge abutments or in trenches, can cause disruption of the pavement surface and a loss of serviceability. None of these, however, are directly related to the design or adequacy of the pavement. Furthermore, the traffic loads are often not major factors in these phenomena because they may be small compared to the weight of the soil mass that is involved. Pavement deterioration due to these phenomena, therefore, must be discounted in evaluating observed pavement conditions for the purpose of developing a pavement design.

The major subgrade mechanisms that contribute to pavement deterioration are deformation and shear failure.

Subgrade Deflection. --The deflection of the subgrade under traffic load results from stresses particularly vertical, transmitted through the pavement system. Both theory and stress measurements show that vertical stresses become smaller with increasing depth below the pavement surface and with increasing horizontal distance from the center of the line of load application, depending on the elastic characteristics of the subgrade and base course (4).

These stresses have a two-fold effect on the subgrade (and on the other pavement layers). First, they produce a downward deflection of the subgrade surface due to the deformation of the soil without appreciable volume change. This can be visualized as the shortening and lateral building of the column of soil immediately below the load similar to the shortening of any axially loaded structural member. If it is assumed that the subgrade is a semi-infinite isotropic homogeneous elastic mass with a modulus of elasticity of E and is momentarily incompressible and that a uniform pressure of q is applied to a square area of width b, the deflection ρ due to deformation will be

$$\rho = \frac{0.6\,qb}{E} \qquad (2)$$

that is, the deflection is the same as for a free-standing column of soil whose height is 0.6 times the width of the column. Of course, neither the distribution of the load nor the shape of the loaded area of the subgrade is as simple as the conditions assumed in this equation. More accurate, and more elaborate, mathematical representations of the deformation deflection of a subgrade are available. All are of the same general form as Eq. 2; therefore, this suffices as a model for illustrating the effects of some of the different factors involved. The deflection in any case is directly proportional to the pressure and the size of the loaded area and inversely proportional to the modulus of elasticity.

The second deflection mechanism is the consolidation or densification of the subgrade. Although the theories of soil settlement due to reduction in the volume of the voids have been primarily applied to foundations of structures, they apply also to the consolidation of the subgrade. The relation between void ratio change and stress increase is more complex than that for elastic deformation and, therefore, a simple expression for consolidation settlement is not available even for homogeneous soils. However, consolidation settlement does increase with increasing stress, not in direct proportion but more nearly in proportion to the log of the increase compared to the original stress due to the soil weight.

Under repeated loadings, progressive consolidation occurs. With each successive cycle of load and unload, the reduction in voids rapidly becomes less. Settlement appears to continue indefinitely, but at an ever decreasing rate. Subgrade deformation and consolidation cause an elongated depression in the wheelpath that is entirely below the original surface level. The deformation deflection is temporary and is recovered after the wheel passes. The major effect is an "alligator" cracking of the surface course if the deflection is sufficiently great. The estimated limiting deflection, based on the U. S. Navy airfield design, is 0.2 in., although some highway departments have suggested limiting deflections of 0.05 in. for major highways. Consolidation deflection causes a permanent rut entirely below the original surface. The rut may be accompanied by longitudinal and possibly transverse cracks. In addition, long longitudinal waves in the rut may be observed where there is severe consolidation.

Shear Failure.--Shear failure of the subgrade, similar to the bearing capacity failure of a foundation, can result if the stresses transmitted to the subgrade through the base and surface courses exceed the strength in a sufficiently large zone. If it is assumed that the subgrade is homogeneous and its properties can be described by the unit weight γ, the cohesion c, and the angle of internal friction φ, and if it is assumed that the pressure transmitted to the subgrade is vertical and uniform over an area of width b, the pressure at which the soil will shear q_o is defined by

$$q_o = \frac{\gamma b}{2} N_\gamma + c N_c + q' N_q \qquad (3)$$

In this expression N_γ, N_c, and N_q are dimensionless functions of the foundation shape and angle of internal friction and q' is the weight of the pavement and base above the subgrade.

Many variations of this expression, originally proposed by Terzaghi (5), have been published. The differences are in the mode of loading and assumed character of the zone of shear failure and they are manifested in differences in the values of the N-factors. So far no analysis has been developed for a nonuniform loading of indefinite width such as that transmitted through the pavement to the subgrade. However, it is to be expected that the general form of the equation will be little changed; instead, the values of N will reflect the nonuniform loading. Therefore, bearing capacities for subgrades computed by Eq. 3 and utilizing the N-values for one of the existing methods of analysis should be approximately proportional to the true bearing capacities. Or, conversely, the safety factor with respect to shear failure computed by Eq. 3 and utilizing certain existing N-factors and the average stresses transmitted to the subgrade through the pavement system should have some reasonably constant relation to the true safety factors.

Whereas the strength parameters c and φ reflect complete soil failure, they may not indicate the development of limited but accumulating shear under repeated loads that are not great enough to produce complete failure. Although little is known about the effects of repeated loading on progressive shear, the indications are that the magnitude of progressive failure increases with the increasing ratio of the actual stress to the failure stress. That is, progressive failure increases with a decrease in safety factor.

Shear in the subgrade is accompanied by a broad deep depression or rut in the wheelpath with the upheaval occurring beyond it. Longitudinal cracking may be severe and

eventually leads to transverse cracking which forms a blocky pattern (6). Shear along the pavement edge may be accompanied by curved cracking and outward movement of the base and surface, and sometimes by severe outward tilting.

Apparent Safety Factor

The stresses computed by any of the elastic theories apply only to the state of elastic equilibrium on which that theory was based. If the elastic state is altered by nonlinear strain or by failure, the stress distribution may be altered. If failure develops suddenly from an elastic state, however, the stresses just before reaching failure are probably not greatly different from those of elastic equilibrium. If it further can be assumed that the pressure, q_o, required for complete failure and that required to initiate failure are approximately the same or proportional, then it is possible to compute an apparent safety factor against failure by

$$SF_a = \frac{\sigma_a}{q_o} \tag{4}$$

In this expression, σ_a is the average vertical stress transmitted to the soil surface by the pavement system, as computed by an appropriate elastic theory, and q_o is the ultimate bearing capacity computed by Eq. 3, utilizing appropriate factors. The apparent safety factor is not the true safety factor (i.e., failure does not necessarily occur at a safety factor of 1), but it is reasonable to assume that both safety factors are proportional.

Summary

Pavement deterioration and failure is the result of a series of complex processes, none of which are clearly understood and only part of which are directly related to the loads supported. Although exact methods of analyzing the mechanical processes of subgrade deflection and shear failure are not available, approximations can be made that point out the relative importance of the different factors involved and also indicate the relative magnitude of possible deformation and the safety against shear failure.

The greatest unknown factors are those which involve the environment: temperature, frost action, groundwater, surface water infiltration, and other moisture changes. These profoundly influence the deformation and shear failure characteristics of all pavement components but particularly those of the subgrade. At the present time, little is known about the direct effects of the environment on the soil and too few facts are available to permit valid empirical correlations to be made.

SURVEY OF GEORGIA PAVEMENTS

A survey of Georgia pavements was undertaken in 1961 to locate typical areas in all four of the geologic regions (Coastal Plain, Piedmont, Blue Ridge, and Appalachian Ridge—Valley) in which comparable pavements had both exhibited good performance and deteriorated badly. An inquiry was sent to each of the Georgia State Highway Department field divisions asking for their suggested locations for study. From these a list of 84 was compiled for examination and testing.

A field examination was made of each location in the late summer, fall, and early winter of 1961. The pavement was examined visually and data on the roadway environment and pavement condition were obtained. A survey of the traffic was made during the period of pavement examination in which the total number of vehicles and the number of heavy trucks in the lane under study was counted and the percentage of heavy trucks estimated. Although such a short count is not a valid indication of the total traffic, it does give some picture of the character of the traffic on pavements for which no accurate information was available.

The typical depth of rutting was measured using a 4-ft straight-edge placed over the wheelpaths. The segment so measured was then photographed and a sketch made

of the pattern of cracking (if any). The dates of construction and repair (if any) were obtained from the field division engineer. He also provided information on the design and construction of the pavement, where it was available. The pavement was marked at the location where samples were to be made, usually in the zone of the failure but not where the failure itself might have disrupted the soil. Finally, a serviceability rating was assigned utilizing the criteria described by Carey (3) and based on the visual observations of the surface condition and its riding qualities.

Sampling

Samples were secured in most of the locations by the Georgia State Highway Department Division of Materials and Tests. The sampling program was necessarily interspersed with the routine drilling and sampling work for new construction, and thus was spread out over several months. Practically all sampling was done in the late winter and spring of 1962 when the soil moisture conditions were likely to be at the highest.

The bituminous pavement was cored where possible and its thickness measured. The thickness of each deeper pavement course was measured and the materials were described visually. Undisturbed samples were secured of each base course layer that contained no gravel and of the top 2 to 3 ft of the subgrade, utilizing 3-in. O.D. thin-wall sample tubes. The samples were sealed in the field with plastic end caps and brought to the Georgia Institute of Technology Soil Engineering Laboratory.

Laboratory Tests

The samples were cut into 6-in. sections using either a high-speed abrasive saw or a metal-cutting band saw. Unfortunately, some of the samples were unsatisfactory because of gravel which caught under the edge of the tube and disturbed the soil or because of faulty sealing. Most, however, were suitable for testing.

Because of the limited amounts of sample available, only one form of test could be utilized. Considered the most representative of field conditions was the undrained triaxial test, utilizing the full sample diameter (approximately 2.8 in.) and no changes in moisture. Where possible, three confining pressures, 10, 20, and 40 psi, were employed; however, in some cases only 10 and 20 psi were used when the amount of sample was limited. The samples, each about 6 in. long, were loaded axially at a controlled strain rate of 0.8 to 1 percent/min. The test data were analyzed on a computer and the results plotted in the form of stress-strain curves from which the initial tangent modulus of elasticity for a confining pressure of 10 psi was found.

AASHO SUBGRADE TESTS

The AASHO test road was constructed to provide as uniform a subgrade as possible, so that initial subgrade variability would not influence the pavement performance. Therefore, the materials utilized were as nearly uniform as possible in composition, and the construction was controlled so that the moisture contents and densities could be kept within narrow limits.

Tests of the subgrade (embankment) base and surface materials were summarized in the AASHO Road Test reports and in other published data on the road (7). These included control tests for quality and physical tests by the U. S. Bureau of Public Roads to determine the structural properties of the compacted materials. In addition, samples were furnished to many state highway departments to be tested by the procedures commonly employed for their own design work. The results of these tests have also been published (8). Limited tests were made of soils in certain of the road embankments which had been removed from test routinely at the programmed end of testing earlier because of deterioration. These included moisture, density, CBR and K-factor tests (1).

Sampling

None of the published data included strength tests of samples of the subgrades as constructed. Four undisturbed samples were secured by the Illinois Division of Highways on about May 1, 1963, well after the spring thaw. These were of the subgrade, commencing 3 in. below the subbase, and were made with 24-in. long, 2-in. O.D. thin-walled tubes. They were sealed at the site and shipped to the Georgia Institute of Technology Soil Engineering Laboratory.

Laboratory Tests

Triaxial tests were made of all four samples utilizing the same method and pressures as for the tests of Georgia subgrades. The results were expressed in stress-strain curves and Mohr diagrams, and are summarized in Table 2. As can be seen, the results are not uniform. There is considerable variation in the densities, moistures, and strengths. With the exception of the samples from Sta. 60 + 00, where gravel made a full program of tests impossible, the samples exhibited comparable angles of internal friction of slightly more than 20° and cohesions between 6.2 and 20 psi. A composite plot of all data shows the weaker materials exhibit an average cohesion of 9.5 psi and an angle of internal friction of 20°. These values were used in subsequent analyses.

For comparison, the BPR tests of subgrade samples, laboratory-compacted to 95 percent of AASHO T99-49 maximum (the specified value), gave c and φ values of 11 psi and 31°, respectively, for Borrow Pit 1 and 8.9 psi and 21° for Pit 2. The corresponding CBR values were 2.7 and 2.5. The cooperative test (8) results were comparable in those cases where the soil was tested under similar conditions of compaction and moisture content.

ANALYSIS OF GEORGIA PAVEMENT PERFORMANCE

The performance of the Georgia pavements was analyzed utilizing the pavement descriptions and serviceability rating. The theoretical bearing capacity and deflection of the subgrade were computed by the methods described. These were correlated to form a semirational basis for pavement design evaluation.

Depth-Stress-Width

A previous paper (4) presented data on the vertical stresses at different depths beneath different pavement systems utilized in Georgia. These tests all indicated that the vertical stress was greatest immediately under the tire and became rapidly less with increasing horizontal distance and increasing vertical depth below the ground surface. For the purpose of analysis, it was assumed that the significant vertical stresses at any depth were those equal to or greater than one-half the maximum vertical stresses at that depth.

The average significant vertical pressures for a 9-kip dual-wheel load (4) were increased by ten-ninths to give the average significant vertical pressures for a 10-kip

TABLE 2

TRIAXIAL TEST DATA AASHO TEST ROAD

Station	Position (ft)	γ_d (pcf)	w (%)	c (psi)	φ (deg)
60 + 00	13.5 ft R of center WB	125	11	51	0
149 + 00	13.5 ft L of center EB	114	14	7.6	24
229 + 00	13.5 ft L of center EB	82	28	6.2	22
360 + 00	13.5 ft R of center WB	113	13	21.5	20
Composite[a]		-	-	9.5	20

[a] Weaker materials.

dual wheel (the present Georgia load limit of 20 kips per axle). A plot of these stresses (Fig. 1) shows the significant vertical stresses beneath different bases as a function of depth beneath the pavement surface. For most Georgia pavement systems, the curve for the 3-in. asphaltic surface and 8-in. topsoil-soil-macadam, or silt base applies. This is almost identical to the stress distribution computed by the Boussinesq theory and should apply reasonably well to all but soil-cement and sand-asphalt bases. The curves for the latter are shown in Figure 1.

The width of the zone of significant vertical stresses was also found from the stress distribution curves (Fig. 2). The curve can be approximated by the straight line whose equation is

$$b = 15 + 0.72\,z \qquad (4)$$

where b is the equivalent width in inches and z is the depth below the pavement surface in inches.

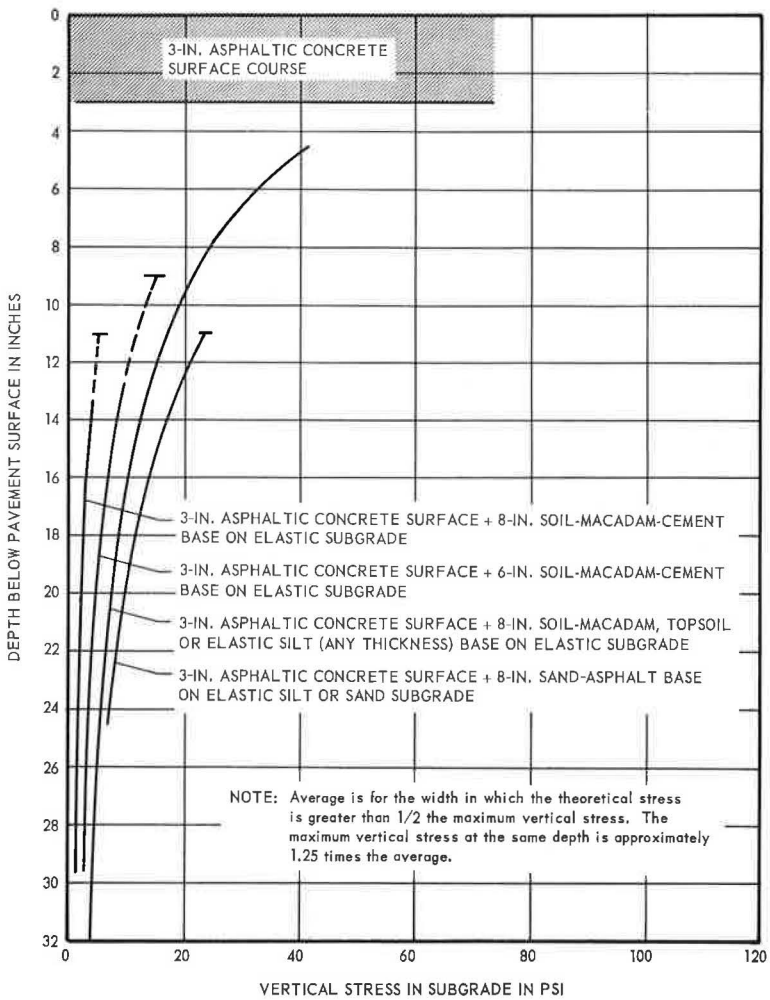

Figure 1. Average significant vertical stress in subgrade for different Georgia base courses and 20-kip axle loads on dual tires.

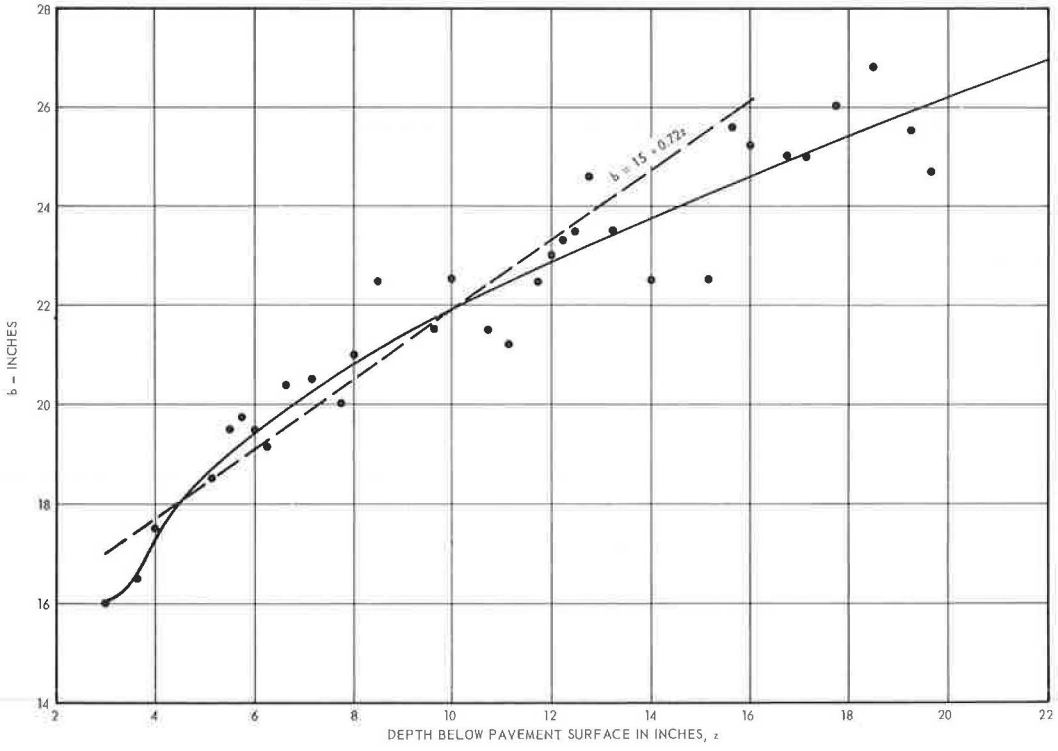

Figure 2. Equivalent width of area of significant vertical pressure in Georgia subgrade.

Deflection—Bearing Capacity

The elastic deformation of each subgrade under a 20-kip axle load was computed from Eq. 2 and the modulus of elasticity for the subgrade at a containing pressure of 10 psi. (The width, b, utilized in the computation was shown in Figure 2. The stress was shown for the depth of the top of the subgrade by Figure 1.) Of course, it would be false to conclude that this represents the true base deflection of the subgrade. However, it should be proportional to the true deflection if the modulus of elasticity determined by the laboratory tests is correct.

The bearing capacity of the subgrade, and in some cases the bearing of each different subgrade layer where the test data differed greatly, was computed from Eq. 3. The c and φ values were those of the soil tests and the b was found from Figure 2. The values of the bearing capacity factors were those computed from the simple Bell-Terzaghi equations as modified by the author (9). For use in these computations the relation was simplified slightly, based on the observation that the total thickness of pavement and base for Georgia is ordinarily 10 to 12 in. In such cases constants can be introduced in the terms involving b, d, and γ with little sacrifice in accuracy (considering the greater error involved in utilizing this or any other existing bearing capacity expression in analyzing pavement capacity).

The vertical stress exerted on the subgrade by the 20-kip axle was found from Figure 1. The ratio of the computed bearing capacity to the stress is the apparent safety factor which is probably not the true safety factor, but should be proportional to it. Further, it would be reasonable to conclude that the lower the safety factor, the greater the possibility of shear failure of the subgrade and the greater the amount of progressive shear.

Traffic

A short-term traffic count was made of each sample section. Data on estimated daily total traffic were obtained from the Georgia Division of Highway Planning. Most estimates were based on actual traffic counting at the regular stations in the area. However, some estimates, particularly for the secondary roads in remote areas, were based largely on experience. In no case was the pavement failure close enough to a point of long-term traffic study that the count can be considered accurate. Both the short-term count at the sample section and the Georgia State Highway Department estimate were utilized in determining the number of trucks per day (other than pickups) on the lane under study. This was converted to an equivalent number of 20-kip axles, utilizing a relationship established by the Alabama State Highway Department in their Loadometer studies (10). The total number of trucks multiplied by the weighting factor gives the equivalent 20-kip axles. The values of the factors used were 0.43 for Interstate and primary roads and 0.32 for secondary roads. The Alabama Loadometer studies were for an 18-kip load. The distribution factors of equivalent 20-kip loads in Georgia would probably be slightly smaller, but in the absence of data, the Alabama figures were used. The daily equivalent 20-kip axle-load figure multiplied by the number of days the pavement was in service gives the total axle loads at the time of the evaluation.

Considering the amount of estimating used to establish this traffic figure, it is likely that it may differ from the true value by 50 percent. An even greater variation is likely on the secondary roads with light traffic where even a moderate use by pulpwood trucks or other local highly specialized vehicles represents the major loading of the pavement.

Serviceability-Safety-Traffic

The serviceability for each pavement area was checked by photographs, measured rut depths, and crack patterns. Greatest weight was given to those factors which reflect the subgrade behavior. For example, although the overall serviceability of a

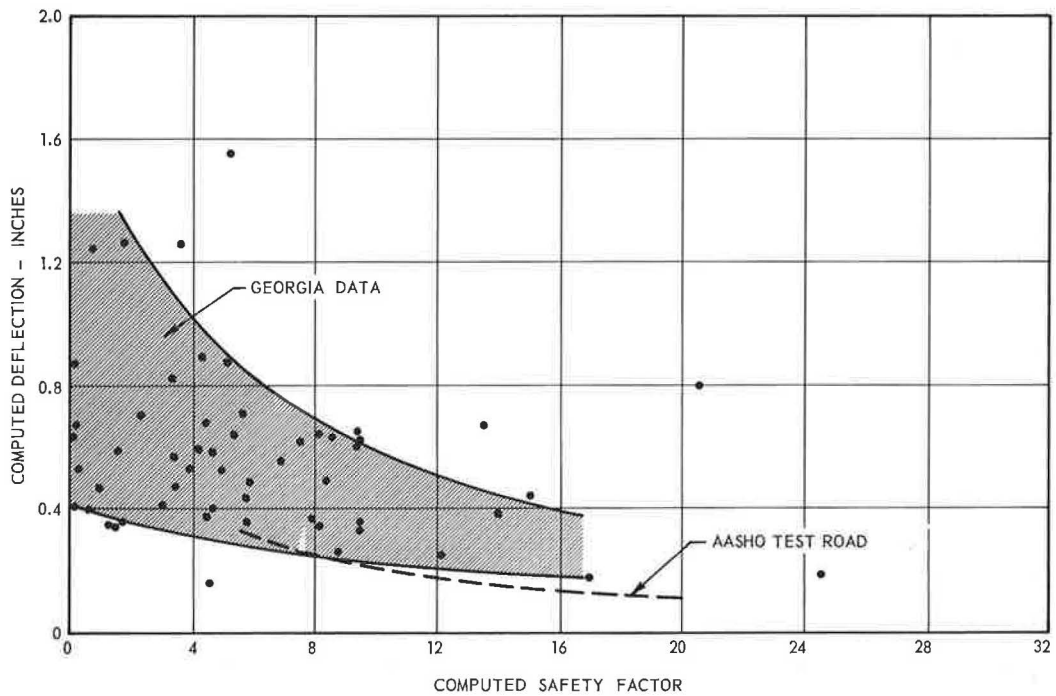

Figure 3. Computed elastic deflection vs computed safety factor of subgrades of Georgia pavements with 20-kip axle loads.

pavement suffering from the peeling of an overlay due to bad bond with the old pavement might be low, the serviceability of the pavement considering the rut depth and longitudinal profile might be high. Because this investigation is concerned with the design of a pavement to fit the subgrade, the subgrade behavior was given greatest weight.

Plots of the serviceability as a function of computed bearing capacity, apparent safety factor, and traffic were made to determine which of these factors was most significant in determining the behavior of the Georgia pavements. A plot of computed deflection vs computed safety factor is shown in Figure 3. Although there is considerable scatter, the relation shows that those pavements having the greatest safety factor against shear failure also exhibit the least elastic deflection; i. e., those soils having the greatest strength are also likely to be the most rigid. This relation also suggests that either deflection or bearing capacity alone might be a satisfactory criterion for design in that one reflects the other to some degree. Because of the limited time available for study and the many factors in both deflection and bearing capacity for which no data were available, no attempt was made to analyze the cause of the scatter.

The plot of serviceability vs apparent safety factor (Fig. 4) also exhibits considerable scatter. However, a general trend is apparent with serviceability decreasing with decreasing safety factor. If the traffic is considered, the trend becomes fairly well defined, with the lighter traffic requiring smaller safety factors than the heavier. Curves were drawn reflecting the largest safety factors required to maintain a given serviceability, for different levels of traffic. In reality, therefore, each curve represents an envelope. There are a few points that do not fit these relations. Some of these with high serviceabilities undoubtedly represent different qualities of initial construction, rather than any deterioration of the pavement. A few exhibit lower serviceabilities because of deterioration other than of the subgrade.

A major unknown factor in the scatter is the fact that the soil test data may not reflect the environmental conditions representative of the greatest degree of deterioration

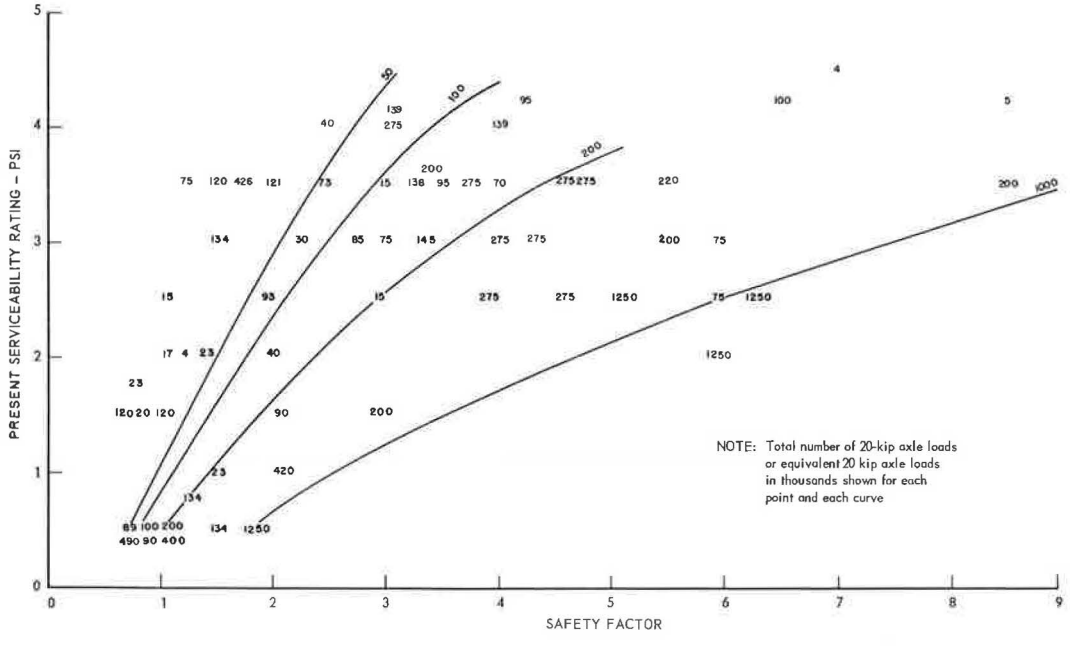

Figure 4. Required safety factors for different present serviceability indexes at end of service period for Georgia pavements and 20-kip axle loads.

and failure. For example, if the subgrade moisture increases in the winter and spring and if failure is most rapid during this period, then the tests should be made of samples obtained during this critical period. Although this was done, it is not known whether the soil at each location was sampled at its worst condition. Moreover, this might not be fair if the traffic during this period of soil weakening was materially less than average. Considering the variable factors which could not be evaluated in this investigation, the degree of correlation shown in Figure 4 is surprising.

AASHO DATA ANALYSIS

AASHO Flexible Pavement Evaluation

The evaluation of the AASHO flexible pavement tests is given in detail in Report 5 (1). A brief review of the program, however, is necessary to provide the background for this analysis.

The entire flexible pavement test program utilized a single subgrade soil, a silty clay classified as A-6 by the AASHO system. This was compacted under close control to densities between 95 and 100 percent of AASHO T99-49 maximum so as to provide as uniform a subgrade as possible and to eliminate the factor of variable subgrade support. The controlled variables were pavement component thickness and traffic. Although a few different base course materials were tested in limited sections, the major emphasis was on the effects of different combinations of surface, base, and subbase thickness under axle loads ranging from 2,000 to 48,000 lb, and with nearly continuous traffic. The serviceability of each pavement section was measured from time to time and a plot of serviceability as a function of the total number of axle loads was made for each pavement section. The results were analyzed statistically to develop empirical relations between axle load, number of axles, pavement design, and performance. The tests effectively demonstrated that serviceability decreased with increasing load and numbers of loads, and decreasing pavement thickness. Curves showing these relationships were developed by assuming a mathematical form and by finding the best fit for the assumed curve by statistical methods.

The method of analysis employed in the AASHO studies does not take into consideration the mechanisms contributing to deterioration or the relative contribution of each. The effect of possible variable subgrade support is not considered. The effect of environment, particularly moisture variation, is also ignored in the primary analysis. Therefore, the AASHO test results cannot be directly applied to the design of Georgia Highways (1, p. 3). Instead, the AASHO data for the 18-kip axle loads (which are nearly equal to the present Georgia legal limit of 20 kips) were analyzed in the same manner as the Georgia data in this report.

Deflection-Bearing Capacity-Traffic

The elastic deflection and bearing capacity of the AASHO subgrade were computed in the same way as for the Georgia subgrades. A single value was utilized for c, φ, and E in all segments, corresponding to the poorer soils tested (the composite on Table 2).

A plot of computed elastic deflection vs computed safety factor (Fig. 5) is well defined, as might be expected, because the only variable involved is pavement thickness. This does, however, suggest the validity of using a single index, either bearing capacity or deflection, as a basis for evaluating subgrade support. A comparison of Figure 5 with Figure 3 is of interest: the AASHO curve in Figure 3 approximately coincides with the lower limit of the Georgia data, suggesting that many of the Georgia soils are more elastic than those of the AASHO subgrade.

A plot of the safety factor of the AASHO pavements vs number of 18-kip axle loads required to reduce the serviceability to 1.5 is shown in Figure 6. A well-defined trend is evident, showing that as the safety factor increases, so does the number of axle loads required to reduce the serviceability to 1.5. Conversely, if a serviceability of 1.5 is demanded at the end of the service life of a pavement, the required safety factor must increase with increasing traffic.

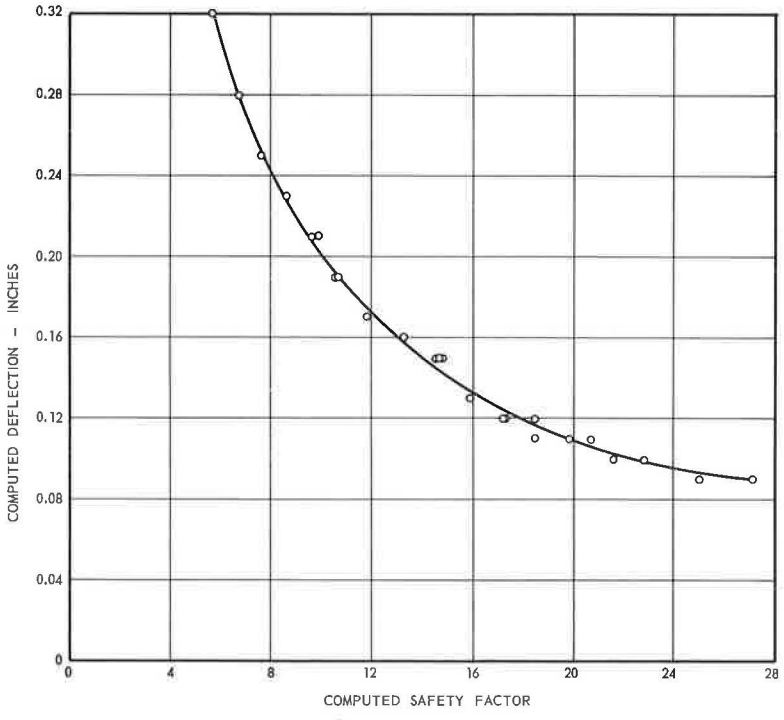

Figure 5. Computed elastic deflection vs computed safety factor of subgrades of AASHO Road Test and 18-kip axle loads.

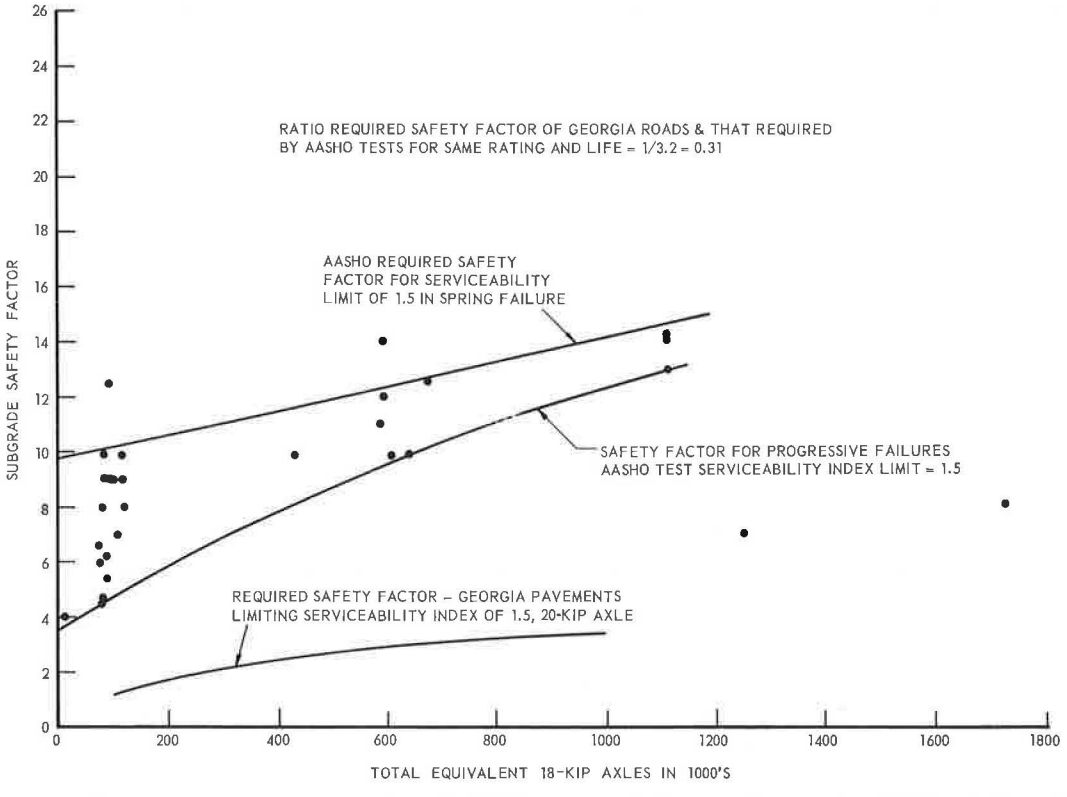

Figure 6. Required safety factor of AASHO pavement to provide serviceability index of 1.5 after different numbers of 18-kip axle loads.

The relationship exhibits considerable scatter, particularly at the lower numbers of axle loads. A study of the individual points shows that those exhibiting the higher safety factors failed suddenly in the spring of 1959 immediately after the thaw period. Two interpretations may be placed on this: (a) the failures were not the result of progressive failure or repeated load; or (b) the soil strength at this time was less than that indicated by the tests of samples made in the late spring of 1963. Those pavements which survived the spring breakup of 1959 exhibited a much better correlation between safety factor and traffic. Of these, however, those points above the lower line represent, for the most part, rather sudden failures corresponding to the spring breakup. The lower curve would seem to represent the more valid relationship between safety factor and traffic. If strength data were available for each test section for the period in which failure developed, the scatter would probably have been much less.

PAVEMENT DESIGN

AASHO Pavement Design

A tentative pavement design method was derived from the AASHO Road Test results by the AASHO committee on design and a draft was presented by Liddle (2). The basis for this development is outlined by Langsner, Huff, and Liddle (11).

The major Road Test correlation is pavement serviceability deterioration (from the initial constructed value) as a function of the pavement design, the axle load, and the number of axle loads. Thus, for a given initial serviceability and a desired serviceability level at the end of the pavement life, and for a required axle load and total traffic, the required pavement design can be found. The correlation is entirely empirical, based on curve fitting, and does not necessarily reflect any consideration of the mechanisms that contribute to failure. The correlation is valid only for the test road subgrade and only if the subgrade properties are uniform and unchanging. An attempt was made to include the variation of the subgrade with the season by assigning a greater weight to the number of load applications occurring during seasons of more rapid deterioration than to those during seasons of less rapid deterioration. The method of determining the factor (1) apparently was purely empirical; the weighting factors were adjusted until the serviceability and total load application data fit the assumed mathematical model with the least variation. This procedure does not indicate the mechanism by which the deterioration is accelerated. In fact, it applies the correction to the traffic rather than to the pavement support factors to which it more logically should apply. Therefore, although it may improve the fit of the AASHO data to an assumed mathematical curve, there is no reason to believe that it might be valid elsewhere.

The pavement design in the main load-performance-traffic-design relationship is expressed in terms of the structural number $\overline{SN}$ or equivalent thickness D; both definitions and symbols are used for the same thing, the first in Liddle's paper (2) and other design memoranda, and the second in the AASHO Report (1). This is related to the actual pavement components by

$$D = \overline{SN} = a_1D_1 + A_2D_2 + A_3D_3 \qquad (5)$$

where D_1, and D_2, and D_3 are the thicknesses in inches of the surface course, the base course and the subbase, respectively. The coefficients a_1, a_2, and a_3 are assumed to be indexes of the relative load-spreading or supporting qualities of each corresponding pavement course. The values found for the AASHO Road Test components varied with the traffic, load and the component thicknesses. The values for the 18-kip axle-load section are given in Table 3.

TABLE 3

VALUES OF COEFFICIENTS FOR 18-KIP AXLE-LOAD SECTION

Course	Coeff.	Unweighted	Weighted
Asphaltic concrete surface	a_1	0.39	0.44
Crushed stone base	a_2	0.15	0.14
Sand, gravel subbase	a_3	0.12	0.11

TABLE 4

COMPARISON OF PAVEMENT COEFFICIENTS

Course	Thickness (in.)	Stress in Course (psi)		Stress Reduction in Layer		
		Top	Bottom	Total (psi)	Per In. (psi)	Comparative a[a]
Surface	4	90	44	46	11.5	0.39
Base	3	44	27	17	5.7	0.19
Subbase	4	27	17	10	2.5	0.08

[a]Assuming surface = 0.39.

Although the AASHO Road Test report (1, p. 36) states that the weighted values indicate that an inch of surfacing ($a_1 = 0.44$) is about three times as effective as an inch of base ($a_2 = 0.14$) or four times as effective as an inch of subbase ($a_3 = 0.11$), this does not necessarily mean that these materials have support qualities or load-spreading abilities in the same ratio. For example, one design of the AASHO Loop 4, where the 18-kip axle load was employed, consisted of the layers shown in Table 4. If the vertical stresses are computed at the top and bottom of each layer using the Boussinesq equation (which applies to a semi-infinite homogeneous isotropic elastic mass), they will be seen to be less at the bottom of each successive course, as shown in the table. The stress reduction in each layer and stress reduction per inch of layer are also shown. The comparison indicates that the first layer is 2 times more effective than the second and 4.6 times more effective than the third. The effectiveness of each layer in terms of the pavement coefficient is tabulated. The resulting values are remarkably similar to the Road Test values for a. Therefore, it must be concluded that the relative values of a_1, a_2, and a_3 do not only reflect the load-spreading or supporting qualities of the pavement materials but also their relative position with respect to the pavement surface.

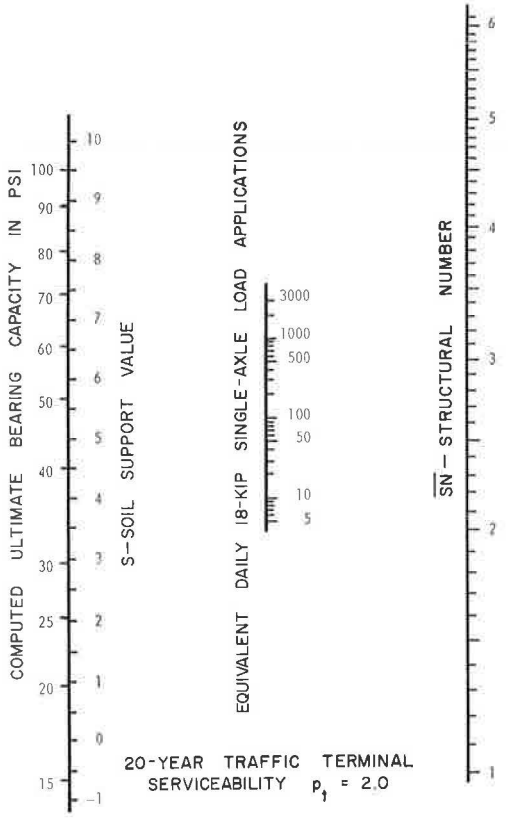

Figure 7. AASHO interim guide to design of flexible pavement (2) adapted to Georgia subgrades.

The Road Test correlation does not include any terms reflecting the subgrade soil support because it was assumed that this was constant and uniform. However, a possible "second" subgrade soil value was inferred from the pavement section with such thick crushed stone bases that the base, in effect, was the subgrade; however, this inference was not checked by any rational procedure. Arbitrary soil support values, S, were assigned to the subgrade and the thick stone base of 3 and 10, respectively. Of course, these values do not necessarily reflect relative support but instead are points of reference.

Nomographic design charts were constructed for the Road Test correlation uti-

lizing an axle load of 18 kips and for terminal serviceabilities of 2 and 2.5. The former is reproduced in Figure 7, from the AASHO Interim Guide for the Design of Flexible Pavements. The same chart has been used by Liddle (2, 11).

Design Constants, Georgia Pavements

The use of the AASHO design charts requires calibration of the soil support scale in terms of some quantitative index or measure of the appropriate property of the subgrade soil for which the pavement is designed. Whereas the AASHO test results do not directly point to the mechanism of pavement deterioration and failure, clues are given by the results of the trenching program. Trenches were cut into pavement sections that had deteriorated to the point of removal from test in 1959. An extensive trench program was undertaken in 1960 when 39 pavement sections were investigated. In each, the transverse profile of the boundary between each of the pavement components and the densities of each layer in and beyond the wheelpath were obtained accurately. These tests indicated that about 25 percent of the thickness change of the pavement layers could be attributed to densification or consolidation of the layers. The remaining change, therefore, must be shear displacement. Such shear displacements can be clearly seen in the transverse profiles of the subgrade surface. Therefore, because it is shown that the major part of the subgrade's contribution to the deterioration of the pavement surface is shear failure, it appears reasonable to presume that the subgrade bearing capacity (its resistance to shear displacement) would be a valid index to the subgrade support of S. On this basis, the AASHO support value would represent an ultimate bearing capacity of 99 psi, based on tests of the samples secured in 1963 some time after the critical period of spring softening. This value probably does not represent the bearing capacity during the periods of most rapid deterioration. This is confirmed by the plot of safety factor vs traffic for the AASHO Road Test (Fig. 6). The lowest curve, which represents the more valid traffic-related deterioration, shows a safety factor of 3.6 required under conditions of very little traffic. The corresponding Georgia data gave a safety factor of about 1 for the same low traffic. Therefore, it is concluded that the actual bearing capacity of the AASHO subgrade was appreciably less than 99 psi during the critical periods of the Road Test.

A plot of the required Georgia subgrade safety factors for the same level of serviceability (1.5), based on Figure 4, is shown for comparison in Figure 6. The Georgia values everywhere are 1/3.2 or 31 percent of the indicated AASHO values. On this basis, the Georgia ultimate bearing capacity equivalent to the Road Test subgrade bearing capacity would be 0.31×99 or 31 psi. This value is recommended for use of pavement design in Georgia as the equivalent of the subgrade support value of 3 (2, 11).

Other values on the subgrade support value scale were established from this key bearing capacity utilizing the AASHO pavement thickness relation for an 18-kip axle load and 100 equivalent axle loads per day. The required safety factors for Georgia pavements for different amounts of traffic and different serviceabilities at the end of the pavement life were found from Figure 4 and plotted in Figure 8. One hundred axles per day for 20 years is a total of 730,000 axle loads. For a serviceability limit of 2.0, the required Georgia safety factor is 4. The safe limit of stress for the correct design would be $\frac{1}{4} \times 31$ or 7.75 psi. The total pavement thickness (3-in. surface plus soil-macadam base) required to maintain the stress at this level, from Figure 1, is 19.5 in. From the AASHO chart for a serviceability of 2, an S of 3 and 100 axles per day require a pavement $\overline{SN}$ of 3.58. The weighted average a for the Georgia pavement, therefore, must be 3.58/19.5 or 0.184.

A second point on the support scale can be found by utilizing a different assumed Georgia ultimate bearing capacity and the computed weighted average a for the Georgia pavement. For example, if the subgrade has an ultimate bearing capacity of 50 psi, the actual stress on the subgrade would be limited to $50/4 = 12.5$ psi. This corresponds in Figure 1 to a total thickness of 13.7 in. Utilizing the previously computed weighted average a, the $\overline{SN}$ would be $13.7 \times 0.184 = 2.52$. From the AASHO chart, the soil support number corresponding to $\overline{SN} = 1.52$ and 100 axle loads daily would be 5.7. Therefore, the S value corresponding to a bearing capacity of 50 psi would be 5.7.

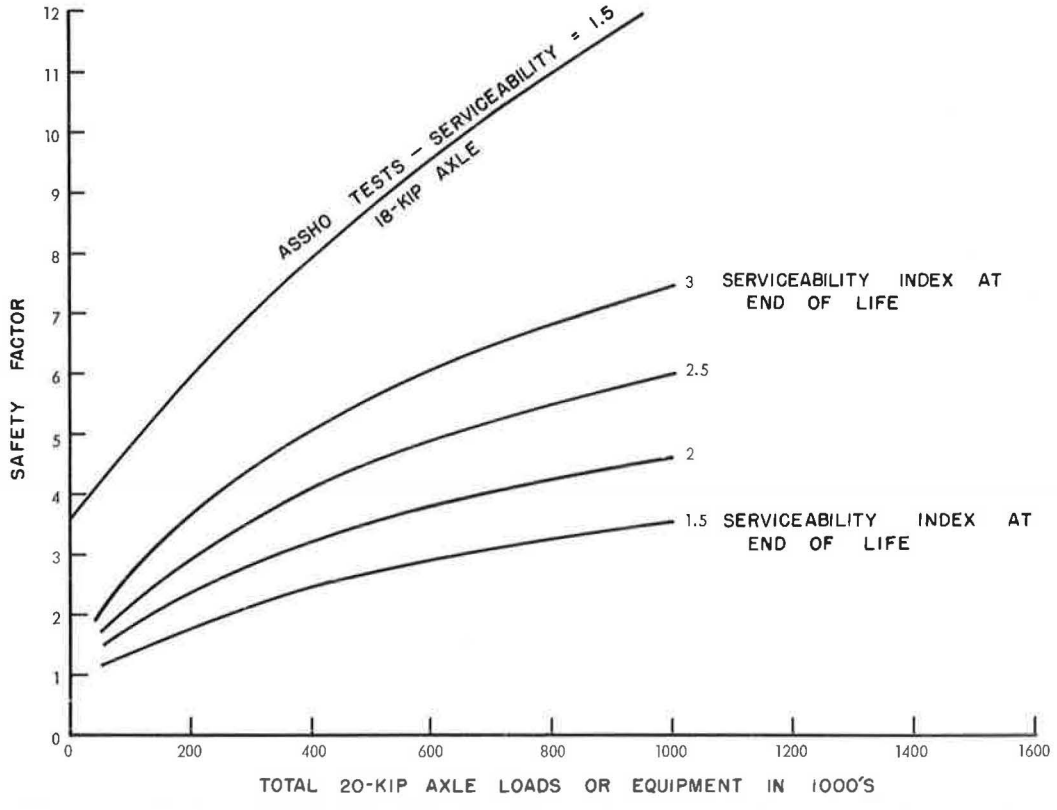

Figure 8. Required safety factors for Georgia subgrades for different numbers of 20-kip axle loads.

By this process the bearing capacities corresponding to various S values were found and are given in Table 5. These values apply to the 100 axle loads daily and the performance rating of 2.0 at the end of the pavement life. However, their applicability to other conditions is probably as valid as the other assumptions made in developing the design method.

In utilizing these values for design, consideration must be given to the test method on which the Georgia evaluations were based. The samples were secured in actual subgrades during the winter and the time of greatest soil moisture and lowest strength. Until data are available on the variations in soil moisture with the season, it is safe only to assume that the limit of capillary saturation is the limiting moisture corresponding to the Georgia test data. It is recommended that the bearing capacity be found from c and φ values determined as follows:

1. Compact two specimens of the subgrade to the lowest density and highest moisture permitted by the construction specifications.
2. Confine each in a triaxial chamber, one at a confinement of 10 psi and the other at 20 psi.
3. Subject each to a head of 1 ft of water from the bottom and allow to saturate until

TABLE 5

RELATION OF S TO COMPUTED ULTIMATE BEARING CAPACITY[a]

Bearing Capacity (psi)	S	Bearing Capacity (psi)	S
15	- 0.7	60	6.6
20	+ 0.9	70	7.4
30	2.9	80	8.2
40	4.5	90	8.9
50	5.7	100	9.5

[a]For using AASHO tentative design chart with subgrade bearing capacities computed from undrained triaxial shear tests of Georgia subgrade soils computed and inundated.

no more water is absorbed (period of saturation to be found by experiment).

4. Load axially until failure occurs, without further change in moisture. For design utilize a seasonal weighting factor of 1 throughout, as in Figure 7.

Determination of the a coefficients for use in the AASHO design method is more difficult because there is little on which to base a correlation. The AASHO values are 0.44 for the asphaltic concrete surface and 0.14 for the crushed stone base. The weighted a for a typical Georgia pavement of 3 in. surface and 8 in. soil-bound macadam would be $3/11 \times 0.44 + 8/11 \times 0.14 = 0.22$. This compares reasonably well with 0.18, indirectly computed from the equivalent thicknesses utilizing the AASHO design chart as previously described.

Based on the subgrade stress studies of the author, the value of 0.44 for the surface appears large. Considering the stress-spreading value of the layers alone, a value of 0.35 is suggested for the asphaltic surface and 0.14 for the stone base. The weighted average of these is 0.197, which is closer to that of the value computed from the bearing study. These values have a ratio of 2.5 to 1, which is close to that found on the basis of the Boussinesq distribution to be applicable to a flexible pavement system employing a granular base.

The a value of the soil-macadam-cement base can be found indirectly from Figure 1. This shows that an 8-in. soil-macadam-cement base (5 psi on subgrade) is equivalent to 22 in. of soil-bound macadam, etc., or would have an a of $22/8 \times 0.14 = 0.38$. The 6-in. soil-macadam-cement base (15 psi) is as effective as 9 in. of soil-bound macadam; it has an a of $9/6 \times 0.14 = 0.21$. At first glance the different a values for the same material might appear contradictory. However, stress theory indicates that the load-spreading ability of a layer capable of supporting tension is a nonlinear function of the layer thickness as well as the material rigidity. For an all-over design value, an a of 0.25 to 0.30 for a soil-macadam-cement base would appear reasonable. This is not greatly different from the value of 0.23 estimated for the AASHO pavements.

The 8-in. thick sand-asphalt base stressed the subgrade to 23 psi which is equivalent to a 5.5-in. thick soil-bound macadam base. The equivalent a value for the sand-asphalt, therefore, would be $5.5/8 \times 0.14 = 0.10$. This is considerably less than the 0.25 estimated from the AASHO test results. (Of course, the AASHO tests did not include a sand-asphalt base; the value was only a guess.) The great difference between the AASHO a values and the values inferred from the Georgia stress tests is possibly the result of the higher Georgia temperatures and resulting lower rigidity, as well as the slower rate of loading.

Alternate Georgia Design Method

An alternate design procedure can be evolved from the Georgia pavement evaluation data:

1. Determine the c and φ of the soil as outlined previously.
2. Compute the ultimate bearing capacity, using an assumed tentative pavement thickness D.
3. Find the appropriate safety factor from Figure 8.
4. Compute the safe bearing capacity by dividing the ultimate bearing capacity, Step 3.
5. Find the total pavement thickness from Figure 1 utilizing the appropriate curve for the type of base course to be employed.

This procedure is no more complicated than that of the AASHO interim guide. It makes use of the AASHO serviceability concept and the traffic-serviceability decline principle. It is based on Georgia performance and on the stress spreading ability of the Georgia base courses. Finally, it is a more nearly rational approach to design than is the AASHO method.

Recommendations for Further Study

Test sections of pavement should be constructed specifically for serviceability-performance studies. These should be a part of the highway system so as to reflect

the use and traffic patterns of real highways. They should be placed on typical subgrades in each geologic region and should be constructed with varying pavement thicknesses and Georgia bases. They should be accompanied by a traffic count station where periodic Loadometer studies can be made to determine the distribution of the heavier axle loads. The soil moisture variation should be measured periodically, and the bearing capacity determined by laboratory tests of samples secured so as to reflect the typical range of moistures, particularly the highest. Pavement serviceability should be determined accurately by profile studies.

Subgrade moisture studies should be undertaken to define the range in moisture content changes for the typical subgrades in each geologic region and each different drainage regime.

Triaxial tests should be made on typical subgrade materials utilizing the procedure outlined in this paper for "saturating" the soils, or when more realistic subgrade moisture data become available, by making the tests at those moistures. The bearing capacities and deflections of these materials should be computed from the appropriate theories and correlated with the geology, soil classification, and region for use in preliminary design.

Finally more realistic theories should be developed for the bearing capacity and deflection of the subgrade and each of the pavement components.

CONCLUSIONS

1. There are numerous causes or factors involved in the failure of a pavement to perform adequately. Of the Georgia pavements studies, however, most were load related.
2. The study of the performance of Georgia pavements disclosed a correlation among the serviceability rating or index, traffic, and computed deflection and bearing capacity of the subgrade.
3. The study of the AASHO data disclosed a similar correlation among these factors.
4. The AASHO subgrade had an ultimate bearing capacity of 99 psi. For comparable load, traffic and performance, Georgia roads required an ultimate bearing capacity of 31 psi. The difference is probably the result of differences in environment. The 31-psi required bearing capacity for Georgia subgrades corresponds to the Soil Support Number 3 of the AASHO design.
5. Georgia pavement thicknesses can also be designed by the use of triaxial tests on subgrade soils tested under field moisture conditions. The required safety factor against a bearing capacity (shear) failure is the required thickness to reduce the stress to that necessary to provide the safe bearing. This factor can be found from graphs of the test data and stress distribution below a pavement.

ACKNOWLEDGMENTS

This work has been sponsored by the Georgia State Highway Department and the U. S. Bureau of Public Roads, through the Engineering Experiment Station of the Georgia Institute of Technology. The author is indebted to T. S. Wallace, T. K. Brasher and D. Wheeless, graduate research assistants; to Dr. A. Schwartz who directed the field studies of the pavements and the laboratory testing; to W. F. Abercrombie, Engineer of Materials and Tests and T. Moreland, Soil Engineer, the Georgia State Highway Department; and to the late W. E. Chastain, Sr., Engineer of Physical Research, Illinois Division of Highways.

REFERENCES

1. The AASHO Road Test, Report 5: Pavement Research. Highway Research Board Spec. Rept. 61E, 1962.
2. Liddle, W. J. Application of AASHO Road Test Results to the Design of Flexible Pavements. Preprint Vol. Supple., Int. Conf. on the Structural Design of Asphalt Pavements, Univ. of Mich., Ann Arbor, 1962.

3. Carey, W. N., Jr., and Irick, P. E. The Pavement Serviceability-Performance Concept. Highway Research Board Bull. 250, pp. 40-58, 1960.
4. Sowers, G. F., and Vesic, A. B. Vertical Stresses in Subgrades Beneath Statically Loaded Flexible Pavements. Highway Research Board Bull. 342, pp. 90-123, 1962.
5. Terzaghi, K. Theoretical Soil Mechanics. New York, John Wiley and Sons, 1941.
6. Hveem, F. N. Types and Causes of Pavement Distress. Highway Research Board Bull. 187, pp. 1-52, 1958.
7. The AASHO Road Test, Report 2: Materials and Construction. Highway Research Board Spec. Rept. 61B, 1962.
8. Shook, J. F., and Fang, A. Y. Cooperative Materials Testing Program at the AASHO Road Test. Highway Research Board Spec. Rept. 66, 1961.
9. Sowers, G. F., and Sowers, G. B. Introductory Soil Mechanics and Foundations. New York, Macmillan Co., 2nd Ed. 1961.
10. Eiland, E. Alabama Highway Departments Use of the AASHO Data. Proc. 6th Alabama Joint Highway Conf., Auburn, April 1963.
11. Langsner, G., Huff, T. S., and Liddle, W. J. Use of Road Test Findings by the AASHO Design Committe. Highway Research Board Spec. Rept. 73, pp. 399-414, 1962.

Low Modulus Pavement on Elastic Foundation

JON HAGSTROM, RICHARD E. CHAMBERS, and EGONS TONS
Respectively, Research Assistant, Senior Research Engineer, and Assistant Professor of Civil Engineering, Department of Civil Engineering, Massachusetts Institute of Technology

The Westergaard theory for a plate on a "heavy liquid foundation" has been applied to the analysis of stresses and deflections in the asphalt-bound layer(s) of a flexible pavement system. A computer program has been developed to give a solution for the symmetrical loading case. Plots of the bending stresses, shear stresses and vertical deflection vs pavement thickness have been made to determine the influence of the various parameters involved in the analysis. It was found that the bending and shear stresses depend on the ratio of the pavement stiffness to the support stiffness, whereas the deflection is determined by the stiffness ratio and the magnitude of the modulus of support reaction.

A limiting stiffness ratio of $E/k \geq 100$ was chosen as a criterion for plate-type behavior in the asphalt-bound layer. This limit, however, was not rigorously determined. Certain limitations as to thickness for given values of the other variables were discovered. Relatively thin asphalt-bound layers give little load spreading action because of their high flexibility. The load is transferred directly to the support, causing large vertical deformations in the support layer. The behavior of very thick asphalt-bound layers approaches that of a single homogeneous layer. Stresses are dependent only on load, and plate theory no longer applies. A computer program for stress-deflection calculations is applied.

•A TYPICAL flexible pavement cross-section may include the natural in-place subgrade, a compacted subgrade, a compacted subbase, a compacted base of treated or plain gravel or crushed rock, and a surface of one or more layers of asphaltic concrete. This vertical variation in the material composition of the highway structure, coupled with the complex nature of the behavior under load of the individual materials, has hindered the development of rational analysis for the stresses and displacements produced by traffic loads.

In 1943, Burmister (1) introduced a theory of stresses and displacements in layered systems based on the assumption that the materials of each layer are ideally elastic. Burmister's analysis provides an exact solution for a given surface loading. The equations are rather cumbersome to work with in practice; however, computer solutions have been developed for a large range of applications (5).

Attempts to correlate theoretical stresses and deflections with actual soil behavior by using Burmister's theory have met with little success. Sowers and Vesic (6) found that the reduction in subgrade stresses predicted by Burmister's theory occurs only when the stiffer top layers have the ability to develop tensile stresses. In general, investigators have concluded that soil properties cannot be accurately described in terms of a single Young's modulus and Poisson's ratio as is assumed in elastic theory.

Paper sponsored by Committee on Flexible Pavement Design and presented at the 44th Annual Meeting.

When the surface layer is fairly stiff in comparison with the support and the deflections are small, the tensile stresses produced in the support will be negligible. Assuming that these conditions are satisfied and that the behavior of the surface layer is consistent with elastic theory, Burmister's equations can be used for the analysis of stresses and deflections in the asphalt-bound layer.

By making certain simplifying assumptions concerning the behavior of the asphalt-bound and supporting layers, the equations for the stresses and displacements can be reduced to a manageable form. This simplified theory was first suggested by Westergaard (7) for use in the design of concrete pavements. It is the purpose of this paper to explore Westergaard's theory as it applies to the analysis of stresses and deflections in the surface layer of a flexible pavement system. The term "surface layer" used in this context is meant to include the asphalt-bound layer(s) only. The treatment in this report is mathematical in nature. It is intended as background material for future research which will include a treatment of asphaltic concrete properties for various time-temperature and loading conditions.

ELASTIC APPROACH

The behavior of asphaltic concrete is not consistent with several of the assumptions of elastic theory. The relation between stress and strain is not, in general, linear; moreover, it is time dependent. However, under certain conditions a flexible pavement will exhibit nearly complete rebound on removal of load, the recovery occurring over some time interval. The amount of deflection under load and the time for recovery on removing the load will depend on the temperature of the pavement and the duration of the load. Baker and Papazian (10) have pointed out that the effect of choosing a particular temperature and time of loading to determine the elastic modulus of the asphalt-bound material is equivalent to selecting a secant modulus. The complexity of the mathematics for rigorous treatment of the viscoelastic theory makes the use of this secant modulus artifice and elastic theory necessary at this time.

APPLICATION OF WESTERGAARD THEORY

Development

Westergaard treats the asphalt-bound layer as a circular plate of infinite extent. The flexural rigidity of the plate can be expressed as:

$$D = \frac{EI}{1 - \mu^2} \tag{1}$$

where

E = modulus of elasticity for plate (psi),
I = moment of inertia for plate ($in.^4$), and
μ = Poisson's ratio.

For a plate of constant thickness, this equation becomes:

$$D = \frac{Eh^3}{12\,(1 - \mu^2)} \tag{2}$$

where h is the thickness of plate in inches. The deflection of a pavement depends not only on its flexural rigidity but also on the stiffness of the support beneath. Westergaard has expressed the stiffness of the support as a modulus of support reaction, k. The modulus is defined mathematically as follows:

$$k = \frac{p}{w} = \frac{\text{reaction of support}}{\text{deflection of support surface}} \tag{3}$$

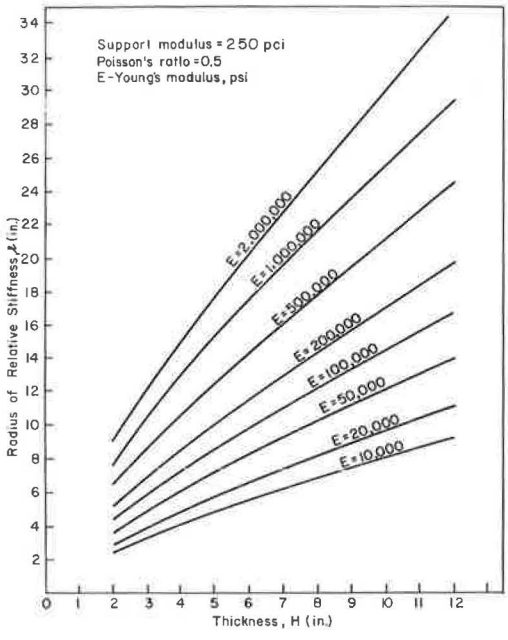

Figure 1. Radius of relative stiffness vs thickness of asphalt-bound layer.

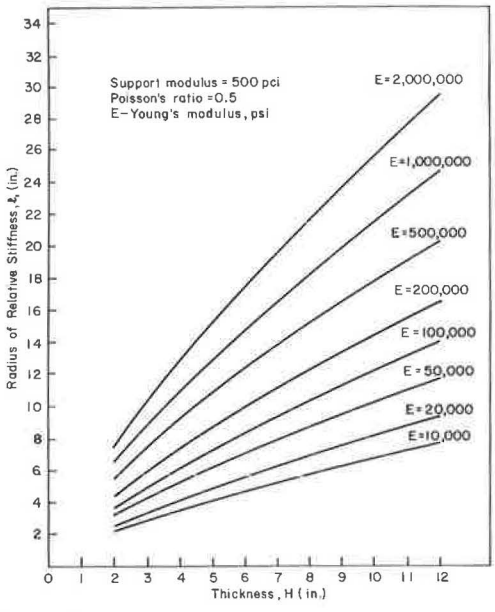

Figure 2. Radius of relative stiffness vs thickness of asphalt-bound layer.

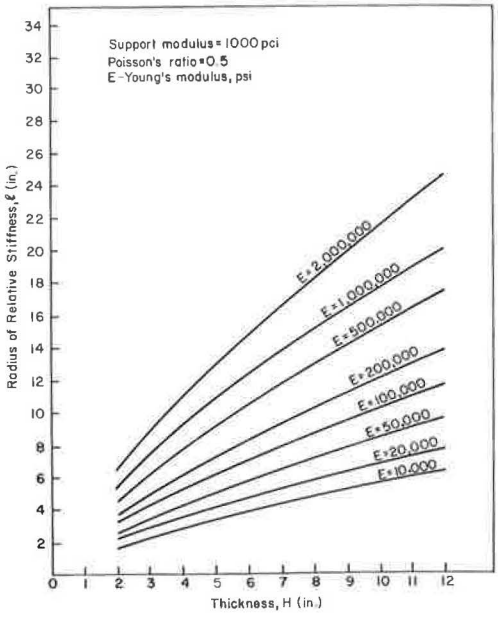

Figure 3. Radius of relative stiffness vs thickness of asphalt-bound layer.

To facilitate the mathematical treatment, Westergaard introduced the term "radius of relative stiffness," denoted by the symbol ℓ and defined mathematically as:

$$\ell^4 = \frac{D}{k} \qquad (4)$$

For a pavement of constant thickness this equation becomes:

$$\ell^4 = \frac{Eh^3}{12\,(1 - \mu^2)k} \qquad (5)$$

Plots of radii of relative thickness vs thicknesses of asphalt-bound layers for varying support moduli are shown in Figures 1 through 3.

To apply this mathematical treatment in an analysis of the forces and deflections due to an interior load on a layered pavement system, the following assumptions must be made:

1. A pavement loaded some distance from the edge can be represented by a circular plate of infinite extent.
2. The reactions of the support are vertical only, are proportional to the deflection of the asphalt-bound layer, and

are independent of the loaded area. The latter portion of this assumption is equivalent to assuming that there is no transfer of stress through shear resistance in the support, analogous to the behavior of a "heavy liquid."

3. The asphalt-bound layer is at every point in contact with the support.
4. Volumetric changes, variations in support properties, temperature, horizontal components of support reaction, and dynamic effects can be neglected or accounted for otherwise.

Support

Because the support, consisting of particulate materials, is neither a perfectly elastic solid nor a heavy liquid, it is necessary to evaluate the support modulus, k, by some sort of plate bearing test. This necessitates the adoption of some standard plate size and testing procedure. Work by the U. S. Bureau of Public Roads (11) indicates that for circular plates with diameters between 26 and 84 in., there is little variation in the pressure required to produce a given deflection. Furthermore, Terzaghi (12) has indicated that a linear relationship between deflection and pressure does exist for some soils up to one-half the bearing capacity of the soil. This justifies the assumption of linearity between reaction and deflection, and negligible transfer of stress by shear resistance in the soil within the limits indicated.

Asphalt-Bound Layer

Westergaard represents the asphalt-bound layer as a circular plate of infinite extent. He assumes that the properties of the asphalt-bound material are consistent with the assumptions of elastic theory (13); that is, the material must be continuous, homogeneous, isotropic, and governed by Hooke's law.

By requiring equilibrium of forces and moments in the three directions of space, a system of six equations with six unknowns can be derived. These six equations can be reduced to a single sixth-order differential equation describing the behavior of an ideally elastic body under load. For a body whose dimension in the vertical direction is much smaller than in the two other directions, the governing sixth-order differential equation can be reduced to the familiar fourth-order differential equation of ordinary plate theory by making several simplifying assumptions:

1. The middle plane of the plate remains unstrained under load.
2. Plane sections remain plane under load.
3. The direct stress in the vertical direction is small in comparison with the other stress components and can be neglected in the stress-strain relations.
4. A plane section normal to the middle plane before loading remains normal under load.

The last assumption is equivalent to stating that the deformation due to vertical shearing stresses is very small and can be neglected.

If the behavior of the asphalt-bound layer under load is to be consistent with plate theory, the asphalt-bound layer must be relatively rigid in comparison with the support layer. However, it is difficult to define the critical E/k value because of the many assumptions involved.

A critical ratio of E/k = 100 is proposed in this paper with the following reasoning:

1. Plate theory requires that the thickness of the plate be small in comparison with the dimensions in the other two directions. For circular plates, it is commonly required that the thickness-radius ratio be greater than 10 (26).
2. The radius of influence of a concentrated load is approximately 4ℓ, where ℓ depends on the E/k ratio and the asphalt-bound layer thickness (14).
3. For values of E/k less than 100, the radius of influence of a concentrated load is at best seven times greater than the asphalt-bound layer thickness.

Because the critical ratio has not been rigorously determined, it should be used only as a general guide. However, it is important to realize that the Westergaard theory becomes increasingly inaccurate as the stiffness of the asphalt-bound layer approaches that of the support. Thus, the application of the theory is limited to conditions which lead to small deflections, the vertical stress at the pavement support interface should not exceed one-half the ultimate bearing stress of the support, and the E/k ratio should be 100 or greater.

Development of Equations

The fourth-order differential equation describing the behavior of a plate can be expressed as follows:

$$\nabla^2 (\nabla^2 w) = \frac{p}{D} \tag{6}$$

where w represents the vertical deflection of the plate, p represents the vertical load, D represents the flexural rigidity of the plate, and ∇^2 represents the Laplace operator which is defined in Cartesian coordinates as $\frac{\partial^2}{\partial x^2} + \frac{\partial^2}{\partial y^2}$. For a plate on a "heavy liquid" foundation where the reaction of the subgrade is vertical only and is proportional to the deflection, w, the differential equation becomes:

$$\nabla^2 (\nabla^2 w) = \frac{p - kw}{D} \tag{7}$$

By representing a tire load on a pavement as a circular load of uniform intensity, the intensity being equal to the tire pressure, Putnam (14) has derived equations for the bending moments in the asphalt-bound layer and for the deflection of the surface of the pavement (Appendix B). Because of the symmetry of the assumed load representation, the moments and deflections are expressed in terms of Bessel functions. Putnam's equations for deflection and bending moment under the center of the circular load are as follows:

$$w_o = \frac{P\ell^2}{\pi D c^2} \left[1 + c\,\mathrm{ker}'c \right] \text{ in.} \tag{8}$$

and

$$m_{max} = \frac{P(1 + \mu)}{2\pi} \left[\frac{1}{c}\,\mathrm{kei}'c \right] \text{ in.-lb/in.} \tag{9}$$

where

P = total load (lb);
μ = Poisson's ratio;
ℓ = radius of relative stiffness (in.);
D = flexural rigidity of the plate (lb-in.^{2});
c = radius of relative load distribution, defined as radius of applied circular load/ℓ;
ker'x = Bessel function with real argument; and
kei'x = Bessel function with real argument.

Using tabulated values for the Bessel functions, these equations provide a relatively simple means of analysis for deflection and maximum bending stresses. These equations can also be adapted to computer analysis and the stresses and deflections can be computed for a range of asphalt-bound layer thicknesses and moduli, and moduli of support reaction.

Moment and Deflection Curves

Figures 4 through 9 show plots of the maximum bending stress (maximum moment per unit length/section modulus per unit length) and the maximum deflection under the center of a 10-kip single-axle wheel load with a 70-psi tire contact pressure vs asphalt-bound layer thickness. The ordinate values have been divided by the total load because the magnitude of the stresses and deflections is a function of the ratio of total load to tire contact pressure (i.e., loaded area) and is not uniquely determined by the magnitude of the load.

The graphs indicate that the bending stresses depend on the ratio of the asphalt-bound layer stiffness to the modulus of support reaction, D/k, and are independent of the magnitude of these quantities. As the asphalt-bound layer decreases, it loses flexural rigidity, and at some point a decrease in the maximum bending stress under the center of the load occurs, as is indicated by the peaking in the curves of Figures 4, 5 and 6. In this range of asphalt-bound layer thickness, the radius of influence of the load is small, on the order of twice the radius of the loaded area. (For a concentrated load, the radius of influence is approximately 4ℓ.) Thus, the load is transferred directly into the support with little spreading by plate action.

For relatively thick asphalt-bound layers, Figures 4, 5 and 6 indicate that the bend-stress tends to become less dependent on the Young's modulus of the asphalt-bound layer and the support modulus. The pavement behavior approaches that of a Boussinesq half space and plate theory breaks down. An increase in asphalt-bound layer thickness beyond 10 to 11 affects only slightly the bending stresses of the structure. It is interesting to note that this 10- to 11-in. boundary for diminishing returns coincides with the optimum pavement thickness determined for a similar range of variables by McLeod (15) with his Burmister-type layered analysis.

The deflection plots indicate that the deflection depends not only on the ratio of plate rigidity to support stiffness but also is greatly affected by the modulus of support reaction, k. Using the deflection curves, it is possible to determine the magnitude of the vertical stress in the soil at the interface. The vertical stress is equal to the deflection multiplied by the modulus of subgrade reaction: $p = kw$.

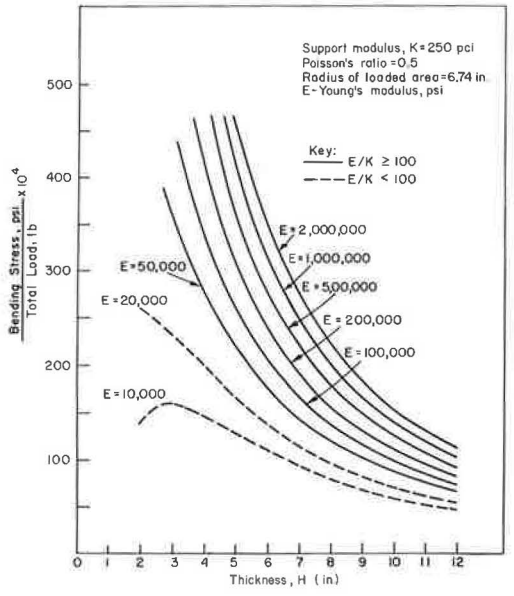

Figure 4. Bending stress vs thickness of asphalt-bound layer for 10-kip load, 70-psi tire pressure.

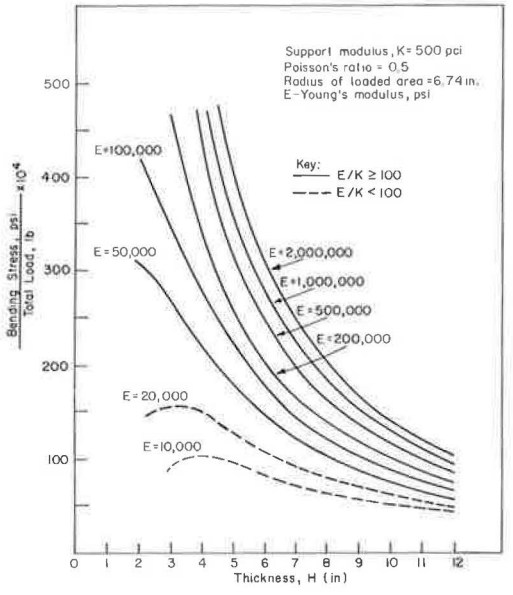

Figure 5. Bending stress vs thickness of asphalt-bound layer for 10-kip load, 70-psi tire pressure.

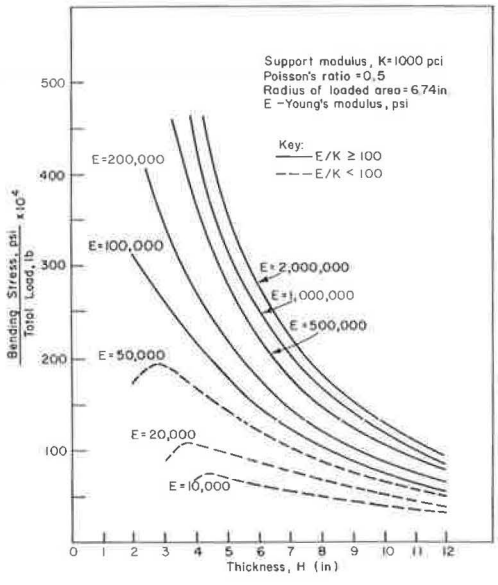

Figure 6. Bending stress vs thickness of asphalt-bound layer for 10-kip load, 70-psi tire pressure.

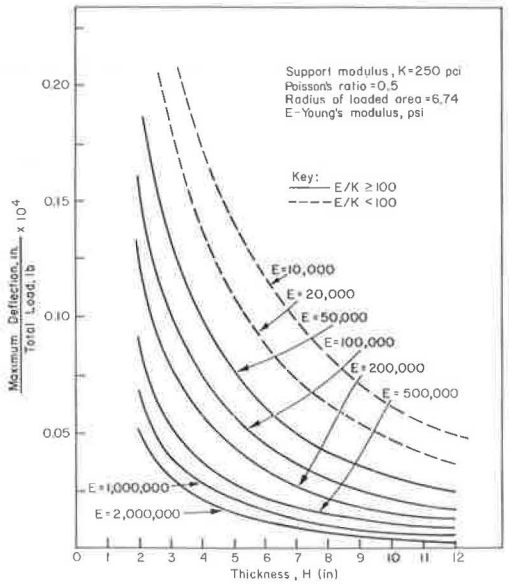

Figure 7. Maximum deflection vs thickness of asphalt-bound layer for 10-kip load, 70-psi tire pressure.

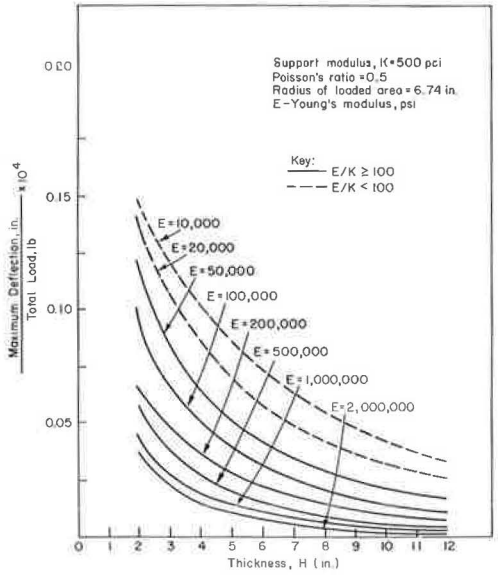

Figure 8. Maximum deflection vs thickness of asphalt-bound layer for 10-kip load, 70-psi tire pressure.

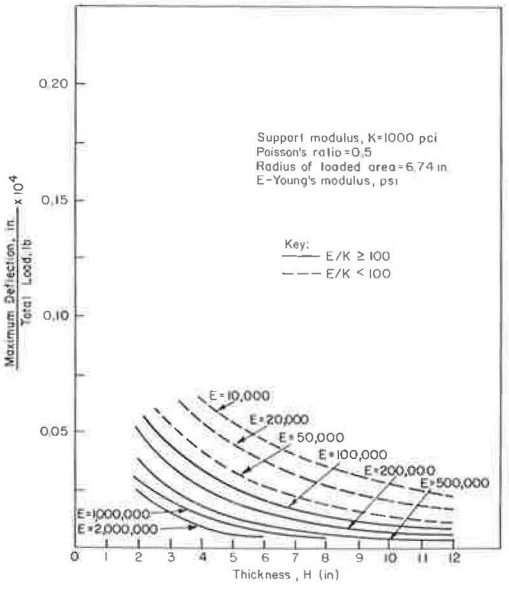

Figure 9. Maximum deflection vs thickness of asphalt-bound layer for 10-kip load, 70-psi tire pressure.

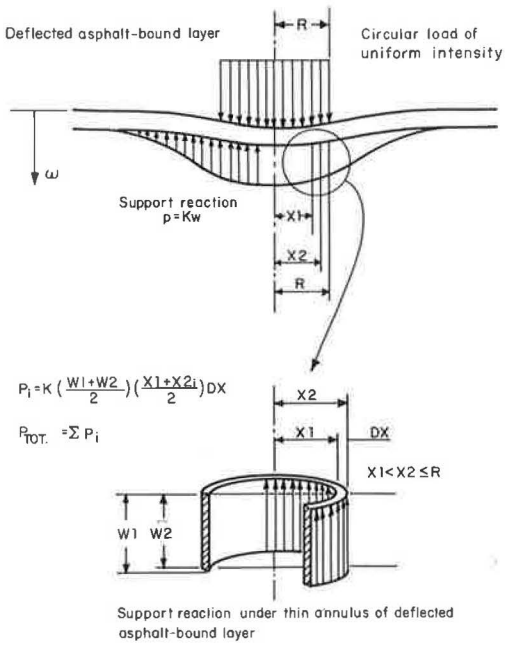

Figure 10. Computation of total support reaction within distance, R, from center of loaded area.

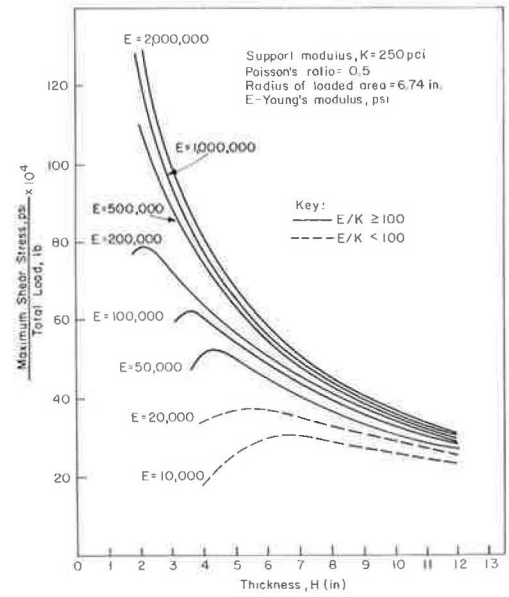

Figure 11. Maximum shear stress vs thickness of asphalt-bound layer for 10-kip load, 70-psi tire pressure.

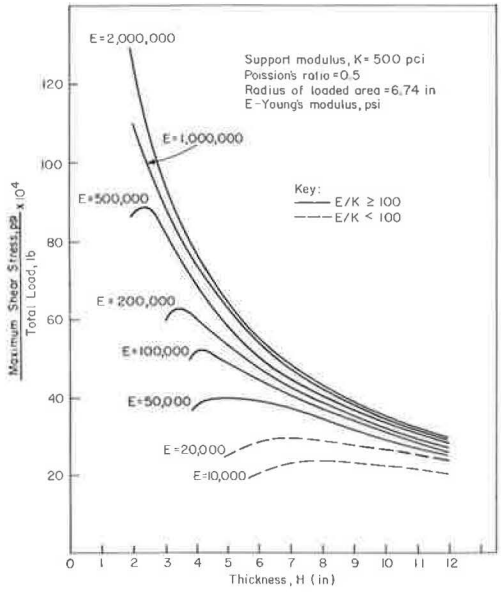

Figure 12. Maximum shear stress vs thickness of asphalt-bound layer for 10-kip load, 70-psi tire pressure.

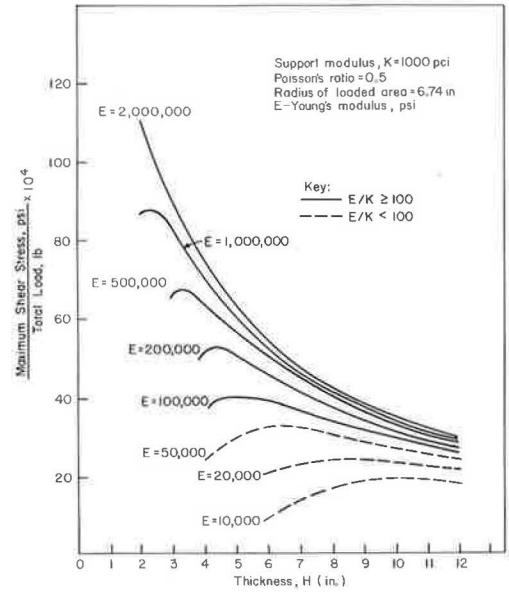

Figure 13. Maximum shear stress vs thickness of asphalt-bound layer for 10-kip load, 70-psi tire pressure.

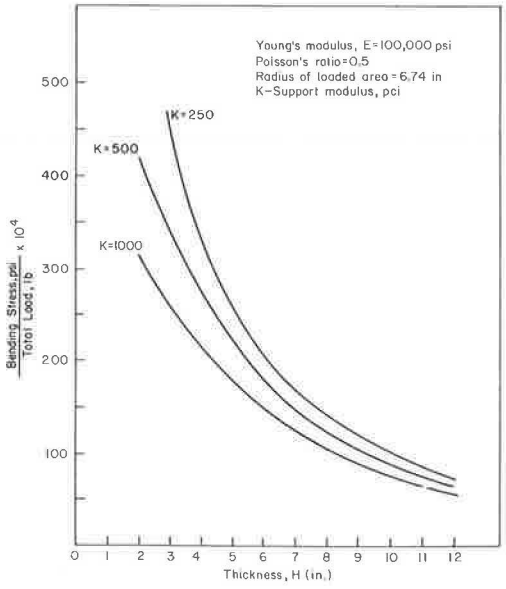

Figure 14. Bending stress vs thickness of asphalt-bound layer for 10-kip load, 70-psi tire pressure.

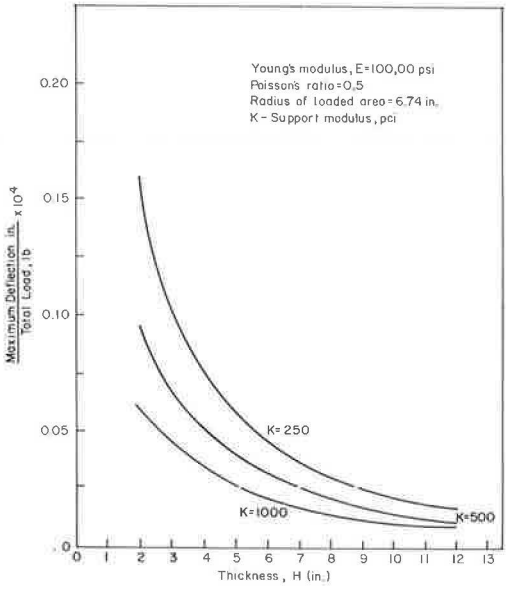

Figure 15. Maximum deflection vs thickness of asphalt-bound layer for 10-kip load, 70-psi tire pressure.

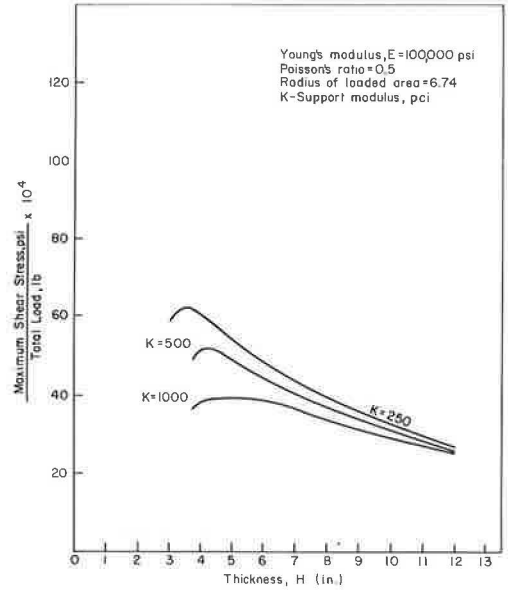

Figure 16. Maximum shear stress vs thickness of asphalt-bound layer for 10-kip load, 70-psi tire pressure.

Vertical Shear

Because of the assumptions made in reducing the general sixth-order differential equation of elastic theory to the fourth-order equation of ordinary plate theory, it is impossible to solve directly for the vertical shear stresses in the asphalt-bound layer. However, the shear force acting over the thickness of the asphalt-bound layer at a point can be determined by evaluating the slope of the moment curve at that point. By assuming a distribution of the shear force over the thickness, a value for the maximum shear stress can be determined.

The shear force at any distance from the center of the applied load can also be determined by computing the magnitude of the total support reaction within the radius of the point being considered, subtracting this reaction from the magnitude of that portion of the applied load which lies within the radius of the point being considered and assuming that the difference in these forces is carried by a shear force distributed uniformly around the perimeter of the cylinder with the radius being considered. The magnitude of the support reaction can be computed by dividing the circular area within the radius being considered into many thin annuli, evaluating the average reaction for each annulus, multiplying the average reaction by the area of the annulus and summing the reactions for each annulus. This procedure is indicated schematically in Figure 10.

Figures 11, 12, and 13 are plots of the maximum shear stress at the edge of the applied load for a 10,000-lb wheel load with 70-psi tire contact pressure. In determining the shear stress, it was assumed that the shear force is distributed parabolically over the asphalt-bound layer thickness. As was the case for the bending stresses, the shear curves exhibit a peak value for relatively thin asphalt-bound layers and the shear stress tends to become independent of E and k for thicknesses greater than the 10- to 11-in. range.

Figures 14, 15, and 16 illustrate an alternative way of plotting the bending stresses, deflections and shear stresses. The Young's modulus value of the asphalt-bound layer is held constant and the ordinates are plotted vs thickness for various values of the support modulus.

CONCLUSIONS

1. When the asphalt-bound layer is fairly rigid in comparison with the support ($E/k \geq 100$), an applied load is spread over the support by the plate action in the asphalt-bound layer. If, in addition, the deflection under load is small, the Westergaard theory will provide a useful analysis.
2. By representing the wheel load as a circular load of uniform intensity, the bending stress under the center of the load can be computed for a given E/k ratio in terms of Bessel functions.
3. Given the E/k ratio and the value of the support modulus, k, the pavement deflection and the vertical stress at the asphalt-bound layer-support interface can be computed.
4. By assuming a parabolic distribution for the shear force over the asphalt-bound layer thickness, it is possible to determine the maximum vertical shear stress acting under the edge of the loaded area.

REFERENCES

1. Burmister, D. M. The Theory of Stresses and Displacements in Layered Systems and Applications to the Design of Airport Runways. Highway Research Board Proc., Vol. 23, pp. 126-148, 1943.
2. Burmister, D. M. The General Theory of Stresses and Displacements in Layered Systems. Jour. of Applied Physics, Vol. 16, Nos. 2, 3 and 5, 1945.
3. Burmister, D. M. Stress and Displacement Characteristics of a Two-Layer Rigid Base Soil System: Influence Diagrams and Practical Applications. Highway Research Board Proc., Vol. 35, pp. 773-814, 1956.
4. Burmister, D. M. Applications of Layered System Concepts and Principles to Interpretations and Evaluations of Asphalt Pavement Performances and to Design and Construction. Internat. Conf. on the Structural Design of Asphalt Pavements, Univ. of Mich., 1962.
5. Mehta, M. R., and Veletoses, A. S. Stresses and Displacements in Layered Systems. Univ. of Illinois, Urbana, June 1959.
6. Sowers, G. F., and Vesic, A. B. Vertical Stresses in Subgrades Beneath Statically Loaded Flexible Pavements. Highway Research Board Bull. 342, pp. 90-123, 1962.
7. Westergaard, H. M. Computation of Stresses in Concrete Roads. Highway Research Board Proc., Vol. 5, Part 1, pp. 90-112, 1925.
8. Westergaard, H. M. Stresses in Concrete Pavements Computed by Theoretical Analysis. Public Roads, Vol. 7, No. 2, April 1926.
9. Westergaard, H. M. Analytical Tools for Judging Results of Structural Tests of Concrete Pavements. Public Roads, Vol. 14, No. 10, Dec. 1933.
10. Baker, R. F., and Papazian, H. S. The Effect of Stiffness Ratio on Pavement Stress Analysis. Highway Research Board Proc., Vol. 39, pp. 61-85, 1960.
11. Teller, L. W., and Sutherland, E. C. The Structural Design of Concrete Pavements. V. An Experimental Study of the Westergaard Analysis of Stress Conditions in Concrete Pavement Slabs of Uniform Thickness. Public Roads, Vol. 23, No. 8, Oct. 1942.

12. Terzaghi, K. Evaluation of Coefficients of Subgrade Reaction. Geotechnique, Vol. 5, Dec. 1955.
13. Wang, C. T. Applied Elasticity. New York, McGraw-Hill, 1953.
14. Putnam, J. O. Theoretical Analysis of the Behavior of Rigid Airfield Pavements for the Case of Interior Loading. unpublished Doctoral Thesis, MIT, 1963.
15. McLeod, Norman W. Some Notes on Pavement Structural Design. Highway Research Record No. 13, pp. 66-141, 1963.
16. Yoder, E. J. Principles of Pavement Design. New York, John Wiley and Sons, 1959.
17. Taylor, D. W. Fundamentals of Soil Mechanics. New York, John Wiley and Sons, 1948.
18. Hogg, A. H. A. Equilibrium of a Thin Plate, Symmetrically Loaded, Resting on an Elastic Foundation of Infinite Depth. Philosophical Magazine, Vol. 25, 1938.
19. McLachlan, N. W. Bessel Functions for Engineers. 2nd Ed., Oxford, Clarendon Press, 1955.
20. Timoshenko, S., and Goodier, J. N. Theory of Elasticity. New York, McGraw-Hill, 1951.
21. Timoshenko, S., and Woinowsky-Krieger, S. Theory of Plates and Shells. 2nd Ed., New York, McGraw-Hill, 1959.
22. Investigations of Pressures and Deflections for Flexible Pavements. U. S. Army Corps of Engineers, Waterways Experiment Station, Vicksburg, Rept. No. 1, Homogeneous Clayey Silt Test Section, Tech. Memo No. 3.323, March 1951.
23. Investigations of Pressures and Deflections for Flexible Pavements. U. S. Army Corps of Engineers, Waterways Experiment Station, Vicksburg, Rept. No. 4, Homogeneous Sand Test Section, Tech. Memo No. 3.323, Dec. 1954.
24. Acum, W. E. A., and Fox, L. Stresses in a Three-Layer System. Great Britain, Bond Research Note No. R. H./1257/WEAA-LF, Nov. 1949.
25. McMahon, T. F., and Yoder, E. J. Design of a Pressure-Sensitive Cell and Model Studies of Pressures in a Flexible Pavement Subgrade. Highway Research Board Proc., Vol. 39, pp. 650-682, 1960.
26. Seely, F. B., and Smith, J. O. Advanced Mechanics of Materials. New York, John Wiley and Sons, 1957.
27. Odemark, N. Investigation as to the Elastic Properties of Soils and Design of Pavement According to the Theory of Elasticity. Statens Vaginstitut, Stockholm, Maddelande No. 77, 1949.

Appendix A

PROGRAM DESCRIPTION

The bending stresses, deflections, and shear stresses plotted in Figures 4 through 9 and 11 through 16 were evaluated using a FORTRAN source program developed from Putnam's equations. The input required by the program includes the design wheel load, the design tire pressure, Young's modulus for the pavement material, Poisson's ratio for the pavement material, and the support modulus. As output, the program lists the bending stress divided by total load, deflection divided by total load, maximum shear stress divided by total load and the ratio of the radius of the loaded area to the radius of relative stiffness of the pavement. These quantities are computed for values of pavement thicknesses ranging from 2 to 12 in. in 2-in. intervals. The input and output formats are consistent with any FORTRAN II processor and can be readily altered for use with any FORTRAN processor. The output format contains Hollerith fields, or H-type alphanumeric data fields, which identify the quantities computed. Figure 17 shows the actual output for a typical analysis.

The reasoning used in the development of the program can be seen in the flow diagram shown in Figure 18.

```
H=   2.00 STRESS=    .0663 DEF=    .00001637 SHEAR=    .00475281 C=   1.5529
H=   4.00 STRESS=    .0345 DEF=    .00000750 SHEAR=    .00614423 C=    .9233
H=   6.00 STRESS=    .0207 DEF=    .00000443 SHEAR=    .00487677 C=    .6812
H=   8.00 STRESS=    .0139 DEF=    .00000300 SHEAR=    .00391795 C=    .5490
H=  10.00 STRESS=    .0100 DEF=    .00000219 SHEAR=    .00324716 C=    .4644
H=  12.00 STRESS=    .0076 DEF=    .00000169 SHEAR=    .00276339 C=    .4050
```

E = 100,000
K = 250
Poisson's ratio = 0.5

Figure 17. Typical program output.

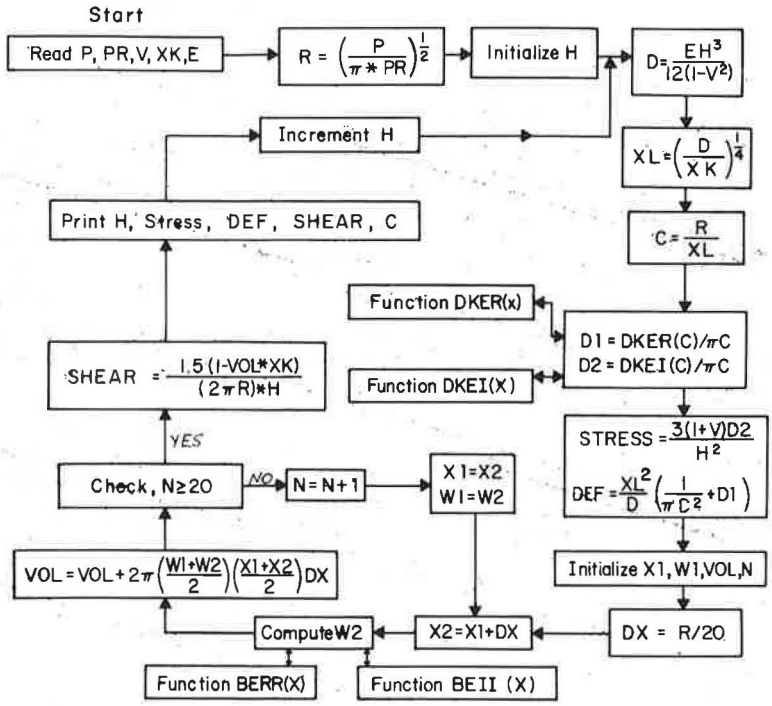

Figure 18. Flow diagram for computer program.

The definitions of the symbols used in the flow chart are as follows:

BEII (X) - bei (x), Bessel function with real argument;
BERR (X) - ber (x), Bessel function with real argument;
C - ratio of relative load distribution, R/XL;
D - flexural rigidity of pavement (lb-in.^{2}/in.);
D1 - function of C;
D2 - function of C;
DEF - deflection under center of load area, divided by the total load (in./lb);
DKEI (Z) - kie'(z), Bessel function with real argument;

DKER(Z) - ker'(z), Bessel function with real argument;

DX - width of annuli used in calculating reaction under loaded area (in.);

E - Young's modulus for pavement material (psi);

H - pavement thickness (in.);

N - number of annuli used to compute subgrade reaction under loaded area;

P - total load applied at surface (lb);

PR - tire contact pressure for applied load (psi);

R - radius of applied load (in.);

SHEAR - maximum vertical shear stress at edge of applied load divided by total load (psi/lb);

STRESS - maximum bending stress under center of applied load divided by total load (psi/lb);

V - Poisson's ratio;

VOL - volume of support reaction diagram divided by modulus of subgrade (cu in.);

W1 - deflection at inner radius of annulus (in.);

W2 - deflection at outer radius of annulus (in.);

XK - modulus of support reaction (pci);

XL - radius of relative load distribution;

X1 - inner radius of annulus; and

X2 - outer radius of annulus.

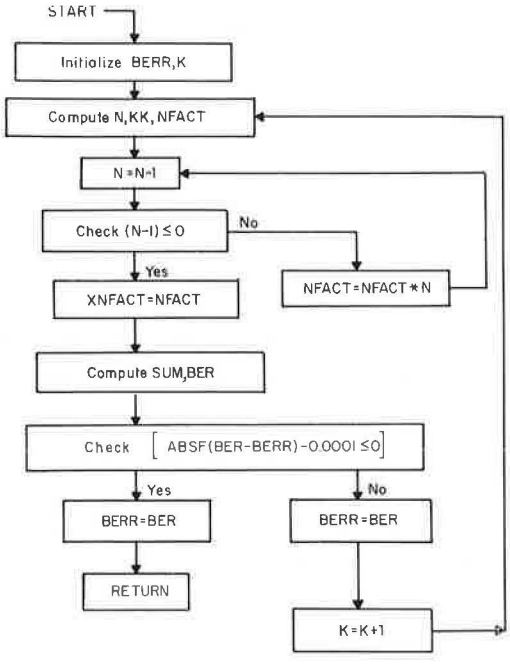

Figure 19. Flow diagram for computer subprogram, FUNCTION BERR (X).

The required Bessel functions are computed using Function Subprograms, otherwise known as FORTRAN functions. The definition for FUNCTION BERR (X) is as follows:

$$\text{BERR}(X) = \text{ber}(x) = \sum_{k=0}^{\infty} (-1)^K \frac{\left(\frac{X}{2}\right)^{4K}}{\left[(2K)\,!\right]^2} \qquad (10)$$

Figure 19 shows the flow diagram for this function. BEII (X) is defined as follows:

$$\text{BEII}(X) = \text{bei}(x) = \sum_{k=0}^{\infty} (-1)^K \frac{\left(\frac{X}{2}\right)^{4K+2}}{\left[(2K+1)\,!\right]^2} \qquad (11)$$

```
C       WESTERGAARD ANALYSIS
      1 FORMAT (5F12.2)
      2 FORMAT (3H H=F5.2,4X,7HSTRESS=F8.4,4X,4HDEF=F12.8,4X,
       16HSHEAR=F12.8,4X,2HC=F8.4)
      3 READ 1, P, PR, V, XK, E
        R=(P/(3.1416*PR))**.5
        DO 7 IH=2,12,2
        H=IH
        D=(E*(H**3))/(12.*(1.-V*V))
        XL=(D/XK)**0.25
        C=R/XL
        D1=DKER(C)/(3.1416*C)
        D2=DKEI(C)/(3.1416*C)
        STRESS=(D2*3.*(1.+V))/(H**2)
        DEF=(XL**2)*((1./(3.1416*(C**2)))+D1)/D
        X1=0.0
        W1=DEF
        DX=R/20.
        VOL=0.0
        N=1
      4 X2=X1+DX
        W2=((XL**2)/D)*((1./(3.1416*(C**2)))+(D1*BERR(X2/XL))
       1+(D2*BEII(X2/XL)))
        VOL=VOL+(1.5708*(W1+W2)*(X1+X2))*DX
        IF(20-N)6,6,5
      5 X1=X2
        W1=W2
        N=N+1
        GO TO 4
      6 SHEAR=(1.5*(1.-(VOL*XK)))/(6.2832*R*H)
      7 PRINT 2, H, STRESS, DEF, SHEAR, C
        GO TO 3
        END


        FUNCTION DKEI(Z)
        A=0.1159-LOGF(Z)
        X=Z/2.
        DKEI     =(A+.5)*X+3.1417*(X**3)/8.-(A+5./3.)*(X**5)/12.
       1-3.1417*(X**7)/576.
        RETURN
        END


        FUNCTION DKER(Z)
        A=0.1159-LOGF(Z)
        X=Z/2.
        DKER     =-.5/X+(3.1417*X/4.)-(.5*(A+1.25)*(X**3))
       1-(3.1417*(X**5)/48.)+((A+(47./24.))*(X**7)/144.)
        RETURN
        END
```

Figure 20.

```
      FUNCTION BEII(X)
      BEII=(.5*X)**2
      K=1
    6 N=2*K+1
      KK=4*K+2
      NFACT=N
    3 N=N-1
      IF(N-1)1,1,2
    2 NFACT=NFACT*N
      GO TO 3
    1 XNFACT=NFACT
      SUM=((-1.)**K)*((.5*X)**KK)/(XNFACT**2)
      BEI=BEII+SUM
      IF(ABSF(BEI-BEII)-.0001)4,4,5
    5 BEII=BEI
      K=K+1
      GO TO 6
    4 BEII=BEI
      RETURN
      END
```

```
      FUNCTION BERR(X)
      BERR=1.
      K=1
    6 N=2*K
      KK=4*K
      NFACT=N
    3 N=N-1
      IF(N-1)1,1,2
    2 NFACT=NFACT*N
      GO TO 3
    1 XNFACT=NFACT
      SUM=((-1.)**K)*((.5*X)**KK)/(XNFACT**2)
      BER=BERR+SUM
      IF(ABSF(BER-BERR)-.0001)4,4,5
    5 BERR=BER
      K=K+1
      GO TO 6
    4 BERR=BER
      RETURN
      END
*     DATA
```

Figure 20. (Cont'd.)

The flow chart for FUNCTION BEII (X) is similar to that of FUNCTION BERR (X) and, therefore, will not be illustrated.

The subprograms used to evaluate DKEI (Z) and DKER (Z) are relatively simple; therefore, they will not be diagramed. These two subprograms are exact for values of the argument less than or equal to one. For values of the argument between 1 and 2, the error is negligible (less than 1 percent), but for values greater than 2 the error increases rapidly. It is for this reason that the quantity C, which is the argument used in this program, is included in the output of the program. An inspection of the program output will reveal the limits of the pavement thickness for which the computed stresses and deflections are exact. For values of $E/k \geq 100$, the solutions for a 10-kip load with a 70-psi tire pressure are accurate for pavement thicknesses greater than 2 in. Bessel functions available as Library Functions in the software of a particular data processing unit can readily be incorporated into the program and the subprograms can be omitted. The log function, natural log, is the only Library Function required by the program as presented here. Figure 20 shows a complete listing of the main FORTRAN program and the required FORTRAN functions.

Appendix B

DERIVATION OF EQUATIONS FOR MOMENT AND DEFLECTION*

The differential equation describing the behavior of a plate on a "heavy liquid" foundation (Eq. 7) becomes in cylindrical coordinates and for a symmetrical loading:

$$\left(\frac{\partial^2}{\partial r^2} + \frac{1}{r}\frac{\partial}{\partial r}\right)\left(\frac{\partial^2 w}{\partial r^2} + \frac{1}{r}\frac{\partial w}{\partial r}\right) = \frac{p - kw}{D} \tag{12}$$

where

p = unit load on plate,
r = radial distance from center of loaded area, and
w = vertical displacement.

For the case of a concentrated load, p is equal to zero except at the center of the plate; therefore, by setting p equal to zero and substituting ℓ^4 for D/k, the governing differential equation becomes:

$$\ell^4\left(\frac{\partial^2}{\partial r^2} + \frac{1}{r}\frac{\partial}{\partial r}\right)\left(\frac{\partial^2 w}{\partial r^2} + \frac{1}{r}\frac{\partial w}{\partial r}\right) + w = 0 \tag{13}$$

The following dimensionless quantities are introduced: $z = w/\ell$ and $x = r/\ell$. Eq. 13 becomes

$$\left(\frac{\partial^2}{\partial x^2} + \frac{1}{x}\frac{\partial}{\partial x}\right)\left(\frac{\partial^2 z}{\partial x^2} + \frac{1}{x}\frac{\partial z}{\partial x}\right) + z = 0 \tag{14}$$

By substituting ∇ for $\frac{\partial}{\partial x^2} + \frac{1}{x}\frac{\partial}{\partial x}$, Eq. 14 becomes

$$\nabla\nabla z - z = 0 \tag{15}$$

*This material is taken from the work of Putnam (14).

The variable $\epsilon = x\sqrt{i}$ is introduced and Eq. 15 becomes

$$\nabla'\nabla'z - z = 0 \tag{16}$$

where the symbol ∇' stands for $\frac{\partial}{\partial\epsilon^2} + \frac{1}{\epsilon}\frac{\partial}{\partial\epsilon}$. Eq. 15 is equivalent to

$$\nabla' (\nabla'z + z) - (\nabla'z + z) = 0 \tag{17}$$

and

$$\nabla' (\nabla'z - z) + (\nabla'z - z) = 0 \tag{18}$$

Thus, it is satisfied by the solution of the Bessel differential equation:

$$\nabla'z + z = \frac{\partial^2 z}{\partial\epsilon^2} + \frac{1}{\epsilon}\frac{\partial z}{\partial\epsilon} + z = 0 \tag{19}$$

and

$$\nabla'z - z = \frac{\partial^2 z}{\partial\epsilon^2} + \frac{1}{\epsilon}\frac{\partial z}{\partial\epsilon} - z = 0 \tag{20}$$

The combined solution of these two equations can be written as:

$$z = B_1 I_0 (x\sqrt{i}) + B_2 I_0 (xi\sqrt{i}) + B_3 K_0 (x\sqrt{i}) + B_4 K_0 (xi\sqrt{i}) \tag{21}$$

where I_0 and K_0 are Bessel functions of the first and second kind and of imaginary argument.

The argument x is real and all functions contained in the solution appear in complex form. The real part of the solution is determined by the introduction of four other functions: $I_0 (x \pm i) = \text{ber } x \pm \text{bei } x$, $K_0 (x \pm i) = \text{ker } x \pm \text{kei } x$, and setting $B_1 + B_2 = C_1\ell$, $B_1 - B_2 = -C_2 i\ell$, $B_3 + B_4 = C_4\ell$, and $B_3 - B_4 = -C_3 i\ell$, where the constants C_1, C_2, C_3 and C_4 are real. The following expression is obtained for the deflection of the plate:

$$w = C_1 \text{ber } x + C_2 \text{bei } x + C_3 \text{kei } x + C_4 \text{ker } x \tag{22}$$

All functions contained in Eq. 22 are real for real values of the argument. The series expressions which are represented by the Kelvin function, for small values of the argument are:

$$\text{ber } x = 1 - \frac{x^4}{4(16)} + \frac{x^8}{4(16)\ (36)\ (64)} \cdots,$$

$$\text{bei } x = \frac{x^2}{4} - \frac{x^6}{(4)\ (16)\ (36)},$$

$$\text{ker } x = (\ln 2 - j - \ln x) + \frac{\pi x^2}{16} - \frac{x^4}{64}\left(\ln 2 - j - \ln x + \frac{3}{2}\right) \cdots, \text{ and}$$

$$\text{kei } x = \frac{-\pi}{4} + (\ln 2 - j - \ln x + 1)\frac{x^2}{4} + \frac{x^4}{256},$$

in which j is 0.57722, Euler's constant; and ln 2 - j = 0.11593. The values of the Kelvin functions and their first derivatives are available in tabulated form for the pertinent values of the argument (19).

The general solution can be used for the analysis of any problem of symmetrical bending of a circular plate resting on a dense liquid foundation. The four constants must be determined for each particular case. For the case of loading under consideration (a concentrated load, P, applied at a point, x = 0, of an infinitely extended plate), the deflection of the plate at some distance, x, must be equal to zero. The functions ber x and bei x increase indefinitely with increasing values of x; therefore, the constants C_1 and C_2 must assume a value of zero to satisfy the boundary condition. The value of ker x becomes infinitely large at the origin, x = 0.

By setting $C_1 = C_2 = C_4 = 0$, the deflection equation (Eq. 22) reduces to

$$w = C_3 \text{ kei } x \tag{23}$$

The constant, C_3, is evaluated by considering the shearing forces. The shearing force, per unit length, is written as:

$$Q_r = -\frac{D}{\ell^3} \frac{d}{dx} \frac{d^2w}{dx^2} + \frac{1}{x} \frac{dw}{dx} \tag{24}$$

By substituting the first terms of the series expression for kei x in Eq. 23 and taking the derivative, the following expression is obtained:

$$Q_r = -\frac{C_3 D}{3} \frac{d}{dx} \left(- \ln x + \frac{\pi x^2}{16} \ldots \right) \tag{25a}$$

$$Q_r = \frac{-C_3 D}{\ell^3} \left(\frac{1}{x} + \frac{\pi x}{8} \ldots \right) \tag{25b}$$

As the value of x decreases, the value of Q_r approaches $\frac{C_3 D}{\ell^3} \frac{1}{x}$.

$$Q_r = \frac{C_3 D}{r \ell^2} \tag{26}$$

The shearing force may also be obtained by distributing the load, P, uniformly over a circumference of radius, r:

$$Q_r = -\frac{P}{2\pi r} \tag{27}$$

Setting Eq. 23 equal to Eq. 27 yields:

$$C_3 = -\frac{P \ell^2}{2\pi D} \tag{28}$$

and

$$w = -\frac{P \ell^2}{2\pi D} \text{ kei } x \tag{29}$$

The value of D can be substituted into Eq. 29 to obtain:

$$w = -\frac{P}{2\pi k \ell^2} \text{ kei } x \tag{30}$$

To obtain the deflection at the center of a uniform circular load, consider an element of the loaded area:

$$dA = r\,d\theta\,dr \tag{31}$$

and the increment of load on the element of area:

$$dP = pdA = \frac{P}{\pi a^2} r\,dr\,d\theta \tag{32}$$

The increment of deflection which is caused at the origin (r = 0) by the load on the element of area is a function of the distance of the load from the origin (r) and is dependent on the direction of the load from the origin (θ). Therefore, by use of the influence function for the concentrated load, Eq. 29, the increment of deflection at the origin caused by the load, dP, at a distance, r, is:

$$dw_O = -\frac{P}{\pi a^2} r\,dr\,d\theta \left(\frac{\ell^2}{2\pi D} \text{ kei } x\right) \tag{33}$$

Because Eq. 33 represents the increment of deflection caused at the center of the loaded area by the load on each element of the area, the total deflection at the origin will be the summation of the increments of deflection:

$$w_O = -\frac{P\ell^2}{\pi a^2 (2\pi D)} \sum_{r=0}^{r=a} \sum_{\theta=0}^{\theta=2\pi} r\,dr \text{ kei } x \tag{34}$$

In the limit Eq. 34 becomes the integral expression for deflection under the center of a distributed load; thus

$$w_O = -\frac{P\ell^2}{\pi a^2 (2\pi D)} \int_0^a \int_0^{2\pi} r\,dr\,d\theta \text{ kei } x \tag{35}$$

By integrating between the limits, $\theta = 0$ and $\theta = 2\pi$, and substituting $x = r/\ell$, Eq. 35 becomes:

$$w_O = -\frac{P\ell^2}{\pi D a^2} \int_0^a r \text{ kei } \left(\frac{r}{\ell}\right) dr \tag{36}$$

A solution to Eq. 36 is written as

$$w_o = \frac{P\ell^2}{\pi D a^2}\left[r\ell \ker'\left(\frac{r}{\ell}\right)\right]_0^a \tag{37}$$

For a value of r = 0, the expression in the brackets of Eq. 37 takes a value of $-\ell^2$; therefore, by substitution of the limits, r = 0 and r = a, Eq. 37 may be written:

$$w_o = \frac{P\ell^2}{\pi a^2 D}\left[\ell^2 + a\ell \ker'\left(\frac{a}{\ell}\right)\right] \tag{38a}$$

or

$$w_o = \frac{P^2}{\pi D}\left[\left(\frac{\ell}{a}\right)^2 + \frac{\ell}{a}\ker'\left(\frac{a}{\ell}\right)\right] \tag{38b}$$

and by substituting the dimensionless parameter, $c = a/\ell$ (the radius of relative load distribution):

$$w_o = \frac{P\ell^2}{\pi D}\left[\frac{1}{c^2} + \frac{1}{c}\ker' c\right] \tag{39a}$$

or

$$w_o = \frac{P\ell^2}{\pi D c^2}\left[1 + c \ker' c\right] \tag{39b}$$

The increment of moment which is produced at the origin by the load on an element of area is a function of the distance from the origin, r, and the direction, θ. However, for the special case of symmetrical loading, represented by the circular area of load distribution, the moment which is produced at the origin may be obtained by integration over the surface of loading by considering the equation of deflection for a concentrated load and the equations of bending for a symmetrically loaded plate:

$$m_r = -D\left(\frac{d^2w}{dr^2} + \frac{\mu}{r}\frac{dw}{dr}\right) \tag{40}$$

and

$$m_t = -D\left(\frac{1}{r}\frac{dw}{dr} + \mu\frac{d^2w}{dr^2}\right) \tag{41}$$

The radial and tangential bending moments are equal at the origin for a symmetrical loading condition, therefore,

$$m_{r=0} = \frac{m_r + m_t}{2} = -D\left(\frac{1+\mu}{2}\right)\left(\frac{d^2w}{dr^2} + \frac{1}{r}\frac{dw}{dr}\right) \tag{42}$$

By considering Eq. 30 for deflection of a concentrated load, and the derivatives:

$$\frac{dw}{dr} = -\frac{P\ell^2}{2\pi D}\,\mathrm{kei}'\frac{r}{\ell} \tag{43a}$$

and

$$\frac{d^2w}{dr^2} = -\frac{P\ell^2}{2\pi D} \text{kei}'' \frac{r}{\ell} \tag{43b}$$

and by adding:

$$\frac{d^2w}{dr^2} + \frac{1}{r}\frac{dw}{dr} = -\frac{P\ell^2}{2\pi D}\left(\text{kei}'' \frac{r}{\ell} + \frac{1}{r}\text{kei}' \frac{r}{\ell}\right)$$

and by substituting the identity relationship:

$$\text{kei}'' \frac{r}{\ell} + \frac{1}{r}\text{kei}' \frac{r}{\ell} = \frac{1}{\ell^2}\text{ker} \frac{r}{\ell}$$

we may obtain

$$\frac{d^2w}{dr^2} + \frac{1}{r}\frac{dw}{dr} = -\frac{P}{2\pi D}\text{ker} \frac{r}{\ell} \tag{44}$$

Thus, the increment of total bending moment produced at the origin by the load on an element of the loaded area is given by:

$$dm = \frac{(1+\mu)}{2}\frac{P}{\pi a^2}\frac{1}{2\pi} r\, dr\, d\theta\, \text{ker}\left(\frac{r}{\ell}\right) \tag{45}$$

and, at the limit, the total bending moment produced at the origin by loading over the circular area is:

$$m = \frac{(1+\mu)P}{2\pi a^2}\int_0^a r\,\text{ker}\left(\frac{r}{\ell}\right) dr \tag{46}$$

and integration of Eq. 46 between the limits of r = 0 and r = a yields:

$$m_{max} = \frac{P(1+\mu)}{2\pi a^2}\left[a\ell\,\text{kei}'\left(\frac{a}{\ell}\right)\right] \tag{47a}$$

or

$$m_{max} = \frac{P(1+\mu)}{2\pi}\left[\frac{1}{c}\text{kei}'\, c\right] \tag{47b}$$

Eq. 47b for the maximum moment and Eq. 39b for the deflection under the center of the loads are the equations used in the computer program to compute STRESS and DEF, respectively.

Layered Pavement Design Method for Massachusetts

EGONS TONS, RICHARD E. CHAMBERS, and MICHAEL A. KAMIN
Respectively, Assistant Professor of Civil Engineering, Senior Research Engineer, Principal Civil Engineer, Massachusetts Department of Public Works

A method for the design of flexible pavements has been developed for Massachusetts. The method is simple, rational and practical, and can be applied immediately on a routine basis in the design office, yet is flexible enough to permit modification as indicated by future research. Data and analyses that evolved from the AASHO Road Test experiments were used as a guide in the development of the design method.

Straightforward conventional procedures have been selected to provide a value for soil support. Preliminary soils data are obtained from geological and soil maps, and borings and samples for test are taken as needed. Laboratory Bearing Ratio and other tests are performed. Test results and boring data are then used as a basis for a Design Bearing Ratio. Traffic factors are computed from anticipated traffic conditions and existing traffic and Loadometer data. The 18-K Daily Equivalent Axle Load is used directly as defined in AASHO procedures.

The Regional Factor as recommended by the AASHO guide was not adopted in its present form. This approach was deemed too specifically related to materials, soils and environment of the test site. To account for possible moisture, frost, traffic, time (aging) and other effects, a blanket increase of 15 percent in Structural Number was introduced. This increase probably approximates a reasonable Regional Factor. More study is needed in this area.

There are an infinite variety of layered pavement systems that will satisfy the strength requirements as dictated by a given soil and traffic. AASHO coefficients of relative strength of various materials for surface, base and subbase were adopted where possible. A new coefficient was derived for the penetrated base. The general design chart correlating DBR values with traffic and structural number permits the use of any type and thickness of surface, base, and subbase, provided the strength coefficient for each material is known. The pavement thicknesses obtained by using the derived design chart are reasonable when compared to past experiences in Massachusetts and other states.

•FIELD EXPERIENCE has formed the basis for proportioning of flexible pavements in Massachusetts as well as in many other states. In an attempt to place pavement design in Massachusetts on a more quantitative basis, a committee was formed of members of the Massachusetts Department of Public Works and of the Department of Civil Engineering of the Massachusetts Institute of Technology; their mission was to review and evaluate available approaches and recommend a practical design method that could

Paper sponsored by Committee on Flexible Pavement Design and presented at the 44th Annual Meeting.

be used immediately in the design office. It was, of course, recognized that any approach adopted would have to be augmented with subsequent research, the direction of which would also be recommended by the committee. This paper covers the first phase of the study, i.e., the background and development of the design method.

There are a variety of sources that can be used as a basis for the design of flexible pavements. There are empirical methods that become so modified with time that the reasons for their existence are vague and often not documented. At the other extreme are theoretical approaches that are oversimplified in assumptions but complicated in application, demanding development of data and techniques not now available. Therefore, it was decided that a new approach, that offered by the AASHO guide, would be a desirable path to follow. Although the AASHO concept is controversial and certainly not conclusive in many respects, it does offer an extensive, well-documented, and well-controlled fund of data as its background. There is also the hope that more information will be developed to strengthen further the AASHO approach.

In essence, the AASHO approach considers: (a) soil supporting capacity, (b) traffic factors, (c) regional variables, and (d) structural capabilities of pavement materials. These factors form the basis for proportioning a pavement section that will serve the riding public for a predictable period of time. Certainly the critical parameters are recognized and the criterion for performance is realistic. A design method based on the AASHO approach should, therefore, be reasonable.

DEFINITIONS OF TERMS

Axle Load.—Load transmitted by a single axle having two single- or dual-tired wheels.

Base Course.—Layer of specified material of designed thickness placed on a subbase or subgrade to support a surface course.

Bearing Ratio (BR).—Stress required to produce a certain penetration, using a standard piston, in a given soil relative to a standard reference stress.

Black Base.—A plant-mixed graded bituminous mixture used under the surface layer.

Design Bearing Ratio (DBR).—That bearing ratio selected as being typical for design purposes of the section under consideration.

18-Kip Equivalence Factor.—Number of applications of an 18,000-lb single-axle load that will have the same effect on the serviceability of a pavement as a single application of a given load.

Equivalent Daily 18-Kip Load.—Average number of equivalent 18-kip load applications that will be applied to the pavement structure in one day.

Freezing Index (FI).—An index of the severity of a winter which takes into account the temperature drop below freezing and the number of days in which this occurs.

Frost Heave.—Increase in elevation of the pavement surface due to ice lens formation in the underlying soils or materials.

Frost Susceptible Material.—A soil in which significant detrimental ice segregation can occur if conditions of moisture and temperature are favorable.

Future Average Daily Traffic (Future ADT).—Estimated average daily traffic at the time that the Terminal Serviceability Index is reached.

Initial Serviceability Index (ISI).—Serviceability index of a newly constructed road before the commencement of traffic.

Layered (Flexible) Pavement.—A pavement structure which maintains intimate contact with and distributes loads to the subgrade and depends on aggregate interlock, particle friction, and cohesion for stability.

Longitudinal Profile.—Contour of the surface grade in the direction of traffic.

Pavement Structure.—Combination of subbase, base course, and surface course placed on a subgrade to support the traffic load and distribute it to the subgrade.

Penetrated Base.—An open-graded crushed rock layer penetrated in the field with asphalt, used under the surface layer.

Present Average Daily Traffic (Present ADT).—Average daily traffic expected to occur immediately after the highway is opened to traffic.

Present Serviceability Index (PSI).—Serviceability index at time of observation.

Regional Factor.—A factor used to adjust the structural number for climatic and environmental conditions.

Serviceability.—Ability of a pavement to serve traffic that it was meant to serve.

Serviceability Index (SI).—A number that estimates ability of a pavement to serve traffic that it was meant to serve. A measure of the roughness, rutting and degree of cracking and patching found in a pavement.

Soil Support Value (S).—An index of the relative ability of a subgrade material to support traffic loads imposed on it by the pavement structure.

Strength Coefficient.—A number indicating relative effectiveness of pavement materials as they contribute to the performance of the pavement structure.

Structural Number.—Product of thickness and strength coefficient of a given layer of the pavement structure. Sum of the structural numbers for all layers is the structural number of the pavement and is an index of the performance of the section.

Subbase.—Layer or layers of specified or selected material of design thickness placed on a subgrade to support a base course.

Subgrade Line.—Level above which the pavement structure and shoulders are constructed.

Subgrade Material.—Material below subgrade line in cuts and embankments and in embankment foundations, extending to such depth as affects the support of the pavement structure.

Subgrade Weakening.—Loss in supporting capacity of subgrade soils due to increase in water content.

Surface (Wearing) Course.—Top layer(s) of the pavement structure that resists the direct stress applied by traffic loads. It provides a smooth riding surface, resists skidding, abrasion and climatic effects, and protects the underlying layers from moisture.

Terminal Serviceability Index (TSI).—Serviceability index at which the pavement is deemed unable to serve the traffic that it was meant to serve; the point at which major resurfacing of the pavement is necessary.

Traffic Analysis (Design) Period.—Number of years that the highway will be in service before the Terminal Serviceability Index is reached.

Transverse Profile.—Contour of surface grade across the roadway.

Truck Weight (Loadometer) Study.—A field survey made for the purpose of obtaining information on trends in weight dimensions, axle spacings, types, loads, etc., of freight vehicles actually using the road.

FACTORS IN PAVEMENT DESIGN

The purpose of a pavement is to provide a smooth riding support for various loaded vehicles. This is achieved by designing and constructing a layered densified composite consisting of various sizes of rock particles, often bound together by some organic or inorganic cementing agent. The function of each layer is as follows (Fig. 1):

1. Surface Layer.—This must resist the high vertical stresses applied under the tire. As it acts as a plate under dynamic conditions, it develops substantial bending and shear stresses as well. The surface must also act as a protective layer to shield the layers beneath from water, provide a smooth wearing surface to afford a satisfactory ride to the user, and reduce stresses on the layers below it.

2. Base Layer.—This must resist high stresses. Although the surface layer acts to reduce them to some degree, the stresses within the base are still high. This is particularly true for bases which underlie thin surface layers. The base must also serve to reduce stresses on the weaker layers below it, and provide a smooth support on which the surface can be laid.

3. Subbase.—This must provide drainage for water that may penetrate the surface layers and also must allow drainage for the water that percolates from below. The drainage function is particularly critical because of the frost conditions found in Massachusetts. The subbase must also resist stress applied from above, and reduce stresses on the underlying soil layer.

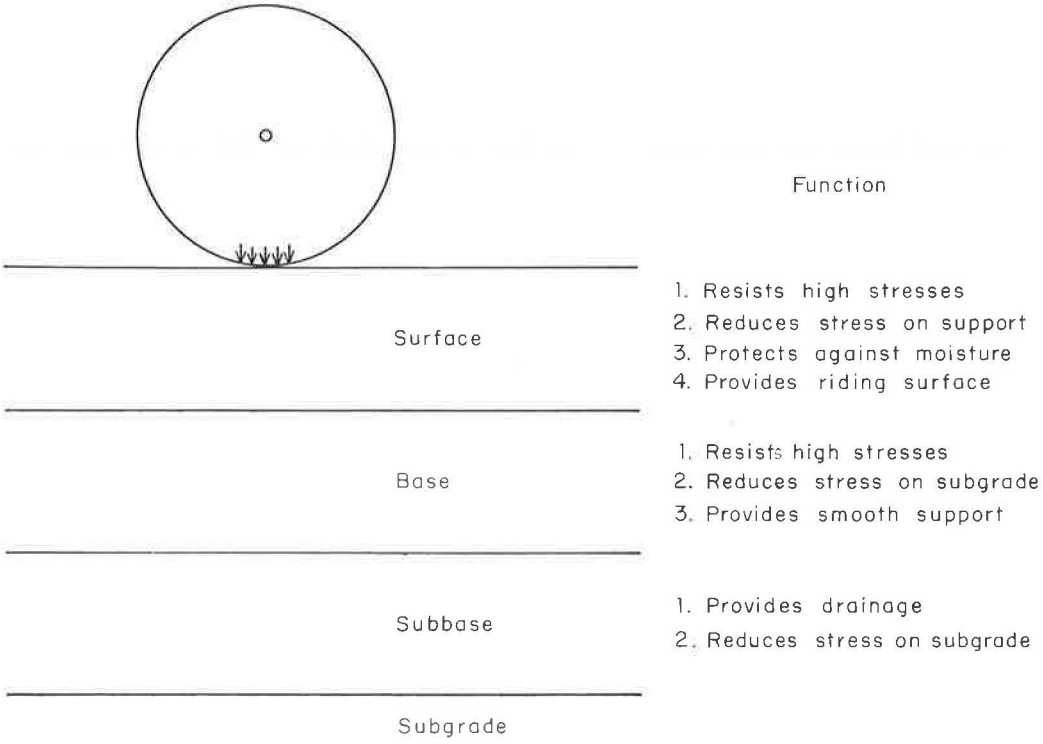

Figure 1. Primary functions of pavement layers.

Static vs Moving Load

The load applied to the layered pavement composite can be static, such as at stop lights, or moving, as encountered in rural and many urban highways. In the methods of design developed in the past, the static load was considered the most critical; therefore, static test values were often used in design. Most of the mileage of the interstate highways and expressways is subjected exclusively to moving loads during its service. Furthermore, the data developed at the AASHO Road Test are based on performance under moving loads(1).

There are materials, such as crushed rock or gravel, which may not have properties influenced by time of load duration. On the other hand, materials like bituminous concrete and some soils can be greatly affected by the speed of load application and by temperature. Therefore, it is necessary for the purposes of design to decide what kind of loading the designed pavement will predominantly serve.

The speed of traffic used in the AASHO Road Test was about 30 mph. On primary highways and most secondary roads, 30 mph and above are frequently encountered, although it is possible that trucks on grades may slow down to below the 30-mph speed.

In this design approach, using the AASHO Road Test findings as background, it was assumed that a moving load would be applied to a given point on the wheelpath for very short durations, usually lasting much less than one second. Figure 2 shows the relationship between speed of given vehicle and the approximate time of load duration at a point the wheel is traversing.

Present Serviceability Index

One of the major contributions towards quantitative measurement of ridability of the pavement is the Present Serviceability Index (PSI) developed during the AASHO Road Test experiments (2). The index can vary between 0 and 5 (4 to 5 = very good; 3 to 4 =

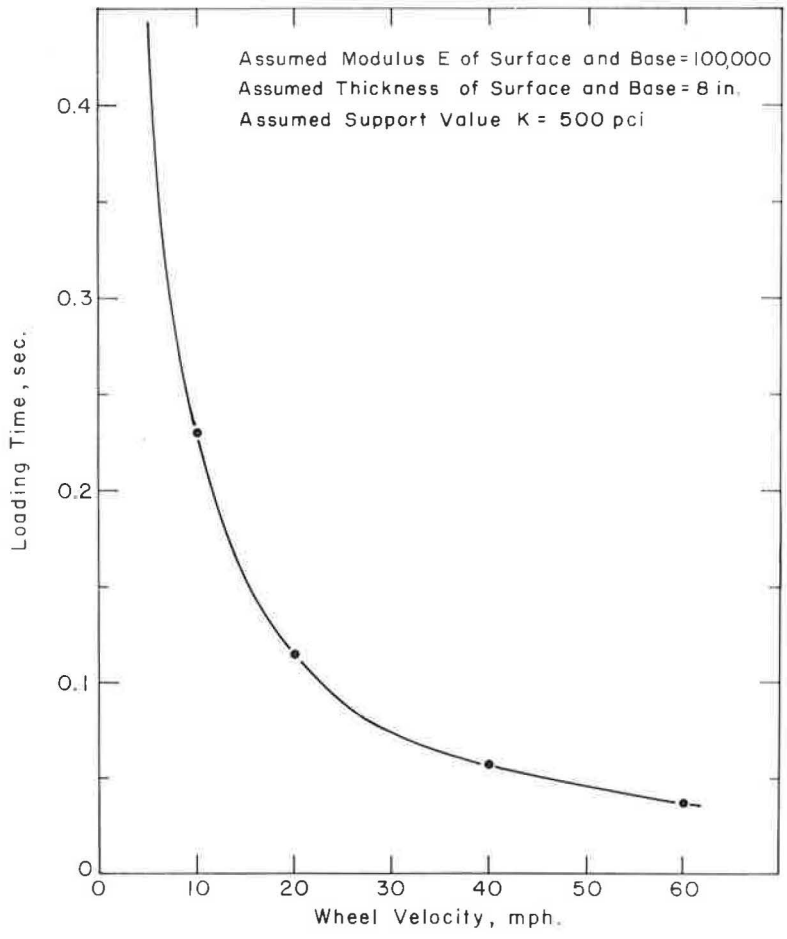

Figure 2. Example of pavement loading time as affected by vehicle speed.

good; 2 to 3 = fair; 1 to 2 = poor; 0 to 1 = very poor). This numbering system was obtained by first sending out various representatives of highway users on designated road sections and asking them to give their evaluation of the condition of the road as to the ability to carry traffic at that time. They were asked to indicate their decision by assigning a number for each section.

The human survey was followed by a mechanical survey, measuring washboarding, rutting, cracking, patching, etc., to determine the relative influence of each of these deficiencies in assigning a PSI for a given section by an "average" user of the road. The most important factors that were found to affect the ridability of the road are: (a) longitudinal profile of the road (washboarding, bumps, etc.), (b) transverse profile of the road (rutting), (c) amount of cracking, and (d) amount of patching. From the AASHO Road Test, the following equation relating these variables was derived (2):

$$PSI = 5.03 - 1.91 \log (1 + SV) - 1.38 RD^2 - 0.01 \sqrt{C + P} \qquad (1)$$

where

SV = mean of the slope variance in the two wheelpaths (longitudinal variation),
C + P = measure of cracking and patching in pavement surface, and
RD = measure of rutting in wheelpaths.

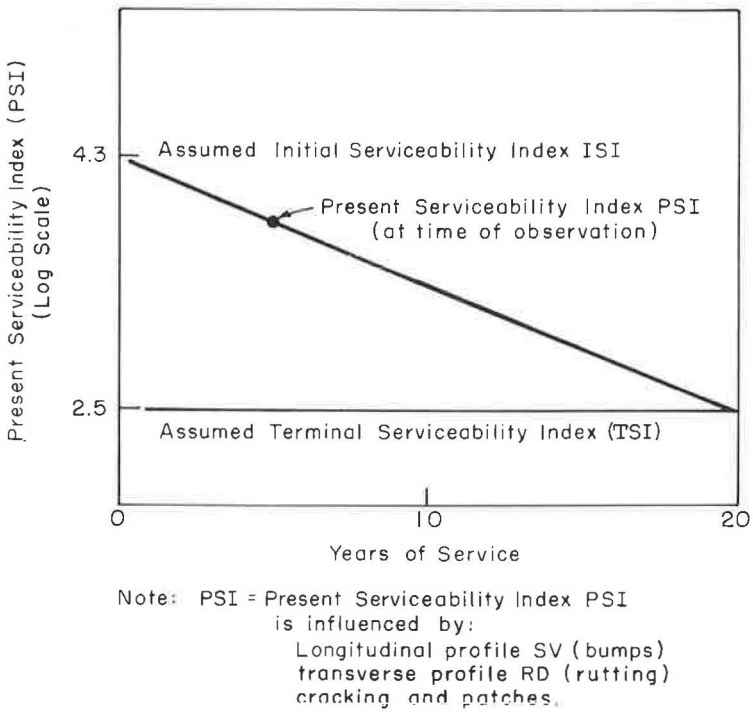

Figure 3. Serviceability index decline with time.

All these variables can be measured on a road and the PSI values can be calculated at any time desired. For primary roads with a high volume of high-speed traffic, a PSI value of 2.5 is often assumed to be the low point, a time when some kind of resurfacing work should be considered. If the initial PSI value is known and the terminal value is assumed to be 2.5, a trend curve with age for PSI can be obtained for a given traffic, as illustrated in Figure 3. That is, the PSI concept can be used as a criterion for the design of a pavement to carry given traffic for, e.g., 20 yr before the PSI value drops to 2.5. At this time, major resurfacing work is needed to restore the riding comfort. This approach is the basis of the design method presented here.

Major Factors Affecting PSI

The amount of roughness, cracking, and patching of a road with time in service will be dictated by many factors. The most important are the following: (a) subgrade, (b) materials in the pavement layers and their arrangement, (c) quality of construction, and (d) traffic. All these factors may not have equal weight under given conditions, but they are all important in general considerations of pavement design. If any of them are neglected, a pavement may have only a fraction of the useful life intended. The PSI defines primarily the smoothness of a road surface, which can be affected by any of the factors mentioned.

SURVEY OF SUBGRADE SOILS

One of the major parameters considered in the AASHO guide approach to pavement design is the supporting capacity offered by the subgrade soil. Because the final cross-section and grades of the highway will depend on the supporting capacity of the soils encountered, a detailed survey of the soils existing along the proposed route must be undertaken early in the design phase. A study of available information on soils and soils types existing in Massachusetts was undertaken as a background for preliminary

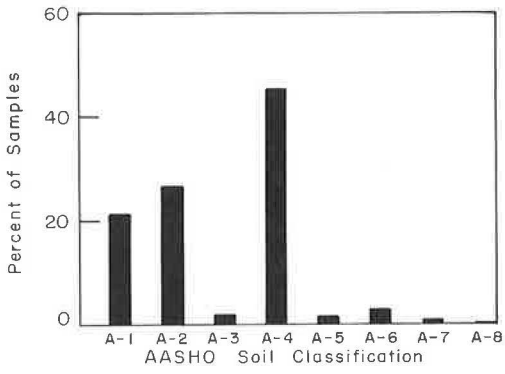

Figure 4. Frequency of soil types from records on existing roads (Mass. Department of Public Works, Materials Division).

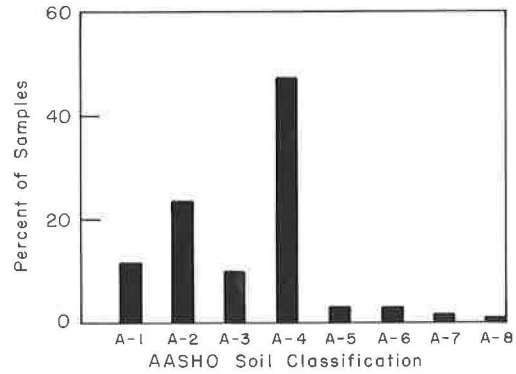

Figure 5. Frequency of soil types from records of Soil Conservation Service (Amherst, Mass.).

surveys along proposed routes. An analysis was made of data available on embankment material on existing roads, and of data developed by the U.S. Soil Conservation Service. Figures 4 and 5 show the distribution of soils types as determined from representative data from these sources. The majority of soils fall into AASHO Classifications A-1 through A-4, with the A-4 materials being predominant.

Maps of value for soils evaluation are currently being prepared by the U.S. Soil Conservation Service and the U. S. Geological Survey; however, it will be several years before either of these sources has information covering all areas of Massachusetts. Data from these agencies should aid in initial route planning, as well as in selection of locations for soil sampling along proposed routes. Topological maps, prepared as a matter of course during the route-planning phase of highway design, should also prove helpful.

Route Survey

A field survey must also be undertaken to determine the locations at which samples for test should be removed. A specialist in the area of soils and geology should accompany the highway designer in an on-site inspection of the proposed route. Observation of characteristics of the terrain such as surface water, rock, outcroppings, variations in soil types, and condition of existing cuts and fills in the area, if present, will provide some index as to the variations to be expected in embankment materials and identify possible problem areas that may need special treatment.

Criteria for Location of Soil Test Samples

The subgrade on which the pavement structure will be placed will seldom, if ever, coincide with the surface of the existing terrain (Fig. 6). To determine the type and strength of the soil on which the pavement will be constructed, soil sampling and testing is necessary. Samples may be obtained either by digging or by boring if the depth required is great. It is important that borings be made in both cuts and fills. The location and spacing of the borings should be determined from the preliminary soil surveys.

In cuts, the pavement is placed on top of soils existing along the predetermined subgrade line. There may be instances where these soils vary greatly in their ability to support the loaded pavement. Especially capricious are so-called transition areas from a cut to a fill. To predict the support abilities of the soils, soil samples for laboratory evaluation are needed from the subgrade level. Borings in cuts should be taken to at least 3 ft below the prescribed subgrade line. Soil profiles should also be plotted from the boring data. Knowledge of the soil properties in cuts is very important

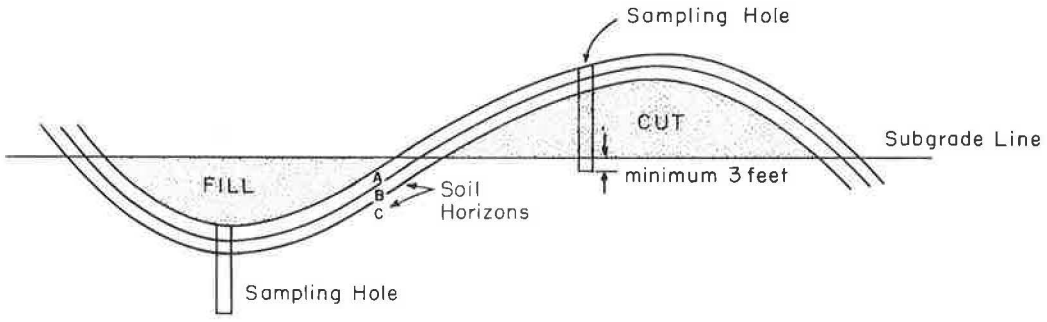

Figure 6. Terrain necessitating soil sampling in cuts and fills.

in this design procedure because the pavement thickness is based primarily on the soil conditions in the cut.

The purpose of taking borings and obtaining soil information under fill areas is different from that of cuts. The excess material from cuts is usually used in fill and the subgrade material will be more or less blended soils from the cut. Therefore, the concern here is the ability of the existing soils to support the fill material rather than the pavement and the traffic load. The depth of borings under fills will depend on circumstances but in most cases should be about equal to the height of the fill material.

SOIL TESTING AND IDENTIFICATION

Strength Test

In most pavement design methods, a "strength" value of the embankment soil forms one basis for proportioning of the pavement structure. In essence, the AASHO approach permits any measure of soil supporting capacity to be used, provided the strength of the AASHO Road Test subgrade is known under the test. (This is a tentative situation; subsequent testing must be performed to determine the extent of correlation that exists with any test method that may be selected.) Thus, virtually complete freedom was allowed in the selection of test for soil supporting capacity.

Strength Test Values Shown in AASHO Guide.—The AASHO Road Test sections were built on one type of soil, A-6, and, therefore, only one point on a soil support scale is available (3). In Figure 7, taken from the AASHO guide, a support value of 3 has been assigned for the A-6 soil. The highest support value on the scale was obtained by analysis of performance of various sections with a thick crushed rock base. Thus, Point 10 represents soils having characteristics of the crushed rock base materials. The support values have been compared with several known test procedures. These comparisons are approximate and were not adopted for the basis of Massachusetts design for the following reasons:

1. Kentucky CBR.—The Kentucky CBR scales given in the AASHO guide (Fig. 7) are basically not Kentucky curves because that state does not use dynamic compaction in preparing specimens. Furthermore, the guide calls for the Modified Proctor compaction (AASHO Method T-180-57) which Massachusetts is not using at the present time.
2. Stabilometer (R) Curves.—The stabilometer scales given in the AASHO guide were studied. The compaction again is not that of the Standard Proctor; also, the R values of Washington State differ from those of California, indicating that the test has not been generally standardized.

Other Laboratory Strength Tests.—Besides the California Bearing Ratio and the stabilometer tests, there are a variety of laboratory procedures, with triaxial tests being quite prominent. Several states use a triaxial test value in their pavement design. The Texas Highway Department was contacted to find out whether any correlation

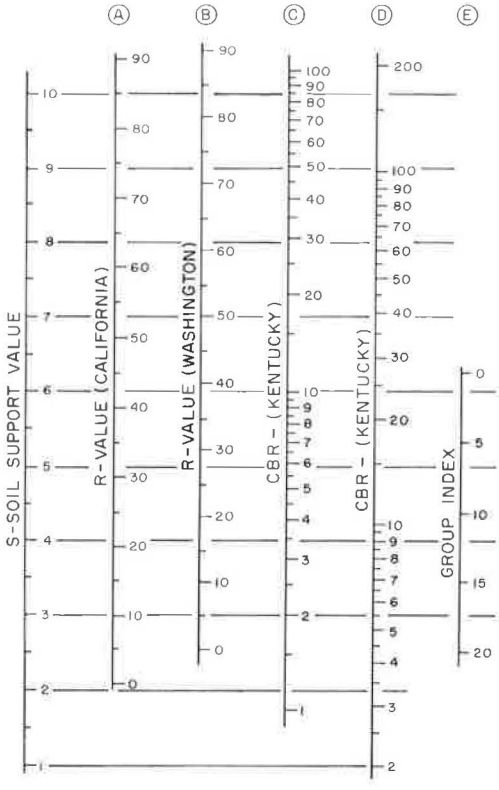

Figure 7. AASHO correlation chart for estimating soil support value (S).

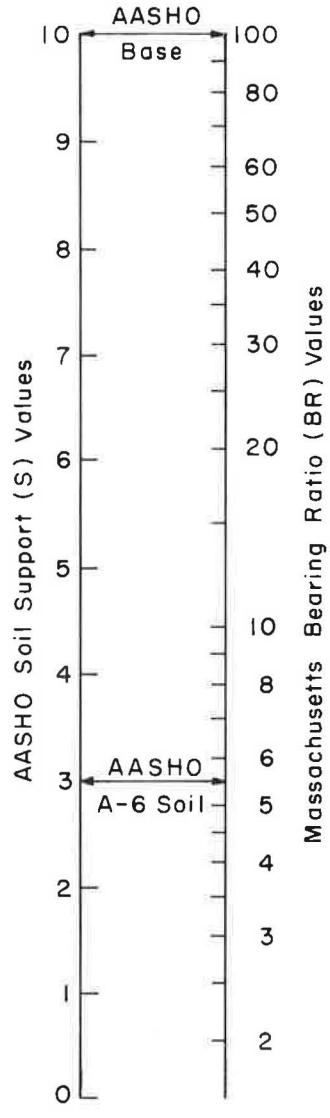

Figure 8. Assumed correlation between Massachusetts bearing ratio (BR) and AASHO soil support value (S).

has been established between the triaxial and the soil support values (S) in the AASHO guide. Apparently such correlation does not exist.

Bearing Ratio for Massachusetts.—It was decided that the Massachusetts test for soil supporting capacity should fit the following requirements:

1. The test should be relatable to the S values of AASHO guide.
2. The test should be well established, so that as much background data as possible could be obtained as needed.
3. Samples should be prepared using Standard Proctor compaction.

It was judged that a bearing ratio test would satisfy these requirements. Therefore, a literature search was undertaken to establish a bearing ratio scale for Massachusetts, tied in with the hypothetical soil support values in the AASHO guide. The most helpful publication in this respect was a paper by Shook and Fang (4), which summarizes all cooperative tests done by various agencies on the AASHO test road materials.

The Massachusetts scale was established by averaging appropriate CBR values for the AASHO test road soil compacted by the Standard Proctor (5.5-lb hammer, 12-in. drop). This bearing ratio value was approximately 5.5 and was assumed to be equal to the soil support value, S = 3. Also, the appropriate bearing ratio values for the crushed rock base material, compacted according to the Standard Proctor method, were averaged. This value was about 100 and it was assumed to be equal to 10 on the soil support scale. Then a logarithmic relationship was assumed between the two established points which resulted in a bearing ratio scale for Massachusetts as shown in Figure 8. Further research and improvement of this scale may be necessary. At the same time, the scale is reasonable if compared to the other attempts made along the same lines. The test basically calls for AASHO T-99-57 compaction, and a 4-day soaking before test. Detailed procedure is given in ASTM D1883-61T.

Classification Tests

Standard soil classification tests should be performed on the subgrade materials. These include: (a) sieve analysis (AASHO Designation T-88-57), (b) hydrometer analysis (AASHO Designation T-88-57), (c) liquid limit (AASHO Designation T-89-60), and (d) plastic limit (AASHO Designation T-90-56). Although these tests are not directly involved in structural design calculations, they should be performed for purposes of identification and determination of the degree of frost susceptibility of the soil.

Desirable Additional Tests

In addition to tests needed for design purposes, three other tests are suggested: (a) volume change, (b) permeability, and (c) unconfined compression. The first two tests are fundamental in describing engineering behavior of soils. A serious thought should be given to incorporating these two tests in design considerations. To achieve this, accumulation of measurements and research is needed. The unconfined compression test can be used only with clays. This simple test, in comparison to the bearing ratio values, should add to the understanding of the strength behavior of cohesive soils in subgrades.

SUBGRADE SUPPORT FOR DESIGN

Selection of Design Bearing Ratio

One of the problems facing the design engineer is the selection of a Design Bearing Ratio value (DBR) for a given section of a roadway. The soils vary widely from place to place, as is illustrated in Figure 9. If the design is based on different bearing ratio values, the cross-section of the pavement may have to be changed every 500 to 1,000 ft. If the lowest bearing ratio value is used, overdesign in most sections will result. The economics of the project and minimum pavement thickness requirements should be the guiding factors for a decision to change a cross-section.

A practical criterion for the selection of the DBR results if normal construction practice is considered. Usually in cut areas practice is to utilize the soils in situ as the subgrade for the pavement. Fill areas, however, are built up from either cut or borrow soils. It is reasonable to expect that the fill, if made up from the cut material, will be at least as strong as the weakest material in the cut. In cases where fill is built up from borrow, the borrow material can be specified as having a given strength. It is clear that the governing factor in the choice of a DBR is the strength of the soil in the cuts; the properties of the soils in fill areas will usually exceed those in the cut area either by nature or by control.

The choice of the DBR within the cut will depend on the variations of strength of the soils. Figure 10 shows three examples of cases that may arise:

1. If the bearing ratio values in the cut do not vary greatly, the DBR should be close to the minimum bearing ratio found. If fill is to be borrow, the borrow must be specified to have a bearing ratio equal to the DBR.

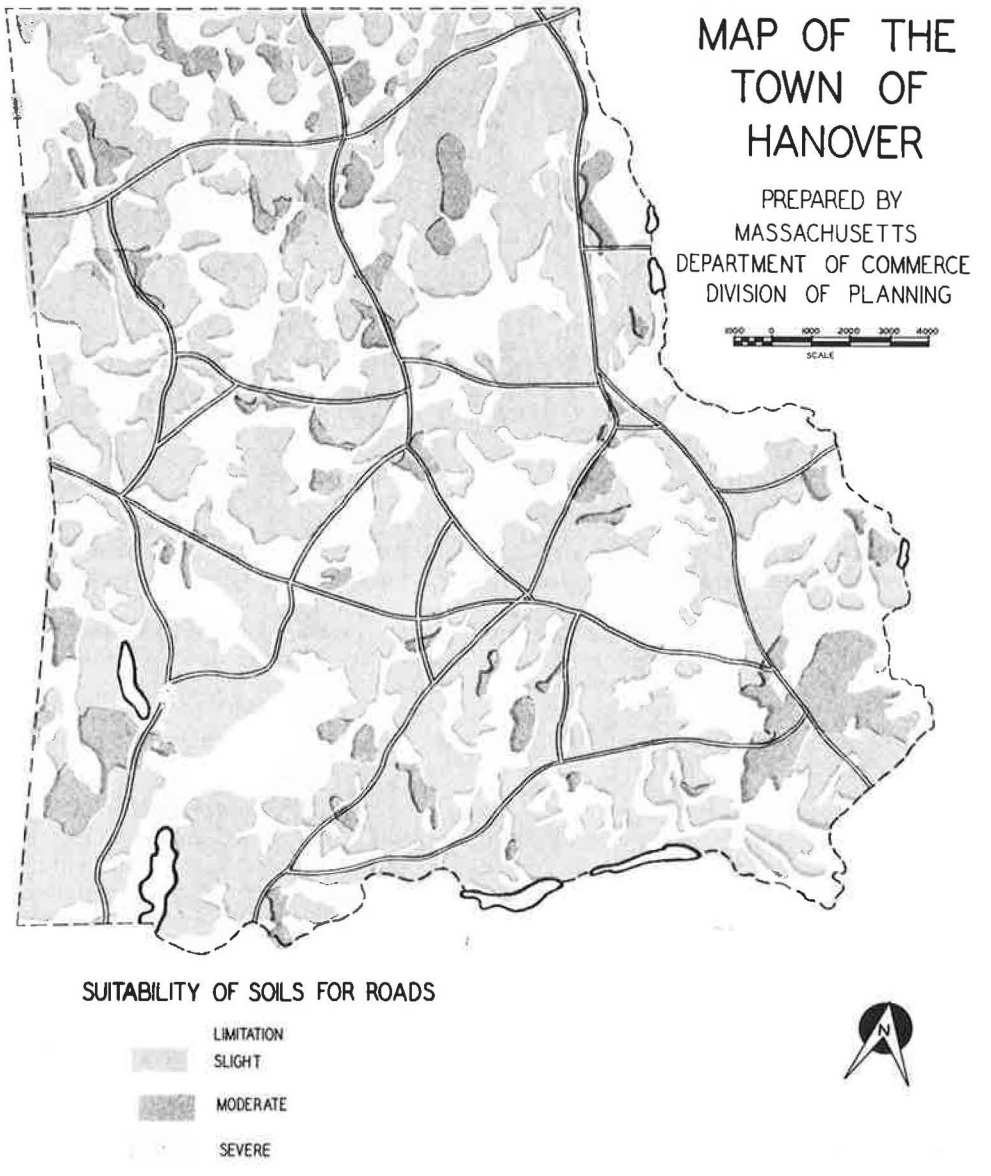

Figure 9. Interpretive map developed by U. S. Soil Conservation Service, showing frequent soil variation in road construction.

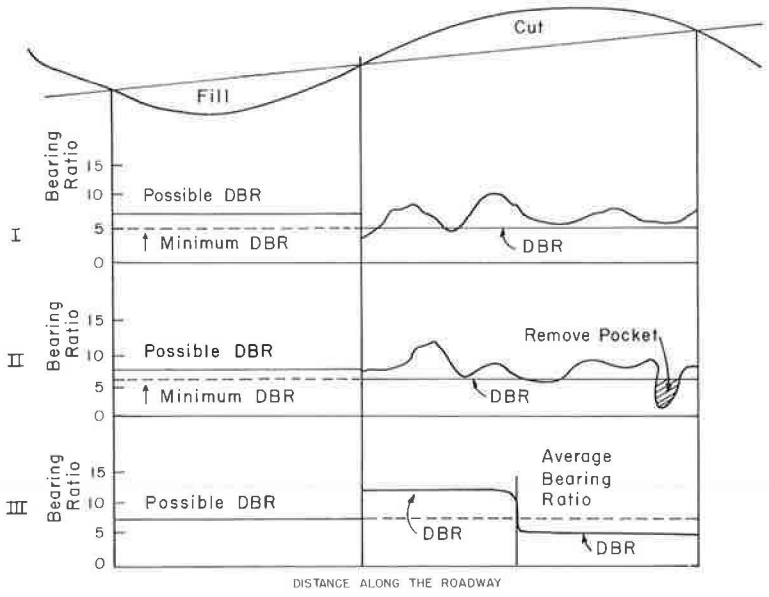

Figure 10. Three examples in selection of Design Bearing Ratio (DBR).

2. If there is a "soft spot" for only a short distance (Fig. 10), it may be more economical to treat this area (dig out or cover up) rather than use the lowest bearing ratio value for a design.

3. If there are changes in soils and two (or more) types of soils exist for relatively long distance (e.g., half a mile or more), a possibility of using two (or more) thicknesses of pavement should be considered.

Soil Support as Affected by Frost and Moisture

Depth of frost penetration is determined by several parameters: (a) freezing index, an index of the severity of a wind, which takes into account the temperature drop below freezing and the number of days in which this occurs; (b) thermal conductivity, which depends on the soil or layer type, density and moisture content; and (c) the volumetric latent heat of fusion, which depends on moisture content and dry density of the soil or layer. Several formulas are available to determine the frost penetration using these parameters.

The U. S. Army Corps of Engineers (5), using the modified Berggren formula derived by Aldrich (6), has developed simple graphical solutions for frost depth determinations under pavements. From these, Figure 11 was plotted for frost depths expected to occur in Massachusetts under average conditions in average soils. The wide variation of penetration is to be expected because of the spread in freezing index from, for example, Cape Cod to the Berkshires. There are, of course, yearly variations in penetration due to climactic changes. The criterion used in the development of Figure 11 was the average freezing index of the three coldest years occurring in a 30-yr interval. It is certain that frost permeates the pavement and well into the supporting soils everywhere in Massachusetts. Frost and its effects on the pavement structure and performance is, therefore, an important consideration in this design study.

Concepts in Frost Design.—Under certain conditions frost heaving can occur, causing severe and dangerous changes in elevation of the pavement surface. Heaving is possible if a certain combination of factors are present: (a) freezing temperatures within the soil, (b) a source of water, and (c) a frost-susceptible material. The depressed temperature starts to freeze the water in the soil. If the soil has a high cap-

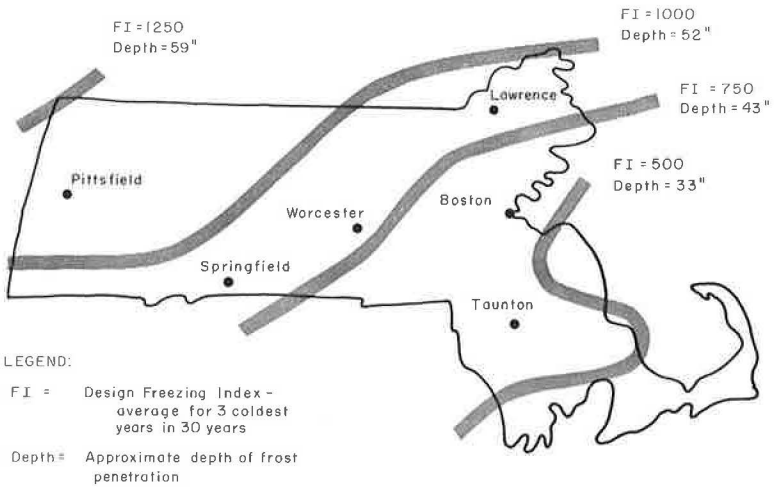

Figure 11. Variation in design freezing index and depth of frost penetration in Massachusetts.

illary tendency, it will act to siphon water from the source. As the new water freezes, lenses are formed which can cause severe changes in elevation at the surface.

The types of soils that possess capillarity always contain fines, but to be frost susceptible they also must be permeable. Thus, for example, sands with relatively large particle size are not considered frost susceptible; such soils as gravels having a high percentage of fines, silts, and varved clays are considered frost susceptible. Criteria for frost susceptibility, which are said to be 85 percent sure, have been developed by the U. S. Army Corps of Engineers (5). These are based on the percentage of fines passing 0.02-mm mesh for given soil types. On this basis, frost susceptibility has been divided into four categories ranging from low susceptibility (F-1) through high susceptibility (F-4). Table 1 gives the criteria for determining the degree of susceptibility for different materials.

TABLE 1

SOIL CLASSIFICATION FOR FROST DESIGN[a]

Frost Group	Soil Type	Finer than 0.02 mm (% by wt)
F-1	Gravelly	3-10
F-2	Gravelly	10-20
	Sands	3-15
F-3	Gravelly	>20
	Sands except very fine silty sands	>15
	Clays with plasticity indexes >12	
F-4	All silts	
	Very fine silty sands	>15
	Clays with plasticity indexes <12	
	Varved clays and other fine-grained banded sediments	

[a]U. S. Army Corps of Engineers (5).

The effects of frost heaving vary with local conditions. If the soils and water conditions are uniform over a reasonable distance, the heave will be uniform, and probably unnoticeable, to the motorist. The problem of heaving may be serious if conditions are variable in localized areas. In this case, differential heaving is possible, and uncomfortable or dangerous bumps may result. It is principally the horizontal variability of soils or water conditions that cause serious effects from frost heaves.

Horizontal variations are taken into account in some agencies. The Corps of

Engineers, for example, uses these as the basic consideration that determines the approach to frost effects in airfields, where maintenance of uniform grade is critical. If variations are high, removal of most or all of the susceptible material is recommended. Such a step is not deemed economically feasible for highway pavements except in unusual circumstances. Michigan, too, considers horizontal variations to be serious. In their study of the problem (7), they found that 98 percent of all heaves occurred in cuts where the soil pattern is variable. In fills, few heaves were observed because, by nature, sharp variations are minimized. Blending of the top 12 in. of the subgrade may be a helpful step in minimizing horizontal variations, and hence frost heave.

Once the soil and select materials of a pavement are frozen, beneficial effects occur. Freezing essentially stabilizes the particulate materials and increases their resistance to deflection. At the AASHO test road a marked decrease in loss of serviceability was observed in the winter months, indicating improved performance.

When frost leaves, significant weakening of the soil and select pavement materials can result. If there are frozen lenses within the soil, thawing essentially leaves a pocket of liquid. This liquid then saturates the surrounding soil. Because the material below remains frozen, the path of escape for the water is upwards. According to the AASHO test results, this weakens the subbase as well as the subgrade soil. Thus, while the gravel acts as a draining layer, it is also weakened in strength.

The Corps of Engineers recommends designing highways for the reduced subgrade strength encountered during spring breakup. They recommend increasing the design traffic number in their design method as an adjustment to, in effect, arrive at a stronger pavement section than would normally be used. The size of the increase depends on the degree of frost susceptibility of the soil under consideration. The Corps of Engineers' approach cannot be applied directly to the AASHO data because the criteria used for measuring performance by the two methods differ.

Massachusetts' Experience with Frost Problems.—A survey was taken of all the district offices of the Massachusetts Department of Public Works regarding their experience with frost problems on major roadways. There were a few isolated cases where serious heaving was reported, for example, in places where springs were found close to the surface. But problems were considered the exception rather than the rule. The Design Committee on its several survey trips made special note of the frequency of heaves. None were apparent, although one area had been marked as such on Route 128.

On the basis of experience, frost heaves do not appear to be a major problem in Massachusetts, although certainly conditions are favorable for them to develop. There are apparently several reasons for this. Massachusetts has been particularly careful to provide good surface and subsurface drainage in their pavements. For example, practice has been to keep the road surface at least 5 ft above free water to allow for drainage. Also, a gravel subbase layer extending to 20 in. below the pavement surface has been provided on major highways. These precautions have, in most cases, probably reduced the amount of free water available to create frost heaving.

The effects of subgrade weakening during spring breakup have not been documented. But these effects, although damaging, are more subtle and would probably not be noticed unless specific study were given to the problem.

AASHO Approach—Regional Factor.—At the AASHO test road, the rate of decay of serviceability was found to vary significantly with season. Indeed, a major conclusion of the research effort was that 80 percent of the sections failed during spring breakup. To account for these variations in performance, deflection data were analyzed. Deflections found in plate bearing tests on many of the test sections were found to vary with season. They were low in the winter, high in spring, and intermediate in summer. By statistical manipulation a weighting function was derived that related serviceability loss and deflection variations (Fig. 12).

The approach recommended by the AASHO guide regarding seasonal variations is to use a regional factor. Although no quantitative means of determining the regional factor is given, consideration is recommended of such factors as finished grade elevation above water, drainage, depth of frost penetration and number of freeze-thaw cycles. Furthermore, other considerations are lumped in with this factor, such as steepness of grade and areas of concentrated stopping or turning. The regional factor, which can

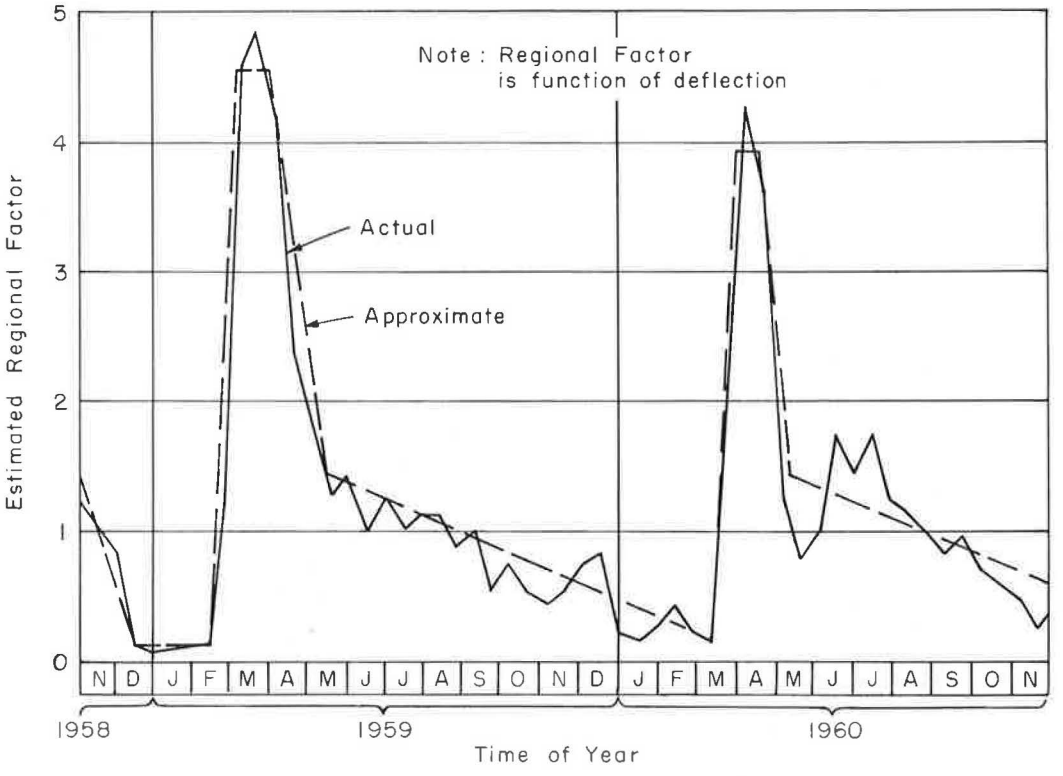

Figure 12. Monthly variations in estimated regional factor for the AASHO test road.

vary from 0.5 to 5.0, can then be applied to adjust the structural proportions of the pavement to account for these effects.

The regional factor should also account for the relative weakening that can occur in soils and materials, depending on their frost susceptibility. Further study of this area should be undertaken to account for seasonal variations in properties of soils and materials.

Recommendations.—Soils and materials should be checked for frost susceptibility according to the Corps of Engineers criteria (Table 1). The F-4 soils, as designated by the Corps of Engineers are highly susceptible and, therefore, offer the possibility of creating significant differential heaves and weakening. Special attention should be given to surface drainage and water table when these materials are encountered. If good drainage is impossible to achieve or if ground or surface water conditions exist near F-4 soils, they should be removed and replaced with less susceptible materials, preferably of the same type as is adjacent to the problem area. The depth of removal should be at least 80 percent of the depth of frost penetration in the area (Fig. 11). Economics and practicality of the specific situation should govern the exact quantity of material to be removed.

Variations in soils cause differential frost heaves and weakening effects. In fills, where the material is randomly deposited and intermixed in the grading operation, the chances of local variations in soils are small. In cuts, soils will be of a more variable nature; therefore, consideration should be given to blending at least the top 12 in. of subgrade in cut areas. To reduce the potential hazards of frost heave and weakening, the present practice of holding surface grade at least 5 ft above free or groundwater should be continued.

Non-frost-susceptible materials should be used in the select materials of all pavement. In all cases, a minimum depth below pavement surface of 20 in. of non-frost-

susceptible material should be provided. Presently, insufficient data are available to determine quantitatively the regional factor. If the regional factor is ignored, the resulting design may not be adequate. Thus, a factor should be introduced to account for: (a) frost weakening effects, (b) Massachusetts construction practice differing from the super-controlled procedures used at the AASHO Road Test, (c) unknown differences in materials properties from those used at the AASHO Road Test, (d) effects of mixed traffic, (e) effects of traffic application over longer periods of time than was possible at the AASHO Road Test, and (f) other unknown factors. It is recommended that a blanket increase of 15 percent be applied to the structural requirements of the pavement. In fact, this is equivalent to a regional factor of 3.

PAVEMENT AS A STRUCTURE

Structural Approach

The design method evolved here is, in essence, a structural design. It differs significantly in its approach from those normally used by the civil engineer in designing bridges, buildings or other structures. Designers of the latter structures usually can estimate the loadings, the stresses within the structure, and the behavior of the materials that they will use. The immensity of the variables that accompany a flexible pavement design have precluded a full rational design treatment, and so the AASHO Road Test and resulting design guide depend heavily on empirical results. Although the state of the art in design theory and materials understanding cannot yet replace empirical methods, it can supplement the AASHO approach and contribute to an understanding of the behavior of the layered pavement as a structural system.

Applicable Theories

There are several theoretical solutions for the stresses and deflections existing in a pavement section when subjected to wheel loads. One simplified solution is that developed by Boussinesq (8) using the theory of elasticity. As it is applied to pavement sections, it must be assumed that the materials in the section have the same elastic properties, i.e., modulus of elasticity and Poisson's ratio. It also must be assumed that the material is elastic. Whereas neither of the assumptions are true for particulate layered systems, the Boussinesq solution provides a first approximation of pavement stresses.

A solution that is more refined than the Boussinesq solution has been offered by Burmister (9). The Burmister solution theoretically is more applicable to the pavement system because it can account for the differing properties in each layer. The solution still assumes that the materials are elastic and, therefore, it suffers some of the weaknesses of the Boussinesq solution.

A third solution extended from the Westergaard (10) theory by our Materials Research Laboratory (11) makes significantly different assumptions than were made by either Boussinesq or Burmister. This theory assumes that an elastic plate rests on a dense liquid foundation. It maintains that the surface layer, the plate, behaves elastically and that the foundation is made up of a bed of independent springs. Thus far, this theory has been developed to consider stresses in the asphalt-bound layer only and the vertical stress applied to the layer below.

Stresses in Pavement Layers

Vertical Stress.—These three theories involve different stiffness parameters and, therefore, it is difficult to compare rigorously values obtained with them. By using some approximations, the plots of variations in vertical stress with depth were obtained (Fig. 13). The Boussinesq theory yields results that are reasonably valid for the static case only, whereas the Burmister and Westergaard theories can be applied to the dynamic or moving load case because they can account for differing properties of the pavement layers.

The plots in Figure 13 clearly illustrate the important structural functions of the surface layer. First, it must support a high stress at the surface; most soils cannot

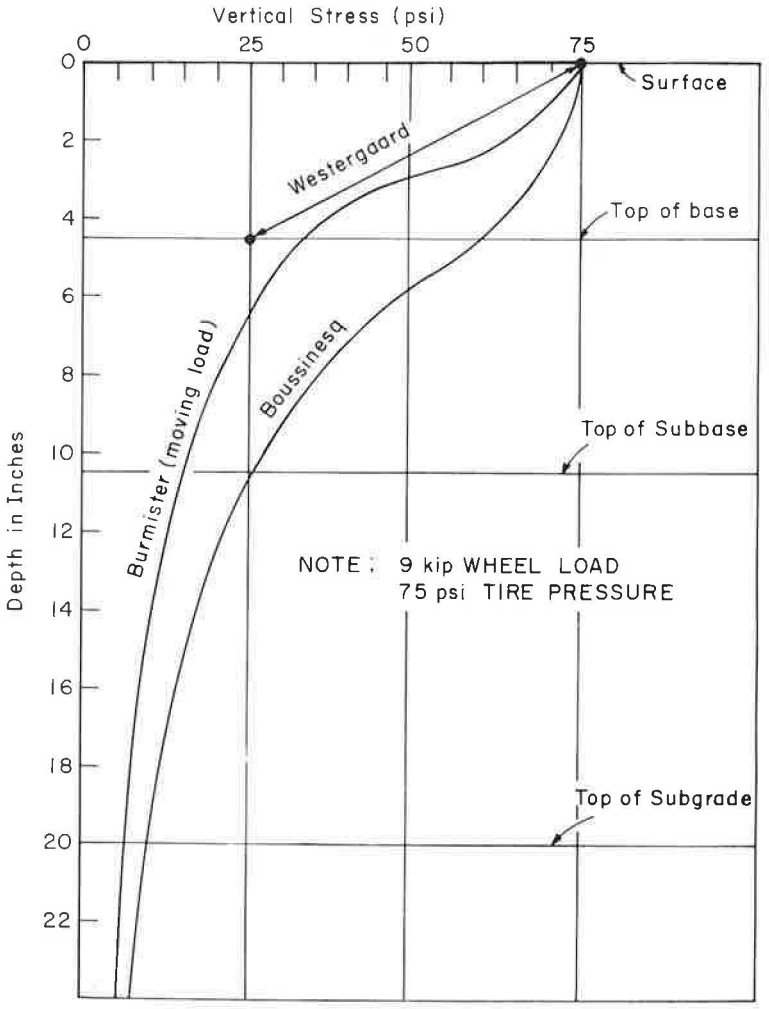

Figure 13. Variations in vertical stress with depth according to various theories.

support such stresses without failure or excessive deformation. Second, for the dynamic moving load case, the surface layer absorbs a significant amount of vertical stress, thereby reducing the stress on the layers below. For the dynamic case, the stress on the top of this particular base layer is around 40 percent of that exerted by the tire at the surface. A reduction of only 20 percent is expected for the static case. If the surface layer is thinner than the $4\frac{1}{2}$ in. shown, the stress reduction will be less, whereas thicker layers will produce the converse result. Thus, the surface layer serves a dual structural function. It carries the high concentrated surface stress and, if thick enough, is capable of reducing the vertical stress applied to the layers below.

The structural role of the base is also illustrated in Figure 13. Despite the stress reduction provided by the surface layer, the top of the base layer is exposed to a substantial stress. For the illustration shown, this stress is about 30 psi. The depth of the base layer is caused for further stress reduction so that the stresses are reduced by about one-half for the 6-in. depth. As with the surface layer, the base resists high stress at its surface and reduces stress on the layers below.

The structural role of the subbase follows that of the base. It still must resist a reasonably high stress of 15 psi which reduces by about one-half over the depth of the

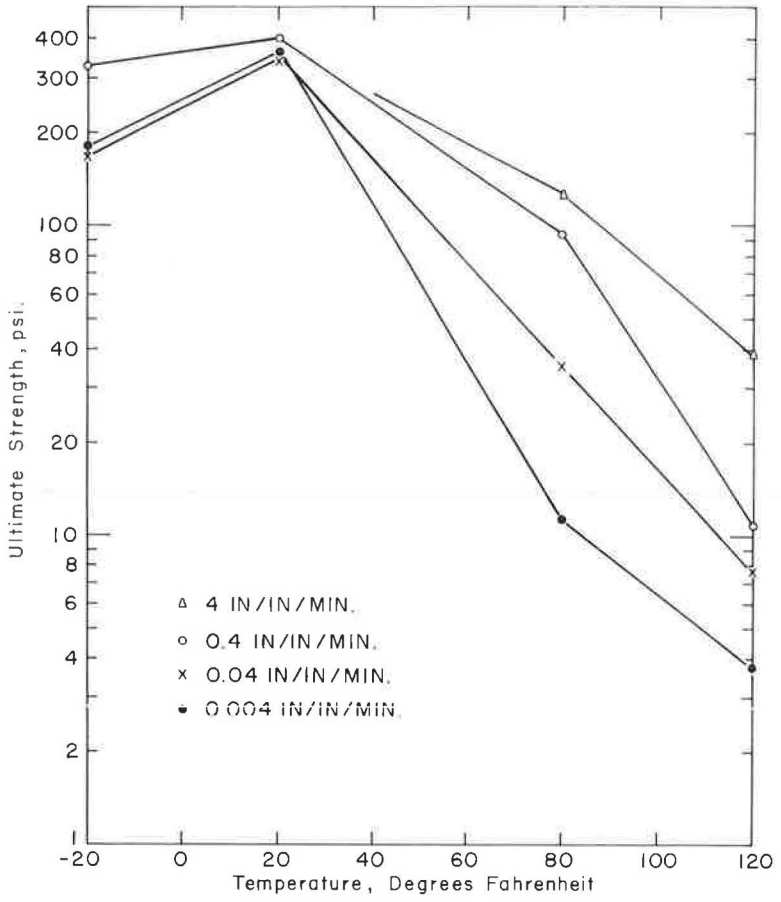

Figure 14. Tensile strength of Massachusetts Class I bituminous concrete top course at various temperatures and rates of loading.

layer. This layer, which is usually gravel in Massachusetts, is in a zone of reasonably high stress; it is important to maintain its quality at a high level because it must act as a drainage layer to select its gradation so that it is not weakened by water.

The subgrade, of course, is the ultimate support for the structure. The stresses on it are a direct function of the action of the layers above. The stresses that are applied to the subgrade surface eventually die out at great depths. The important consideration here is that the materials above distribute the stress so that this layer is subjected to tolerable stress levels.

Each layer in the pavement structure has a dual role to fulfill. First, the layer must be strong enough to sustain the load from above without failure or excessive permanent deformation. Second, it must be stiff and/or deep enough to keep the stress on the layer below at a tolerable level. Although these functions are qualitatively clear from the preceding analysis, the exact parameters that govern these functions have not yet been fully developed.

Stresses in Surface Layer.—The theoretical analysis just discussed dealt with the variations of vertical stress with depth and materials of the pavement section. Theory has been developed to explore further the stresses in the critical surface layer, particularly as it acts as a plate. This plate action occurs when the moving load condition is coupled with the materials properties under dynamic loads. The action is one of stiffening so that the applied load tends to spread over a large area of the underlying layers. In so doing, flexural stresses are brought into play. To provide an estimate

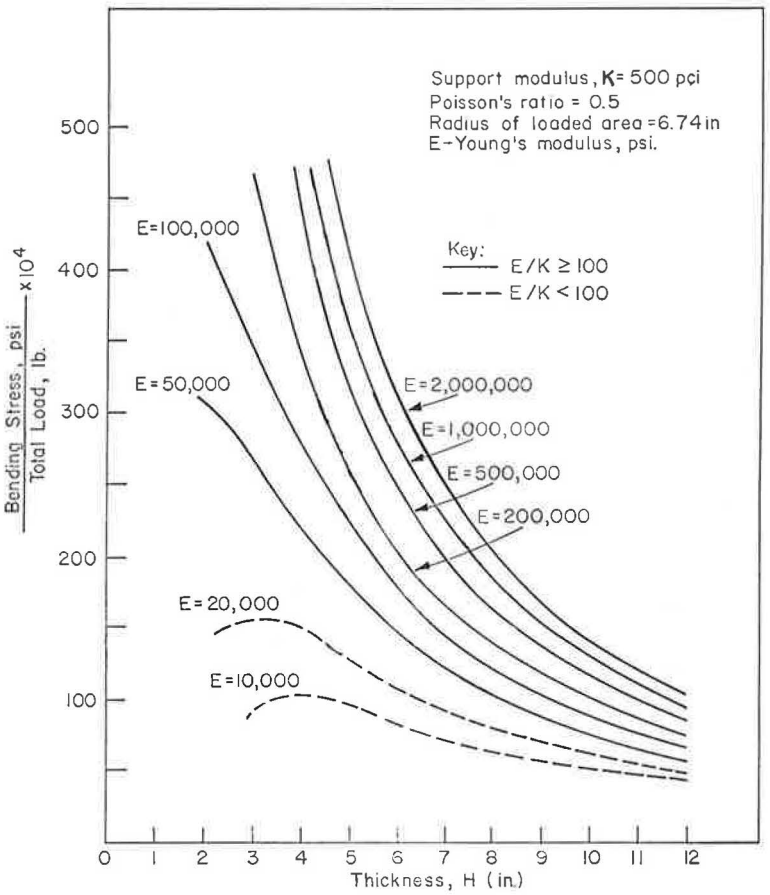

Figure 15. Bending stress vs thickness of asphalt-bound layer for 10-kip load, 70-psi tire pressure.

of the severity of stress in the surface layer, the dynamic properties of the bituminous surface are used in conjunction with layered pavement analysis.

Bituminous concrete, being a viscoelastic material, displays time- and temperature-dependent properties. Ideally, from viscoelastic theory, the effects of time and temperature are superimposable. That is, the modulus of a viscoelastic material may be altered from a given value by changing either temperature or the rate of loading. Thus, a material will offer more resistance to deformation if the rate of loading is increased or the temperature of the material is depressed. Clearly, no single value of modulus can be representative of bituminous concrete. A reasonable value for normal temperature and vehicle velocity can be taken as 100,000 psi for purposes of the ensuing discussion.

The tensile strength of bituminous concrete will also vary with temperature and rate of loading. Figure 14 is a plot of tensile strength of bituminous concrete with rate and temperature of test (12). At temperatures below the glass transition point of asphalt, the tensile strength is relatively unaffected by test rate and has a value of a few hundred psi. At temperatures above the glass transition point, test rate has significant influence on the tensile strength. Loading times at even slow vehicle speeds are much less than a second, representing several orders of magnitude faster loading than those shown in Figure 14. The limiting strength under such high loading rates would approach the strength observed at or below the glass transition point. A reasonable estimate of this value from the plot is 300 psi for Massachusetts-type bituminous surface course.

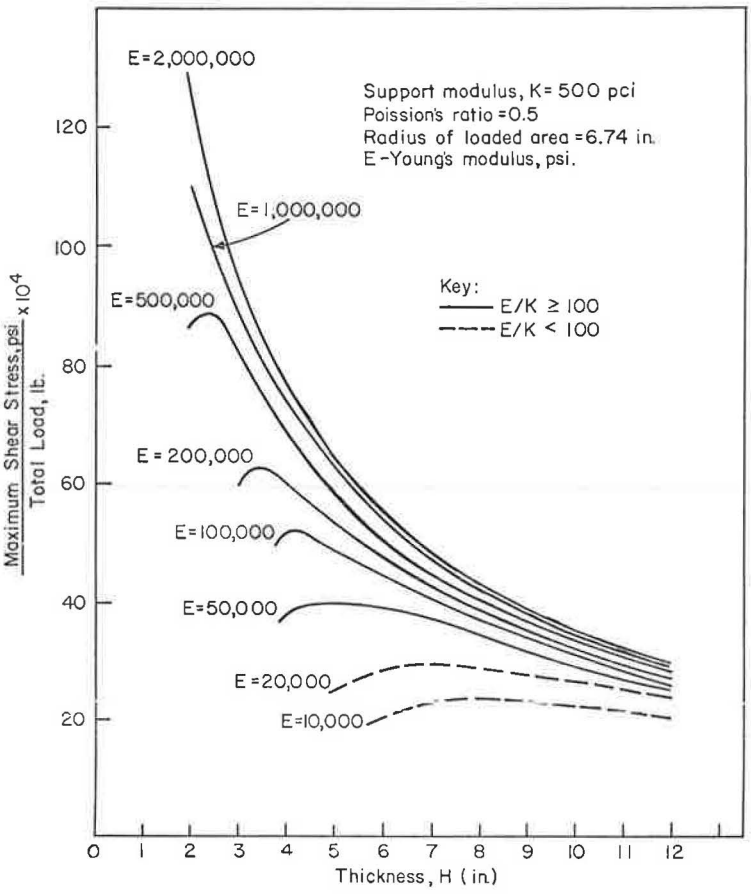

Figure 16. Maximum shear stress vs thickness of asphalt-bound layer for 10-kip load, 70-psi tire pressure.

Westergaard's Analysis Applied to Bituminous Concrete.—The Westergaard analysis was originally developed for use in concrete pavement design. It remains as the principal method by which airfield pavement is proportioned. Putnam (13) extended the Westergaard analysis to cover a broader range of problems than was considered in the original work. This enabled Hagstrom et al. (11) to study bituminous concrete using the Westergaard theory.

The accuracy of the Westergaard approach depends on certain conditions of relative stiffness. If the stiffness of the plate or top layer is substantially higher than that of the supporting foundation, the theory will be reasonably accurate. Such is the case if the dynamic properties of bituminous concrete are used in conjunction with reasonable values for the supporting media.

Figure 15 is a plot of the variation in bending stress with pavement thickness as derived by Hagstrom. Constant reasonable values are assumed for the support modulus (500 pci) and loading (a 10,000-lb single load simulating two 5,000-lb single wheels). The range of moduli shown represents the variation of the modulus of bituminous concrete that may occur under reasonable rates of loading and temperature conditions. The dashed curves represent areas where application of the theory is questionable because the stiffness of the surface layer is not sufficiently large when compared to the foundation stiffness. The curves in Figure 15 illustrate the strong influence that depth of section has in reducing bending stress within the top layer. For example, with the conditions discussed earlier, a modulus of 100,000 psi and tensile strength of 300 psi,

the depth required so that the section would just fail under the loading is $3\frac{1}{2}$ in. If fatigue effects are considered, the allowable working stress might be about one-half of the test value, or 150 psi. Thus, to sustain repeated loadings, a depth of 7 in. would be required. Of course, tensile failure of the flexural section implies cracking on the under surface that will eventually reflect through to the surface. Clearly, to reduce cracking, the bituminous layers should be as thick as economically possible.

The previous analysis probably relates directly to the studies of black bases at the AASHO Road Test. It was found that black bases offered significant improvement in pavement performance. The well-graded cohesive base layers served to add depth and, hence, flexural capacity to the surface layer. This would then reflect itself in retention of serviceability.

There are a number of assumptions necessary to develop the preceding discussion. But changing the modulus of the bituminous layer by a factor of two alters the stress by perhaps 10 percent. Varying the foundation modulus by a factor of two changes the bending stress by a maximum of 10 percent at reasonable depths. More recent work by Hagstrom shows that a more exact analysis for dual wheels yields results about 20 percent lower than assumed. On the other hand, wheel loads may in practice exceed those assumed here. Significant latitude in assumptions is possible without altering the general conclusion regarding the analysis.

Hagstrom also obtained values for shear stress existing in the bituminous layer. Figure 16 shows the variation in shear stress with pavement thickness for the same conditions assumed in the bending analysis. For the practical range of moduli and thickness of the bituminous layer, the shear stress is usually less than 100 psi. Although dynamic values of the shear strength of bituminous concrete are not available, it would be expected that the shear strength is of the same order as the tensile strength. Thus, shear strength does not appear to be a criterion governing the top layer of pavement.

COEFFICIENTS OF RELATIVE STRENGTH FOR SUBBASE, BASE AND SURFACE

The preceding theoretical discussion indicated that conventional theory and test values could be applied to the surface layer to provide a reasonable estimate of failure conditions. However, as subsequent layers are treated, the analysis becomes more complex and the important parameters remain unknown. At present, there are severe limits to theory as it applies to the complex action of these non-cohesive layers.

In the absence of theoretical treatment of the layered pavement system, empirical methods were used at the AASHO Road Test. A statistical factorial experiment was designed in which several thicknesses and combinations of materials were placed in a number of test sections. By monitoring the traffic and serviceability, the relative contribution of each material to performance could be obtained. This relative contribution to performance can be assigned to the pavement materials in the form of coefficients.

Coefficients of Various Layers

Table 2 gives the coefficients for various materials as provided by the AASHO guide. Of interest is the relative contribution that each material makes to the performance of a section. For example, 1-in. plant-mixed bituminous concrete (coefficient = 0.44) is equivalent to 3 in. of crushed stone (coefficient = 0.14) or 4 in. of gravel (coefficient = 0.11). This is the first time that quantitative relative values for the performance of materials have been made available to the designer. Although there is as yet no theoretical grasp or means of measuring the coefficients of materials that differ from the AASHO materials, a valuable incentive has been established.

Current Massachusetts practice is to use a penetrated crushed stone base. Because the AASHO guide did not give coefficients for this material, a value had to be estimated for design purposes. The coefficient for crushed stone in the base layer is 0.14, and the coefficient for a black base is 0.34. The strength of a penetrated base should be greater than crushed stone because it is bound by asphalt. Yet the penetrated base cannot be as effective as a well-graded black base because of its open gradation and incomplete penetration of the asphalt. It was decided on the basis of these considerations

TABLE 2

MATERIALS COEFFICIENTS

Pavement Component	Coefficient		
	a_1	a_2	a_3
(a) Surface Course			
Road-mix (low stability)	0.20	-	-
Plant-mix (high stability)	0.44[a]	-	-
Sand asphalt	0.40	-	-
(b) Base Course			
Sandy gravel	-	0.07	-
Crushed stone	-	0.14[a]	-
Cement-treated (no-soil-cement):			
≥650 psi[b]	-	0.23[a]	-
400-650 psi	-	0.20	-
≤400 psi	-	0.15	-
Bituminous-treated:			
Coarse-graded	-	0.34[a]	-
Penetrated stone	-	0.24[c]	-
Sand asphalt	-	0.30	-
Lime-treated	-	0.15-0.30	-
(c) Subbase			
Sandy gravel	-	-	0.11[a]
Sand or sandy clay	-	-	0.05-0.10

[a]Based on results of AASHO Road Test, all other coefficients estimated.
[b]Compressive strength at 7 days.
[c]Estimated by Massachusetts Design Committee.

that a simple average of the coefficients for crushed stone and black base would be a reasonable approximation. Thus, a value of 0.24 was selected as the coefficient for penetrated stone.

Structural Number Concept

The coefficients as derived can be employed directly in the design of the pavement. The anticipated traffic, environmental and soil conditions can be combined to yield a required structural number (SN). The SN can be derived from any arrangement of materials for which the coefficients are known. The thickness of each material multiplied by its coefficient yields the materials contribution to the total SN. Obviously, the types and thicknesses of materials can be manipulated, within limits, to produce a section to meet economic or other criteria.

EQUIVALENT DAILY 18-KIP AXLE LOADING

In addition to a knowledge of the characteristics of soils and paving materials, it is necessary for the adequate design of pavement elements to have certain traffic data and a criterion for the quality of service that is expected for a specified length of time.

Most of the traffic data required for geometric design will be used for the structural design of pavements. These include present average daily traffic (present ADT), future average daily traffic (future ADT), and the percentage of trucks (T). For structural design purposes, the traffic is assumed to be equally divided between the two directions. In addition to these traffic parameters, the daily overall truck traffic and lane distribution of trucks must be ascertained.

An analysis of the relationship between T for the entire day and ADT on Massachusetts highways shows that the overall daily truck traffic is three or more times greater than the peak-hour truck percentage. Because of this, a multiplying factor of 3 will be used to convert the T given for geometric design purposes to obtain the overall daily truck percentage.

Because there are no local data available relative to the distribution of truck traffic by lanes, the recommendations of two recognized organizations will be used. The Thickness Design Manual Series No. 1 (Ms-1), 7th edition, September 1963, by the Asphalt Institute and the Manual of Instructions for Pavement Evaluation Survey, August 1962, by AASHO suggest the following, in effect, identical distribution percentages for the most heavily traveled lanes:

1. If there are four traffic lanes (two in each direction), the percentage of trucks using the design lane is 90 percent of the total number of trucks in one direction.
2. If there are six or more lanes (three or more in each direction), the percentage of trucks using the design lane is 80 percent of the total number of trucks in one direction.

These lanes will hereafter be designated as the design lanes, i.e., the thickness of all other lanes will be the same as that of the design lane.

The AASHO method of determining the relative effects of different axle loadings on pavement performance is used in this design procedure. The AASHO concept relates the destructive effects of mixed axle loads to equivalent 18-kip single-axle loads. The distribution and magnitude of the various axle loads are indicated in Tables W-4A, W-4B and W-4C of the Massachusetts Truck Weight Study. (Truck Weight Study and Loadometer Study are used interchangeably; they refer to the same data.) The "All Stations, All Systems" tabulation of the Truck Weight Study is the source of these data.

The axle-load intervals used in the Truck Weight Study differ from those suggested in the AASHO guide. This required that new equivalence factors be established to fit the intervals of the Truck Weight Study. This was done by plotting the equivalence factors for small intervals (3, Appendix F), and then taking the average value of the interval of interest from the plot. The choice of Truck Weight Study axle-load intervals makes it possible to take advantage of the existing Massachusetts Traffic Planning Department computer program and eliminate the regrouping of axle load.

When the traffic data and truck weight study data are applied as shown in the Appendix to the AASHO guide, a value T_{18}, i.e., equivalent daily 18-kip applications, is obtained. The value of T_{18} is applied to the design chart in combination with soils data (DBR) to obtain a SN from which pavement layer thicknesses can be determined.

STRUCTURAL DESIGN CHARTS

There are two basic structural design charts included herein: one for a Terminal Serviceability Index (TSI) of 2.5 for high-volume high-speed roads (Fig. 17), and the other for a TSI of 2.0 for less traveled roads (Fig. 18). Any proposed combinations of pavement materials may be explored using these charts as a basis.

Variables

The charts were obtained using the AASHO guide, correlating the DBR scale with the AASHO S scale and increasing the SN value by 15 percent for the various traffic volumes.

The design numbers needed before the SN can be obtained are: (a) DBR of the soil, (b) equivalent 18-kip daily loadings, and (c) materials and their strength coefficients used in the pavement layers.

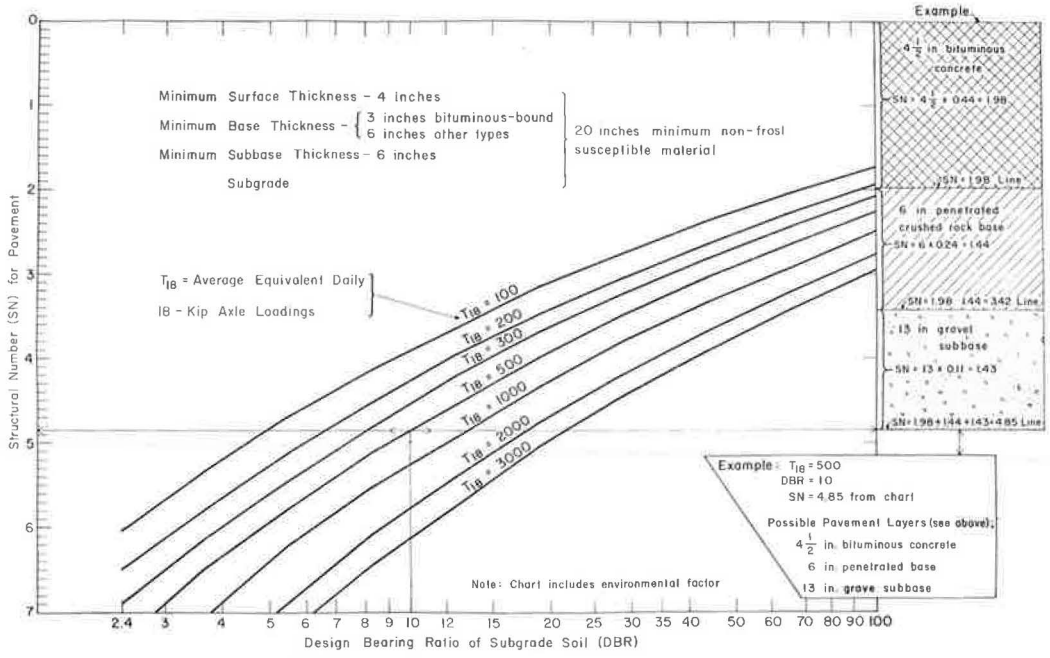

Figure 17. Structural design chart for pavements with TSI = 2.5 and 20-yr traffic analysis (for interstate, federal-aid-primary, and major state highways).

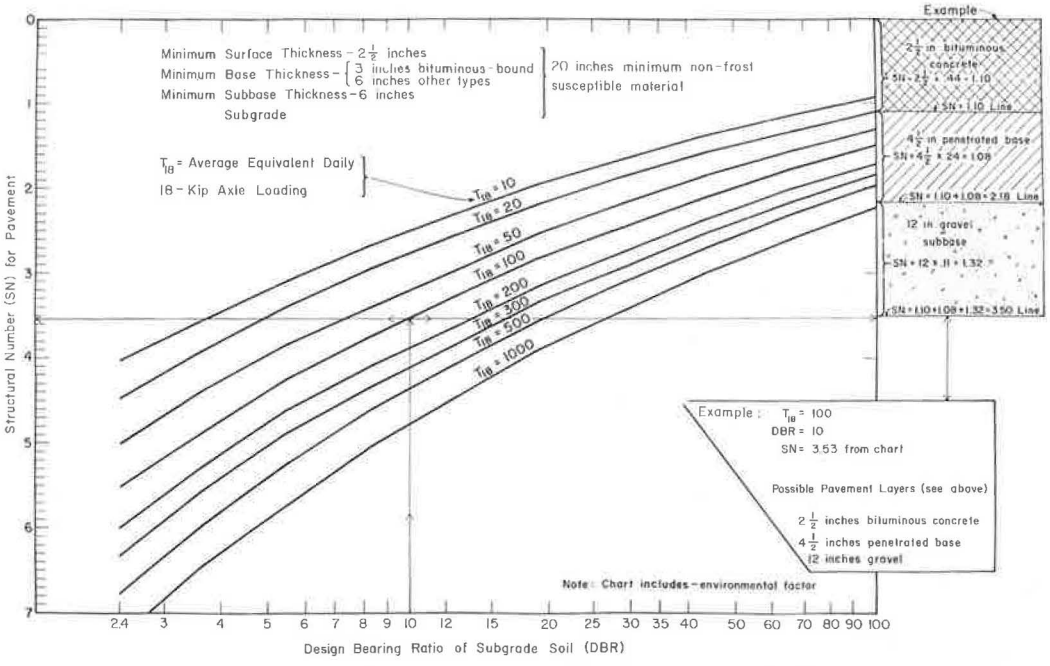

Figure 18. Structural design chart for pavements with TSI = 2.0 and 20-yr traffic analysis (for roads other than interstate, federal-aid-primary, and major state highways).

Design Using Various Materials

The two basic design charts (Figs. 17 and 18) can be used to design with various types of materials, provided their structural coefficients are known or can be estimated. An example for the design is given on the charts. It must be emphasized that the charts give a required SN and not pavement thickness for a given design DBR and traffic combination. Because each material in the layered system has a different strength coefficient, the total thickness of a pavement will vary for a given DBR and traffic number (DBR and T_{18}).

The charts can be used for any road. One can assume certain thickness of asphaltic concrete for the surface, multiply the strength coefficient of this layer by the thickness, and add necessary rock or gravel layers for a foundation to meet the required SN.

Bituminous Concrete/Penetrated Base/Gravel.—Current Massachusetts practice in flexible pavement design is to use a bituminous concrete surface supported by penetrated crushed rock base and gravel. If the designer wants to use these particular materials and knows the desired thicknesses of the surface and the base, a specific design chart can be easily prepared. For instance, a popular cross-section may have $4\frac{1}{2}$-in. bituminous surface, 6-in. penetrated base, and variable gravel thickness. The thickness of each layer is multiplied by the appropriate strength coefficient and a SN for each material can be represented on the chart. The main variable is the gravel layer, except where the DBR's are high or the traffic number, T_{18}, is low.

Again it must be emphasized that the charts are based on SN rather than pavement thickness. For illustration, Figure 19 shows the result of replacing the SN with thickness for a specific combination of materials.

Bituminous Concrete/Black Base/Gravel.—A similar chart can be prepared for pavement with a bituminous base (black base). The 6-in. penetrated crushed rock base is approximately equal to 4 in. of black base.

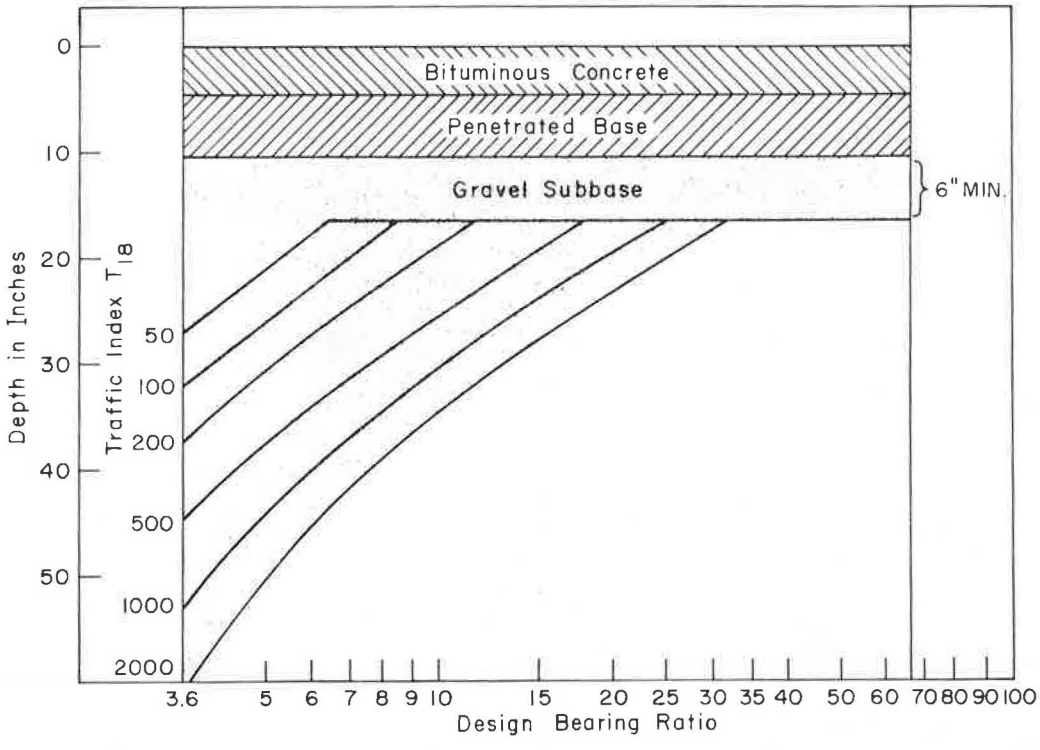

Figure 19. Thickness of pavements for a given combination of materials (not to be used for design purposes); TSI = 2.5.

CONCLUDING REMARKS

The layered pavement design method developed for Massachusetts recognizes characteristics of soils, traffic, and materials as the parameters of major influence in the retention of serviceability of a pavement. Where possible, the results of the AASHO Road Test were used to assess quantitatively the influence of the major parameters. In addition, the special problems related to frost penetration into pavements, frost heaving and spring breakup have been analyzed and recommendations have been made concerning detection, control and treatment of frost-susceptible materials. The pavement structure was analyzed using layered theory to demonstrate the critical action of each layer. The importance of using deep surface layers to reduce cracking was particularly evident from this analysis. The procedure has been developed in such a way that it can be integrated into the sequence of present Massachusetts practice in highway planning, design, and construction.

It was recognized at the outset of this study that although the design method to be developed should represent an improvement over existing constant section design, there would be a necessity for further research in areas where knowledge was found to be particularly deficient. Future research should be directed toward the evaluation of the structural support offered by soils and pavement materials, and variations in this support with environmental conditions. Results of this work should provide a better means for assessment and control of the structural capacity of the pavement components than is currently available.

ACKNOWLEDGMENTS

The work described herein was carried out under the sponsorship of the U. S. Bureau of Public Roads and the Massachusetts Department of Public Works. In the course of this work, the authors called on members of many state highway and federal agencies and drew on the special talents of many in the Massachusetts Department of Public Works and at the Massachusetts Institute of Technology. The number of contributors is so great that it is not possible to give individual credits; the help of all has been invaluable.

REFERENCES

1. The AASHO Road Test, Report 3: Traffic Operations and Pavement Maintenance. Highway Research Board Spec. Rept. 61C, 1962.
2. Carey, W. N., Jr., and Irick, P. E. The Pavement Serviceability-Performance Concept. Highway Research Board Bull. 250, pp. 40-58, 1960.
3. AASHO Interim Guide for the Design of Flexible Pavement Structures. Oct. 12, 1962.
4. Shook, J. F., and Fang, H. Y. Cooperative Materials Testing Program at the AASHO Road Test. Highway Research Board Spec. Rept. 66, 1961.
5. Engineering and Design, Pavement Design for Frost Conditions. U. S. Army, Corps of Engineers, Rept. EM 1110-1-306, May 1962.
6. Aldrich, H. P. Frost Penetration Below Highway and Airfield Pavements. Highway Research Board Bull. 135, pp. 124-149, 1956.
7. Stokstad, O. L. Frost Action in Michigan. Symposium on Frost Heave and Frost Action on Soils. Highway Research Board Spec. Publ., 1951.
8. Boussinesq, J. Application of Potential Theory in a Study of Equilibrium and Motion of Elastic Solids. Paris, 1885.
9. Burmister, D. M. The General Theory of Stresses and Displacements in Layered Soil Systems. Jour. of Applied Physics, Vol. 16, 1945.
10. Westergaard, H. M. Theory of Concrete Pavement Design. Highway Research Board Proc., Vol. 7, Pt. 1, pp. 175-181, 1927.
11. Hagstrom, J., Chambers, R. E., and Tons, E. Low Modulus Pavement on Elastic Foundation. MIT, Dept. of Civil Engineering, Res. Rept. R64-11, April 1964.
12. Tons, E., and Krokosky, E. M. Tensile Properties of Dense Bituminous Concrete. Proc. 38th Annual Meeting AAPT.

13. Putnam, J. O. Theoretical Analysis of the Behavior of Rigid Airfield Pavements for the Case of Interior Loading. Unpublished Doctoral Thesis, MIT, 1963.
14. Helmer, R. A. Nuclear Moisture—Density Research Project. Oklahoma Highway Dept., 1963.
15. The AASHO Road Test. Highway Research Board Spec. Repts. 61A-G, 1962.
16. Proc. Int. Conf. on the Structural Design of Asphalt Pavements, Univ. of Michigan, Aug. 1962.
17. The AASHO Road Test. Highway Research Board Spec. Rept. 73, 1962.